Methods Development for the Synthesis of Biologically Relevant Porphyrins and Porphyrin Rigid Linker Arrays

Submitted by

Elisabeth Sitte (M.Sc.)

Trinity College Dublin, the University of Dublin

A thesis submitted to Trinity College Dublin, the University of Dublin,

for the degree of

Doctor of Philosophy

Under the supervision of Prof. Dr. Mathias O. Senge

May 2022

Declaration

I declare that this thesis has not been submitted as an exercise for a degree at this or any other university and it is entirely my own work.

I agree to deposit this thesis in the University's open access institutional repository or allow the library to do so on my behalf, subject to Irish Copyright Legislation and Trinity College Library conditions of use and acknowledgement.

I consent to the examiner retaining a copy of the thesis beyond the examining period, should they so wish (EU GDPR May 2018).

Unpublished and/or published work of others is duly acknowledged in the text wherever included.

Signed:_____

May 2022 Trinity College Dublin

„Nobody said it was easy
No one ever said it would be this hard“

Coldplay, *The Scientist*

“I shall be telling this with a sigh
Somewhere ages and ages hence:
Two roads diverged in a wood, and I –
I took the one less travelled by,
And that has made all the difference.”

Robert Frost, *The Road Not Taken*

Summary

The research carried out herein focuses on two main aspects: The synthesis of new derivatives of naturally occurring porphyrins and the preparation of non-natural chromophore-rigid linker conjugates as potential bioisosteres and mimics of photosynthetic systems.

Chapter 1 comprises a general introduction. Synthetic advances and applications of naturally occurring porphyrins, especially protoporphyrin IX, are described. Furthermore, the concept of conjugating non-natural porphyrins and other chromophores to a bicyclo[1.1.1]pentane (BCP) rigid linker unit to study biologically relevant processes is introduced. The special properties, synthetic modifications and applications of the BCP motif are discussed.

While the synthetic accessibility of natural porphyrins is limited, at the same time there is a demand for new derivatives for biochemical and medicinal applications. Chapter 2 describes the development of synthetic methods for the functionalisation of protoporphyrin IX dimethyl ester (PPIX-DME) by palladium-catalysed cross coupling reactions. Initially, procedures for the selective bromination of the vinyl groups of PPIX-DME were studied. Optimization of the reaction conditions resulted in yields of di-brominated PPIX-DME of up to 84%. Suzuki and Sonogashira coupling reactions were successfully performed on this precursor and the substrate scope was studied for these reactions. Good to high yields were generally obtained for simple aromatic substrates, while the yields were reduced for sterically demanding arenes and phenyl derivatives with certain functional groups such as a methyl carboxylate ester moiety. PPIX-DME diyne free base and Zn(II) derivatives, obtained by Sonogashira coupling reaction, were used as precursors for Cu(I)-catalysed 1,3-dipolar azide-alkyne cycloaddition (“click“) reactions. The procedures described herein represent robust and versatile methods for the easy functionalisation of PPIX-DME.

After synthetic methods for the bromination and coupling reactions on PPIX-DME had been established the aim was to synthesise PPIX-DME-fluorophore triads as potential theranostic bio-probes (Chapter 3). A Suzuki coupling of a boronic acid substituted BODIPY dye with di-brominated PPIX-DME yielded a triad consisting of one porphyrin und two BODIPY units. Preliminary studies indicated that energy transfer from the BODIPY moieties to the porphyrin occurred. To retain the BODIPY’s fluorescence in the conjugate, the aim was to reduce the rate of BODIPY-to-porphyrin energy transfer. Two different pathways were explored. A Sn(IV)PPIX-DME complex with two axially ligated BODIPY units was

synthesised and its UV-Vis absorption and emission properties were studied. While some fluorescence originating from the BODIPY units was observed the complex‘ overall emission was low. A third triad was prepared by a Sonogashira coupling reaction of di-brominated PPIX-DME and α-distyryl-substituted BODIPY, which exhibits red-shifted absorption and emission maxima compared to α-unsubstituted BODIPYs. Preliminary spectroscopic results indicated that upon excitation of the conjugate at different wavelengths, energy transfer between the porphyrin and BODIPY moieties occurred in both directions.

The potential of new synthetic strategies for the preparation of BCP-chromophore conjugates under “click“-type conditions is discussed in Chapter 4. 1-Azido-3-iodo-BCP was reacted with different ethynyl-substituted chromophores and small molecules to give the corresponding BCP-substituted 1,2,3-triazoles. In some of these reactions, the formation of 5-iodo-1,2,3-triazoles as side products was observed. Following this, the reaction conditions towards the Cu(I)-catalysed formation of BCP 5-iodotriazoles from 1-azido-3-iodo-BCP and terminal alkynes were optimised. Five examples of BCP-substituted 5-iodotriazoles were synthesised subsequently in moderate to good yields. When the cycloaddition reaction was carried out under similar conditions but in the presence of a Pd(II) catalyst, 5-alkynylated 1,4,5-tri-substituted BCP triazoles could be formed. Five derivatives of such 5-alkynylated triazoles were prepared by this single-step one-pot procedure in moderate yields. The obtained products have promise as bioisosteres in medicinal chemistry applications. As a means to assess the compounds‘ potential as bioisosteres, intermolecular interactions in the crystals of several BCP triazoles were studied.

Finally, a variety of BCP-linked chromophore arrays were prepared as potential electron/energy transfer model systems (Chapter 5). The BCP motif was incorporated as a rigid, non-conjugated linker unit between different donor and acceptor moieties with the goal of arranging the substituents in a defined spatial manner while preventing any undesired electronic coupling between them. An electron-deficient (15-(pentafluorophenyl)-10,20-diphenylporphyrinato)zinc(II) moiety was employed as an energy acceptor unit and connected *via* the BCP linker to BODIPY, pyrene and (10,15,20-triphenylporphyrinato)zinc(II) donor units. BCP-linked 15-(pentafluorophenyl)-10,20-diphenylporphyrin dyads with two different metal centres, Zn(II) and Ni(II) as well as Zn(II) and Cu(II), respectively, were also prepared. X-ray analysis of some of the prepared arrays gave information about the mutual orientation of donor and acceptor moieties in the solid state. Detailed spectroscopic measurements on these compounds to study electron/energy transfer through the BCP linker are underway.

Publications

1. J. M. O'Brien, **E. Sitte**, K. J. Flanagan, H. Kühner, L. J. Hallen, D. Gibbons, M. O. Senge, Functionalization of Deutero- and Protoporphyrin IX Dimethyl Esters via Palladium-Catalyzed Coupling Reactions, *J. Org. Chem.* **2019**, *84*, 6158–6173.

2. **E. Sitte**, M. O. Senge, The Red Color of Life Transformed – Synthetic Advances and Emerging Applications of Protoporphyrin IX in Chemical Biology, *Eur. J. Org. Chem.* **2020**, 3171–3191.

   Invited for journal front cover of issue 22/2021.

3. **E. Sitte**, B. Twamley, N. Grover, M. O. Senge, Investigation of the Reactivity of 1-Azido-3-iodobicyclo[1.1.1]pentane under "Click" Reaction Conditions, *J. Org. Chem.* **2021**, *86*, 1238–1245.

   Invited for supplementary cover of issue 1/2021.

Notes on publications:

Chapter 1 contains details from publication 2.

Chapter 2 contains details from publication 1.

Chapter 4 contains details from publication 3.

Conference Abstracts

E. Sitte, J. M. O'Brien, M. O. Senge "Exploration of Novel Functionalization Reactions for Naturally Occurring Porphyrins" in GDCh Wissenschaftsforum Chemie 2017 (10.09.17–14.09.17), Berlin, Germany, Abstract book: 7210_14254.

E. Sitte, M. A. Filatov, K. J. Flanagan, H. Savoi, R. W. Boyle, M. O. Senge "Light for Life – Simultaneous Photosensitization and Optical Imaging Using BODIPY-anthracene Dyads" in GDCh Wissenschaftsforum Chemie 2017 (10.09.2017–14.09.2017), Berlin, Germany, Abstract book: 7210_14255.

L. Hallen, **E. Sitte**, M. O. Senge "Exploration of Novel Functionalization Reactions for Naturally Occurring Porphyrins" in CSCB Symposium (08.12.2017), Dublin, Ireland, Abstract book: P41.

L. Hallen, **E. Sitte**, M. O. Senge "Exploration of Novel Functionalization Reactions for Naturally Occurring Porphyrins" in RSC Organic Division – Ireland Regional Meeting (02.05.18), Belfast, United Kingdom, Abstract book: P3.

E. Sitte, J. M. O'Brien, K. J. Flanagan, M. O. Senge "Exploration of Novel Functionalization Reactions for Naturally Occurring Porphyrins" in 5th ESP Photobiology School (11.06.2018–17.06.2018), Brixen, Italy, Abstract book: P24.

E. Sitte, J. M. O'Brien, K. J. Flanagan, M. O. Senge "Exploration of Novel Functionalization Reactions for Naturally Occurring Porphyrins" in Gordon Research Conference on Chemistry and Biology of Tetrapyrroles (15.07.2018–20.07.2018), Newport, USA, Abstract book: P31b.

E. Sitte, J. M. O'Brien, K. J. Flanagan, M. O. Senge "Exploration of Novel Functionalization Reactions for Naturally Occurring Porphyrins" in 17th Congress of the International Union of Photobiology and 18th Congress of the European Society for Photobiology 2019 (25.08.2019–30.08.2019), Barcelona, Spain, Abstract book: ESP-IUPB04432.

E. Sitte, J. M. O'Brien, K. J. Flanagan, M. O. Senge "Exploration of Novel Functionalization Reactions for Naturally Occurring Porphyrins" in GDCh-Wissenschaftsforum Chemie 2019 (15.09.2019–18.09.2019), Aachen, Germany, Abstract book: 8454_21918.

E. Sitte, M. O. Senge, „Towards Fluorescent Bio-Probes: Protoporphyrin IX-BODIPY Triads" in 27th Lecture Conference on Photochemistry (online) (14.09.2020–15.09.2020), Abstract book: ST-03.

E. Sitte, B. Twamley, N. Grover, M. O. Senge „Investigation of the reactivity of 1-azido-3-iodobicyclo[1.1.1]pentane under “click” conditions“ in ACS Spring 2021 (online) (05.04.2021–30.04.2021), Abstract book: 3537021.

Acknowledgements

First and foremost, I would like to thank Prof. Dr. Mathias O. Senge for giving me the opportunity to carry out this research under his supervision. I am very grateful that Mathias gave me the chance to join his group, for his faith in me from the beginning on, his support and encouragement to think independently and to explore and develop my interests and skills. The Senge Lab is a place with great physical and intellectual resources and I am very glad that I was able to do my PhD in such an environment. I would also like to thank the Sydney E. Auchinleck Foundation and Trinity College Dublin for their financial support.

A big thank you to all the present and past members of the Senge group, Alina, Keith, Marc, Marie, Gemma, Stefan, Mikhail, Ganapathi, Susan, Jessica, Karolis, Bhavya, Dáire, Nitika, Piotr, Zoi, Harry, Chris, Asterios and Claire for their continuous support and advice, help with proof-reading my thesis and for making the lab such a great place to work in which I enjoyed coming back to almost every day. There was never a lack of people to listen to a problem, to offer help when needed or to come for a coffee/tea/pint. I will keep all our nights out, dinners, trips, concerts, conferences, hikes, swims, movie nights, explorations,... in best memory. It's been mostly because of these amazing lab mates that PhD has been a truly unique journey! My special thanks to Nitika for her help with the BCP projects and for being a constant source of knowledge, guidance and support in all lab- and life-related matters, to Jessica for sharing the deutero/proto IX project with me and to Chris for the X-ray work. I would also like to thank our visiting students Lukas, Hannes, Heather, Elizabeth and Julie for supporting me in the projects .

Many thanks to Dr. John O'Brien for running so many of my NMR samples with very quick turnaround and to Dr. Brendan Twamley for his sophisticated crystal structure analyses and for never turning down even those crystals which did not look promising. I am also very grateful to Dr. Manuel Rüther for his NMR analysis, Dr. Gary Hessman and Dr. Martin Feeney for mass spectrometry measurements and all the administrative and technical stuff in the chemistry department.

Last but not least, I would like to say a huge thank you to my family, especially my parents, grandparents and my brother Robert for their belief in me and their support which never faltered, neither in the moments when I called in the middle of the night nor when I forgot to reach out to them for too many days on end. Taking this step in my life would not have been possible without you.

List of Abbreviations

°C	degree Celsius
Ac	acetyl
acac	acetylacetonate
acetone-d_6	deuterated acetone
Ar	aryl
ATP	adenosine triphosphate
BCO	bicyclo[2.2.2]octane
BCP	bicyclo[1.1.1]pentane
BODIPY	4,4-difluoro-4-bora-3a,4a-diaza-*s*-indacene
CYP	cytochrome P450
br	broad
calcd.	calculated
d	doublet (NMR)
DCC	*N*,*N*'-dicyclohexylcarbodiimide
DCM	dichloromethane
dd	doublet of doublets
DDQ	2,3-dichloro-5,6-dicyano-1,4-benzoquinone
dec.	decomposition
DIPEA	*N*,*N*'-diisopropylethylamine
$DMBP^{2+}$	1,1'-dimethyl-4,4'-bipyridinium
DMF	*N*,*N*'-dimethylformamide
DMSO	dimethyl sulfoxide
DMSO-d_6	deuterated DMSO
DPM	dipyrromethane
dr	diastereomeric ratio
EDC	1-ethyl-3-(3-dimethylaminopropyl)carbodiimide
e.g.	*exempli gratia* (for example)
eq.	equivalent(s)
er	enantiomeric ratio
ESI	electrospray ionization
EtOAc	ethyl acetate
et al.	*et alii*/*et aliae* (lat. and others)
Et	ethyl
EtOH	ethanol

FMO	frontier molecular orbital
FRET	Förster resonance energy transfer
GooF	Goodness of Fit
HATU	hexafluorophosphate azabenzotriazole tetramethyl uranium
HBTU	hexafluorophosphate benzotriazole tetramethyl uronium
H-NOX	heme nitric oxide/oxygen binding domain
HOBt	1-hydroxybenzotriazole
HRMS	high resolution mass spectrometry
HSA	human serum albumin
Hz	hertz
iPr	isopropyl
IR	infrared
J	coupling constant
kcal	kilocalorie
L	litre
M	molarity
m	multiplet
m	*meta*
MALDI	matrix assisted laser desorption ionization
*m*CPBA	*meta*-chloroperoxybenzoic acid
Me	methyl
MeOH	methanol
min	minute
mL	millilitre
mol%	mole fraction
M.p.	melting point
MPIX	mesoporphyrin IX
MS	mass spectrometry
m/*z*	mass-to-charge ratio
n. d.	not determined
NADPH	nicotine adenine dinucleotide phosphate
NHS	*N*-hydroxysuccinimide
NIS	*N*-iodosuccinimide
NBS	*N*-bromosuccinimide
NMR	nuclear magnetic resonance
o	*ortho*

p	*para*
Pd_2dba_3	tris(dibenzylideneacetone)dipalladium(0)
$Pd(dppf)Cl_2$	[1,1'-bis(diphenylphosphino)ferrocene]palladium(II) dichloride
$Pd(OAc)_2$	palladium(II) acetate
$Pd(PPh_3)_4$	tetrakis(triphenylphosphine)palladium(0)
PDT	photodynamic therapy
PET	photoinduced electron transfer
Ph	phenyl
PIFA	bis(trifluoroacetoxy)-iodobenzene
PPIX	protoporphyrin IX
PPIX-DME	protoporphyrin IX dimethyl ester
ppm	parts per million
p-Tol	*para*-tolyl
PVA	polyvinylalcohol
pyridine-d_5	deuterated pyridine
q	quartet (NMR)
r.t.	room temperature
R_f	retention factor
s	singlet (NMR)
SET	single electron transfer
SiO_2	silica gel
S_0	singlet ground state
S_1	first excited singlet state
S_2	second excited singlet state
t	triplet (NMR)
TBAF	tetrabutylammonium fluoride
t-Bu	*tert*-butyl
TEA	triethylamine
TFA	trifluoroacetic acid
TFA-d	deuterated TFA
THF	tetrahydrofuran
TLC	thin layer chromatography
TMS	trimethylsilyl
T_1	first excited triplet state
toluene-d_8	deuterated toluene
TPP	tetraphenylporphyrin

UV	ultraviolet
Vis	visible
v/v	volume per volume
XRD	X-ray diffraction
δ	chemical shift (NMR)
Δ	heat
µmol	micromoles
λ	wavelength

Table of Contents

Chapter 1. Introduction

1.1 The Chemistry of Porphyrins

Porphyrins are tetrapyrrolic macrocycles that play a central role in various natural processes. They act as prosthetic groups of proteins and enzymes. Prominent examples are hemoglobin and myoglobin that transport oxygen in blood and in muscle tissue, cytochromes of type c which are required for cellular respiration, cytochromes of the P450 family that are involved in biosynthesis as well as drug metabolism, and catalases and peroxidases which help in the detoxification of organisms.[1] The closely related chlorins and bacteriochlorins act as photosynthetic pigments in plants and bacteria[2] and the corrinoid vitamin B_{12} is a precursor of coenzyme B_{12} and methylcobalamin, two enzyme cofactors.[3] The synthesis of these compounds and investigation of their properties has preoccupied chemists for more than a century. Concomitantly, the preparation of non-natural porphyrin derivatives has surged. Their chemical and photophysical properties have been harnessed for a plethora of applications such as cancer therapy,[4] catalysis,[5] sensing[6] and light harvesting.[7]

1.1.1 The Porphyrin Macrocycle

Porphyrins comprise of four pyrrole moieties which are connected *via* methine bridges in the *α*-positions. The tautomeric porphyrin core structures (**1.1a**, **1.1b**) are shown in Scheme 1. The porphyrin macrocycle possesses 18 π-electrons along the shortest cyclic path (18[annulene]), thus obeying Hückel's[8] [4n+2] rule for aromatic compounds.[9] In the traditional view it was assumed that porphyrin aromaticity is based on the 18[annulene] pathway shown in Scheme 1.1.[10] Later studies suggest that this is not the preferred aromatic pathway and that all 26 π-electrons contribute to the ring current.[11] Chlorins and bacteriochlorins such as chlorophyll a (**1.5**) and bacteriochlorophyll a (**1.6**) (Figure 1.1) are tetrapyrroles which form the photosynthetic pigments in plants and bacteria. In contrast to the porphyrin core, one or two reduced double bonds are reduced, resulting in 24 or 22 π-electrons in the ring.[11b] The inner core pyrrolic hydrogen atoms of porphyrins can tautomerise in association with a shift of the shortest aromatic path of the macrocycle. The tautomer with the hydrogen atoms in *cis*-position is believed to be less favoured in most porphyrins than the *trans*-tautomer due to its higher energy. Interconversion from one *trans*-tautomer to the other takes place *via* formation of the *cis*-tautomer as an intermediate and subsequent rapid tunnelling to the *trans*-tautomer.[12] As synthesised, the porphyrin core is occupied by two protons; such porphyrins without metals are termed free base. Porphyrins

can act as Lewis acids, coordinating metal ions after the loss of two protons. These metal complexes show different absorption spectra compared to free-base porphyrins.[13]

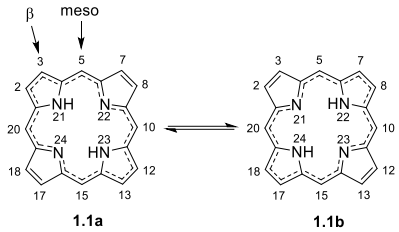

Scheme 1.1. N-H tautomerism in the porphyrin core. The shortest π-electron path, the specific numbering of the porphyrin macrocycle and meso- and β-positions are indicated.

The porphyrin macrocycle can be substituted at the meso-positions (methine carbons) and/or the β-positions (β-pyrrolic carbons). An example of a simple meso-substituted porphyrin is 5,10,15,20-tetraphenylporphyrin (compound **1.10**, Scheme 1.2). In this compound, the *ortho*-carbons of the phenyl ring are in steric repulsion with the hydrogen atoms in the β-positions of the porphyrin core, resulting in a rotational barrier for the phenyl rings and their non-coplanar orientation relative to the porphyrin core (Figure 1.1).[14]

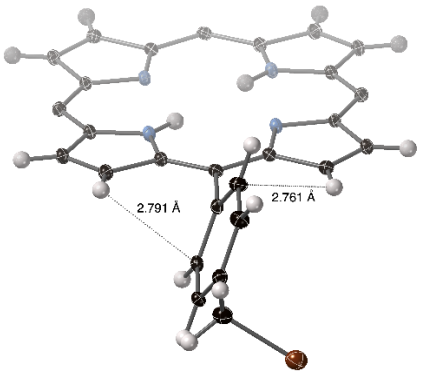

Figure 1.1. Representation of the steric repulsion between the β-hydrogens of the porphyrin macrocycle and the *ortho*-carbons of the meso-phenyl substituent at a distance of 2.791 Å, resulting a rotation of the phenyl ring out of the macrocycle plane.[4d]

meso-Substituted porphyrins have a vast importance in porphyrin research, whereas all naturally occurring tetrapyrroles are β-substituted. Prominent examples in this respect are protoporphyrin IX (PPIX) (**1.2**) which is the iron-free precursor of heme b (**1.3**), and the intermediates in heme biosynthesis, coproporphyrinogen and uroporphyrinogen (Figure 1.2).[15] The functional tetrapyrroles utilised in nature are mostly metal complexes: heme contains Fe(II), chlorophylls contain Mg(II) and vitamin B_{12} (**1.7**) is a Co(III) complex (Figure 1.2).

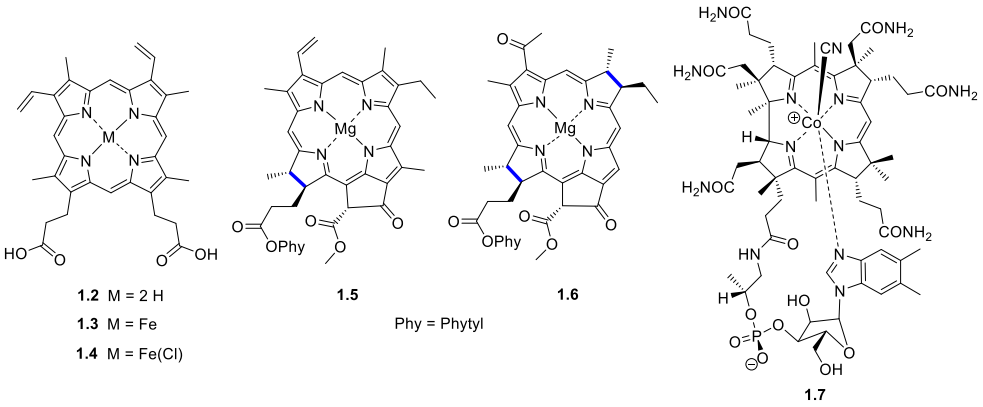

Figure 1.2. Structures of some naturally occurring pigments: Protoporphyrin IX (**1.2**), heme b (**1.3**), hemin (**1.4**), chlorophyll a (**1.5**), bacteriochlorophyll a (**1.6**) and vitamin B_{12} (**1.7**). Reduced bonds of the chlorophylls are highlighted in blue.

Known as "the pigments of life", porphyrinoids such as porphyrins and chlorophylls strongly absorb visible light. The absorption spectrum of free base porphyrins is typically characterised by a strong absorption band in the region between 380 and 500 nm, the Soret band, which corresponds to the $S_0 \rightarrow S_2$ electronic transition, and four weaker bands between 500 and 750 nm, the Q bands, corresponding to the $S_0 \rightarrow S_1$ transition. The relative intensity of the Q bands depends on the type and position of the porphyrin substituents.[13a]

1.1.2 Strategies for Porphyrin Synthesis

Chemist's efforts to determine the structures of the pigments of life began more than 150 years ago. A pioneering work was carried out by Stokes in the second half of the 19th century, who found two different kinds of chlorophyll, a and b, as components of green leaves.[2a,16] In the beginning of the 20th century, Richard Willstätter intensely investigated the structure of chlorophylls. He discovered that chlorophylls contain magnesium.[2a,17] In the 1920s the Munich-based chemist Hans Fischer focused his studies on another natural tetrapyrrole, the red blood pigment heme. In a remarkable effort he developed total syntheses of the biosynthetic heme precursor protoporphyrin IX and heme in its oxidised form, hemin (**1.4**, Figure 1.2).[18] This marked a cornerstone in the development of synthetic porphyrin chemistry. In 1940, Fischer also proposed the structure of chlorophyll a.[19] Later, Fischer's structure was confirmed when Robert Burns Woodward developed a total synthesis for chlorophyll a, setting another milestone in preparative tetrapyrrole chemistry.[20] Woodward also made a major contribution to the total synthesis of vitamin B_{12}, a ring-contracted porphyrinoid (corrin), a few years later, together with Swiss chemist Albert Eschenmoser.[21] These syntheses, developed over many years, required great efforts.[22]

In parallel to developments of the lengthy and intricate syntheses of natural tetrapyrroles, the preparation of simpler non-natural symmetric porphyrins was investigated. The underlying idea was that porphyrins can be prepared by the condensation of aldehydes and pyrroles in a one-pot reaction. The first such reaction was developed by Rothemund in 1935 and later optimised by himself. It involved the condensation of formaldehyde and pyrrole in a methanol/pyridine mixture under a nitrogen atmosphere for 30 h to yield a trace amount of porphyrin (< 1%) (conditions a in Scheme 1.2).[23] This method was later revised by Adler, who in 1967 proposed the reaction of pyrrole and benzaldehyde in refluxing propionic acid for 30 minutes in the open air (conditions b in Scheme 1.2). This procedure uses an acidic solvent which also acts as a catalyst for the condensation and reduces the reaction time compared to the Rothemund synthesis. Therefore, the reaction yield was improved significantly to about 20% but the formation of chlorin side products was observed.[24]

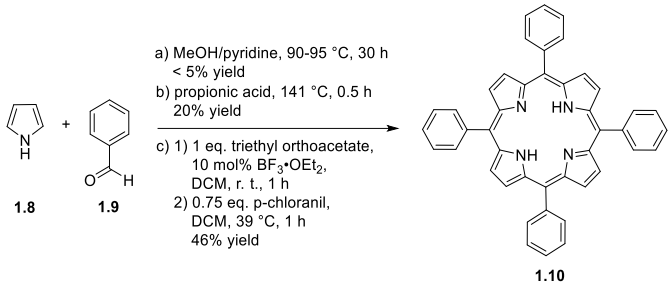

Scheme 1.2. Syntheses of 5,10,15,20-tetraphenylporphyrin (**1.10**) according to the procedures developed by Rothemund (conditions a),[23] Adler (conditions b)[24] and Lindsey (conditions c)[25] and co-workers.

A milestone in the synthesis of meso-substituted porphyrins was achieved by Lindsey in 1986. His group expanded the substrate scope of porphyrin condensation reactions to aldehydes with sensitive functional groups by introducing milder reaction conditions than their predecessors in this field, thereby also reducing the formation of tarry by-products.[25] In the original procedure, benzaldehyde and pyrrole were condensed in dichloromethane (DCM) under a nitrogen atmosphere using boron trifluoride diethyl etherate as a catalyst. Subsequent addition of an oxidant (2,3-dichloro-5,6-dicyano-*p*-benzoquinone (DDQ) or *p*-chloranil) led to the oxidation of the formed porphyrinogen to porphyrin (Scheme 1.2).[25a] This proved to be a viable method to prepare 5,10,15,20-tetraphenylporphyrin (**1.10**) in up to 50% yield and porphyrins with different substituents usually in 30–40% yield.

Unsymmetrically meso-substituted porphyrins of the A_x- or ABCD-type series (Figure 1.3) can be synthesised by mixed condensations whereby different aldehydes are used in a one-pot reaction with pyrrole (Scheme 1.3). The drawback of this approach is that various reaction products are formed, thus the yields are usually low and the separation of the

different products is tedious.[26] Different methods towards the synthesis of unsymmetrically substituted porphyrins have been developed in which the formation of the desired product can be controlled. These different routes follow two main approaches: the total synthesis from pyrrolic building blocks and the functionalisation of pre-formed porphyrins.[27] A classic example for the synthesis of meso-substituted 5,15-A_2-type as well as unsymmetrical β-substituted porphyrins is the MacDonald [2+2] condensation[28] of dipyrromethanes (**1.12**) with aldehydes (Scheme 1.3). The use of specially-functionalised dipyrromethanes (**1.11**) in the [2+2] route can also enable the synthesis of AB_2C- and ABCD-type porphyrins.[29] Dipyrromethane can also be reacted with 2.0 eq. of 2-formylpyrrole and 1.0 eq. of an aldehyde in a [2+1+1] addition instead to yield mono-substituted A_1-type porphyrin.[30] The [3+1] condensation of tripyrranes (**1.13**) with pyrrole and aldehydes can be applied for the synthesis of different porphyrin systems, among others 5,10-A_2-type porphyrins.[31] The synthesis of a linear tetrapyrrole (bilane, **1.14**) precursor and subsequent cyclisation, e.g. *via* metal-templation, is another rational route towards the preparation of unsymmetrical porphyrins.[29a,32]

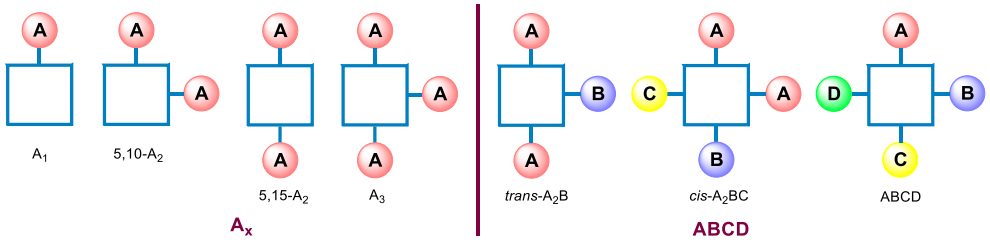

Figure 1.3. Schematic representation of selected porphyrins from the A_x- and ABCD-type series.

A second strategy for the synthesis of unsymmetrical meso-substituted porphyrins is the functionalisation of the free positions of a pre-formed macrocycle. In principle, this can be done on the unsubstituted porphyrin ("porphine"). However this is not a route commonly taken due to the low solubility and limitations in synthetic access to this compound despite the advances made in the last decades.[27,33] Usually, a combination of condensation strategies and post-functionalisation of the obtained porphyrin is used in order to prepare porphyrins with specific substituent patterns. Electrophilic halogenations at the porphyrin free meso- as well as β-positions can be achieved by different methodologies.[34] Especially useful for further synthetic modifications are bromination[35] and iodination[36] to give meso-halogenated porphyrins **1.16a** or **1.16b** which enable for subsequent transition-metal catalysed coupling reactions and addition of a variety of possible substituents to the free positions (Scheme 1.4).[37] Such transformations include Suzuki-Miyaura,[38] Sonogashira,[36,39] Negishi,[35c,40] Stille,[35c,41] Heck,[42] and Buchwald-Hartwig[43] reactions.

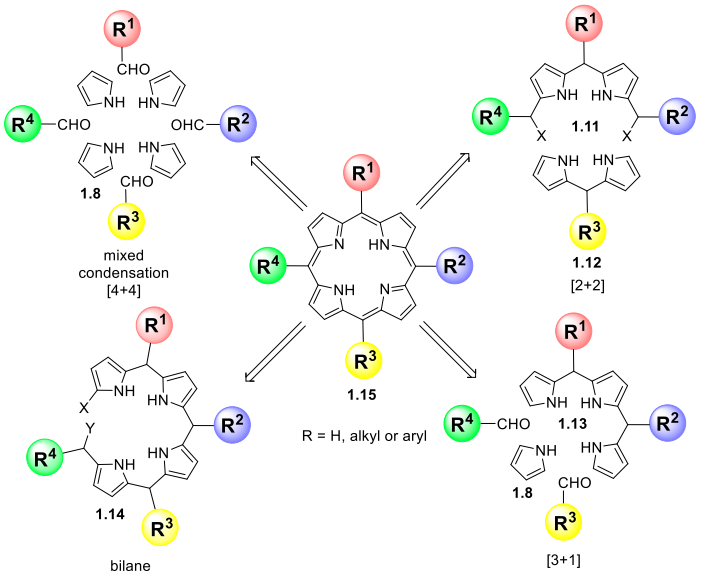

Scheme 1.3. Retrosynthetic analysis of different routes towards the synthesis of porphyrins with mixed meso-substituents.

Likewise, porphyrin functionalisation can be achieved using organometallic reagents. Organolithium reagents were found to undergo nucleophilic addition reactions to free meso-positions of porphyrins (**1.17**). Alkyl- as well as aryllithium reagents proved to be reactive.[44] This method allows for stepwise addition of substituents to the meso-positions, thus enables construction of porphyrins with mixed substituent patterns (**1.18**).[45] Reaction preferentially takes place at the meso-positions, whereby the use of bulky reagents can also lead to partial addition to the β-positions due to steric effects. A modified protocol can be used for the synthesis of directly meso-meso-linked bisporphyrins.[46] There is a vast toolkit of other porphyrin functionalisation reactions which cannot be covered in detail here.

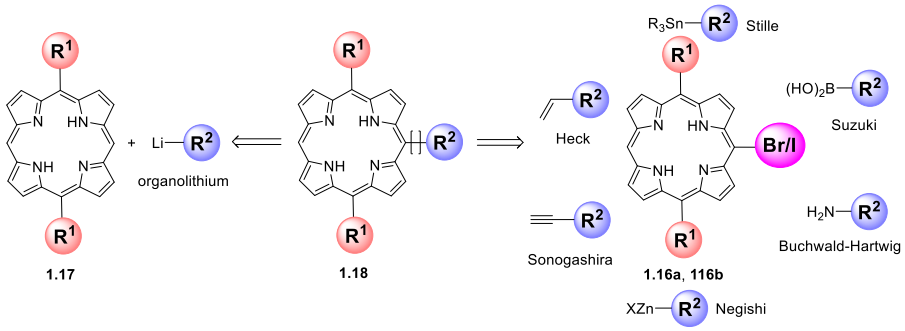

Scheme 1.4. Retrosynthetic analysis of selected possibilities for the functionalisation of an exemplary 5,15-A_2 porphyrin.

1.2 Protoporphyrin IX – Nature's Red Colour

Protoporphyrin IX (PPIX) (**1.2**) is primarily known as the biosynthetic precursor of heme b, the red blood pigment, and other hemes which are found as a prosthetic group in several hemoproteins and enzymes such as hemoglobin, myoglobin, cyctochromes, catalases and peroxidases. Heme's functions in organisms are versatile, ranging from oxygen binding and transport to electron transport and catalysis of redox reactions.[1] Heme b (**1.3**) is the most abundant of the hemes. It consists of a porphyrin ligand, PPIX and a Fe(II) centre (Figure 1.2). The porphyrin macrocycle carries two propionate, two vinyl and four methyl groups in the β-positions while the meso-positions remain free. While the heme metal centre imparts anchoring to proteins by axial ligation to amino acid residues, resulting in penta- or hexacoordinated Fe,[1a] the peripheral substituents on the porphyrin core can also play a role in fixing the prosthetic group inside the heme binding pocket of the protein. The propionate moieties of heme have been shown to engage in electrostatic interactions such as hydrogen bonds with different residues of the protein backbone,[47] whereas the vinyl groups can form covalent bonds with cysteine residues, generating so-called heme c.[1a]

While heme is prone to oxidation at its iron centre, protoporphyrin IX does not suffer from this difficulty. Protoporphyrin IX has gained considerable research interest in recent years. As an important natural product, it provides biocompatibility and can interact with biomolecules; thus, it can be used to modulate molecular or cellular functions.[48] Currently it is widely studied in biomedicine for applications such as photodynamic therapy (PDT),[49] antimicrobial and antiviral phototherapy,[50] biosensing,[51] bioimaging,[52] catalysis[53] and interference with biochemical pathways.[54] Additionally, the inherent properties of PPIX as a porphyrin, the wide range of biological functions manifested in nature through manipulation of the macrocycle conformation,[55] its ready availability and the possibility of facile attachment of groups at its propionate moieties[56] renders it a compound frequently

employed for a variety of other applications such as sensing,[57] light harvesting,[58] electrochemistry[59] as well as uses in supramolecular chemistry.[60]

1.2.1 Total Synthesis of Protoporphyrin IX

In the 1920s Hans Fischer extensively investigated the total synthesis of tetrapyrroles. Highlights were the synthesis of deuteroporphyrin IX in 1928,[61] followed by the first syntheses of PPIX, hematoporphyrin and hemin one year later.[18] The synthesis of the unsymmetrically β-substituted PPIX, which earned the German chemist the Nobel Prize for Chemistry in 1930, was intricate and lengthy. It started with the synthesis of different pyrroles that were reacted to yield the 5,5'-bromo- and 5,5'-methyl-substituted dipyrromethenes **1.19** and **1.20**, respectively, which were condensed in a succinic acid melt to give deuteroporphyrin IX (**1.21**) (Scheme 1.5). Iron(III) insertion, followed by acetylation and reduction yielded hematoporphyrin (**1.22**), which was converted to PPIX (**1.2**) by dehydration.[18,61]

Later, approaches for the *de novo* synthesis of PPIX were developed, mainly by Smith and co-workers.[62] To prepare deuterated derivatives of PPIX dimethyl ester (**1.23**), Smith applied different strategies. One comprised a MacDonald 2+2 condensation of 5,5'-formyl-dipyrromethane **1.24** with 5,5'-unsubstituted dipyrromethane **1.25**. The cyclisation to **1.26** was achieved by *p*-toluenesulfonic acid and zinc acetate. Hereafter, the 3,8-vinyl groups were generated by base-catalysed dehydrochlorination at the 2-chloroethyl moieties of **1.27**, followed by demetallation and esterification.[62a] Alternatively, **1.2** was prepared *via* condensation of the phosphoryl chloride complex of amido-dipyrromethane **1.28** with 5-unsubstituted dipyrromethane **1.29** to give bilane **1.30** which was further converted to the biscarboxylate **1.31** and cyclised using trichloroacetic acid and trimethyl orthoformate. Acetylation to give **1.32**, hydrogenation and reoxidation of the porphyrin macrocycle yielded **1.33** as precursor for PPIX dimethyl ester.[62a]

A different approach for the synthesis of **1.2** involved the formation of tripyrrene **1.36** and then *a,c*-biladiene **1.37** from dipyrromethane **1.34** and subsequent condensations with formyl-pyrrole **1.35**. Cyclisation of the linear tetrapyrrole using a copper(II) salt and demetallation afforded **1.33**, which can be converted to **1.2**.[62b,d-f,h-m,63] More recently, the PPIX dimethyl ester precursor **1.40** was prepared from a condensation of 5,5'-diiodo- and 5,5'-diformyl-dipyrromethanes **1.38** and **1.39** by Martin *et al.*[64] The vinyl groups were obtained by reduction and dehydration of acetyl moieties in the 3,8-positions of the porphyrin ring.

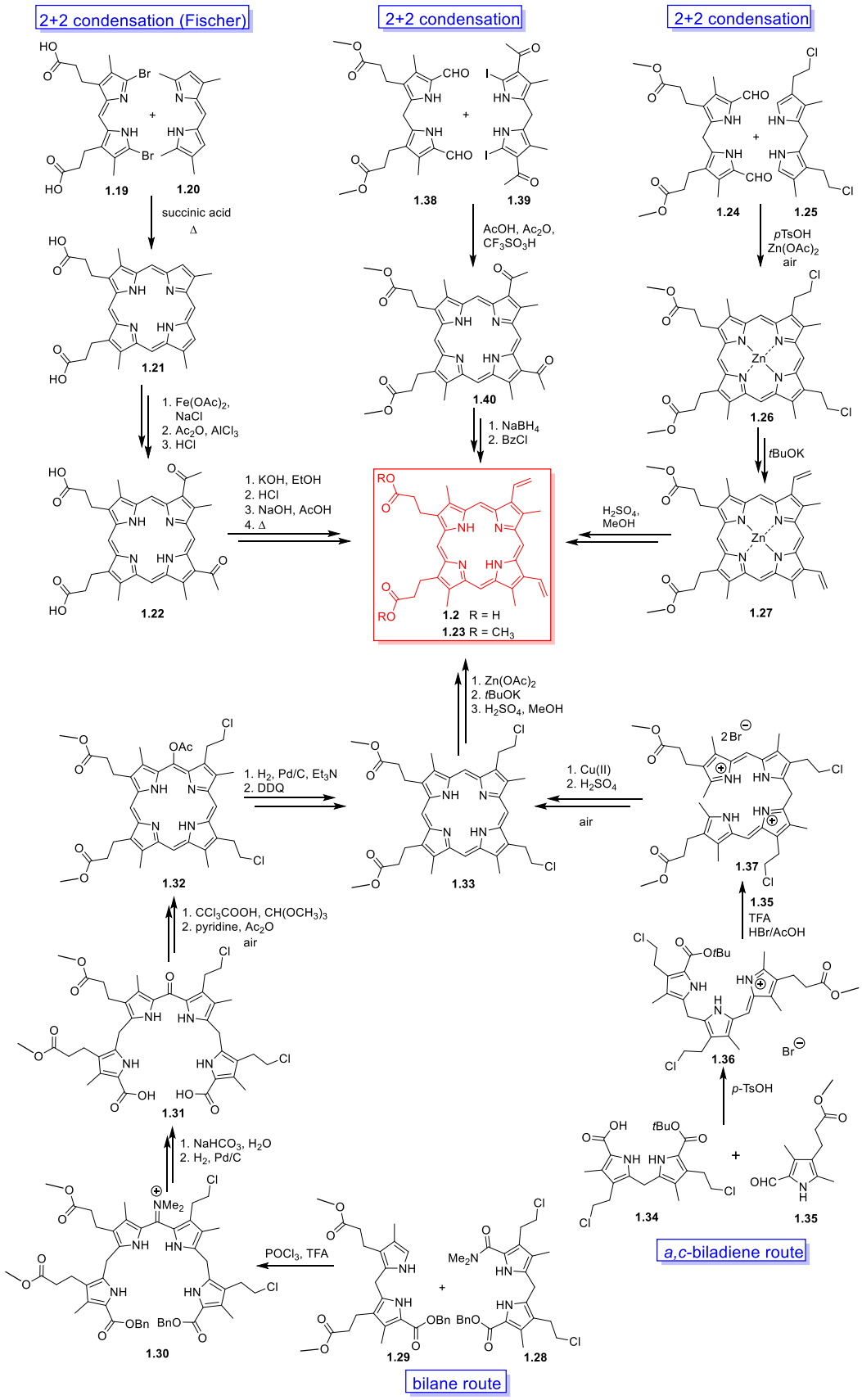

Scheme 1.5. Different routes towards the total synthesis of PPIX (**1.2**) and protoporphyrin IX dimethyl ester (PPIX-DME) (**1.23**).

1.2.2 Substituent Modifications

The interest in PPIX has led to the development of a range of functionalisation reactions for the vinyl groups and propionic acid moieties, the majority of whom has been discussed in a comprehensive review by Pavlov.[56] A selection of frequently applied functionalisation reactions for PPIX (**1.2**), PPIX-DME (**1.23**) and their metal complexes, is given in Scheme 1.6. Among the vinyl group derivatisations are hydrobromination using hydrobromic acid in combination with acetic acid and subsequent nucleophilic substitution,[56,65] mono- and dihydroxylation[56,65b,c,66] and subsequent conversion to aldehydes,[14,65b,66] acetyls,[56,67] alkynes,[56,68] esters[56,65b,69] as well as hydroformylation.[70] Metal-catalysed C-C bond formation reactions have been performed on PPIX vinyl groups, including olefin metathesis[56,71] and Heck reactions.[56,72] Multiple PPIX conjugates have been prepared by ester,[56,66b,73] thioester[56,74] and amide[56,65e,73b,75] formation at the carboxylic moieties (Scheme 1.6). The free meso-positions of PPIX can be formylated using a Vilsmeier reaction whereupon regioisomeric mixtures are obtained.[76] Although long-established reactions such as amide couplings form the basis for most of PPIX synthetic chemistry and are widely applied for the generation of functional derivatives, some advances to broaden the synthetic spectrum of **1.2** and **1.23** have been made more recently and are detailed hereafter.

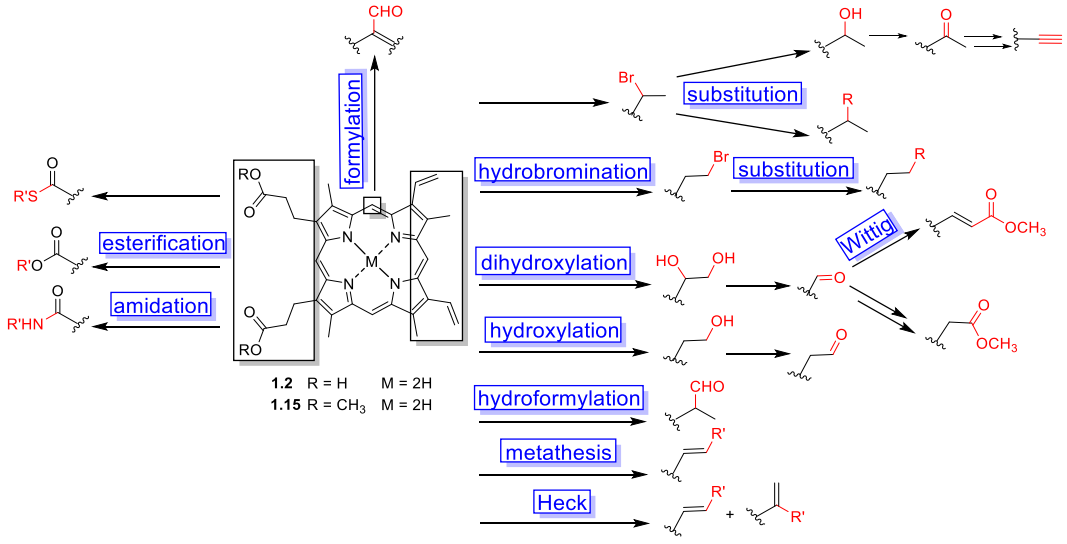

Scheme 1.6. Selected substituent and macrocycle modification on PPIX (**1.2**), PPIX-DME (**1.23**) and their metal complexes.

A new method for the conversion of the vinyl groups of **1.23** to formyl and acetyl moieties, respectively, while circumventing the use of OsO_4 was introduced by Oba and co-workers.[77] Reaction of the vinyl groups with iodine and PIFA in ethylene glycol/1,2-dichloroethane gave a diiodoether porphyrin which was converted to 3,8-diacetyl porphyrin.

An iodohydrin porphyrin was also synthesised in a similar manner which was converted to the 3,8-diformyl derivative of PPIX-DME.

PPIX-DME monoaldehyde **1.40**, synthesised as previously reported,[65,78] was condensed with amines yielding azido- and alkynyl-functionalised porphyrin derivatives, e.g., **1.41a** and **1.41b** (**Scheme 1.7**). Subsequent copper-catalysed azide-alkyne cycloaddition with vitamin B_{12} derivatives afforded molecular hybrid molecules.[79]

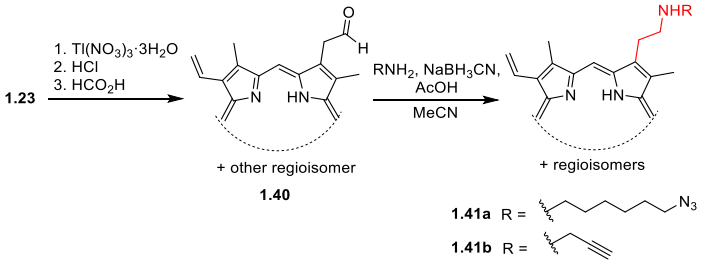

Scheme 1.7. Synthesis of amine-substituted PPIX derivatives *via* condensation with monoformyl-PPIX-DME.

As mentioned previously, hydrobromination of the vinyl groups, followed by nucleophilic substitution is a versatile tool for addition of various substituents to the vinyl-half of PPIX.[65] This reaction was used to prepare tertiary alkylamine-substituted PPIX-DME.[80] Substitution reactions with long aliphatic alcohols instead yielded PPIX lipids. These photosensitiser-appended lipids were assembled into liposomes, forming platforms for sensitiser delivery in aqueous solution.[81] Bishydroxylation of the vinyl groups of PPIX-DME gave the tetraalcohol[66a] as a useful building block which was further reacted with carborane carbonyl chloride to obtain a porphyrin carrying four carboranyl esters.[67a,82] Boronated porphyrins are used in boron neutron capture therapy and PDT.[84]

Electrocyclic reactions involving the vinyl groups of PPIX-DME with diazo compounds are known to produce chlorins.[56,83] This was expanded by Cavaleiro's group who reacted **1.23** with maleic anhydride, followed by addition of nucleophiles to the anhydride moiety giving amphiphilic chlorins e.g. **1.42a** and **1.42b**.[85] Similarly, Uchoa *et al.* synthesised photodynamically active chlorins by a Diels-Alder reaction of **1.23** with maleimides. The cycloaddition products **1.43a**–**1.43c** did not show any π-π-stacking induced self-aggregation due their *endo* conformation.[86] A combined Knoevenagel hetero Diels-Alder reaction on the vinyl groups of Zn complex **1.27** with coumarine, quinolone and naphthoquinoline derivatives was carried out in order to obtain new photosensitiser-natural product conjugates, e.g., **1.44a** and **1.44b** (Scheme 1.8).[87]

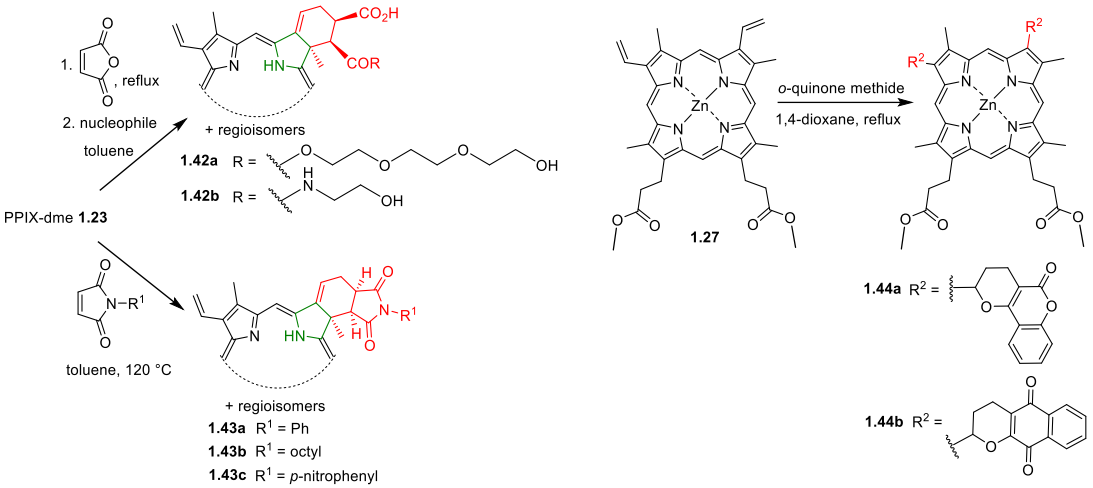

Scheme 1.8. Cycloaddition reactions of the vinyl groups of PPIX-DME **1.23** and its Zn(II) complex **1.27**.

The PPIX vinyl groups are also suitable sites for olefin cross-metathesis reactions and have been subjected to the attachment of different aliphatic side chains using a second generation Grubbs catalyst.[71] Cavaleiro and co-workers synthesised glycoprotoporphyrin derivatives as photosensitisers with increased water-solubility and membrane interaction by this method.[88] Tetraalkyl-substituted as well as amphiphilic PPIX derivatives were synthesised in a similar manner. The tails introduced mediated solvophobicity-induced self-assembly of the porphyrins.[89]

The tendency of vinyl groups to undergo radical additions was exploited to synthesise PPIX containing polymers by free-radical copolymerisation.[90] Reaction of **1.2** with monomers such as acrylamide, methacrylic acid and *N*,*N*'-methylenebisacrylamide was achieved using radical initiators and the resulting polymers were used for spectrophotometric detection of metal ions[90a,b] and as a hydrogel-based pH sensor in a glass electrode.[90c] Incorporation of **1.2** or **1.23** in poly(*N*-isopropylacrylamide) hydrogels circumvented the low water-solubility of these photosensitisers and their tendency to form aggregates in polar solvents.[90d,e] Such biocompatible hydrogels show potential for the clinical administration of PPIX as a photosensitiser.

Heck coupling reactions on the vinyl groups of **1.23** were first carried out by using mercurated arenes as coupling substrates.[72a,c] Later, Castella *et al.* implemented a Pd-catalysed coupling reaction of **1.27** and different halo-aryl compounds which yielded mixtures of regioisomers **1.45a**–**1.45d**.[72b] A similar approach was taken to immobilise PPIX-DME on silicon surfaces. This involved bromination of thienyl-functionalised surfaces using NBS and subsequent coupling of the bromo-heteroarenes with **1.23** using $Pd(PPh_3)_4$ (Scheme 1.9).[91]

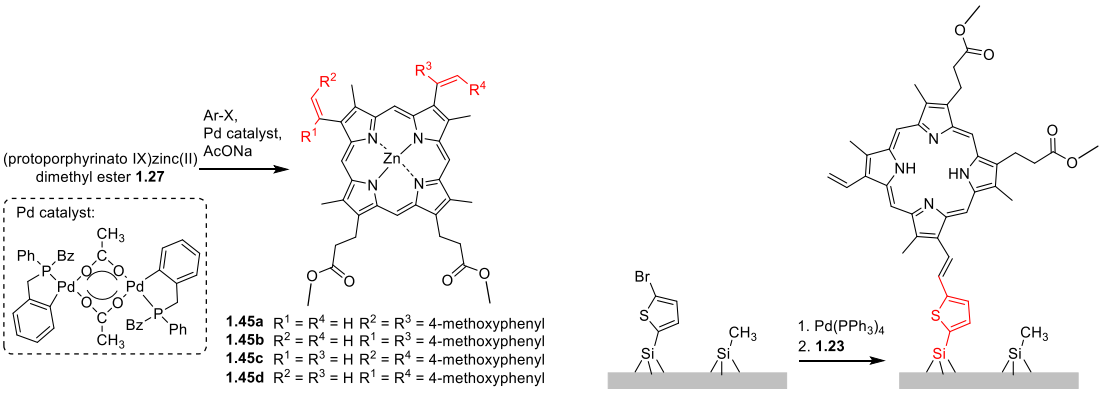

Scheme 1.9. Heck reactions using PPIX-DME and (protoporphyrinato IX)zinc(II) dimethyl ester.

Modification of the propionic acid moieties presents the simplest means to transform **1.2** and is frequently applied for the generation of porphyrin derivatives with specific functionalities and for the attachment of porphyrins to molecules and materials. Reactions at the carbonyl group such as esterifications and amidations are usually straightforward and can be used for the synthesis of a wide range of porphyrin derivatives. Hence, peptide coupling reactions with PPIX are well established in the literature.[56,65e,73b,75] This type of functionalisation has remained the main route for the synthesis of PPIX derivatives, be it for the generation of therapeutics,[49e,74,75,80,92] imaging,[92d,93] sensing,[94] materials chemistry,[95] photooxidation catalysis,[96] use in electrochemistry,[97] as biomimetics,[98] as modulated biomolecules[99] and for supramolecular assemblies.[89,100]

Various strategies were applied to effect amide bond formation on **1.2** or hemin (**1.4**) (Scheme 1.10). Activation of the carboxylic acid by reaction with carbodiimides such as 1-ethyl-3-(3-dimethylaminopropyl)carbodiimide (EDC)[49e,92b,c,f,j,t-v,101] or *N*,*N*'-dicyclohexylcarbodiimide (DCC),[92d,l,93,100a] respectively, and subsequent formation of the *N*-hydroxysuccinimide (NHS) esters, followed by reaction with the amine coupling substrates reliably, yields PPIX mono- and bisamide products **1.46** and **1.47**.

Alternatively, DCC[75a,92d,r,94] and EDC[89,100b,100d] were used in combination with 1-hydroxybenzotriazole (HOBt) to form active carboxylate esters which easily reacted with amines. In other cases, amide bond formation on PPIX and hemin was effected by use of the potent peptide coupling agents hexafluorophosphate azabenzotriazole tetramethyl uronium (HATU)[92k,n] and hexafluorophosphate benzotriazole tetramethyl uronium (HBTU),[92i,p,96b,98,102] respectively, in combination with a tertiary amine base. Dorota Gryko and co-workers screened different conditions for the coupling of amino acids to PPIX. The best yields were obtained using a combination of HBTU, HOBt and *N*,*N*-diisopropylethylamine (DIPEA). [102]

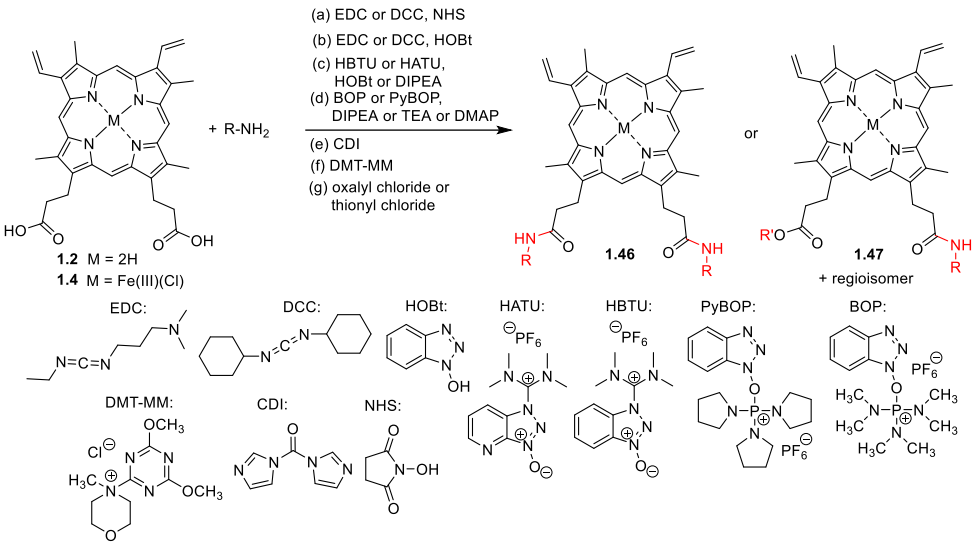

Scheme 1.10. Different strategies for amide bond formation at the PPIX carboxylic acid moieties.

More examples of PPIX functionalisation can be found in comprehensive reviews on this topic.[56,103]

1.2.3 Protoporphyrin IX in Chemical Biology Applications

PPIX's inherent tendency to interact with certain biomolecules has been exploited to create biochemical tools. A selection of examples in two fields of chemical biology that PPIX has found entry in will be introduced hereafter. More examples can be found elsewhere.[103]

1.2.3.1 Protoporphyrin IX-DNA-Complex Sensing Devices

Guanine-rich nucleic acid-segments form particular secondary structures *in vivo* which function as regulators of genome and telomere stability as well as gene activity.[51a,104] In such sequences the formation of guanine-quartets (G-quartets) *via* Hoogsteen base pairing can lead to the arrangement of the respective DNA or RNA sequences in four-stranded helices, the so-called G-quadruplexes (Figure 1.4).[105] Together with other molecules, these motifs have drawn attention as biochemical tools for *in vitro* applications such as DNAzymes to catalyse redox reactions in a peroxidase-like fashion, as well as for the detection of enzymatic activity, nucleic acids, proteins, small molecules and metal ions.[105,106]

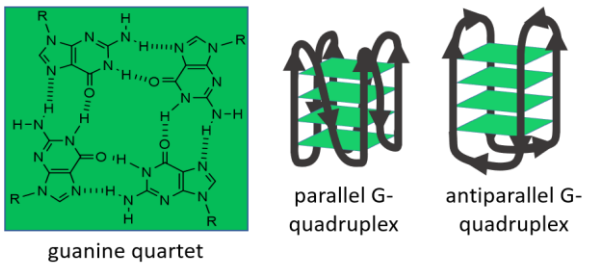

Figure 1.4. Hydrogen bonding in a guanine quartet and schematic representation of parallel and antiparallel G-quadruplex conformations.

The conformation of the G-quadruplex is strongly dependent on the presence of certain metal ions interacting with the carbonyl oxygen atoms of the guanine bases inside the quartet. Moreover, the G-quartet constitutes a plane of aromatic moieties that can interact with aromatic molecules *via* π-π-interactions. Such interactions can be used to detect G-quadruplex formation or to form functional entities such as DNAzymes. Among the compounds with G-quadruplex binding abilities are tetrapyrroles such as phthalocyanines and porphyrins.[51a,107] Notably, hemin binding for generation of DNAzymes with peroxidase-like activity and for development of molecular sensing devices has found widespread attention and has been discussed in several reviews.[105,106,107a,108] PPIX and its Zn(II) complex in combination with G-quadruplex structures are used as biosensors.

The hydrophobic character of PPIX facilitates formation of micellar aggregates in aqueous solution which quenches the molecules' fluorescence.[109] Disruption of the aggregates by binding to the G-quadruplex enhances the fluorescence of PPIX by a factor of 16. PPIX is reported to selectively bind to parallel G-quadruplex conformers.[51a,110] (Protoporphyrinato IX)zinc(II) (Zn(II)PPIX) (**1.48**) also shows a significant increase in fluorescence upon G-quadruplex binding.[111] Hence, both molecules can be used as fluorogenic reporters for G-quadruplex formation which finds application for various sensing purposes. Another

Detection of Nucleic Acids

G-quadruplexes in combination with PPIX or Zn(II)PPIX have commonly been used for nucleic acid detection *in vitro*; e.g., for miRNA and DNA. Generally, the detection process involves an initial binding event of the target nucleic acid with another DNA strand. This triggers a cascade which usually includes a signal amplification process and the recruitment of a G-quadruplex forming DNA sequence. Once G-quadruplexes form they bind to the porphyrin probes which results in an enhanced fluorescence signal.[51b,c,112] A similar strategy was also used for measurements of the length of DNA segments.[113] Figure 1.5 shows an example of nucleic acid detection by Zn(II)PPIX-G-quadruplex assemblies.[51c]

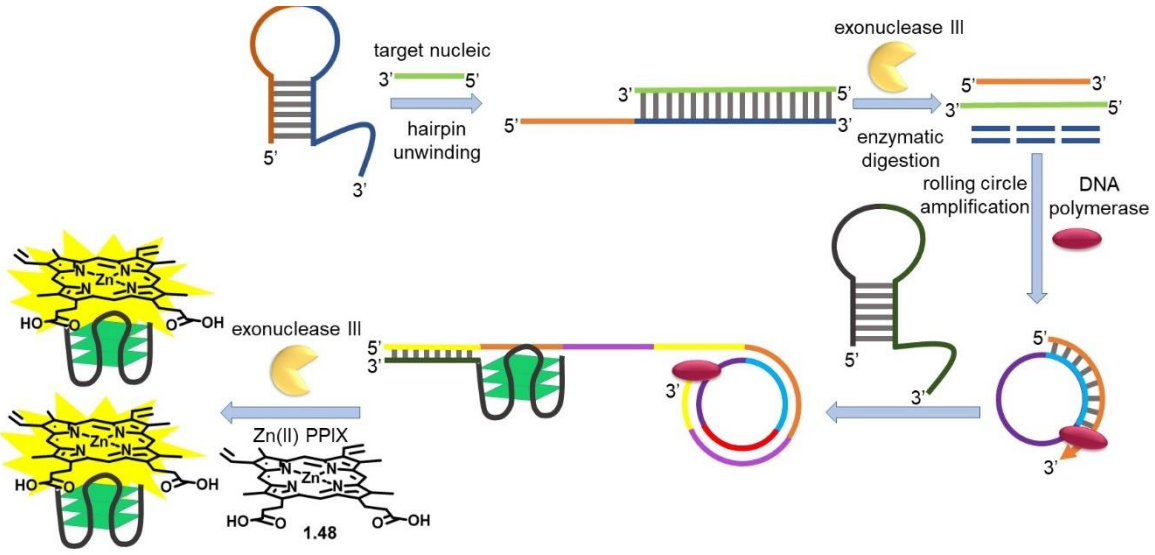

Figure 1.5. Exemplary nucleic acid detection with Zn(II)PPIX G-quadruplex biosensors. Binding of the target nucleic acid unwinds the DNA hairpin. Subsequent digestion by exonuclease III liberates a DNA single strand that acts as a primer for rolling circle amplification. Binding of a G-rich hairpin to the amplified DNA sequence causes refolding of the hairpin to a G-quadruplex structure. Liberation of G-quadruplexes by exonucleases and binding of Zn(II)PPIX (**1.48**) results in a fluorescence signal.

Detection of Enzymatic Activity

G-quadruplexes can be used to detect the activity of enzymes, e.g., for monitoring telomerase activity.[114] Maintenance of telomeres, the terminals of chromosomes in human cells, by telomerase is usually inhibited in normal cells, while telomerase is active in the majority of tumor cells.[115] Therefore, telomerase activity serve as a marker for the development of malignancies. Telomeres contain TTAGGG repeat sequences; thus, they form G-quadruplex structures themselves. Colourimetric assays with hemin exploiting the peroxidase-like activity of telomeric G-quadruplexes have been used to detect telomerase activity.[114] A now classic system by Willner and co-workers quantified the activity of telomerase in cancer cell lysates based on the fluorescence of Zn(II)PPIX. A telomerase primer served as a substrate to be telomerised by the enzyme from the cell extracts and G-quadruplex formation in the so-obtained telomere repeats was detected by (protoporphyrinato IX)zinc(II) binding and its fluorescence response.[112c]

The activities of other DNA-editing and -degrading enzymes have been monitored by using a combination of G-quadruplexes and PPIX or Zn(II)PPIX.[116] Detection of DNA methylation

patterns, an epigenetic modification accomplished by DNA methyltransferases, is also a means of early cancer recognition.[117] Methylation of adenines in the sequence of a DNA hairpin probe led to recognition of the methylated sites by endonuclease Dpn1 and liberation of single stranded DNA. After undergoing an amplification cascade, G-quadruplexes were recruited that bound Zn(II)PPIX.[116a,b] Other enzymatic activities detected by G-quadruplex/PPIX systems include uracil glycosylase and endonuclease S1 activities.[116c,d]

Detection of Metal Ions

The inherent property of G-quadruplexes to take on different conformations of different stabilities upon binding to various metal ions has been used for fluorescent detection of metals, including K^+, Na^+, Pb^{2+} and Hg^{2+} with PPIX as a signal reporter.[105a,118,110,112,111,119] A yet different strategy was applied for the detection of Cu^{2+} ions using a PPIX/G-quadruplex system. G-quadruplex-based DNAzymes can catalyse the insertion of Cu(II) and Zn(II) into mesoporphyrin IX[120] This finding was implemented by Wang and co-workers who developed a Cu^{2+} sensor based on G-quadruplex-catalysed metalation of PPIX. Upon Cu(II) insertion the fluorescence of the PPIX/G-quadruplex was quenched.[121]

Detection of Small Molecules and Proteins

G-quadruplex-based sensing devices have also been used for the detection of small molecules,[112c,112e,122] proteins[123] and cells.[124] The nucleotide ATP could be detected using an aptamer-forming DNA sequence that only assembled to a G-quadruplex structure upon ATP binding. Zn(II)PPIX binding gave fluorescent indication of the DNA structural change.[112c]

A similar method was used for detection of the mycotoxin ochratoxin A. G-quadruplex formation upon binding of ochratoxin A to the DNA aptamer and recruitment of Zn(II)PPIX effected the fluorescent signal readout.[122a] A protein-binding DNA aptamer in combination with a G-quadruplex and Zn(II)PPIX was also used for thrombin detection.[123]

Porphyrins themselves can also be detected with such systems. Competitive binding of PPIX and hemin to a G-quadruplex structure was used for hemin detection. Hemin replaced PPIX bound to G-quadruplex, thereby quenching the fluorescence of the system.[122c]

Lastly, G-quadruplex systems were used for the cellular delivery of PPIX as a photosensitiser and fluorescent probe.[124] By binding to the G-quadruplex the low solubility of PPIX in aqueous medium can be overcome. More importantly, the G-quadruplex aptamers can be designed to bind to specific cellular proteins, which can mediate cell and cell organelle targeting. This way, PPIX/G-quadruplexes can act as cancer therapeutics in

PDT and cancer cell imaging tools. Wang and co-workers reported that nucleolin, a protein that is overexpressed in cancer cells, can act as a PPIX/G-quadruplex target and can impart binding of this system on the cell surface[124a] as well its internalisation.[124b]

1.2.3.2 Reconstitution of Hemoproteins with Non-Natural Cofactors

The reconstitution of hemoproteins with non-natural metallo-porphyrin cofactors is a potent tool to tweak enzymes to perform specific chemical reactions *in vitro*. While the metal complexes are the catalytically active part, the protein provides the scaffold for substrate binding, macrocycle conformational control, and orientation relative to the metal cofactor; thus, it impacts the activity and selectivity of the reaction. Modulation of chemical transformations by metallo-enzymes therefore can be achieved by alteration of the metal centre, its ligand and the protein environment.[125]

In exemplary work Marletta and co-workers explored different ways of modulating hemoproteins from the heme nitric oxide/oxygen binding domain (H-NOX) family to produce proteins with altered functions. Engineering of the heme binding pocket of the protein by mutagenesis as well as replacement of the native heme cofactor with Ru(II) mesoporphyrin IX were employed to modulate the NO and O_2 binding abilities of H-NOX rendering it a potential sensor for these gases.[126] Stable complexes of H-NOX proteins with the paramagnetic heme analogues Mn(II)/(III)PPIX and Gd(III)PPIX were assessed as magnetic resonance imaging (MRI) contrast agents that do not suffer from leaching of toxic metal into the tissue.[127] A different tool used by Nierth and Marletta for the modification of H-NOX hemoproteins was synthetic modification of the porphyrin scaffold. An alkynyl moiety was introduced in one of the meso-positions of heme. After reconstitution of H-NOX with the modified heme cofactor, this left a synthetic handle for attachment of fluorophores or groups that alter the redox potential of the cofactor.[128] These key advancements illustrate the potential of cofactor reconstitution in hemoproteins as a tool to produce biomolecules with altered or enhanced functionalities.

Oxidation/Reduction Catalysts

Nature employs heme-dependent enzymes such as catalase, cytochrome P450 enzymes, nitric oxide synthase and peroxidases to catalyse redox reactions.[1b] Replacing iron by other metals can help to elucidate the mechanism of action of heme enzymes and can also yield oxidizing/reducing enzymes with altered catalytic activity and substrate scope. One promising candidate for hemoprotein reconstitution is (protoporphyrinato)manganese(III) (Mn(III)PPIX). It has been used to replace heme in different proteins and these constructs have been evaluated for their peroxidase-like activity. H_2O_2 cleavage by Mn(III) enzymes to

give O_2 and H_2O passes through H_2O_2 binding to the metal centre and oxidation to high valent Mn-oxo complexes Mn(IV)=O or Mn(V)=O, a process equivalent to native heme-based peroxidases. However, Mn(III)PPIX reconstituted proteins were shown to be less efficient in cleaving peroxides compared to their native iron-containing counterparts.[129]

More engineered metalloproteins were tested for their ability to catalyse redox reactions thereafter. Zhang and co-workers successfully modulated the peroxidase-like activity of Mn(III)PPIX reconstituted myoglobin by altering the protein scaffold. Amino acid residue replacements showed that His64 in the wild-type protein was crucial for enzymatic activity. This was imparted by hydrogen bond formation between His64 and H_2O_2, thereby facilitating H_2O_2 binding to the Mn(III) centre. Additional introduction of the residue His43 led to a 5-fold increase in H_2O_2 activation by the enzyme, probably by formation of an additional hydrogen bond between His43 and H_2O_2 and facilitated O-O bond cleavage (Scheme 1.11).[130]

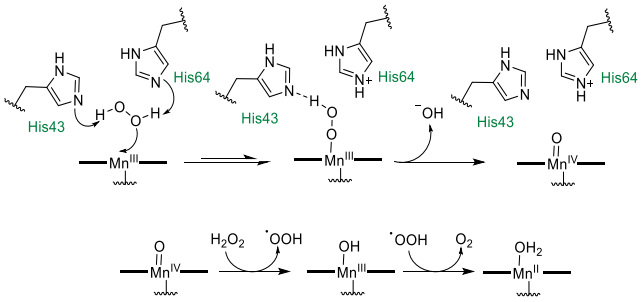

Scheme 1.11. Proposed mechanism for H_2O_2 splitting in a Mn(III)PPIX reconstituted F43H myoglobin mutant, assisted by amino acid residues His43 and His64.

Mn(III)PPIX reconstituted proteins were used to catalyse the oxidation of organic compounds.[131] A Mn(IV)-oxo complex was produced from Mn(III)PPIX myoglobin by addition of the oxidant *meta*-chloroperoxybenzoic acid (*m*CPBA). This oxidative Mn(IV) intermediate was capable of catalysing C-H bond cleavage in 1,4-cyclohexadiene yielding benzene, a reaction that could not be catalysed by native myoglobin.[131a] An engineered Mn(III)PPIX myoglobin in which the amino acid residues Leu29 and Phe43 had been replaced with His was successfully used for the epoxidation of the styrene double bond using oxone as an oxidant in place of H_2O_2.[131b]

Mn(III)PPIX (counterion was not specified) in combination with genetically engineered human serum albumin (HSA) was also employed as an artificial superoxide dismutase. Wild-type HSA Mn(III)PPIX showed only little activity in dismutating the reactive superoxide radical anion $O_2^{\bullet-}$, whereas, when the proximal amino acid residue Tyr161 was replaced by

Leu *via* site-directed mutagenesis, the catalytic activity increased by a factor of 5.5. Presumably, this was due to removal of Tyr161 as an axial ligand for Mn(III)PPIX and exchange with a non-coordinating residue. This led to formation of a superoxide dismutase where the metalloporphyrin plane and catalytic cavity are not blocked by a coordinating amino acid residue.[53c]

Upon mutation of Tyr161 in HSA to a His residue instead and incorporation of Mn(III)PPIX (**1.49**) into the binding pocket, the protein showed catalase activity. This ability of Mn(III)PPIX-HSA to catalyse the degradation of H_2O_2 was exploited by covalently conjugating it to hemoglobin (Figure 1.6). In this cluster, the engineered HSA acted as a protective wrap for hemoglobin, which is prone to oxidation by self-produced and surrounding H_2O_2. Thereby, hemoglobin was protected from oxidation by H_2O_2 which renders the protein-hybrid promising for use as a hemoglobin-based O_2 carrier (HBOC), e.g., for therapeutics.[132]

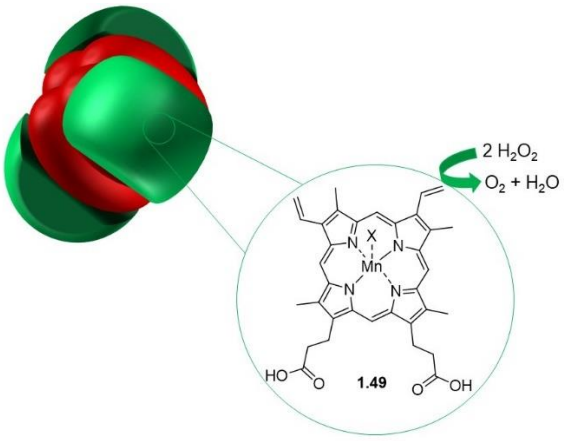

Figure 1.6. Schematic representation of a protein cluster consisting of three Mn(III)PPIX (counterion not specified) (**1.49**) reconstituted HSA units (green) wrapped covalently around hemoglobin (red). The HSA units feature catalase activity.

Carbene Insertion Catalysts

Engineered and natural hemoproteins are highly promising catalysts for abiological reactions, especially C-H bond activation reactions. Among those are N-H, and S-H insertions, as well as cyclopropanations and aziridinations.[53a,b] However, use of heme as a co-factor in abiological catalysis restricts the applicability to a limited set of reactions. Considering the importance of transition metal catalysis in modern synthetic chemistry, the replacement of heme-iron by different transition metals could lead to a drastic expansion of the scope of accessible ‘heme’-enzyme-catalysed reactions. Hence, reconstitution of heme

enzymes with metallo-PPIX complexes to catalyse chemical transformations of C-H bonds in small molecules have been attempted.[133]

A (chloro)(protoporphyrinato)manganese(III) [Mn(III)PPIX(Cl)] myoglobin complex was tested for its catalytic activity towards the hydroxylation of ethylbenzene to 1-phenylethanol, but was found to be inactive. Only the Mn(III)porphycene(Cl) analogue showed efficacy in catalysing the reaction.[133a] Mn(II) and Co(II)PPIX myoglobin complexes were shown to catalyse intramolecular C-H amination reactions of arylsulfonyl azides. Engineering the protein active site by point mutations resulted in enhanced stereo- and enantioselectivity in ring closure reactions of the substrate. The substrate total turnover numbers of both, Mn(II)- and Co(II)porphyrin reconstituted myoglobins were found to be lower (142 and 64, respectively) compared to wild-type myoglobin (181).[133b]

Hartwig and co-workers systematically screened a library of myoglobins reconstituted with different metallo-PPIX and metallo-mesoporphyrin IX cofactors for their catalytic activity in C-C bond forming reactions which were not catalysed by wild-type myoglobin. Two model reactions were chosen to test the different metalloproteins: an intramolecular carbene insertion into a C-H bond and cycloadditions of carbenes to alkenes (cyclopropanation). The best turnover numbers for both reactions (>60) were obtained using an axially methyl-ligated iridium complex (methyl)(mesoporphyrinato IX)iridium(III) [Ir(III)MPIX(Me)] (**1.50**) as cofactor (Figure 1.7). A stepwise evolution of the protein scaffold was carried out in order to optimise the stereoselectivities of both reactions. Exchanging different amino acids in the inner and outer coordination sphere of the enzyme resulted in good to high enantiomeric and diastereomeric ratios (*er* and *dr)* for formation of the asymmetric products; yet, the substrate turnover numbers were low.[134]

In order to improve substrate conversion rates a cytochrome P450 hemoprotein (CYP119) from a thermophilic archaeon was employed as a protein scaffold instead of myoglobin. The thermostable CYP119 enzyme is involved in stereoselective biosynthetic transformations of C-H bonds in its wild-type form. Reconstitution of CYP119 with Ir(III)MPIX(Me) (**1.50**) and directed evolution of the apoprotein to enhance the substrate affinity yielded an enzyme with vastly increased efficiency in C-H carbene insertion reactions; more than 4000 times higher than that of the wild-type heme enzyme. The artificial enzyme catalysed reactions with turnover numbers up to 35 000 and up to 94% *ee*.[135] The Ir(III)MPIX(Me)–CYP119 system was also adapted for the catalysis of stereoselective cyclopropanation reactions for a variety of olefinic substrates (Figure 1.7).[136]

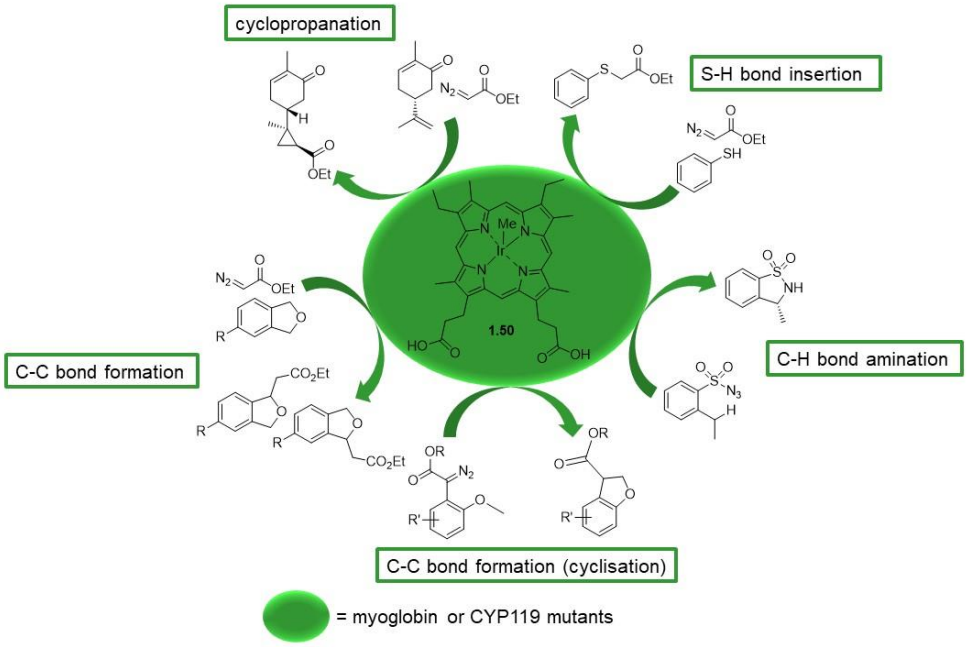

Figure 1.7. C-C bond formation, cyclopropanation S-H bond insertion and C-H bond amination reactions catalysed by (methyl)(mesoporphyrinato IX)iridium(III) [Ir(III)MPIX(Me)] (**1.50**) reconstituted myoglobin or CYP119 mutants, respectively.

The same group expanded the scope of reactions to be catalysed by similar engineered protein systems with good efficiencies to intramolecular C-H bond amination of sulfonyl azides and carbene insertions into C-H bonds of 4-substituted phthalans (Figure 1.7).[137]

Fasan and co-workers used such an approach with different metallo-PPIX and -MPIX complexes for carbene insertion reactions into N-H, S-H and C-H bonds, as well as cyclopropanations. For N-H insertion, myoglobin variants containing heme as a cofactor showed the highest turnover numbers and product yields. The same was found for cyclopropanation reactions. S-H and C-H insertions were most efficiently catalysed by engineered Ir(III)MPIX(Me)-myoglobin (Figure 1.7).[138]

Construction of Photosensitive Proteins

Embedding metallo-PPIX photosensitisers in a protein matrix prevents aggregation-induced quenching of their excited states and additionally allows for tuning of the sensitisers' properties and their orientation towards electron-accepting substrates, e.g., by modulating the coordination sphere of the protein.

Photosensitive proteins are often used in assemblies as models for native light-harvesting complexes. In the present context, a hexameric heme protein isolated from a marine bacterium was reconstituted with the photosensitisers Zn(II)PPIX and Zn(II)chlorin e_6 [(15-

carboxymethyl-3^1,3^2-didehydro-rhodochlorinato)zinc(II)]. Each of the six subunits bound one tetrapyrrole metal complex, leading to the arrangement of the photosensitisers in a spatially and conformationally defined manner (Figure 1.8). After irradiation, the energy migration between the subunits of the complex was studied. The researchers found indication that singlet-singlet annihilation takes place in the oligomeric hemoprotein.[58b]

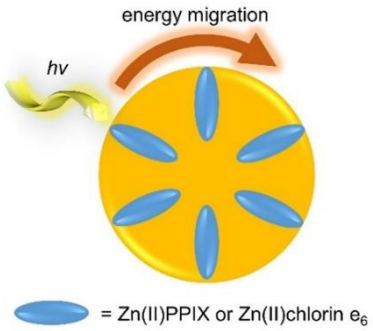

Figure 1.8. Hexameric heme protein reconstituted with Zn(II)PPIX and Zn(II)chlorin e_6 for studies of energy migration in the complex.

Komadsu, Tsuchida and co-workers were the first ones to use a Zn(II)PPIX-based protein complex for photosensitised water reduction. For this Zn(II)PPIX (**1.48**) was incorporated into HSA and the construct was combined with the electron mediator 1,1'-dimethyl-4,4'-bipyridinium ($DMBP^{2+}$) (**1.52**), colloidal Pt-polyvinylalcohol (PVA) particles as an electron transfer catalyst, and triethanolamine (**1.54**) as a sacrificial electron donor for restoration of the photosensitiser (Figure 1.9). Photoinduced Electron Transfer (PET) was found to take place only *via* the triplet state pathway of the photosensitiser to form radical cation **1.51**. The system showed good efficiency for photosensitised reduction of water to hydrogen when compared to the (5,10,15,20-tetrakis(*N*-methylpyridinium-4-yl)porphyrinato)zinc(II)–HSA complex.[139]

Hayashi *et al.* also investigated in the use of light-sensitive proteins for catalytic processes. They reconstituted apomyoglobin with Zn(II)PPIX that was modified at the carboxylic acid moieties to carry charged groups which can attract ionic electron acceptors *via* electrostatic interactions. The PET from the photosensitiser to the acceptor was studied.[75f,140] Later they used these findings to develop a system for photocatalytic reduction of H_2O to H_2 based on Zn(II)PPIX reconstituted myoglobin.[141]

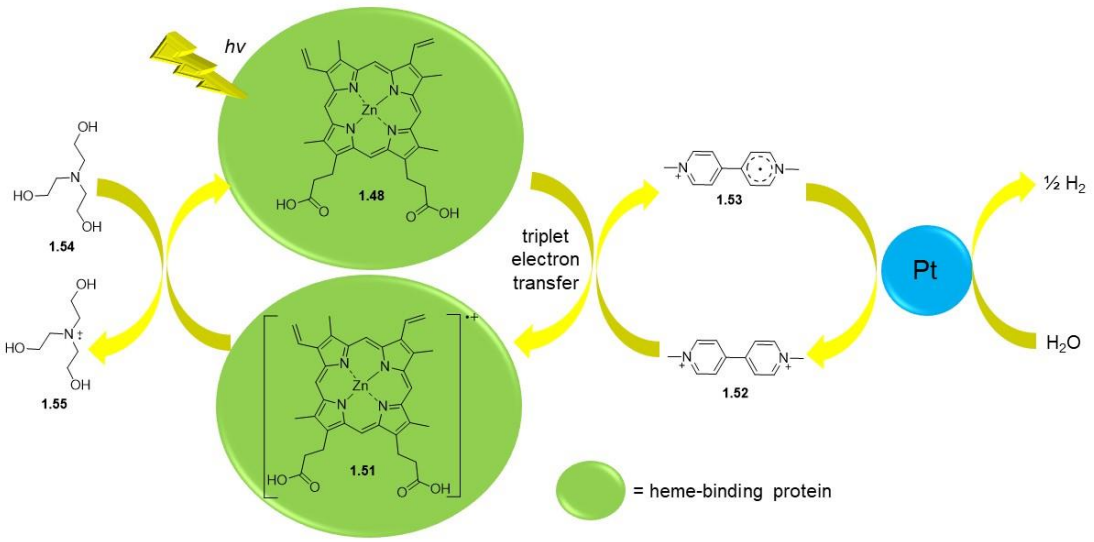

Figure 1.9. Schematic representation of photosensitised water reduction with a Zn(II)PPIX (**1.48**) reconstituted heme-binding protein as the photosensitiser, 1,1'-dimethyl-4,4'-bipyridinium ($DMBP^{2+}$, **1.52**) as the electron mediator, colloidal Pt as the reduction catalyst and triethanolamine (**1.54**) as the sacrificial electron donor.

A similar approach was later used for the generation of a photocurrent induced by gold surface-immobilised photosensitiser-protein assemblies. Several layers of cytochrome b_{562} reconstituted with Zn(II)PPIX derivatives were attached to the gold surface *via* immobilisation of the porphyrin on the surface and irradiation with monochromatic light generated a photocurrent which was significantly enhanced compared to a surface with a single layer of photoactive hemoproteins.[97b] Assembly of the metalloprotein rods with opposite orientation in regards to the gold electrode *via* immobilisation of the apoprotein on the surface also resulted in photocurrent generation.[142]

Co(II)PPIX reconstituted myoglobin (oxidation state of the catalytically active species not specified) was also used for photoinduced hydrogen production in water. The protein assembly showed a 3-fold higher turnover number compared to free Co(II)PPIX. The catalytic activity could be increased by altering the secondary coordination sphere of the protein using point mutations. E.g., the H64A and H97/64A mutants showed higher activity than the wild-type myoglobin porphyrin complex.[143]

1.3 Bicyclo[1.1.1]pentane as a Rigid Linker Motif for Multichromophore Arrays

As shown in section 1.2, a chromophores' spatial arrangement, separation, relative orientation and immediate environment influence observed reactivity, photophysical and electron-transfer characteristics. Often, in organic chemistry, linking of two molecules of interest is performed with aryl rings or alkyl chains. For studying chromophores, the rigidity of an aryl ring with the electronic isolation of the alkyl group is required. These properties can be provided by saturated rigid linkers, such as bicyclo[1.1.1]pentane (**1.56**), bicyclo[2.2.2]octane (**1.57**), cubane (**1.58**), triptycene (**1.59**), and adamantane (**1.60**) (Figure 1.10).[144]

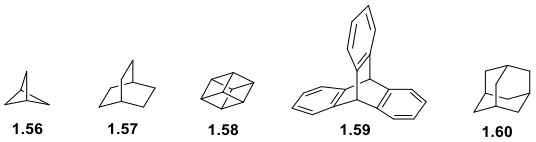

Figure 1.10. A selection of rigid hydrocarbon linkers: bicyclo[1.1.1]pentane (**1.56**), bicyclo[2.2.2]octane (**1.57**), cubane (**1.58**), triptycene (**1.59**), and adamantane (**1.60**).

For the design of rigid linker-bridged chromophore model systems, an understanding of chromophore arrays in nature is important. In the following, such an exemplary system will be described in more detail.

1.3.1 Multichromophore Arrays in Nature

Natural tetrapyrroles such as chlorophylls, bacteriochlorophylls and hemes, e.g., in cytochromes, play a crucial role in electron and energy transfer processes in nature. Oxygenic photosynthesis, employed by green plants and photosynthetic bacteria, is the fundamental mechanism for carbon fixation on earth and the main source of food and oxygen. Following light harvesting by antenna pigments it involves a range of energy and electron transfer processes between the pigments and other small molecules which ultimately result in the splitting of water to produce O_2 and the fixation of CO_2 into carbohydrates (Figure 1.11). In brief, photosynthesis in plants involves the action of two light-driven reaction centres in the photosystems I and II which consist of pigments attached to proteins and are located in the thylakoid membrane of the chloroplasts, and a dark reaction, the Calvin-Benson cycle, which takes place in the chloroplast stroma. In the light reaction, water is split into oxygen, protons and electrons, the protons and electrons are transferred through the membrane to produce adenosine triphosphate (ATP) and nicotinamide adenine dinucleotide phosphate (NADPH). These energy storage molecules

are then used in the dark reaction to construct carbohydrates from CO_2. The integral part of each of the two photosystems comprises a pair of chlorophylls, the so-called special pair, which is surrounded by protein complexes containing hundreds of carotenoid and chlorophyll antenna pigments. These act as light harvesting complexes by collecting energy from excitation by visible light and funnelling it to the special pair of chlorophylls in the reaction centre. The pigments of the light harvesting complexes display a variety of different absorption characteristics and energy levels, their involvement in light harvesting and energy transfer increases the spectral and spatial cross-section of the special pair. The energy passed onto the reaction centre causes excitation of the special pair followed by charge separation, i.e. the transfer of an electron to an acceptor molecule.[145]

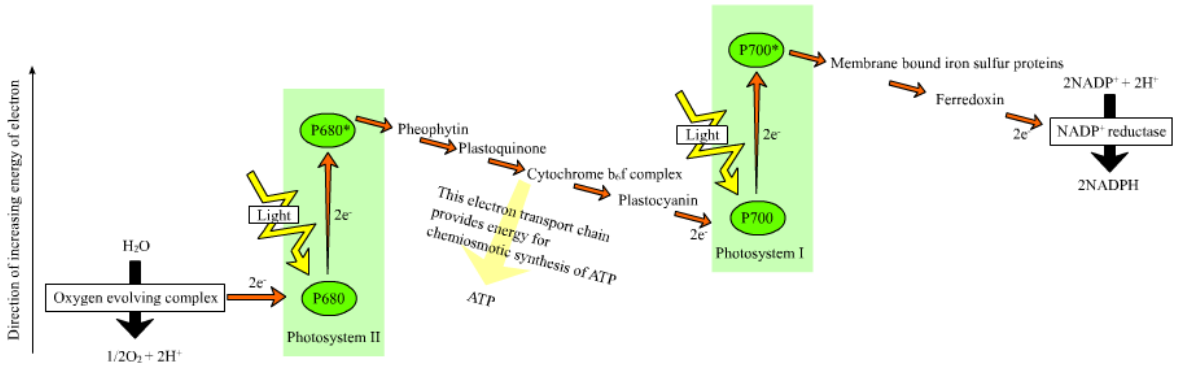

Figure 1.11. Schematic representation of energy and electron transport processes during oxygenic photosynthesis. From: https://en.wikipedia.org/wiki/Photosynthesis#/media/File:Z-scheme.png © 2005 Bensaccount, licensed under: https://creativecommons.org/licenses/by-sa/3.0/deed.en.

Understanding the mechanisms of electron and energy transfer in photosynthesis as well as other natural processes such as the oxidative phosphorylation in cellular respiration has been a key interest of scientists for many years. Various model systems have been designed in which tetrapyrroles have been attached to suitable energy donor or acceptor units *via* covalent bonding or non-covalent interactions. The use of such synthetic models as mimics of natural systems has proven useful to study the influence of parameters such as donor-acceptor distance, orientation and solvent on the interactions between donor and acceptor moieties.[146] It is considered that, for example, in bacterial reaction centres, this electron transfer between donor and acceptor molecules can be mediated through the medium such as amino acid residues of the protein environment. The medium participating in the electron transfer is called a “bridge”. The molecular orbitals of the bridge can participate in the electron transfer and facilitate it without formation of an intermediate kinetic state; a so-called superexchange mechanism. Thereby, the nature of the bridge between donor and acceptor is important – the bridge orbitals need to exhibit a favourable orientation relative to the donor and acceptor orbitals and also need to be energetically close to the

interacting donor orbital.[145a] In biological systems, the participants in electron transfer are fixed in a defined position inside the membrane and generally do not come into close contact with each other. In this sense, such electron transfer between membrane-bound molecules can be compared to long-range electron transfer of covalently connected donor-acceptor systems, that is, the electron transfer rate depends not only on intrinsic and thermodynamic factors but also on the donor-acceptor distance and their mutual orientation.[147] The variation of electron transfer rates with distance is described by the exponential decay constant β and it is dependent on the bridging unit which connects the two moieties. Saturated hydrocarbon linkages can function as mediators for electronic coupling through σ-π-interaction, the transfer rate for this kind of bridge typically decays with ≈ 1.0 $Å^{-1}$.[148] For conjugated alkenes and phenylenevinylene bridges the distance dependence of the electron transfer can become very weak with decay constants as low as 0.04 $Å^{-1}$.[148a, 149] For aromatic rings the constant is usually lower than for alkyl bridges (0.4–0.8 $Å^{-1}$) but strongly depends on the dihedral angle between the rings.[148a]

Considering these aspects, a good model system for studying electron and energy transfer processes should have a defined geometry with a fixed distance and relative orientation between the donor and acceptor moieties. This can be achieved by the introduction of steric hindrance to give structural rigidity.[150] In addition, the donor and acceptor units should be only weakly coupled electronically so that the properties of the single units are retained. However, for the study of electron transfer processes some electronic interaction between the moieties should be present. Rigid hydrocarbon linkers such as bicyclo[1.1.1]pentane, cubane, bicyclo[2.2.2]octane and triptycene are bridging units whose substituents are arranged in a defined spatial manner and distance. They are non-conjugating, hence they significantly decrease electronic coupling between the substituents and they restrict rotation around the central unit. The potential of such molecules as linkers in the investigation of electron transfer processes has been discussed.[144] Especially interesting is the bicyclo[1.1.1]pentane unit because it shows notable electron transfer through its hydrocarbon scaffold, making it a possible mediator for electron transfer.[144a] Hence, in the following, specific properties of the BCP unit as well as its synthetic transformations and applications will be discussed.

1.3.2 Physicochemical Properties of [1.1.1]Propellane and Bicyclo[1.1.1]pentane

Bicyclo[1.1.1]pentane (BCP) (**1.56**) is the smallest member of the family of bicyclic bridged hydrocarbons. It was first synthesised by Wiberg in 1964[151] and its properties were studied soon after.[152] The synthesis was accomplished by an anti-Markovnikov addition of HBr to

the methylenecyclobutane precursor **1.61**, followed by basic hydrolysis of the carboxylic acid ester and brominative decarboxylation using mercuric oxide and bromine (Scheme 1.12). Subsequent treatment with sodium in dioxane yielded BCP.

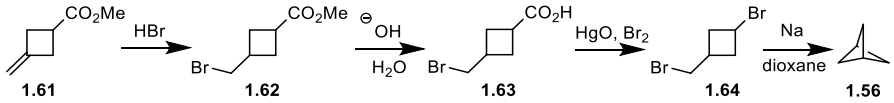

Scheme 1.12. First synthesis of bicyclo[1.1.1]pentane (**1.56**).[151]

This synthesis was followed by the preparation of tricyclic [1.1.1]propellane (**1.66**) by Wiberg *et al*. in 1982.[153] The name "propellane" had previously been suggested by Ginsburg for tricyclic hydrocarbon scaffolds.[154] The synthesis of [1.1.1]propellane was later optimised;[155] today it is usually prepared form the tetrahalide **1.65** by reaction with an organolithium reagent in diethyl ether according to the procedure developed by Szeimies and co-workers (Scheme 1.13).[155a,b] Uchiyama and co-workers developed a system for the on-demand preparation of the unstable propellane by encapsulating 1,3-diiodo-BCP in α-cyclodextrin where it is significantly stabilised and could be stored for 65 days with no decomposition detected. 1,3-Diiodo-BCP was released from the capsule using organic solvents and converted to propellane *via* UV irradiation or tributylphosphine- and hydrazine-mediated deiodination.[156] [1.1.1]Propellane is now commonly used as a precursor for the synthesis of BCP derivatives *via* strain-release reactions.

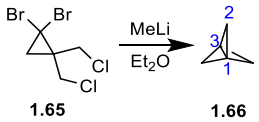

Scheme 1.13. Preparation of [1.1.1]propellane (**1.66**) according to Szeimies and co-workers.[155a,b] Specific numbering of the [1.1.1]propellane molecule is indicated in blue.

The character of the central bond between the so-called bridgehead carbons C1 and C3 (Scheme 1.13) in [1.1.1]propellane is a subject of debate. Theories revolve around it exhibiting characteristics of a covalent bond with high p-orbital contribution,[155b,157] a charge-shift bond[144a,158] and a diradical[144a,157b] but the true nature of the bond remains unclear so far.[144b] The strength of the central bond was calculated to be relatively low with 60 kcal/mol.[153,159] [1.1.1]Propellane shows an inverted tetrahedral geometry at the bridgehead carbons as well as remarkable orbital hybridisation of the bridgehead atoms. The central C1-C3 bond has a high p-character and is strongly represented in the HOMO of the molecule, resulting in a reactivity which in some cases is comparable to that of alkenes. At the same time, the C1-C2 bonds of the carbon cage show sp^2-character.[155b,157] [1.1.1]Propellane is a highly strained molecule with a ring strain of 98 kcal/mol[160] owing to

different contributing parameters, notably angle strain (Baeyer strain[161]), conformational strain (Pitzer strain[162]) and transannular strain (Prelog strain[163]).[144a] Breaking of the C1-C3 bond releases the strain by about one third yielding BCP with a strain energy of 68 kcal/mol.[160] The remaining high strain of the BCP scaffold can be explained by the geometry of the molecule and orbital hybridisation. The two bridgehead carbons in BCP interact at 1.845 Å[164] or 1.874 Å,[165] one of the shortest non-bonded C-C distances reported in the literature. The exocyclic C-H bonds on the bridgehead carbons exhibit a high s-character of 34%, indicating sp^2-hybridisation rather than sp^3.[144a,166] The back lobes of the exocyclic bridgehead orbitals partially overlap and cause repulsion between C1 and C3. This phenomenon contributes to the high ring strain and a destabilisation of the BCP ground state.[159b,167] Despite its strain BCP shows good kinetic stability.[168] The C1-C3 non-bonded separation can be modulated by the introduction of different substituents at the bridgehead carbons. Electron-withdrawing moieties reduce the electron occupancy in the exocyclic orbitals and therefore weaken the repulsion and shorten the distance between the bridgehead carbons.[167] The shortest inter-bridgehead distance of 1.80 Å was measured when BCP was bound to a pyridinium salt,[169] while longer C1-C3 distances were observed for aryl and alkyl substituents such as [n]staffanes.[170] Substituents can also induce steric influence on the BCP scaffold.[144a] BCP itself exerts an electron-withdrawing effect on the moieties it is bound to which, again, can be explained by the high s-character of the bonding hybrid orbitals.[157a,171] Thus, BCP-1-carboxylic acid as well as BCP-2-carboxylic acid are significantly more acidic than other aliphatic carboxylic acids with notably less s-character of the bonding orbitals.[172] Interaction between the bridgehead carbon atoms as well as σ conjugation through the BCP skeleton makes BCP a good mediator for electron transfer.[144a] BCP is therefore the shortest possible rigid linker between two molecular units, such as chromophoric moieties, that does not engage in π-conjugation between these systems.[173] Hence, it isolates the π-clouds of two linked systems, while potentially still allowing for some electronic communication through the BCP scaffold. A rigid linker system such as BCP also enables the arrangement of molecular moieties with a defined orientation towards each other, i.e. with an angle of 180°.[144a]

1.3.3 Bridgehead Modifications of Bicyclo[1.1.1]pentane

The unique electronic and structural properties of the BCP skeleton have spurred immense interest in BCP as a versatile synthetic tecton and the variety of methods employed for its functionalisation has increased drastically in recent years. In most of the cases, [1.1.1]propellane is used as the precursor for functionalisation reactions and substituents are added to the bridgehead carbons by taking advantage of the reactivity of the central

bond. The relief of strain in the molecule by cleavage of the central bond is often described to be the main driving force for reactions on [1.1.1]propellane making the molecule reactive towards addition of radicals as well as nucleophiles and electrophiles (Scheme 1.14). However, it was suggested that strain release cannot be the sole factor determining the omniphilic reactivity of [1.1.1]propellane.[174] In a recent study, Sterling *et al*. propose that [1.1.1]propellane's reactivity is more driven by the change in electron delocalisation over the hydrocarbon cage.[175] [1.1.1]Propellane is more reactive than alkenes, whose reactivity it has been compared to, since non-activated alkenes usually do not react with nucleophiles.[157b,144a] Radical attacks at [1.1.1]propellane proceed rapidly, they are about 2-3 times faster than on styrene.[157b] The bicyclopentyl radical (**1.67g**) which forms upon attack is kinetically relatively stable; there is an energy barrier to opening of the bicyclopentane ring of 26 kcal/mol.[176] For this reason, the bicyclopentyl radical can be trapped by another radical to give bridgehead-substituted BCP (**1.67h**). Reaction of the bicyclopentyl radical with [1.1.1]propellane can lead to the formation of BCP oligomers, the [n]staffanes (**1.67j**).[177]

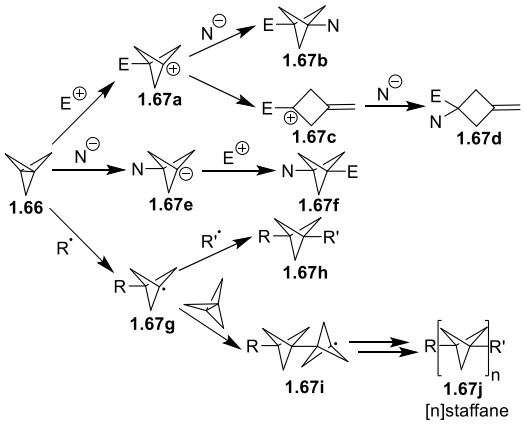

Scheme 1.14. Reactions on [1.1.1]propellane – attacks of electrophiles ($E^{\oplus}$), nucleophiles ($N^{\ominus}$) and radicals ($R^{\cdot}$).

Nucleophilic attack at [1.1.1]propellane yields an intermediate carbanion (**1.67e**) which is trapped by an electrophile. By contrast, the carbocation derived from addition of an electrophile to the central bond most commonly rearranges upon ring-opening to the corresponding methylenecyclobutyl cation (**1.67c**). Bicyclobutyl cations are only stable if they carry electronegative substituents.[157b]

A variety of free radical additions to [1.1.1]propellane were described by Wiberg *et al*., including reactions with iodine, thiols and disulfides, halomethanes, aldehydes and *tert*-butyl hypochlorite.[178] Kaszynski and Michl reported the photoinduced addition of butanedione to [1.1.1]propellane to obtain diacetyl-BCP (**1.68**) (Scheme 1.15). This

compound was further converted to the BCP dicarboxylic acid (**1.69**) which can be transformed to the acid chloride (**1.70**) and the ester (**1.71**).[179] More recently, the insertion of [1.1.1]propellane into 1,2-dicarbonyls and subsequent functionalisation reactions inside a continuous flow photochemical reactor was reported.[180] The so obtained carbonyl compounds are versatile precursors for the synthesis of functionalised BCP such as by amide coupling reactions[181] and for the synthesis of biologically relevant BCPs.[182] A BCP-1-carboxylic acid derivative was included in Baran's work on Fe-catalysed redox-active ester couplings. The decarboxylative coupling with Ph_2Zn afforded phenylated BCP in 35% yield.[183]

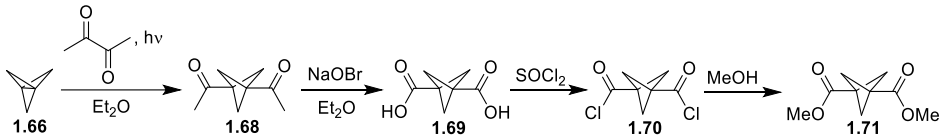

Scheme 1.15. Preparation of different carbonyl-substituted BCPs according to Kaszynski and Michl.[179]

The addition of thiophenol to propellanes is assumed to proceed *via* a radical mechanism as well and this reaction has been known for a long time.[178b,184] However, only recently the potential of thiol additions to [1.1.1]propellane as simple functionalisation reactions has been explored by the group of Bräse (Scheme 1.16).[185] The reaction was shown to take place for a vast number of substrates, including various thioalkanes as well as activated and deactivated thioarenes.[185a] Oxidation and amination or imination yielded pharmaceutically interesting sulfoxides (**1.78**), sulfones (**1.77**), sulfonamides (**1.76**) and sulfoximines (**1.72**, **1.73**).[185b,c] Sulfonamides and sulfonyl fluorides were also synthesised form BCP carboxylic acid derivatives in four steps.[186] UV-light-mediated insertion of [1.1.1]propellane in disulfide bonds led to the formation of 1,3-dithio-substituted BCPs (**1.79**).[187] Wu *et. al.* used thiolating and selenating agents RSO_2SCF_3 and RSO_2SeCF_3 in reaction with [1.1.1]propellane to produce BCP derivatives with sulfonyl- and trifluoromethylthio- (**1.80**) or –seleno-substituents (**1.81**).[188]

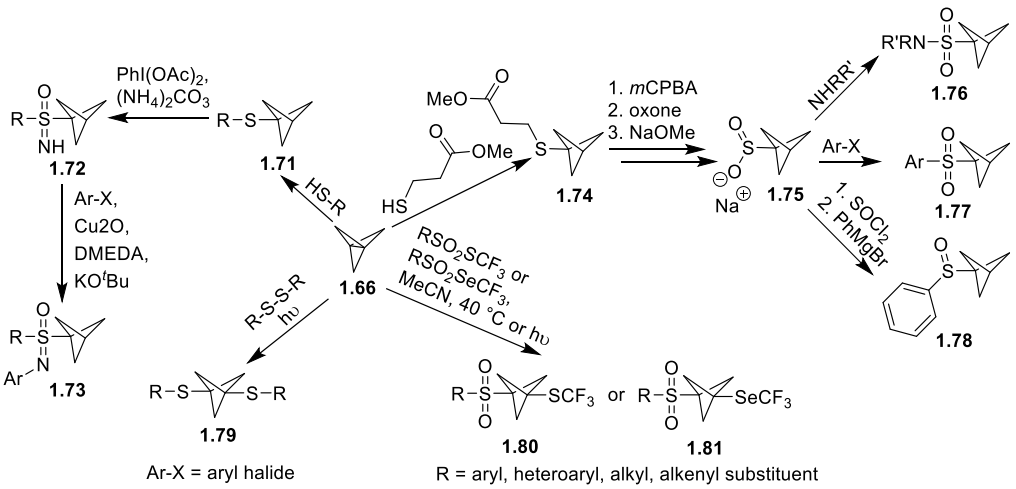

Scheme 1.16. Transformations of [1.1.1]propellane based on thiol and disulfide additions.

A considerable amount of research has been devoted to the introduction of amine moieties at the BCP bridgehead carbons. Amine-substituted BCP is a useful building block for easy functionalisation and especially for the conjugation to drugs. The bicyclo[1.1.1]pentane-1-amine hydrochloride (**1.83**) was traditionally prepared from bicyclo[1.1.1]pentane-1-carboxylic acid (**1.82**) *via* Schmidt reaction using NaN_3 and H_2SO_4 (Scheme 1.17).[189] Alternatively, Pätzel *et al*. transformed BCP carboxylic acid **1.84** to the Boc-protected amine **1.85** using diphenylphosphoryl azide (DPPA) in combination with *tert*-butanol,[182c] a procedure later adapted and modified by other groups.[190] Stannylation of BCP followed by lithiation and amination proved to be a viable route for bicyclo[1.1.1]pentane-1-amine (**1.88**) synthesis; however, in a low yield.[191] The generation of BCP amine was still limited by yields, scalability and use of toxic or dangerous reagents, which led to investigations of BCP amine synthesis directly from the propellane precursor.

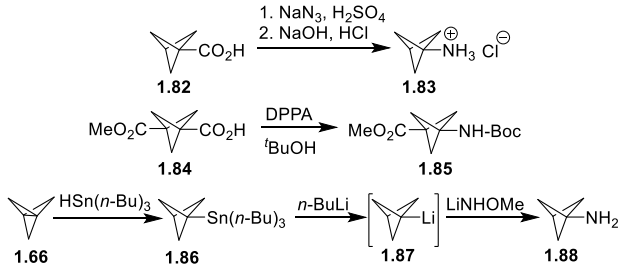

Scheme 1.17. Traditional routes towards the synthesis of BCP amines from different BCP precursors.

Bunker *et al*. employed a manganese-catalysed addition of di-*tert*-butyl-azodicarboxylate to [1.1.1]propellane *via* a free radical mechanism which yielded Boc-protected BCP hydrazine **1.89** (Scheme 1.18). Deprotection and subsequent hydrogenation using PtO_2/H_2 afforded the bicyclo[1.1.1]pentane-1-amine hydrochloride salt (**1.83**) in 79% overall yield in three

steps.[192] Later, Uchiyama and co-workers used a similar approach for the synthesis of 1,3-di-substituted bicyclo[1.1.1]pentane-1-hydrazines and bicyclo[1.1.1]pentane-1-amines. In a multicomponent reaction, [1.1.1]propellane, di-*tert*-butyl-azodicarboxylate and an aryl or alkyl hydrazine were combined with iron phthalocyanine (Fe(Pc)) as a catalyst and *tert*-butyl-hydroperoxide as an oxidant. So-obtained protected BCP hydrazines (**1.90)** could be reduced to amines (**1.91**).[193]

Another route towards amine-substituted BCP is the reduction of the respective BCP azide. Initial attempts to reduce 1-azido-3-iodobicyclo[1.1.1]pentane (**1.92**) with lithium aluminium hydride or $Pd(OH)_2/C/H_2$, respectively, were either not successful[188b] or resulted in low yields.[192] Adsool and co-workers succeeded in developing a procedure for the reduction of 1-azido-3-iodobicyclo[1.1.1]pentane to bicyclo[1.1.1]pentane-1-amine hydroiodide (**1.93**) on a large scale. In the same study, 1-azido-3-iodobicyclo[1.1.1]pentane was also employed as a substrate for 1,3-dipolar cycloaddition ("click") reactions with different alkynes.[194] The same group developed a protocol for the introduction of substituents in the 3-position of BCP amine. 3-Phenylbicyclo[1.1.1]pentan-1-amine hydrochloride (**1.95**) was synthesised by reaction of 1-azido-3-iodobicyclo[1.1.1]pentane with tetrabutylammonium cyanoborohydride (TBACB), AIBN and benzene and subsequent reduction of the azide moiety. Alternatively, "click" reactions were performed on 1-azido-3-phenylbicyclo[1.1.1]pentane. However, more complex substrates for reactions at the 3-position of BCP produced regioisomeric mixtures.[195]

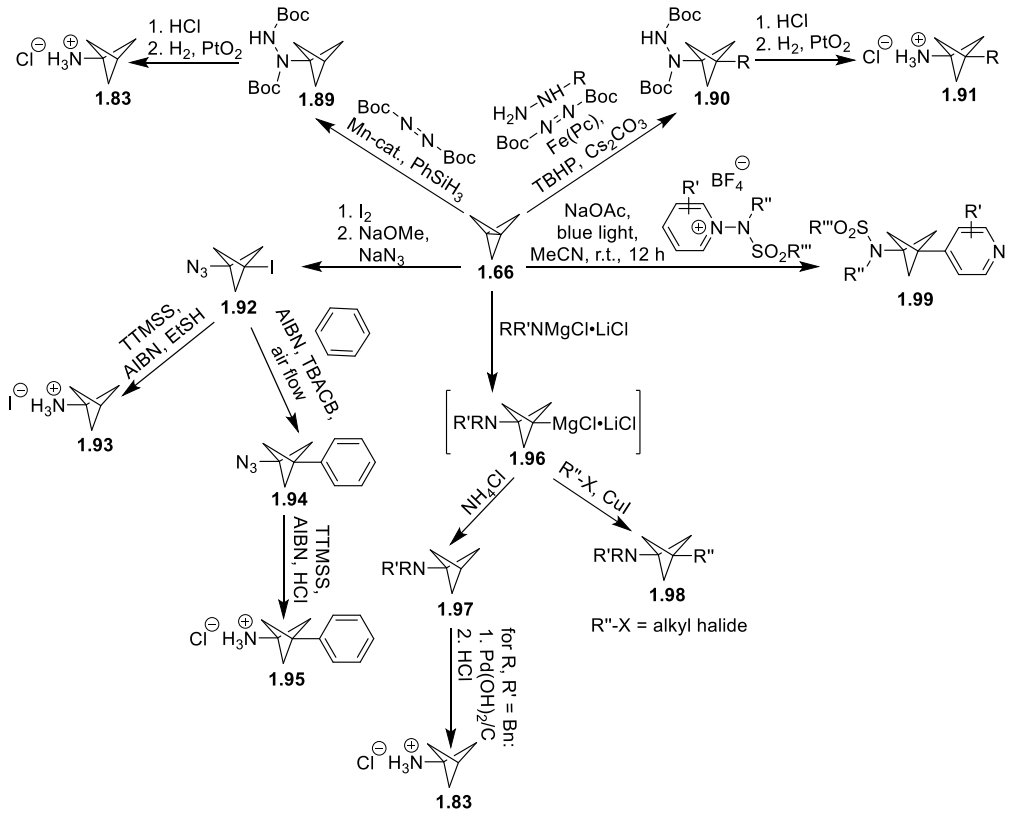

Scheme 1.18. Synthesis of BCP amines from [1.1.1]propellane precursor.

A method introduced by Baran and co-workers reduced the amount of steps required for BCP amine synthesis and enabled direct coupling of functional amines, such as drug molecuels. The innate reactivity of the spring-loaded central bond of [1.1.1]propellane and other strain-release reagents was exploited for the addition of turbo-amide reagents (RR'NMgCl•LiCl).[196] Primary BCP amines obtained by this (i.e. from **1.97**) and other methods can be applied to the corresponding BCP azides which serve as precursors for "click" reactions.[197] The reaction of [1.1.1]propellane with RR'NMgCl•LiCl forms an aminated BCP magnesium species (**1.96**) as an intermediate. This intermediate can undergo Cu-catalysed reaction with alkyl iodides and electrophiles to obtain 3-substituted BCP amines (**1.98**).[198] An interesting approach towards sulphonamide-substituted BCPs was employed by Shin *et al.* who added *N*-aminopyridinium salts to [1.1.1]propellane under irradiation with blue light. The *N*-aminopyridinium salt acts as a bifunctional reagent which forms an electron donor-acceptor complex with [1.1.1]propellane. In a single electron transfer process, an amidyl radical is formed which then undergoes reaction with propellane. The BCP radical derived thereof then traps the remaining pyridyl group at the C4 position, giving 1,3-aminopyridylated BCP (**1.99**).[199]

The reactivity of [1.1.1]propellane had previously been harnessed in a similar manner by addition reactions with Grignard reagents and organolithium reagents.[157b] Notably, BCP Grignard reagents (**1.100**) were generated from [1.1.1]propellane and were further reacted with aryl halides *via* Pd- or Ni-catalysed cross-coupling reactions to produce symmetrically and unsymmetrically 1,3-di-substituted BCP building blocks (**1.101**) (Scheme 1.19). Cross-couplings can proceed either directly from the BCP Grignard reagent in a Kumada-type reaction or after transmetalation with a Zn salt in a Negishi-type reaction.[173,200] Initially, long reaction times of 3–7 days were required for generation of the BCP Grignard reagent. Later, optimisation of the reaction conditions led to faster formation of the BCP magnesium species in 0.75–3 h.[200c] Aggarwal and co-workers reacted BCP Grignard reagents with alkenylboronic acid pinacol esters. The BCP boronate complexes (**1.102**) which formed as reaction intermediates underwent a 1,2-metallate rearrangement either directly or upon addition of an electrophile to yield alkylated BCP derivatives (**1.103**).[201] α-Chiral BCP alkenyls were synthesised using a similar strategy. In the first step, the BCP Grignard reagent **1.100** was formed, which was then reacted with $ZnCl_2$, an enantioselective Ir catalyst – $[Ir(cod)Cl]_2$ with a phosphoramidite ligand – and a Boc-protected allylic alcohol to form α-chiral di-functionalised BCP derivatives **1.104**.[202] Viyas *et al.* reacted BCP Grignard reagents with aryl-, ethynyl- and alkenyl-aldehydes followed by oxidation with MnO_2 to give the acylated BCP derivatives **1.105**. Subsequent asymmetric transfer hydrogenation using a chiral Ru catalyst gave α-chiral BCP alcohols **1.106**.[203]

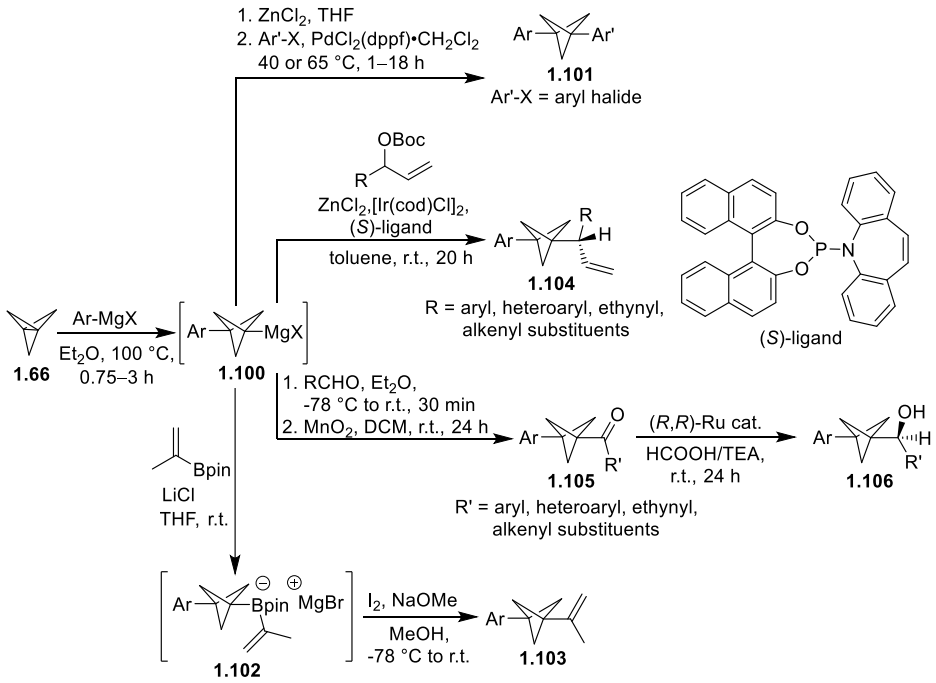

Scheme 1.19. Formation of BCP Grignard reagent **1.100** which can be reacted to give different di-substituted BCP derivatives according to procedures by Knochel,[200c] Aggarwal,[201, 202] Wills[203] and co-workers, respectively.

The reaction of [1.1.1]propellane with organolithium reagents can yield valuable BCP building blocks which, in theory, can be used for a variety of reactions. In practical terms, the lithiation reaction is more difficult to implement because it is rather fast and can lead to the oligomerisation of BCP units.[157b,182a] Wiberg *et al*. accomplished the synthesis of bicyclo[1.1.1]pentyllithium from thiophenol-substituted BCP by reaction with lithium di-*tert*-butylbiphenylide. This was followed by the addition of electrophiles such as aldehydes, carboxylic acid esters, peroxides, trimethylsilyl chloride and tributyltin chloride. The reactivity could be modulated by lithium copper exchange. The BCP cuprate was used for conjugate addition to enones and reactions with alkyl halides, among others.[178b,204] Lithiation of BCP was also achieved by reaction of 3-substituted 1-iodobicyclo[1.1.1]pentane with *tert*-butyllithium (*t*-BuLi) or lithium di-*tert*-butylbiphenylide.[200b]

The addition of alkyl halides across the central bond of [1.1.1]propellane is a tool for functionalisation which has been applied since the early days of propellane chemistry. This can be achieved when a solution containing [1.1.1]propellane and the alkyl halide is irradiated with a mercury lamp or when methyl lithium is added to the reaction mixture (Scheme 1.20).[200b,205] The use of specific chemicals as radical initiators for the addition

reaction is another strategy which bears the advantages of being more mild and functional group-tolerant. Anderson and co-workers employed triethylborane (BEt_3) as an initiator for the synthesis of 1-halo-3-substituted BCPs (**1.107**) from [1.1.1]propellane and alkyl halides. The reaction was found to be tolerant towards the presence of different functional groups and biomolecules such as a nucleoside and a peptide. 1-Iodo-3-substituted BCPs obtained *via* this method could easily be further functionalised. Iodine-lithium exchange with *t*BuLi yielded a precursor suitable for Pd-catalysed coupling reactions to yield all-carbon di-substituted BCPs (**1.113**).[206] In further studies, 1-iodo-3-substituted BCPs obtained by this method were also subjected to Fe-catalysed Kumada cross-coupling reactions with Grignard reagents to obtain **1.113**.[207] Alternatively, deiodination using TTMSS and BEt_3 gave 3-unsubstituted BCP products (**1.115**).[206] The insertion of [1.1.1]propellane in alkyl halide bonds of α-halo carbonyls containing a chiral auxiliary was also used for the preparation of α-chiral BCPs. Synthesis of the 1-iodo-3-substituted BCP building blocks using BEt_3 was followed by deiodination with TTMSS. Chiral centres in the α-position of the carbonyl substituent were introduced in a diastereoselective manner by deprotonation with sodium bis(trimethylsilyl)amide ($NaN(SiMe_3)_2$) and addition of electrophiles.[208] The synthesis of α-chiral BCP compounds was also achieved without chiral auxiliaries but use of a chiral dirhodium catalyst instead. Notably, in this case preformed 1-aryl-BCP underwent direct C-H functionalisation at the 3-position with aryl diazoacetate substrates.[209]

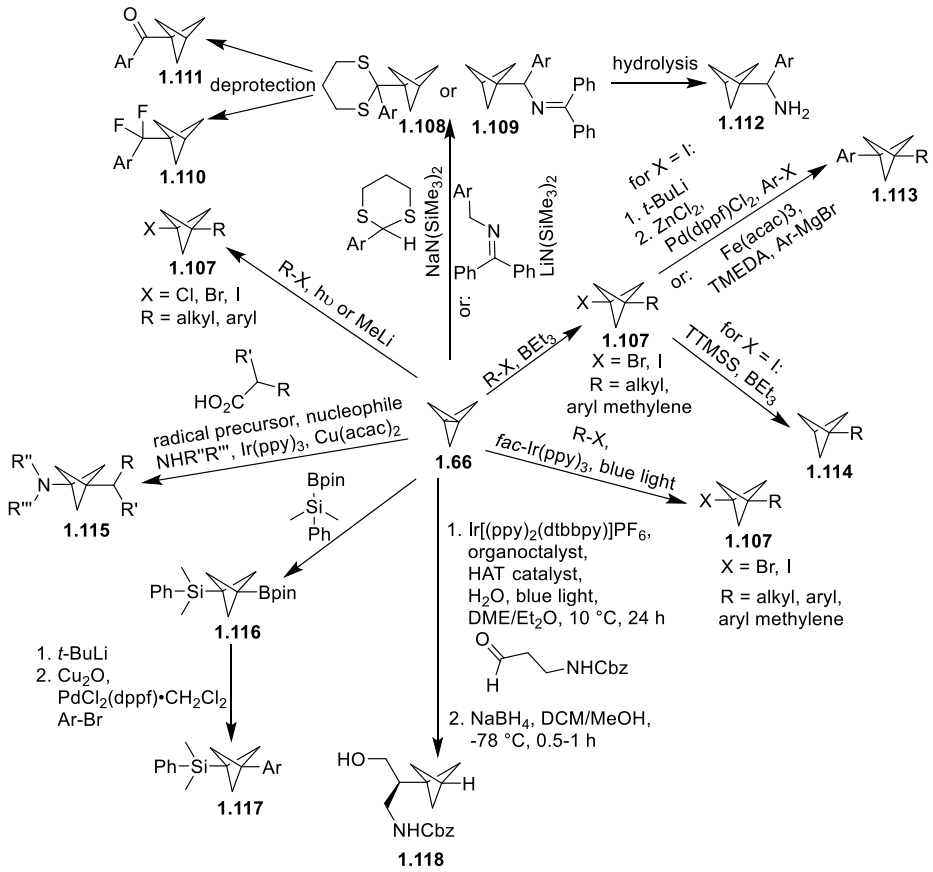

Scheme 1.20. Selected recent methods for the synthesis of functionalised BCPs by the insertion of [1.1.1]propellane into chemical bonds.

The concept of light- or chemical-induced bond insertion of [1.1.1]propellane was also applied for non-halogenated compounds. UV-light promoted silaboration gave BCP building blocks with silyl and boronic ester moieties on the bridgehead carbons (**1.116**). The boronic ester functional group subsequently was used for a variety of transformations, notably a Suzuki-Miyaura type coupling reaction using *t*-BuLi, Cu_2O and $PdCl_2(dppf)•CH_2Cl_2$ giving 1-silyl-3-aryl-substituted BCPs (**1.117**).[210] The use of dilauroyl peroxide promoted the insertion of [1.1.1]propellane in the sulfur-α-carbon bond of xanthates.[211]

A different approach towards the addition of alkyl and aryl halides to [1.1.1]propellane under mild reaction conditions is the use of *fac*-tris(2-phenylpyridine)iridium(III) (*fac*-$Ir(ppy)_3$) as a photocatalyst. In this case the reaction can be carried out under irradiation with blue light.[212] Later, Anderson and co-workers employed photoredox organocatalysis using Ir[(ppy)2(dtbbpy)]PF_6 as a photocatalyst, a pyrrolidine organocatalyst, and a hydrogen atom transfer (HAT) catalyst to directly produce α-chiral BCP derivatives. Reaction with a set of α-substituted aldehydes under blue light irradiation and subsequent reduction with $NaBH_4$

gave the mono-substituted BCP products in commonly good yields and high enantiomeric excess (**1.118**).[213] The combination of an Ir-photoredox-catalyst with a second transition metal catalyst for substrate activation opens up new pathways for cross-coupling reactions. Zhang *et al*. combined Ir-catalysed activation of a radical precursor under blue light irradiation with Cu-based activation of nucleophilic substrates for a three-component coupling reaction with [1.1.1]propellane. The procedure yielded unsymmetrically 1,3-di-substituted BCPs (**1.115**) in a single step.[214] A similar approach was taken by VanHeyst *et al*. who merged Ir- and Ni-catalysis for C-C coupling of BCP trifluoroborate salts with aryl halides.[215]

Another approach towards carbon-carbon bond formation on BCP is the deprotonation of C-H-acidic compounds with strong bases and reaction of the resulting carbanion with [1.1.1]propellane. Walsh and co-workers used $LiN(SiMe_3)_2$ and $NaN(SiMe_3)_2$ for the reaction of ketimines[216] and aryl-dithianes,[217] respectively, with [1.1.1]propellane to yield mono-substituted BCPs (**1.108** and **1.109**). The addition of ketimines is predicted to take place *via* a radical pathway, where the ketimine anion initially transfers an electron to [1.1.1]propellane (single electron transfer, SET) and then undergoes radical-radical coupling with the so-formed BCP radical anion. BCP ketimine derivatives can be transformed into amines (**1.112**) by hydrolysis.[216] In the case of dithiane the reaction is assumed to take place by nucleophilic addition of the carbanion species to [1.1.1]propellane. BCP-dithianes were converted to ketone (**1.111**) and *gem*-difluoro-derivatives (**1.110**).[217]

1.3.4 Applications of Bicyclo[1.1.1]pentane

The special properties of BCP have made this molecule find application in several fields ranging from materials sciences to medicinal chemistry. Features of BCP that are exploited therein are its 3D-shape, the ability to hold substituents in a defined spatial manner at a short distance and the possibility of electron transfer through the BCP cage.

Particular attention has been drawn to the use of BCP in medicinal chemistry and BCP has found entry into several drugs. An underlying concept is that the increase of the proportion of sp^3 carbon centres or saturation in a drug candidate adds complexity to the molecule, thus enables the access of a larger chemical space and increases the likelihood that the molecule can complement the spatial requirements of the drug target. Furthermore, a higher degree of saturation can also improve the drug's solubility and its target selectivity due to the added 3-dimensionality.[218]

Among other 3D hydrocarbon scaffolds, BCP has been used as an aliphatic bioisostere for phenyl rings in drug candidates (**1.119**–**1.133**, Figure 1.11).[182b,182d,219] In a classic example, Stepan *et al*. demonstrated that replacing the fluorophenyl ring in the γ-secretase inhibitor BMS-706,163 with a BCP moiety (**1.119**) positively influenced factors such as the aqueous solubility, passive permeability and metabolic stability.[182d]

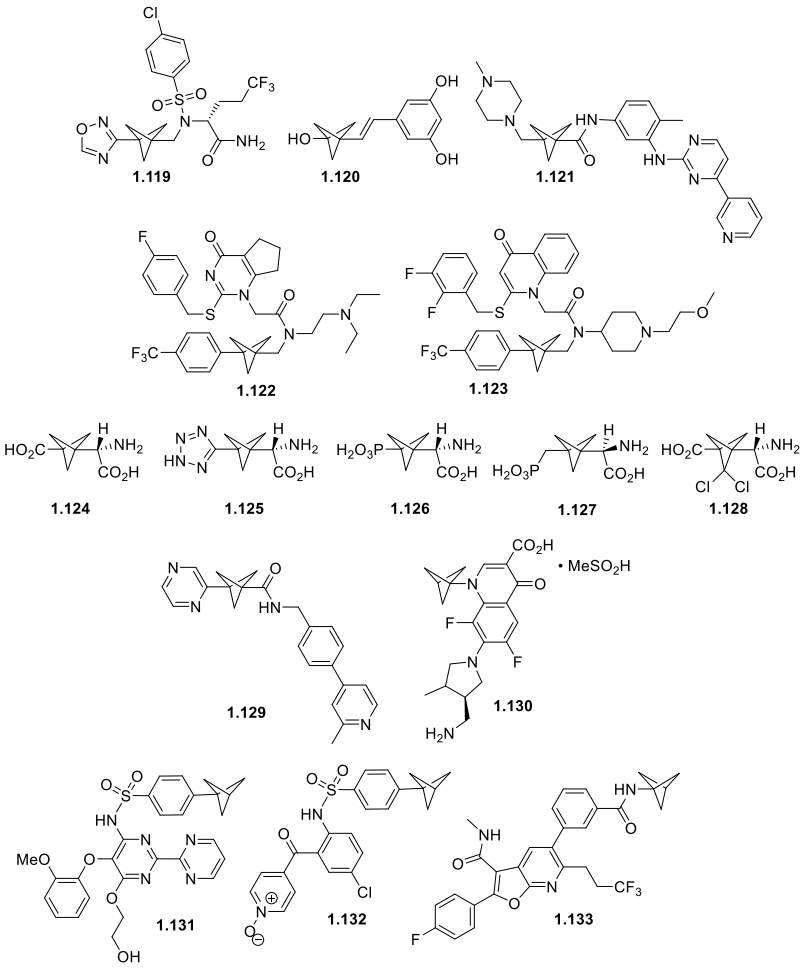

Figure 1.11. Structures of different biologically active compounds in which BCP has been used as a bioisosteric replacement of the phenyl ring or the *tert*-butyl moiety.

Several other studies highlighted positive effects of replacing phenyl moieties with BCP. Auberson *et al*. investigated changes in the physicochemical properties of building blocks in which the phenyl ring had been replaced with a BCP moiety. The bioisosteric substitution was found to enhance the compound's solubility and to decrease non-specific binding.[219c] Better solubility, improved absorption and higher metabolic stability was also determined for a BCP-containing resveratrol analogue.[219b] Resveratrol is a natural product with suspected beneficial properties for the treatment of different illnesses, e.g. cancer, but low bioavailability.[220] Incorporation of BCP instead of one phenyl ring markedly improved the *in vivo* pharmacokinetic properties of the compound (**1.120**) while its antiproliferative activity

in cancer cell lines was retained.[219b] Replacement of the phenyl moiety in imatinib, an ABL1 kinase inhibitor and drug for the treatment of leukemias, with BCP likewise increased the thermodynamic solubility of the drug (**1.121**).[219d] Improved solubility and a low clearance was described for two BCP-containing derivatives of the $LpPLA_2$ inhibitors darapladib (BCP-derivative: **1.122**) and rilapladip (**1.123**) which was attributed to the inclusion of more 3-dimensionality in the molecules and reduction of the aromatic ring count.[219e]

Pellicciari *et al*. incorporated BCP into (carboxyphenyl)glycine (CPG)-based drugs instead of the phenyl ring. The (*S*)-stereoisomer, (*S*)-(+)-2-(3'-carboxybicyclo[1.1.1]pentyl)glycine (*S*-CBPG) (**1.124**), showed good selectivity and potency as a metabotropic glutamate receptor 1 (mGluR1) antagonist and partial activity as a metabotropic glutamate receptor 5 (mGluR5) agonist. This finding indicated that the phenyl moiety is not required for interaction of the ligand with the receptor and the BCP was found as an appropriate spacer, positioning the two substituents on the bridgehead carbons in a defined coplanar orientation.[182b,219h] It was suggested that the activity of *S*-CBPG as a glutamate antagonist for mGluR1 and an agonist for mGluR5 could be used as a tool to discriminate between the physiological effects caused by either of these receptors from the same family (group I).[219i] The neuroprotective effect of *S*-CBPG was analysed *in vivo* and *in vitro*. It was found that *S*-CBPG reduced neuronal death in brain cells that were exposed to oxygen-glucose-depriving conditions as well as CA1 pyramidal cell injury following transient global ischemia in gerbils.[219j] Structural modifications were implemented on *S*-CBPG to tune the activity of the drug candidate. Replacement of the bridgehead carboxy group with a tetrazolyl moiety lowered the compound's (**1.125**) potency as an mGluR1 antagonist but enhanced its selectivity since no affinity for mGluR5 was observed anymore.[219g] When the bridgehead carboxy group in both stereoisomers was replaced with a phosphonic acid moiety instead, the *S*-isomer (**1.126**) was found to be selective and moderately potent as an agonist for the group III mGlu receptor 4.[221] Phosphonomethyl derivatives of (bicyclo[1.1.1]pentyl)glycine, were prepared as well. Especially the *R*-derivative of this amino acid (**1.127**) showed good potency and selectivity as an antagonist of an ionotropic glutamate receptor, the NMDA receptor.[219l] An interesting effect was observed when the BCP bridge in *S*-CBPG was substituted with two chlorine atoms to give (2*S*)-(2′,2′-dichloro-3′-carboxybicyclo[1.1.1]pentyl)glycine (**1.128**): The dichloro-derivative of *S*-CBPG acted as glutamate antagonist at both, mGluR1 and mGluR5. It was reasoned that the loss of the agonistic activity at mGluR5 was caused by the increased steric hindrance imparted by the chlorine substituents.[219k]

However, the replacement of phenyl moieties with a bioisostere whilst retaining the compound's bioactivity is not always possible. When BCP was incorporated in place of

benzene into an inhibitor of the Wnt pathway the derivative (**1.129**) was completely inactive in cell assays. This finding showed that specific steric, electronic and stereoelectronic effects imparted by the phenyl moiety can be crucial for a drug's activity.[219f]

BCP has been also been used as a bioisostere of other chemical moieties, notably as an analogue of the *tert*-butyl group.[189c,222] Barbachyn *et al*. strived to find an alternative to N-1-*tert*-butyl-substituted quinolines as bactericidal agents against Gram-positive bacteria.[189c] Related *N*-1-*tert*-butyl-substituted naphthyridine derivatives had previously shown high activity as antibacterial agents[223] while the quinoline series was found to be less active.[224] Replacement of the *tert*-butyl group in quinolines with the sterically less demanding BCP unit yielded a quinoline derivative (**1.130**) which showed improved bactericidal activity compared to ciprofloxazin against different Gram-positive bacteria.[189c] The physicochemical effects of the replacement of the *tert*-butyl group with BCP units in two clinically approved drugs, bosentan (**1.131**) and vercirnon (**1.132**), was studied by Westphal *et al*. The activity of the drugs was retained upon BCP incorporation and in case of BCP-bosentan even increased. Yet, BCP-vercirnon showed higher clearance rates in mouse and rat microsomes than the parent drug, pointing towards a lower metabolic stability in these organisms.[222b] Synthesis of 7-azabenzofurans for pan-genotypic inhibition of the hepatitis C virus NS5B polymerase revealed a BCP-containing derivative (**1.133**) as a candidate with good activity and appreciable pharmacokinetic profile.[222a]

Incorporation of the BCP moiety into several more bioactive compounds, e.g. in place of cyclohexyl rings, piperidyl rings and parts of amino acids has been reported.[182e,182c,225] Several pharmaceutical companies have incorporated BCP into patented drug candidates (**1.134**-**1.140**) (Figure 1.12).[196b, 226]

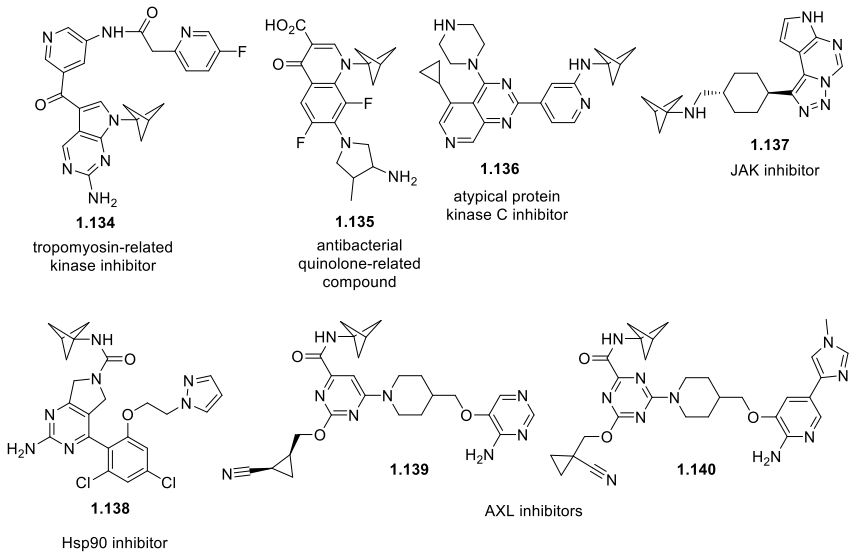

Figure 1.12. Patented drug candidates containing BCP as a bioisostere.

The special nature of the BCP molecule makes it an interesting object for the study of electron and energy transfer through its cage. BCP can act as a transmitter of π-electrons between the two bridgehead substituents.[157a] In presence of a donor and an acceptor substituent, electron transmission can occur, e.g. from the lone pair π orbital of the donor (-NH_2) to a σ* orbital of a BCP core C-C bond and from a BCP C-C bond σ orbital to a π orbital of the acceptor substituent (phenyl ring). The π-interaction between donor and acceptor substituents through the hydrocarbon cage is very pronounced for BCP monomers. By contrast, in 3,3'-substituted BCP dimers, the [2]staffanes, electron delocalisation occurs from the -NH_2 lone pair into the BCP cage it is bound to but the second cage carrying the acceptor phenyl substituent is less involved in the interaction. Substituent interactions in [n]staffanes with n ≥ 3 are based on the long-range polar effect while the π-transfer effect and electronegativity have almost no contribution anymore.[227] Obeng *et al*. assembled monolayers of bridgehead-dithiol-substituted [n]staffanes with n = 1-4 on gold electrodes. The free thiol moieties were subsequently functionalised with pentaaammineruthenium(II). Detection of an oxidation-reduction wave of the Ru(II)/Ru(III) redox couple indicated electron transfer across the monolayer.[228]

BCP represents the shortest saturated linker which allows for arrangements of the bridgehead substituents in a 180° fashion. Thus, it was recognised as an attractive linker system for a photochromic unit and a fluorescent dye. The mutual orientation of the dipole moments of the two chromophores that are aligned by the rigid BCP unit as well as the short distance between them creates the prerequisites for highly efficient Förster resonance

energy transfer (FRET) from the fluorophore to the closed photochromic unit. At the same time, direct overlap of the π-systems through the BCP spacer is inhibited, preventing perturbations caused by conjugation.[182a,173]

Chapter 2. Methods Development for the Functionalisation of Protoporphyrin IX Dimethyl Ester

While nowadays transition metal-catalysed coupling reactions find widespread application in porphyrin synthesis, functionalisation of naturally occurring porphyrins such as protoporphyrin IX by these methodologies has been less explored. In this chapter, the halogenation of protoporphyrin IX dimethyl ester (PPIX-DME) vinyl groups is described. Several strategies for the modification of brominated PPIX-DME by transition metal-catalysed coupling reactions are evaluated and presented thereafter.

2.1 Use of Transition Metal-Catalysed Coupling Reactions for Porphyrin Functionalisation

The use of transition metal-catalysed coupling reactions as a tool to form C-C bonds has undergone a surge in the past few decades. Among the most prominent examples for such transformations are the Suzuki-Miyaura,[38a] Sonogashira,[39] Mizoroki-Heck,[42a] Negishi,[40a] Mitiga-Kosugi-Stille[41] and Buchwald-Hartwig[43a,b] reactions. The use of transition metal-catalysed methodologies has also reformed the porphyrin chemistry field. A plethora of reaction protocols have been developed for the meso- and β-functionalisation of the porphyrin core as well as of peripheral substituents. The developments in the field allow for facile stepwise construction of unsymmetrical porphyrins, the synthesis of porphyrin dimers and oligomers and fused porphyrins, to name only a few.[37a] The prerequisite for metal-catalysed coupling reactions is the presence of suitable functional groups in the porphyrin precursors which essentially comprise halogens, boronic acids/boronate esters, terminal alkenes and alkynes.

Borylated porphyrins can be obtained by direct Ir-catalysed C-H functionalisation with bispinacolate $(Bpin)_2$ (Scheme 2.1). The reaction is regioselective for the porphyrin β-positions. Under the original reaction procedure developed by Osuka and coworkers, the mono-borylated free-base porphyrin product **2.1** formed along with a regioisomeric mixture of diborylated porphyrins **2.7** and **2.8**. The borylation also proceeded with the Ni(II) and Cu(II) complexes of the diaryl-porphyrin (**2.2** and **2.3**).[229] The borylated products can serve as precursors for Suzuki-Miyaura coupling reactions. Precursors with the most versatile applicability, however, are halogenated porphyrins, since they can be used as starting materials for all the different kinds of coupling reactions. Although the solubility of brominated porphyrins can be comparably low,[37a] brominations are the most widely investigated halogenation reactions on porphyrins since they occur quite easily and

because brominated porphyrins readily undergo transition metal-catalysed coupling reactions. While iodinated compounds are also very reactive in C-C bond forming reactions, known methods for the iodination of porphyrins are limited.[230]

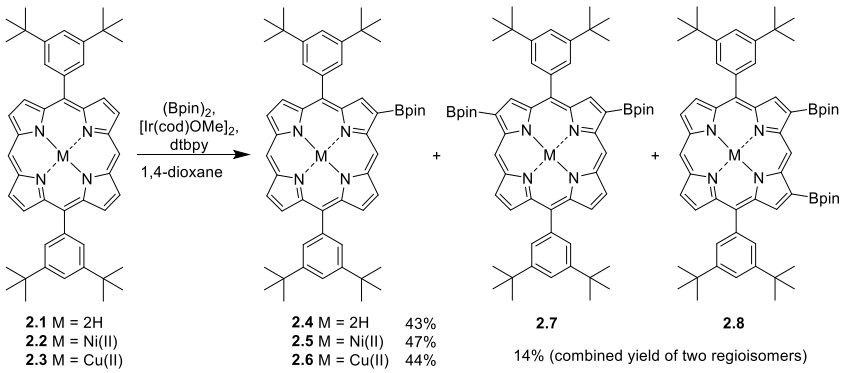

Scheme 2.1. Ir-catalysed borylation of the 5,15-diarylporphyrin β-positions.

Typically, higher electron density is located on the porphyrin meso positions, therefore these positions are more reactive towards electrophilic bromination. Different protocols have been applied, most of them either use *N*-bromosuccinimide (NBS), liquid Br_2, pyridinium bromide perbromide (PBPB), *N*-bromoacetamide or hydrobromic acid as brominating agents. The bromination with Br_2 requires the use of metalated porphyrins, otherwise decomposition of the porphyrin macrocycle can occur. Meso-aryl substituents increase the reactivity of porphyrins at the other free meso positions because they enhance the electron density of the porphyrin system.[230] Hence, the choice of suitable brominating agents strongly depends on the electronics and steric demand of the porphyrin used, as well as the number and positions of the bromine substituents to be added to the macrocycle. For example, selective β-bromination can be achieved and was reported, among others, for the di-bromination of the 3- and 8-positions of deuteroporphyrin dimethyl ester (DPIX-DME, **2.9**) using either PBPB or NBS at 0 °C (Scheme 2.2).[65d, 231]

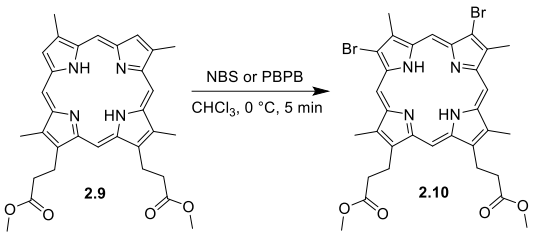

Scheme 2.2. Bromination of the β-positions of deuteroporphyrin dimethyl ester with *N*-bromosuccinimide or pyridinium bromide perbromide, respectively.

The meso-mono- and di-iodinations of 5,15-diarylporphyrins are typically carried out using bis(trifluoroacetoxy)-iodobenzene (PIFA) and I_2 or $AgPF_6$ and I_2 in a mixture of chloroform and pyridine.[34,36]

With borylated or halogenated porphyrin precursors at hand, functionalisation *via* various types of Pd-catalysed cross-coupling reactions is easily possible and a plethora of procedures have been reported. Halogenated porphyrins can either directly be reacted with a coupling partner of choice which carries a suitable functional group or they can first be converted into borylated or ethynylated porphyrins and then reacted with organic halides. Important is the choice of the reaction solvent due to the generally rather low solubility of porphyrins. It should also be considered that the transition metal catalyst or co-catalyst can insert into the porphyrin macrocycle, therefore the use of metalated porphyrin precursors is advisable for most cross-coupling reactions.[34]

An exemplary mechanism for a Suzuki coupling reaction is shown in Scheme 2.3. The Pd(0) catalyst is either added as such or reduced *in situ* from a Pd(II) pre-catalyst. It then undergoes an oxidative addition with the aryl or alkenyl halide substrate to form a Pd(II) complex. The following transmetallation step in which the second aryl or alkenyl substituent is transferred from the boronic acid/ester to Pd(II) is assisted by a base. The base aids in the substitution of the halide ligand on the Pd(II) as well as in making the boronate complex more nucleophilic. The two aryl/alkenyl ligands on the Pd(II) catalyst then undergo C-C bond formation upon reductive elimination from the catalyst and recovery of the Pd(0) species.[232]

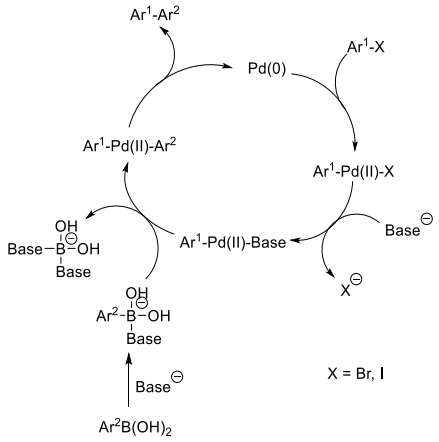

Scheme 2.3. General mechanism for a Suzuki coupling reaction between an aryl halide and an arylboronic acid.

While there is a remarkable variety of procedures reported for the transition metal-catalysed modification of synthetic porphyrins, there are only a few reports about the use of such transformations for naturally occurring porphyrins such as protoporphyrin IX and their closely related derivatives, deuteroporphyrin IX and mesoporphyrin IX.

Especially deuteroporphyrin IX dimethyl ester with its two free β-positions has been subjected to metal-catalysed reactions. One of the first of such reactions reported was a Heck reaction on the mercurated β-positions of the Zn(II) complex of DPIX-DME (**2.11**) (Scheme 2.4). The mercuration was effected by mercury(II) acetate and subsequent treatment with NaCl to give the bis-mercuriochloride porphyrin. Reaction of **2.11** with ethene or methyl acrylate under catalysis by $LiPdCl_3$ and demetalation gave protoporphyrin IX dimethyl ester (PPIX-DME) and coproporphyrin IX dimethyl ester, respectively. A similar procedure was also used for the synthesis of harderoporphyrin and isoharderoporphyrin.[233] Likewise, a Pd-catalysed Stille coupling reaction was carried out on **2.11** (Scheme 2.4). The chloromercurio-moieties in Zn(II)DPIX-DME can also be replaced with bromine or iodine to give the β-halogenated porphyrin derivatives.[234] Later, the substrate scope for Heck reactions on mercurated Zn(II)DPIX-DME was expanded significantly by using different alkenyl, acryl and styrene derivatives as coupling partners.[42b,235] Ali and van Lier employed Sonogashira coupling methodologies on regioisomeric mixtures of mono-iodinated DPIX-DME Zn(II) and Ni(II) metal complexes (Scheme 2.4).[236]

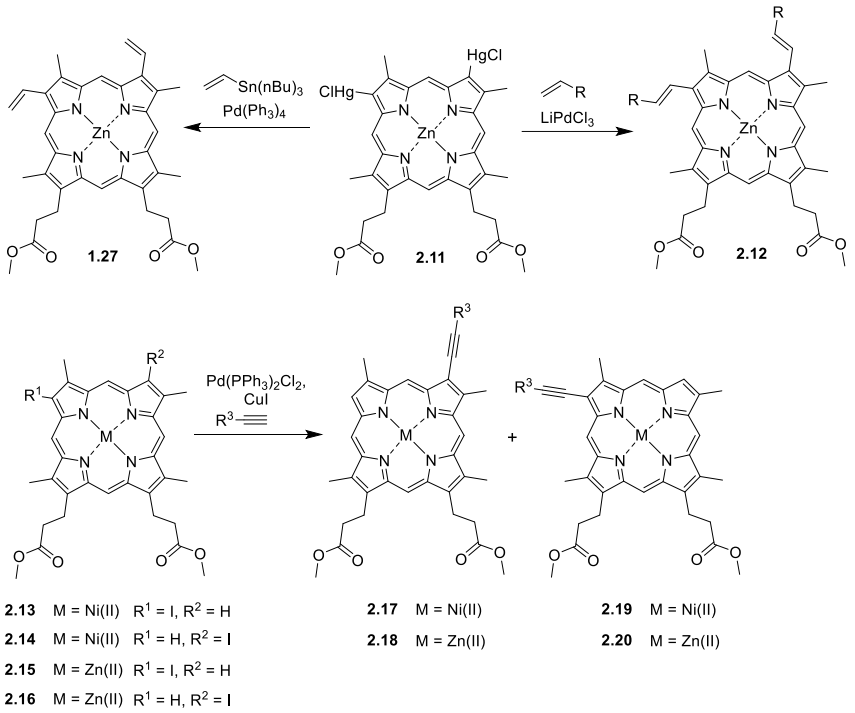

Scheme 2.4. Pd-catalysed Heck, Stille and Sonogashira coupling reactions on metal complexes of deuteroporphyrin dimethyl ester.

Reports of Pd-catalysed coupling reactions on PPIX-DME are more limited. The vinyl groups of this porphyrin can be functionalised *via* Heck coupling reactions. This has been exploited by reacting Zn(II)PPIX-DME (**1.27**) with phenylmercuric chloride under catalysis by $LiPdCl_3$. The reaction yielded only the *E*,*E*-isomer of the vinyl-extended porphyrin (**2.21**).[72a] Castella *et al.* used aryl bromides and iodides for Pd-catalysed Heck reactions on the Zn(II)PPIX-DME vinyl groups (Scheme 2.5). While complete conversion of the starting material was achieved under optimised reaction conditions, mixtures of four different regioisomers (**2.22**–**2.25**) formed which could not be separated easily and the tedious purification limited the yield.[72b]

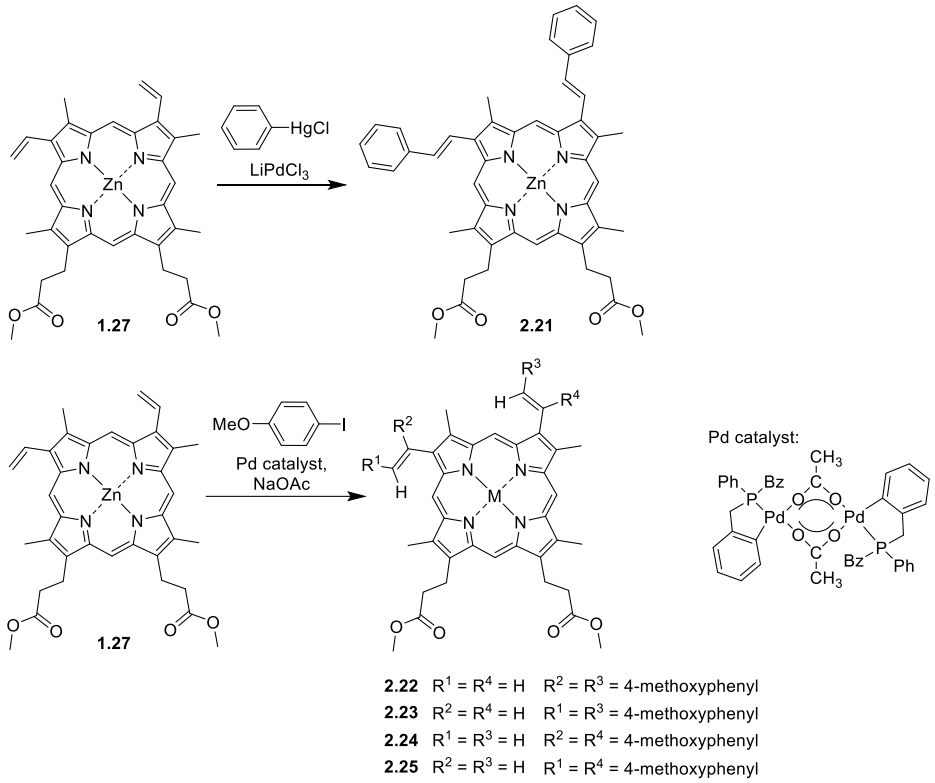

Scheme 2.5. Heck coupling reactions carried out on the vinyl groups of PPIX-DME.

Vinyl group chemistry on PPIX-DME was further employed using ruthenium-catalysed olefin cross-metathesis (Scheme 2.6). A second generation Grubbs catalyst was used to catalyse the reaction between Zn(II)PPIX-DME and free base PPIX-DME (**1.23**), respectively, with aliphatic alkenes. The reaction products **2.26** and **2.27** formed as 50:1 and 40:1 mixtures of *E*- and *Z*-isomers. The reaction was found to be sensitive to the alkene substrate. It proceeded efficiently for electron-rich alkenes, while the yields were decreased significantly for electron-deficient substrates.[71]

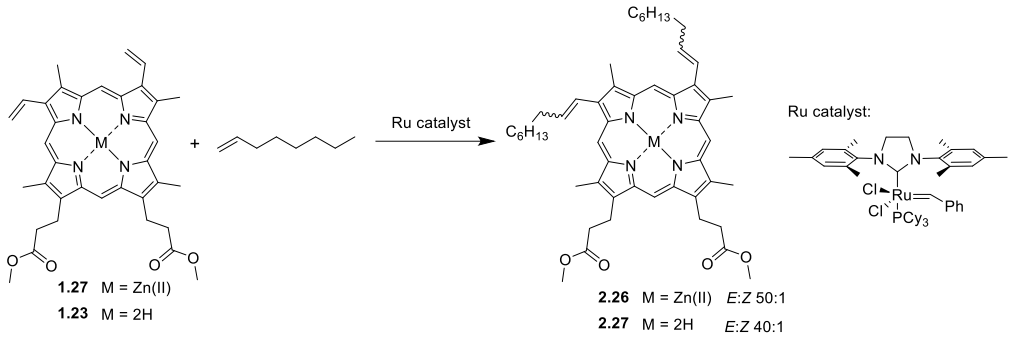

Scheme 2.6. Olefin cross metathesis on the PPIX-DME and Zn(II)PPIX-DME vinyl groups using a 2nd generation Grubbs catalyst.

2.2 Objectives

As a parent structure of protein prosthetic groups in most living organisms, protoporphyrin IX and its derivatives are highly interesting for the study and manipulation of biological systems. Protoporphyrin IX derivatives with enhanced hydrophilicity and tumour tissue selectivity or altered absorption properties and singlet oxygen quantum yields could find application in PDT. Furthermore, protoporphyrin IX derivatives have potential applications as competitive inhibitors of enzymes or as prosthetic groups in novel metalloprotein catalysts.[53c,58b,75f,97b,129–143] Derivatives of protoporphyrin IX which carry appropriate fluorescent moieties could be used as bio-imaging tools.[52]

Although the development of protoporphyrin IX chemistry has been an intense area of research for several decades, only little advances have been made to update protoporphyrin IX functionalisation reactions by use of modern synthetic methods. Particularly desirable are palladium-catalysed cross-coupling reactions which open up an easy opportunity towards the formation of a plethora of products from one simple porphyrin precursor. The establishment of reaction conditions for cross-coupling reactions on protoporphyrin IX would, therefore, enable the targeted and broadly scoped synthesis of protoporphyrin IX derivatives for a variety of biomedical applications.

The aim of this study was to first synthesise different protoporphyrin IX derivatives containing non-natural metals. These compounds will be of interest for the study of non-natural porphyrins' protein binding activities and as potential antimicrobial agents. Furthermore, the functionalisation of protoporphyrin IX vinyl groups was investigated.

Transition metal-catalysed reactions on PPIX-DME derivatives have been limited to reactions which employ the unsubstituted vinyl groups as reaction partners. Utilisation of

the vinyl groups for different kinds of transition metal-catalysed cross-coupling reactions requires procedures for their halogenation or borylation while retaining the double bond, hence the terminal sp^2 carbon centre. It was intended to develop such a protocol for the vinyl group halogenation of PPIX derivatives and to test these compounds‘ utility for Pd-catalysed cross-coupling reactions.

Conditions for selective halogenation of the vinyl groups were investigated first, followed by testing of different reactions of the Suzuki-Miyaura and Sonogashira type. Development of such reaction protocols enables the attachment of moieties with varying degrees of bulk and different functional groups to protoporphyrin IX that potentially change the interaction of the prosthetic group with the binding pocket when reconstituted with proteins. The overall goal was the development and optimisation of different synthetic tools for facile and variable protoporphyrin IX functionalisation.

2.3 Synthesis of Protoporphyrin IX Dimethyl Ester Metal Complexes

In 1999, Srinivasan and coworkers discovered that PPIX complexes with non-natural metals exhibit antibacterial activity against Gram-positive and Gram-negative bacteria as well as Mycobacteria.[237] Bacterial growth inhibition by these compounds was attributed to their uptake into the bacterial cell, which proceeds either through a “Trojan horse” mechanism or occurs *via* direct penetration of the membrane. The Trojan horse pathway involves binding of the abiological porphyrins to proteins that are normally responsible for shuttling heme into the bacterial cells and “tricking” these proteins into transporting the non-natural heme analogues instead. Once in the cell, the metallo-protoporphyrins are assumed to cause cytotoxicity through various effects: inhibition of heme-dependent enzymes, release of cytotoxic metals, promotion of reactive oxygen species (ROS) generation and interference with iron-dependent processes.[238]

Another mode of action is the inhibition of heme transport through the membrane by irreversible binding of metallo-protoporphyrins IX to proteins involved in the bacterial heme uptake.[238b,239] As pathogenic bacteria rely on acquisition of iron from the host organism, these findings suggest potential application of non-natural PPIX metal complexes as antibiotics. Pathogenic bacteria sequester iron from their host organism by uptake of either free metal ions or of heme. Thus, bacterial heme uptake can be exploited for the delivery of drugs into the bacterial cell or the heme transporting complex can be blocked to deprive the bacterium of its iron source.[238a]

It was attempted to synthesise some of the known PPIX-DME metal complexes for potential tests of their cytotoxicity. As a general synthetic plan, protoporphyrin IX disodium salt (**2.28**) was converted into its dimethyl ester (PPIX-DME, **1.23**), by sulfuric acid-catalysed esterification as reported by Hultquist *et al.*,[240] to increase the solubility of the porphyrin (Scheme 2.7). This ensured easier handling of metal insertion reactions. Afterwards, metal complex formation reactions with zinc, copper, cobalt, silver, ruthenium and manganese were carried out. Reaction conditions for the different metals were used as indicated in Scheme 2.7.

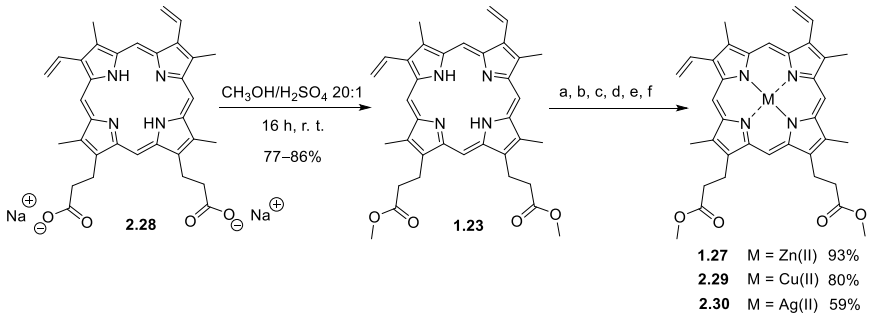

Scheme 2.7. Transformation of protoporphyrin IX disodium salt into its dimethyl ester by acid-catalysed esterification and subsequent metal insertion reactions. Conditions for metal insertions are as follows: a) zinc insertion: $Zn(OAc)_2$•2 H_2O (3.0 eq.), DCM/MeOH 3:1, 30 °C, 1.5 h, b) copper insertion: $Cu(OAc)_2$ (4.9 eq.), DCM/MeOH 3:1, 40 °C, 0.5 h, c) cobalt insertion: $Co(OAc)_2$•4 H_2O (5.0 eq.), DMF, 153 °C, 1 h, d) silver insertion: AgOAc (6.0 eq.), DCM/MeOH 3:1, 40 °C, 1 h, e) ruthenium insertion: $Ru_3(CO)_{12}$ (1.1 eq.), DMF, 153 °C, 24 h, f) manganese insertion: 1. $Mn(OAc)_2$•4 H_2O, DMF, 120 °C, 24 h, 2. $(Bu)_4NCl$ (106 eq.), DCM/MeOH 2:3, r.t., 45 min.

Zinc, copper and silver insertion into PPIX-DME using the corresponding metal acetates $Zn(OAc)_2$•2H_2O, $Cu(OAc)_2$ and AgOAc were accomplished in DCM/MeOH 3:1 as a solvent system under gentle heating (30–40 °C).[241] The respective metalloporphyrins **1.27**, **2.29** and **2.30** were isolated in 93%, 80% and 59% yield, respectively. However, it was found that other metal insertions which needed higher reaction temperatures did not give the desired products as easily. The reaction of PPIX-DME with $Co(OAc)_2$•4H_2O in DMF at 153 °C[61] yielded Co(II)PPIX-DME, but the product could not be purified sufficiently. An attempted ruthenium insertion with $Ru_3(CO)_{12}$ in DMF at 153 °C[242] led to a partial reduction of the vinyl groups, while manganese insertion with $Mn(OAc)_2$·4 H_2O in DMF at 120 °C[241] caused complete decomposition of the porphyrin. Very likely, the high temperature of metal insertions that were carried out in DMF caused side reactions at the sensitive β-substituents of PPIX-DME.

The porphyrin metal complexes **1.27**, **2.29** and **2.30** which were obtained in moderate to good yields were subjected to basic hydrolysis to convert the propionate methyl ester moieties into propionic acid chains, thus giving the protoporphyrin IX Zn(II) (**1.48**), Cu(II) (**2.31**) and Ag(II) (**2.32**) complexes in 85%, 65% and 45% yield, respectively (Scheme 2.8**Scheme**).

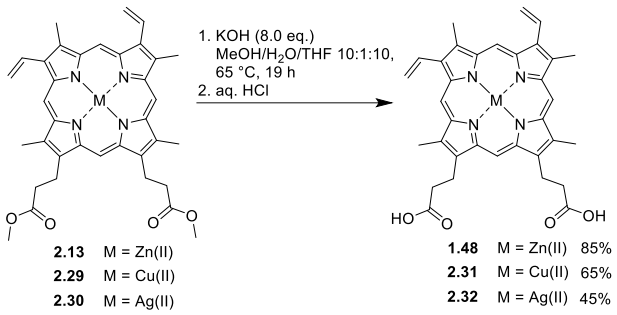

Scheme 2.8. Hydrolysis of ester moieties of PPIX-DME metal complexes using KOH to give protoporphyrin IX Zn(II) (**1.48**), Cu(II) (**2.31**), and Ag(II) (**2.32**) complexes.

2.4 Modification of Protoporphyrin IX Dimethyl Ester Vinyl Groups by Transition Metal-Catalysed Reactions

2.4.1 Halogenation

So far, only a few reactions of vinyl arm extensions are known for protoporphyrin IX where the substituent is not bound *via* a heteroatom and in which the vinyl double bond, thus conjugation with the porphyrin core, is retained. It was aimed to develop a method for halogenation of the vinyl group under conservation of the double bond. This would provide a valuable starting material for coupling reactions to extend the vinyl arms. No indications of bromo- or iodo-vinyl PPIX-DME were found in the literature.

However, C-H bond halogenations have been reported previously for the vinyl groups of related chlorins (Scheme 2.9).[243] Khadira *et al*. brominated pyropheophorbide a methyl ester (**2.33**) by addition of NBS (2.0 eq.) in batches to a refluxing solution of the chlorin in 1,2-dichloroethane. The selective formation of the *E*-isomer (*E*)-3^2-bromopyropheophorbide a methyl ester (**2.34**) in 78% was reported.[243a] On the other hand, Cao *et al*. brominated the vinyl group of chlorin e_6 trimethyl ester (**2.35**) by treating a solution of the chlorin in a DCM/Et_2O 1:1 mixture by dropwise addition of Br_2 (excess) at -97 °C. A mixture of the monobrominated product **2.36** and a chlorin brominated at the vinyl group as well as in one of the meso positions (**2.37**) was obtained. The two products could be separated by silica gel column chromatography.[243b]

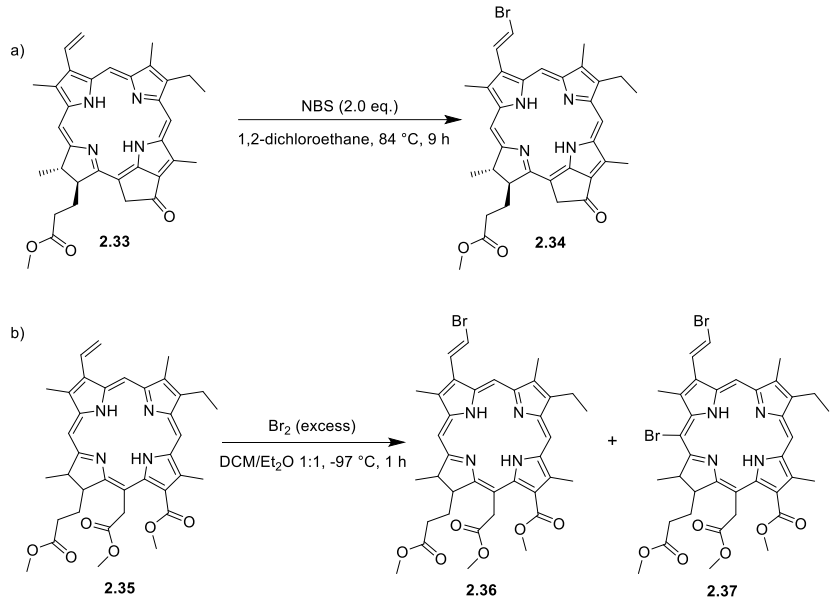

Scheme 2.9. Bromination reactions on the vinyl groups of pyropheophorbide a methyl ester (**2.33**) and chlorin e_6 trimethyl ester (**2.35**).

Based on the procedure reported by Khadira *et al*.,[243a] a bromination of the PPIX-DME vinyl groups was attempted under similar conditions using NBS in 1,2-dichloroethane (1,2-DCE) at 84 °C (Scheme 2.10, Table 2.1). In a first attempt, a solution of PPIX-DME in 1,2-DCE was treated with 2.2 eq. NBS and the mixture was stirred at 84 °C for 18 h (Table 2.1, entry a). The di-brominated product **2.39** was isolated after silica gel column chromatography in a low yield of 9%. Significant decomposition of the porphyrins in the reaction mixture and side product formation was observed. When the reaction time was decreased to 5.5 h to reduce decomposition of the porphyrin and the amount of added NBS was increased to 3.0 eq. the di-brominated product could be isolated in 22% yield (Table 2.1, entry b). The low yields were partly attributed to decomposition as well as significant side product formation. ^{1}H NMR analysis and HR-MALDI-MS of one of the isolated by-products indicated that more than two brominations had occurred on the porphyrin. Solely reducing the reaction time only resulted in an incremental increase in yield (Table 2.1, entry c). However, shortening the reaction time and decreasing the amount of NBS used to 2.2 eq. led to an increase in yield up to 40% (Table 2.1, entry d). When the solvent was changed to DCM and the reaction temperature was lowered to 40 °C, no product formation was observed.

Since in several attempts using NBS as the brominating agent the yield of the di-brominated product could not be increased beyond 40%, it was decided to test a different brominating agent. Pyridinium bromide perbromide (PBPB) has been used previously for the β-bromination of deuteroporphyrin IX dimethyl ester.[65d,230a] Hence, this reagent was

employed for the next bromination attempt. Reaction of **1.23** with 2.2 eq. PBPB in chloroform at 61 °C for 3 h resulted in formation of **2.39** in 84% yield (Table 2.1, entry f).

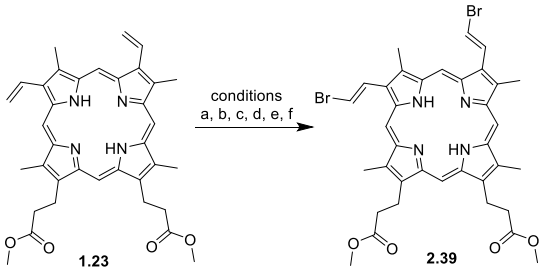

Scheme 2.10. Testing of different reaction conditions for the bromination of the vinyl groups of PPIX-DME (**1.23**). For bromination reaction conditions see Table 2.1.

Table 2.1. Different reaction conditions tested for the di-bromination of PPIX-DME (**1.23**) according to Scheme 2.9.

entry	reagents	temp.	solvents	time	yield
a	NBS (2.2 eq.)	84 °C	1,2-DCE	18 h	9%
b	NBS (3.0 eq.)	84 °C	1,2-DCE	5.5 h	22%
c	NBS (3.0 eq.)	84 °C	1,2-DCE	3 h	25%
d	NBS (2.2 eq.)	84 °C	1,2-DCE	2.5 h	40%
e	NBS (2.2 eq.)	40 °C	DCM	5 h	n. d.
f	PHPB (2.2 eq.)	61 °C	$CHCl_3$	3 h	84%

The higher yield of this reaction compared to former attempts using NBS mainly is attributed to less side product formation as indicated by TLC analysis. So far, only assumptions can be made about the reasons for this. The most plausible one might be that bromine, which is liberated from PBPB, undergoes electrophilic addition to the vinylic double bond first under formation of a bromonium ion. One possibility is that the intermediate is attacked by the remaining bromide to give a 1,2-dibromoethyl-substituent on the porphyrin core. Subsequently, free pyridine, originating from the brominating agent, can help in the elimination of hydrogen bromide whereby the double bond is reformed.[244] Otherwise, deprotonation might already occur in the bromonium intermediate, resulting in the same β-bromo-vinyl porphyrin. When NBS is used instead, the reaction might proceed in a similar way, but possibly succinimide is not a strong enough base to aid in the elimination of hydrogen bromide. Furthermore, PBPB is known to be a milder brominating agent than NBS and due to its lower reactivity less side products are formed.[245]

Attempts to iodinate the PPIX-DME vinyl groups using NIS in 1,2-DCE at 84 °C or with I_2 and PIFA in 1,2-DCE at 84 °C resulted in decomposition of the porphyrin starting material (Scheme 2.11a). Next, substitution of the bromine atoms in **2.39** with iodines by a Finkelstein-type halide exchange was attempted. A modified literature procedure was applied using KI as an iodine source, CuI as a catalyst and 2,2‘-bipyridine as a ligand, but no product formation was observed (Scheme 2.11b).[246]

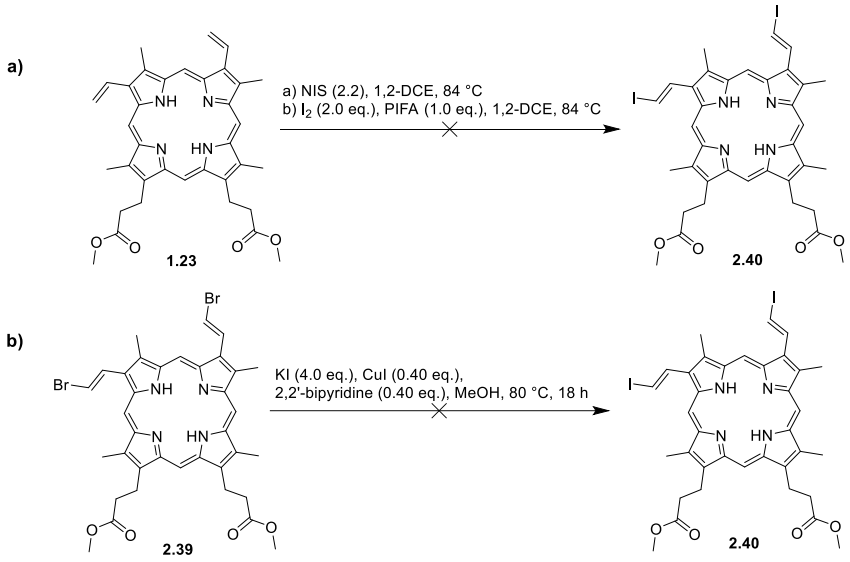

Scheme 2.11. Attempted iodination of the PPIX-DME vinyl groups using different halogenation procedures starting from either (a) PPIX-DME **1.23** or (b) di-brominated PPIX-DME **2.39**.

2.4.2 Suzuki-Miyaura Cross-Coupling Reactions

Since attempts to iodinate PPIX-DME were unsuccessful, focus instead was put on the use of di-brominated PPIX-DME (**2.39**), a precursor which could be prepared in reproducibly high yields. First, it was sought to devise protocols for Suzuki-Miyaura cross-coupling reactions at the vinyl positions of **2.39**. In this type of reaction, an organohalide or pseudohalide is coupled with an organoboron compound by using a palladium or nickel catalyst and a base.[246] The Suzuki-Miyaura reaction is one of the most popular coupling reactions in porphyrin chemistry,[37a] among other reasons due to its mild reaction conditions, the ready availability and stability of the starting materials and the high functional group tolerance.[247,248]

For the Suzuki coupling on **2.39** a modified literature procedure by Moylan *et al*. was applied.[249] Reaction of **2.39** with 4-tolylboronic acid (20 eq.), $Pd(dppf)Cl_2$ (0.20 eq.) as the catalyst and Cs_2CO_3 (20 eq.) as the base in THF at 61 °C for 18 h yielded the bis-coupled product **2.41** in 86% (Scheme 2.12, conditions a). The promising result obtained in this first attempt of the coupling reaction prompted us to test these reaction conditions for more

substrates. Starting materials containing functional groups such as a formyl or methoxy moiety, respectively, in the 4-position of the phenyl ring were well tolerated and gave the respective bis-coupled products **2.43** and **2.42** in 67% and 63% yield. The reaction with (4-(methoxycarbonyl)phenyl)boronic acid pinacol ester proceeded with slightly less efficiency, giving the coupling product **2.44** in 49% yield, which was probably due to a lower solubility of the boronic acid pinacol ester in the reaction mixture. The reactivity of bulky substrates was investigated as well. While reaction of **2.39** with anthracen-9-ylboronic acid resulted in formation of **2.45** in a moderate yield of 59%, the reaction with 1-methyl-1*H*-indole-5-boronic acid resulted in the formation of the di-substituted product **2.46** in only 30%.

Different coupling conditions were employed for the reaction of **2.39** with 4-[(trimethylsilyl)ethynyl]phenylboronic acid pinacol ester. In an initial reaction carried out under the standard coupling conditions, an *in situ* deprotection of the TMS-ethynyl moiety was observed. It was assumed that the deprotection in the reaction mixture led to a reduced overall yield due to a Glaser homocoupling side reaction between the unprotected ethynes.[250] In order to preserve the silyl protecting groups, thereby preventing side reactions and allowing full characterisation of the material, the base was changed to K_3PO_4 (20 eq.) and $Pd(PPh_3)_4$ (0.10 eq.) was used as a catalyst (Scheme 2.10, conditions b). Subsequent deprotection with TBAF gave **2.47** in 32% overall yield.

Attempts to couple **2.39** with 4-dimethylanilineboronic acid only resulted in the formation of trace amounts of compound **2.49** and coupling with 4-pyridinylboronic acid did not yield any product. The low reactivity of pyridinylboronic acids in cross-coupling reactions is a known phenomenon and is attributed to the heterocycles' electron-deficiency and therefore low transmetallation rate and to their tendency to undergo protodeboronation.[251] Change of the catalyst to $Pd(PPh_3)_4$ and use of DMF/toluene 1:1 as a solvent system for the reaction with 4-pyridinylboronic acid, as reported by Hwang *et al.*,[252] did not lead to any product formation either.

To probe if the coupling reaction can take place on sp^3-hybridised carbon centres, **2.39** was reacted with 4-butylboronic acid under the same conditions as employed for aryl substrates. No product formation was observed in this case which indicates that the reaction is not efficient for alkylboronic acids and the conditions will have to be optimised for coupling with such substrates.

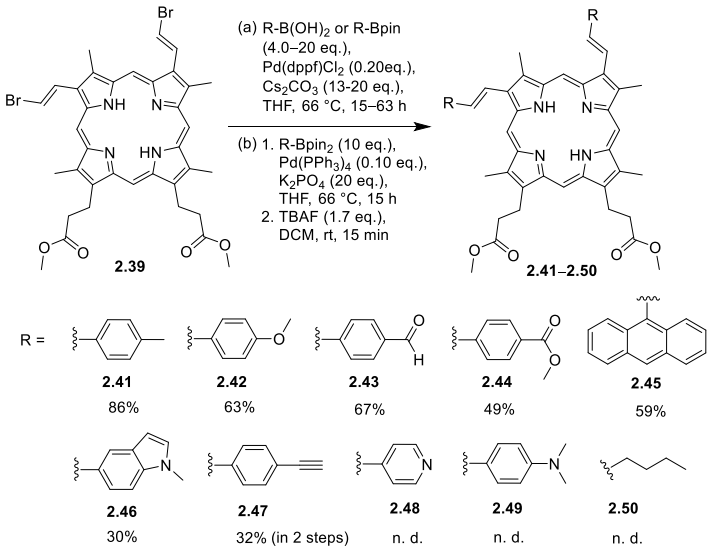

Scheme 2.12. Suzuki-Miyaura coupling reactions of dibromo-PPIX-DME with different boronic acids and boronic acid pinacol esters. n.d. – not determined

It was also attempted to develop a procedure for the borylation of the PPIX-DME vinyl groups to obtain protoporphyrin derivatives that can be reacted with organic halides in Suzuki-Miyaura reactions. One of the most commonly applied borylation procedures is the Pd-catalysed reaction of aryl halides with bis(pinacolato)diboron as developed by Miyaura and coworkers in 1995.[253] An alternative method developed by Masuda *et al.* substitutes the diboron with less expensive pinacolborane.[253,254] The latter procedure was applied for the borylation of PPIX-DME, using HBpin (20 eq.), $PdCl_2(PPh_3)_4$ (0.20 eq.) and TEA (20 eq.) in 1,2-DCE at 84 °C.[38b] The bisborylated product **2.51** was isolated in 48% yield (Scheme 2.12).

Subsequently, exploratory reactions of **2.51** with 4-bromotoluene (**2.52**) were carried out with optimisation of the procedure being attempted (Scheme 2.13, Table 2.2). Based on a method by Bakar *et al.*[255] that was applied for coupling reactions with meso-borylated porphyrins, catalyst $Pd(PPh_3)_4$ (0.20 eq.) and Cs_2CO_3 (4.0 eq.) were used in THF (Table 2.2, entry a). Coupling product **2.41** was obtained in only 16% yield. Another procedure was employed that had been reported by Hata *et al.*[229b] for coupling reactions with β-borylated porphyrins. The use of of $Pd_2(dba)_3$ (0.10 eq.), of PPh_3 (0.40 eq.) and of Cs_2CO_3 (3.0 eq.) in a toluene/DMSO 2:1 mixture led to complete decomposition of the porphyrin within 2 h (Table 2.2, entry b). The product was obtained in 25% yield when **2.39** was reacted with 4-bromotoluene in THF, $Pd(dppf)Cl_2$ was used as a catalyst and Cs_2CO_3 as a base. It is evident that the reaction conditions which gave the best yield (25%) are equivalent to the ones used for Suzuki-Miyaura couplings with **2.39**. However, this yield was still much lower compared to when **2.39** was reacted with 4-tolylboronic acid (86% yield). It is assumed that

this is partly due to the protodeboronation of borylated porphyrin **2.51** as well as a lower solubility of the borylated porphyrin in the reaction mixture.

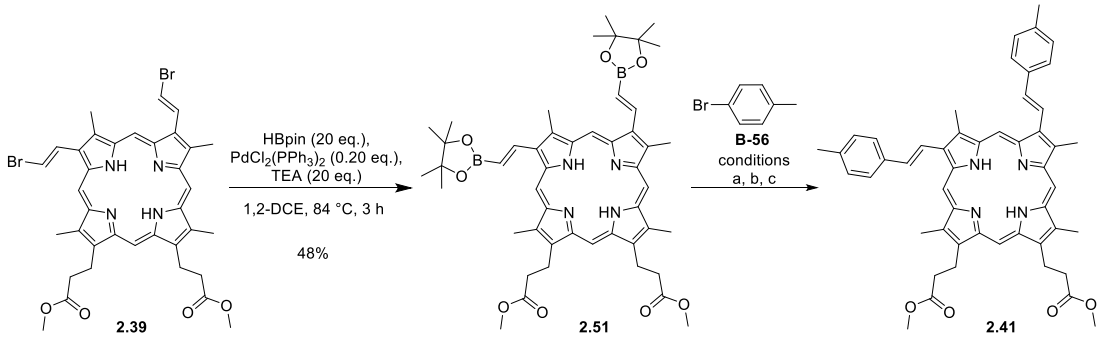

Scheme 2.13. Borylation of dibromo-PPIX-DME to give bisborylated PPIX-DME (**2.51**) and subsequent Suzuki-Miyaura coupling with 4-bromotoluene (**2.52**) to give **2.41**. For Suzuki-Miyaura reaction conditions see Table 2.2.

Table 2.2. Reaction conditions for the Suzuki-Miyaura cross-coupling of bisborylated PPIX-DME **2.51** with 4-bromotoluene (**2.52**) according to Scheme 2.13. n. d. – not determined

entry	reagents	temp.	solvents	time	yield
a	**2.52** (2.5 eq.), $Pd(PPh_3)_4$ (0.20 eq.), Cs_2CO_3 (4.0 eq.),	66 °C	THF	17 h	16%
b	**2.52** (4.0 eq.), $Pd_2(dba)_3$ (0.10 eq.), PPh_3 (0.40 eq.), Cs_2CO_3 (3.0 eq.)	80 °C	toluene/DMSO 2:1	2 h	n. d.
c	**2.52** (4.0 eq.), $Pd(dppf)Cl_2$ (0.20 eq.), Cs_2CO_3 (20 eq.)	66 °C	THF	16 h	25%

Although the Suzuki coupling with borylated PPIX-DME **2.51** opens the possibility for the use of a different range of coupling substrates, this reaction was found to be much less efficient under the conditions employed than Suzuki coupling on di-brominated PPIX-DME **2.39**. Hence, the latter reaction is suggested to be more applicable for the functionalisation of PPIX-DME in less steps and a better yield.

2.4.3 Sonogashira Cross-Coupling Reactions

A popular tool for the functionalisation of porphyrins are Sonogashira coupling reactions between aryl or alkenyl halides and acetylene-appended compounds. In the classical way, the reaction involves a palladium catalyst and a copper co-catalyst that activates the acetylene moiety for transfer to the palladium(II) species.[39,256] A commonly applied alternative is the copper-free Sonogashira coupling that does not make use of a copper catalyst. Instead, the amine bases present in the reaction mixture are assumed to aid in the deprotonation of the acetylene.[257]

It was attempted to append the PPIX-DME vinyl groups with a protected acetylene moiety (Scheme 2.13). After deprotection of the ethyne, the so functionalised protoporphyrin derivative could then serve as a building block for further coupling reactions using organohalides.

Cu(II) insertion in the porphyrin macrocycle can occur during the traditional Cu-catalysed Sonogashira reaction conditions. This can be circumvented by using a metalated porphyrin precursor, e.g. with Zn(II) or Ni(II). In order to save additional metalation and demetalation steps it was decided to test copper-free Sonogashira coupling conditions on free base di-brominated PPIX-DME first (Scheme 2.14). Reaction of **2.39** with trimethylsilylacetylene (2.0 eq.) using $Pd_2(dba)_3$ (0.10 eq.) as a catalyst and $AsPh_3$ (0.10eq.) in a solvent mixture of toluene and TEA (Table 2.3, entry a) did not yield any product and mostly starting material was recovered. The same result was achieved when the solvent was changed to a mixture to THF/TEA and the amounts of TMS-acetylene (4.0 eq.), Pd catalyst (0.40 eq.) and co-catalyst (4.0 eq.) were increased (Table 2.3, entry b). In contrast, when CuI (0.20 eq.) was used as a co-catalyst along with $Pd(PPh_3)_2Cl_2$ (0.10 eq.) in the reaction of **2.39** with trimethylsilylacetylene (4.0 eq.) in a THF/TEA mixture (Table 2.3, entry c), complete conversion of the starting material was achieved and the bis-coupled product **2.53** was isolated in 97% yield. No Cu(II) insertion into the porphyrin was observed in this reaction. Subsequently, the silyl protection groups on the alkyne moieties of **2.53** were removed in a standard procedure with TBAF (2.2 eq.) to yield a porphyrin with free acetylene moieties **2.54** in 86%.

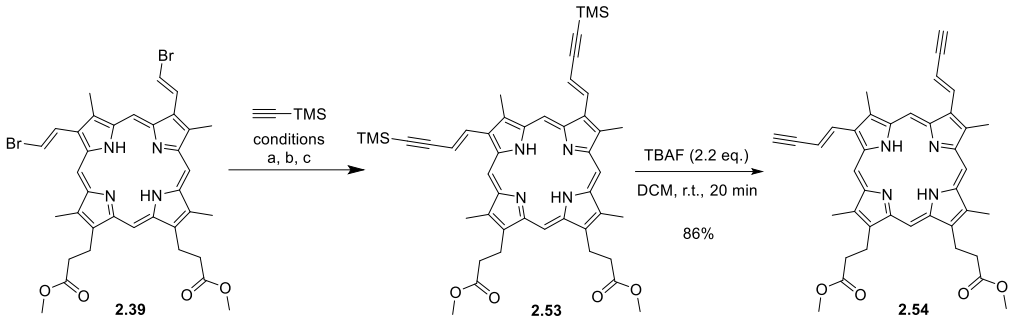

Scheme 2.14. Sonogashira coupling reaction on dibromo-PPIX-DME to give diethynyl-substituted PPIX-DME (**2.53**) and subsequent deprotection with TBAF to yield **2.54**. For Sonogashira coupling conditions see Table 2.3.

Table 2.3. Reaction conditions for the Sonogashira coupling reaction on di-brominated PPIX-DME **2.39** with TMS-acetylene according to Scheme 2.14. n. d. – not determined

entry	reagents	temp.	solvents	time	yield
a	TMS-acetylene (2.0 eq.), $Pd_2(dba)_3$ (0.10 eq.), $AsPh_3$ (0.1 eq.)	40 °C	toluene/TEA 3:1	16 h	n. d.
b	TMS-acetylene (4.0 eq.), $Pd_2(dba)_3$ (0.40 eq.), $AsPh_3$ (4.0 eq.)	35 °C	THF/TEA 2:1	23 h	n. d.
c	TMS-acetylene (4.0 eq.), $Pd(PPh_3)_2Cl_2$ (0.10 eq.), CuI (0.20 eq.)	r. t.	THF/TEA 1:1	16 h	97%

With conditions for the efficient transformation of **2.39** under Sonogashira coupling conditions at hand, this reaction was carried out with more substrates (Scheme 2.15). The reaction with phenylacetylene gave full conversion of the porphyrin starting material and the respective product could be isolated in 97% yield. Conversely, reaction with the more electron-deficient methyl 4-ethynylbenzoate did not lead to complete conversion to the di-substituted product **2.39**, resulting in only 35% yield of the desired compound and a significant amount of recovered starting material. An interchanging cationic and anionic pathway of the Sonogashira reaction mediated by the electron-rich or electron-poor nature of the alkyne was proposed by Ljungdahl *et al*.[258] The reaction conditions applied herein may promote the cationic pathway, thereby disfavouring the reaction with electron-poor substrates.

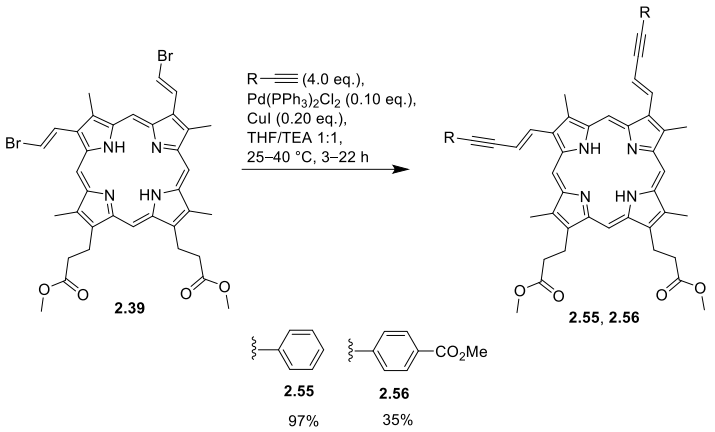

Scheme 2.15. Sonogashira coupling reaction of dibromo-PPIX-DME with phenylacetylene and methyl 4-ethynylbenzoate to yield vinyl-extended porphyrins **2.55** and **2.56**.

Nevertheless, Sonogashira coupling reactions proved as another viable route for the Pd-catalysed functionalisation of di-brominated PPIX-DME. The ethynylated compound **2.54** can also serve as a useful precursor for Sonogashira coupling reactions with organohalide substrates as well as for cycloaddition reactions such as the Cu-catalysed azide-alkyne 1,3-dipolar cycloaddition (”click“ reaction).[259]

2.4.4 Cu-Catalysed Azide-Alkyne 1,3-Dipolar Cycloaddition Reactions

The alkynyl moiety is a very versatile functional group which can be modified in different ways. Among the most widely performed reactions on alkynes are cycloaddition reactions. In 2002, Sharpless and Meldal independently reported on a transformation of the Huisgen 1,3-dipolar cycloaddition reaction procedure which subsequently became one of the most useful tools in medicinal chemistry.[259,260] This reaction, also termed as “click” reaction, connects an azide and an alkyne under copper-catalysis and is generally characterised by its high yields, a large substrate scope and a high selectivity.[261] Since the first use of the Cu-catalysed “click” reaction in porphyrin chemistry by Collman *et al*. in 2006,[262] this reaction has found widespread application in the field, e.g., for the production of photosensitisers, polymers and materials.[263]

It was intended to use acetylene-appended PPIX-DME **2.54** which had previously been prepared in high yields by Sonogashira coupling reaction as a starting material for Cu-catalysed azide-alkyne “click” reactions. As reaction substrates, bromine containing organic azides were chosen because introduction of the bromine moieties would add a synthetic handle to the porphyrin which could subsequently be used for further extension of the vinyl arms. 1-Azido-2-bromobenzene **2.58**, 1-azido-3-bromobenzene **2.59** and 1-azido-4-bromobenzene **2.60** (Scheme 2.16) were synthesised from the respective bromoaniline

precursors by a diazotisation of the amine with $NaNO_2$ and HCl and subsequent nucleophilic substitution of the diazonium moiety with azide.[264]

It was intended to use a protocol for a “click” reaction catalysed by Cu and since Cu(II) insertion into the porphyrin was anticipated in this reaction, Zn(II) insertion into diyne porphyrin **2.54** was attempted first. When the porphyrin was stirred with $Zn(OAc)_2$•2 H_2O (6.0 eq.) in a DCM/MeOH 3:1 mixture at r.t. for 72 h no complete conversion of the starting material was observed by TLC analysis (Scheme 2.16). Changing the solvent to chloroform/MeOH 3:1 and heating the mixture to 61 °C for 24 h also resulted in formation of a mixture of the Zn(II)-coordinated product and free base starting material. The inability to fully metalate the starting material with Zn(II) would result in an overall decrease in yield, hence it was decided to proceed with the “click” reactions using the free base diyne porphyrin **2.54**.

For the “click” reaction, **2.54** was reacted with the azides **2.58**–**2.60** (4.0 eq.), sodium ascorbate (2.0 eq.) and $CuSO_4$•5 H_2O (2.0 eq.) in DMF at 100 °C for 1 h (Scheme 2.16). As opposed to the Sonogashira coupling reactions with the free base PPIX-DME derivative **2.39**, in this reaction Cu(II) insertion into the porphyrin was observed. This was attributed to the high reaction temperature as well as the relatively larger amount of Cu salt used. Formation of the porphyrin Cu(II) complexes **2.62** and **2.63** in coupling reactions with 1-azido-3-bromobenzene and 1-azido-4-bromobenzene was observed while the reaction with 1-azido-2-bromobenzene only resulted in the formation of trace amounts of the “click” product **2.61**. Presumably, steric hindrance with the 2-bromo-substituent inhibited the reaction with **2.58**. Demetallation of the of the Cu(II) porphyrins was carried out by stirring the crude products in a 10:1 mixture of chloroform and concentrated H_2SO_4 at 0 °C for 5 min, followed by an aqueous work-up. The low temperature and short exposure to the acidic solution ensured that the PPIX-DME ester groups remained intact during the demetalation. The two “click” products **2.65** and **2.66** were isolated in 49% and 43% yield, respectively.

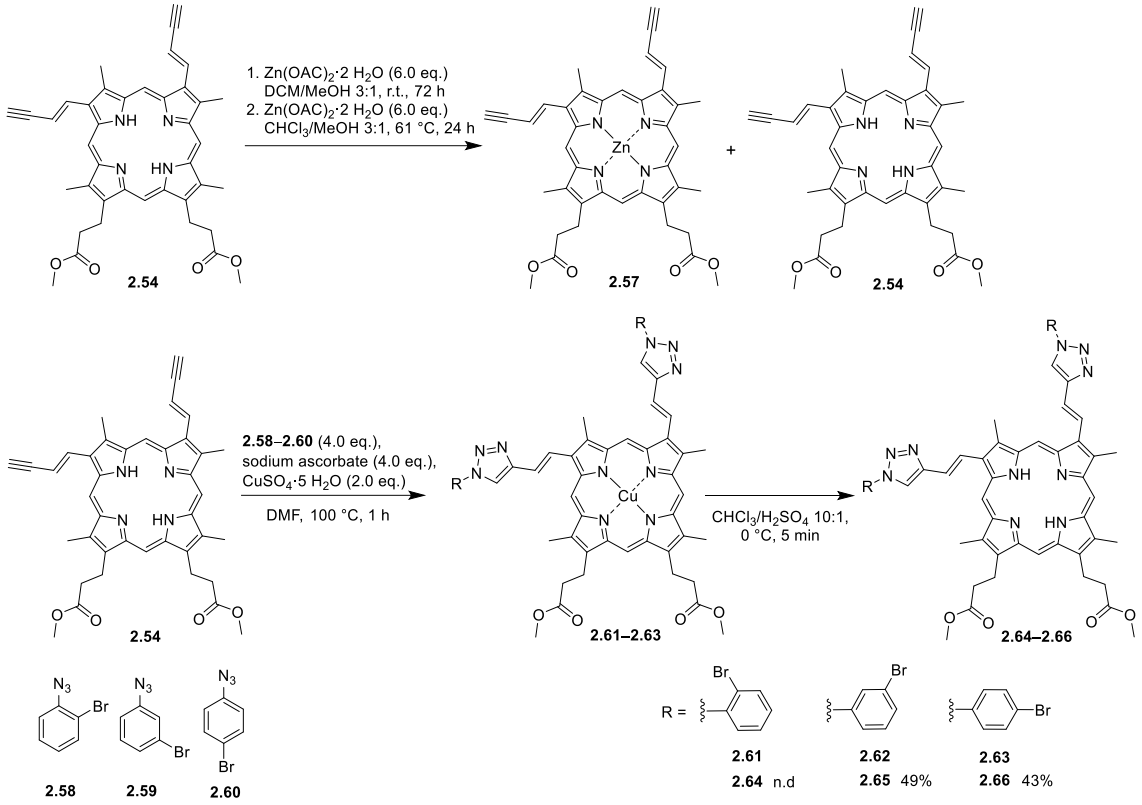

Scheme 2.16. Attempted zinc insertion into diyne porphyrin **2.58,** which did not go to completion, and "click" reactions with free base diyne **2.58** and different 1-azidobromobenzenes.

The observed Cu(II) insertion into the PPIX-DME derivative likely reduced the yield of the "click" reaction by reduction of the amount of catalyst present in the reaction mixture and also necessitated another synthetic step, the removal of Cu(II) from the porphyrin core. To overcome this complication, it was decided to repeat the "click" reaction with a metallated porphyrin precursor. Zn(II) insertion was attempted again, this time with TMS-protected diyne porphyrin **2.53**. Heating of a solution of **2.53** and $Zn(OAc)_2$•2 H_2O (3.0 eq.) in DCM/MeOH (3:1) to 40 °C for 1.5 h led to incomplete conversion of the starting material to the Zn(II) complex. More $Zn(OAc)_2$•2 H_2O (1.0 eq.) was added and the mixture was heated for another 1 h (Scheme 2.17). Since the reaction was still not complete after this time, separation of the Zn(II) inserted product and the free base porphyrin by column chromatography on neutral aluminium oxide was necessary to isolate the product **2.67** in 74% yield. Presumably, the difficulties in inserting zinc into the alkynyl-substituted PPIX-DME as opposed to unsubstituted PPIX-DME arise from electronic changes in the porphyrin macrocycle upon the addition of electron-withdrawing moieties. These changes disfavoured the coordination of Zn^{2+}. Subsequent deprotection of **2.67** with TBAF afforded diyne **2.57**. This porphyrin was introduced to a "click" reaction under equivalent conditions as employed previously for the free base porphyrin but this time the reaction mixture was left to stir for

5 h. Some difficulties were encountered in the purification of the product which presumably were due to coordination of the central Zn(II) to heteroatoms of the porphyrin or azide starting material. Only upon addition of pyridine as a ligand for zinc to break these interactions the pure “click” product **2.68** could be obtained in 28% yield. The relatively low yield of the reaction may be due to these difficulties in purification and, possibly, binding of azide starting material to the central zinc metal in the reaction mixture. Ways to bypass these obstacles could be the use of different reaction conditions which employ solvents that coordinate to Zn(II) more strongly than azide or the use of a precursor porphyrin containing a non-coordinating metal such as nickel.

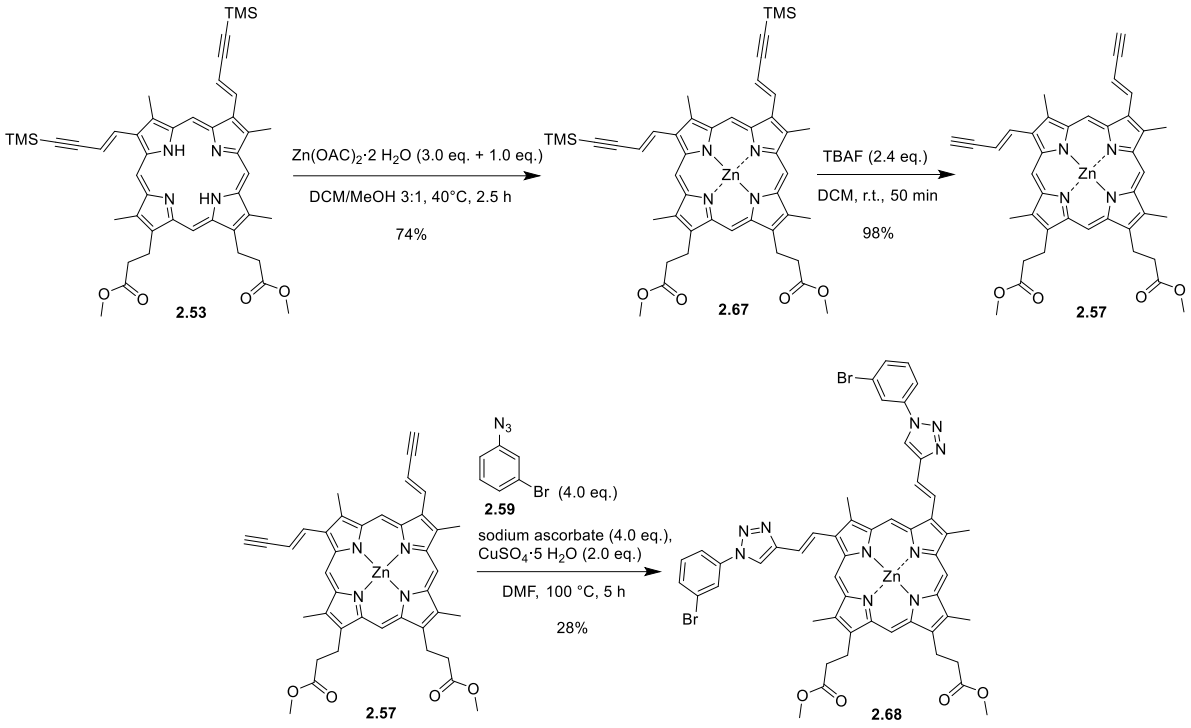

Scheme 2.17. Zinc insertion into porphyrin **2.53**, followed by deprotection and “click“ reaction with 1-azido-2-bromobenzene to yield the zinc complex of 1,2,3-triazole porphyrin **2.68**.

2.5 Conclusion and Outlook

Nature’s porphyrin allrounder, PPIX, has made its way into a multitude of disciplines all across the natural sciences due to its inherent chemical and physical properties, ready availability and relevance in biochemistry. Therefore, developing simple methods to synthesise new functional PPIX derivatives in a broad scope are highly sought after.

In the course of this work, complex formation of protoporphyrin IX with different metals was studied and protoporphyrin IX zinc, copper and silver complexes were successfully synthesised. Subsequently, it was intended to prepare a di-halogenated PPIX-DME precursor and to devise procedures for Pd-catalysed coupling reactions on this molecule to be able to easily modify the porphyrin with different kinds of substrates. Di-brominated PPIX-DME was prepared in a high yield after optimisation of the reaction conditions. The vinyl-bromides could also be converted into boronic ester moieties by Suzuki-Miyaura coupling as well as acetylene moieties by Sonogashira coupling reaction, to obtain two more PPIX-DME derivatives appended with functional groups. As a result, three reactive precursors were obtained which can be used for different kinds of further modifications.

With the possibility to prepare sufficient amounts of the di-brominated precursor, protocols for Suzuki-Miyaura coupling reactions on this porphyrin could be tested. Eight PPIX-DME derivatives were prepared by Suzuki-Miyaura coupling reactions using a variety of substrates with different electronic properties and steric demands. The products were isolated in moderate to high yields. For simple tolylboronic acid, a high yield of 86% was obtained while when the bulkier 9-anthraceneboronic acid (59%) and boronic acids carrying functional groups like formyl and acetylene moieties were used, the yield was decreased (67% and 32%, respectively). The reaction conditions applied were not suitable for couplings with pyridine and amine containing substrates as well as alkylboronic acids. Different protocols will have to be devised for coupling reactions with these compounds.

A procedure for Sonogashira coupling reactions with dibromo-PPIX-DME was also implemented and three ethynyl-linked PPIX-DME derivatives were prepared. PPIX-DME carrying two TMS-acetylene moieties was formed in an excellent yield (98%). After deprotection, PPIX-DME diyne and its Zn(II) complex were employed as starting materials for copper-catalysed 1,3-dipolar azide-alkyne cycloadditions. This procedure proved to be a viable route for the formation of PPIX-DME triazoles in moderate yields (28–49%).

Hence, it was shown that PPIX-DME derivatives can easily be transformed by classical Pd-catalysed coupling reactions as well “click“ reactions. This can possibly add to the recently investigated applications of PPIX in photodynamic therapy, bioactive materials, biorthogonal reactions and drug delivery systems.[92q,265]

Chapter 3. Synthesis of Protoporphyrin IX Dimethyl Ester-Fluorophore Triads

Among its various applications described in Chapter 1, protoporphyrin IX is widely used as a photosensitiser for photodynamic therapy (PDT). Herein, the synthesis of conjugates of protoporphyrin IX dimethyl ester (PPIX-DME) with fluorescent BODIPY dyes is attempted with the aim of preparing potential new theranostic probes for simultaneous therapy and bioimaging. After an introduction to the concepts of PDT and theranostic porphyrin agents, our approaches towards the synthesis of PPIX-DME-BODIPY triads will be presented.

3.1 Porphyrin-Fluorophore Conjugates as Theranostic Agents

The 22π electron macrocyclic structure of porphyrins causes them to strongly absorb light in the visible region of the spectrum. They typically display one strong absorption band between 380–500 nm, the Soret band, and several weaker bands between 500-750 nm, known as Q bands. The intensity and number of Q-bands depends on the porphyrin‘s substituents as well as on whether it is bound to a metal or present in its protonated or free-base form.[13b] Their optical properties, i.e. their strong absorption of visible light, makes porphyrins a suitable core structure for photosensitisers.[266] Photosensitisers are molecules used in photodynamic therapy (PDT), a form of clinical treatment that is applied to treat oesophagal, cervical, gastrical, lung and skin cancers. They also find therapeutic application against age-related macular degeneration and psoriasis and can be used for the inactivation of bacteria.[267] PDT involves the administration of a non-toxic photosensitiser, such as a porphyrin, that preferentially localises in malignant tissue.[268] Photosensitisers undergo transitions to the first or higher singlet excited states (S_1, S_2 or S_n) upon irradiation with light of a wavelength they strongly absorb (Figure 3.1). While the singlet excited state can be quenched by non-radiative decay (internal conversion) or fluorescence, photosensitisers show comparably high intersystem crossing rates to give triplet excited states (T_1, T_n). The molecule in its triplet excited state can then undergo bimolecular reactions with surrounding molecules. Two general pathways are possible for the bimolecular quenching: 1. The photosensitiser directly interacts with substrate molecules in the surrounding tissue by electron transfer, generating highly reactive, cytotoxic intermediates such as free radicals (type I reactions). 2. Energy transfer from the triplet state to ground state oxygen in the tissue (triplet oxygen, $^3O_2$) to generate oxygen in one of its singlet states ($^1O_2$) (type II reaction). Singlet oxygen exhibits a very short lifetime, thus $^1O_2$ is highly reactive and rapidly enters oxidative reactions with cellular molecules such as nucleic acids and enzymes. Both

mechanisms ultimately lead to the destruction of tumour cells, however, type II reactions are thought to be of more relevance to PDT.[269] Photosensitisers affect cellular structures as well as the vascular system and immune response. The impact of PDT is based on all these factors.[270] For clinical applications of a photosensitiser certain criteria are commonly desirable. These include the absorption of light in the desired region of the spectrum (see below), non-toxicity and solubility, the display of selective targeting of the tumour tissue, and an appropriate half-life under biological conditions.[270]

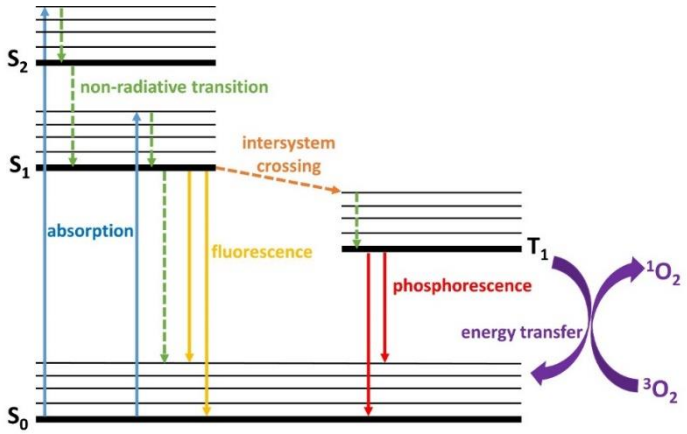

Figure 3.1. Schematic Jablonski representation of the photophysical processes a molecule can undergo upon irradiation with light. Absorption of a photon leads to excitation of the molecule from its ground state (S_0) to its first, second or higher singlet excited states (S_1, S_2, S_n). Higher excited states decay to the first singlet excited state *via* non-radiative transitions. The first excited singlet state can be quenched by three different pathways: Non-radiative decay or emission of photons (fluorescence) to populate the singlet ground state or intersystem crossing to the triplet state (T_1). The excited triplet state of the molecule can be deactivated to the singlet ground state either by emission of photons (phosphorescence) or energy transfer. For a photosensitiser the energy acceptor is triplet oxygen ($^3O_2$), which is converted to singlet oxygen ($^1O_2$).

Research is on-going to develop photosensitisers with improved clearance rates, tumour targeting and photophysical properties.[267a,271] Common photosensitisers include porphyrins, phthalocyanines, chlorins, and other dyes such as rose bengal, methylene blue and boron-dipyrromethene (BODIPY) dyes.[272] The ideal photosensitiser should meet several criteria. Among others, these comprise stability, minimal dark toxicity, preferential uptake into tumour tissue, rapid clearance from the body, high triplet state quantum yields and lifetimes, efficient production of singlet oxygen and reactive oxygen species and, importantly, they should show significant absorption at longer wavelengths (650–800 nm). This wavelength range is referred to as the ”phototherapeutic window“. Light of wavelengths below 650 nm is absorbed by endogenous chromophores and achieves less deep tissue penetration.[273] While upon irradiation at 630 nm the effective penetration depth of light

(irradiance reduced to 37%) is about 1–3 mm, for irradiation at 700–850 nm the penetration depth is approximately doubled.[4c] In addition, light scattering is reduced at longer wavelengths. On the other hand, light with wavelengths >800 nm does not have sufficient energy to generate singlet oxygen.[272,273] Conventional porphyrins show rather weak absorption in the "phototherapeutic window", while chlorins and bacteriochlorins exhibit an enhanced last Q band and therefore strong absorption above 600 nm.[272] However, especially bacteriochlorin derivatives often show low stability.[65a,274] Still, among the most commonly applied photosensitisers are two compounds that are closely related to naturally occurring porphyrins: Photofrin, a haematoporphyrin derivative, which is clinically approved for the treatment of several cancers, such as lung, bladder, gastric and cervical, and δ-aminolevulinic acid (ALA), a precursor in the biosynthetic pathway of protoporphyrin IX that is converted to the porphyrin *in situ*. ALA is used for acne treatment.[4c]

Apart from serving as therapeutic agents, porphyrins can also be used as *in vivo* imaging tools because they show emission in the red or near-infrared region. The affinity of porphyrins for accumulation in neoplastic tissue can be used to locate tumours and to monitor the efficacy of tumour treatment with photosensitisers. This property has even found application in fluorescence-guided surgery. In addition, porphyrins and their metal complexes have emerged in other *in vivo* imaging applications such as radio-, photoacoustic, positron emission tomography (PET) and magnetic resonance (MR) imaging.[275]

The therapeutic effects and emissive properties of porphyrins can be exploited simultaneously to obtain molecules with dual functionality, e.g., act as both a photosensitiser and fluorescence imaging agent. Such compounds are referred to as "theranostics". However, the use of porphyrins as theranostic agents suffers from the limitations of porphyrin photosensitisers, namely their weak absorption at higher wavelengths, and thus limited tissue penetration of the excitation light. In addition, for theranostic materials, a strong fluorescence response is a vital requirement and many PDT-active porphyrins with high singlet oxygen production show low fluorescence quantum yields.[276] One approach to overcome this is the conjugation of porphyrins to a fluorescent dye, which shows absorption and emission properties that complement the porphyrin's functionality. At the same time, such fluorophores can function as antenna systems for the photosensitiser. They harvest light in a spectral window where the photosensitiser absorbs poorly and then transfers the energy to the sensitiser *via* Förster resonance energy transfer (FRET)[277] and/or Dexter energy transfer[278] (Figure 3.2). FRET is a phenomenon where an electron in a donor molecule or moiety is excited to a higher energy electronic state upon

absorption of a photon. When the electron relaxes to a lower energy electronic state, energy is transferred to an acceptor through dipole-dipole coupling interactions. Prerequisites for FRET to take place are a spectral overlap between the donor's emission and the acceptor's absorption profiles as well as spatial vicinity of donor and acceptor. FRET is strongly distance-dependent where the transfer rate correlates with r^{-6} to the donor-acceptor distance *r*. The transfer rate is described by Equation 3.1.

$$E = \frac{1}{1 + \left(\frac{r}{R_0}\right)^6}$$

Equation 3.1. Calculation of the FRET efficiency (E) where r is donor-acceptor distance and R_0 is the Förster radius, distance with 50% transfer efficiency.

Additionally, the relative orientation of the donor and acceptor plays an important role in optimal dipole-dipole interactions.[279] On the other hand, the Dexter mechanism is based on electron exchange interactions. It includes transfer of an excited state electron from the donor to the acceptor and exchange of a ground-state electron from the acceptor to the donor, resulting in electronic excitation of the acceptor (quencher). This process requires favourable overlap of the orbitals of the two partners.[280]

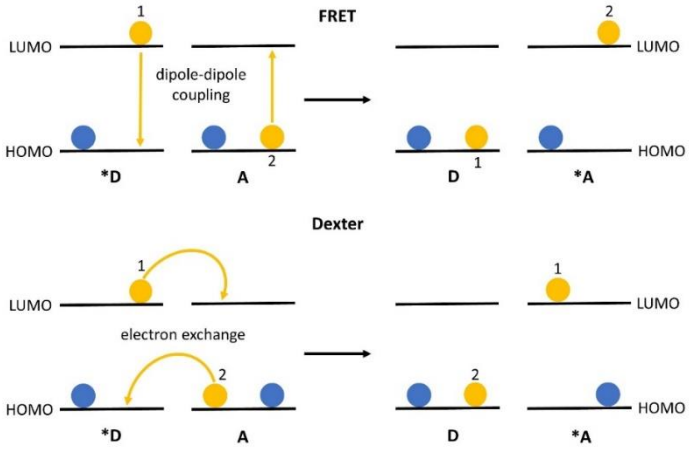

Figure 3.2. Simplified representation of FRET and Dexter energy and electron transfer mechanisms. In FRET, an electron from an excited donor (D*) orbital relaxes to the ground state and, *via* dipole-dipole coupling, induces the transition of a ground state electron of the acceptor (A) to an excited state. The Dexter mechanism includes transfer of an excited electron of the donor to the acceptor. In the exchange, a ground state electron of the acceptor is transferred to the donor's HOMO, resulting in quenching of the excited state of the donor and simultaneous excitation of the acceptor.

A dual function dyad based on a tetrapyrrole photosensitiser was first reported in 2005 and was composed of a chlorin, 2-[1-hexyloxyethyl]-2-devinyl pyropheophorbide a, and a

cyanine dye and showed strong absorption and emission in the near-infrared >800 nm region (**3.1**, Figure 3.3).[281] Later, a cyanine dye was used to link two bacteriochlorin derivatives (**3.2**, Figure 3.3). In this triad, efficient FRET from the cyanine to the bacteriochlorin moieties was observed while the cyanine still retained some emission, enabling its use as a moiety for fluorescence imaging. Conjugation to the dye caused a 3- to 4-fold reduction in the photosensitising activity of the bacteriochlorin, which presumably was attributed to π-π stacking of the conjugates.[282] Panchenko *et al*. synthesised a dyad composed of a bacteriochlorin e derivative and a naphthalimide fragment (**3.3**, Figure 3.3). The compound proved to be an effective photosensitiser with an activity comparable to the free bacteriochlorin but the fluorescence of the naphthalimide moiety was quenched by FRET to the bacteriochlorin. However, the naphthalimide fluorescence could still be detected *in vitro* due to photobleaching of the bacteriochlorin acceptor, and thus inhibition of FRET.[283]

BODIPY dyes have also been employed in conjunction with tetrapyrroles to form theranostic PDT compounds. Van Lier and co-workers coupled BODIPYs to the meso and β positions of Zn(II) phthalocyanines to obtain multimodality molecules, which can simultaneously serve as fluorescence imaging probes, photosensitisers and, potentially, PET agents (**3.4**, Figure 3.3). The BODIPY moieties acted as antenna chromophores, which transferred energy to the phthalocyanine unit whilst the BODIPY emission band was still observed in the conjugates.[284]

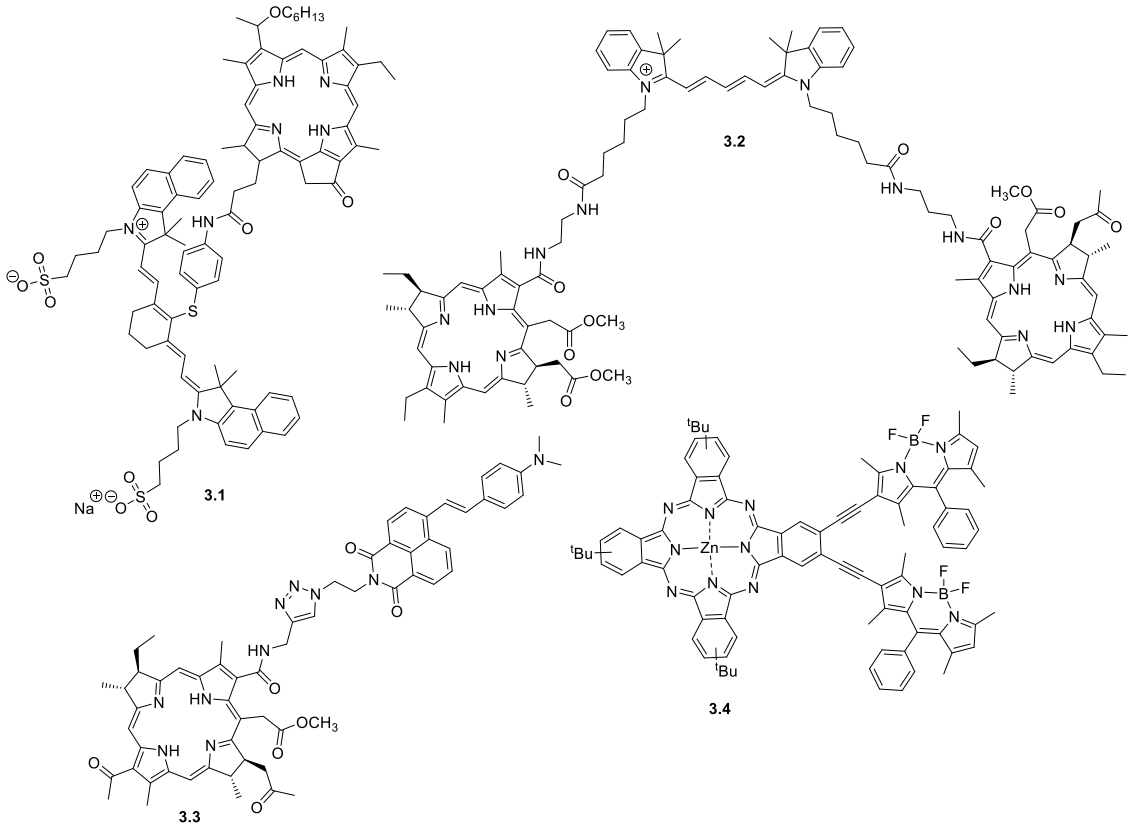

Figure 3.3. Structures of some theranostic tetrapyrrole-fluorescent dye conjugates.

BODIPY dyes have attracted attention as fluorophores due to their strong absorption band, at approximately 500 nm, and high fluorescence quantum yields. They also show relatively good stability and are relatively insensitive to pH and polarity changes. Modifications on their structures can be employed to change the photophysical properties of the BODIPYs. In addition, in most cases their synthesis is facile.[285]

A variety of tetrapyrrole-BODIPY conjugates have been reported in the literature where BODIPY moieties mostly function as light harvesting antenna moieties, which transfer energy to the tetrapyrrole or *vice versa*. These advances have been reviewed, among others, by Ravikanth and co-workers.[286] However, reports of such conjugates as theranostic tools for fluorescence imaging and PDT are scarce.

3.2 Objectives

Protoporphyrin IX has been evaluated as a potent photosensitiser, either when formed endogenously from its ALA precursor or when administered exogenously, usually when attached to a tumour tissue targeting moiety.[103,287] In general, the fluorescence of PPIX can be used to monitor the porphyrin‘s localisation in cells and in living organisms. However, this approach comes with several limitations, e.g., some overlap of the PPIX absorption

spectrum with that of hemoglobin in the blood. In addition, when PPIX is excited directly, it produces singlet oxygen species which cause photobleaching of the photosensitiser, thus PPIX fluorescence decreases.[288]

Herein, it was aimed to synthesise PPIX-based probes, which carry BODIPY moieties for potential physiological imaging applications. BODIPY dyes typically show excellent fluorescence properties. It was anticipated that, when conjugated to PPIX, the BODIPY moieties could serve as fluorophores, which cover a different spectral absorption range to that of simple PPIX. Thus, they have the potential to give a stronger fluorescence response and the direct excitation of PPIX could be avoided.

After efficient methodologies for bromination and Pd-catalysed coupling reactions on PPIX-DME (**1.23**) have been developed (see Chapter 2), BODIPY dyes, with varying photophysical properties, will be coupled to di-brominated PPIX-DME. These include a conventional BODIPY dye displaying green light absorption and emission as well a distyryl-BODIPY and an aza-BODIPY derivative, both exhibiting red light absorption and emission. Different methods for linking the units will be employed, including Sonogashira coupling reactions *via* an ethynyl linker and Suzuki-Miyaura coupling reactions for direct BODIPY-porphyrin linkage. In addition, the synthesis of a porphyrin-BODIPY triad with the BODIPY moieties axially coordinated to the Sn(IV) metal centre of the porphyrin will be investigated.

The absorption and emission properties of the so-obtained porphyrin-BODIPY triads should be investigated to determine to what extent the individual photophysical properties of the moieties are retained and if indications of energy transfer between the units can be found.

3.3 Synthetic Approaches towards the Attachment of Different BODIPY Dyes to PPIX-DME

3.3.1 Synthesis of a PPIX-DME-BODIPY Dye Conjugate

Based on previous investigations concerning bromination and Pd-catalysed coupling reactions on PPIX-DME, it was decided to use the same reaction sequence for the attachment of a BODIPY dye to di-brominated PPIX-DME **2.39**. A BODIPY with a phenylboronic acid substituent in the meso-position (**3.7**) was synthesised in a one-pot procedure from 2,4-dimethylpyrrole **3.5** and (4-formylphenyl)boronic acid **3.6** as reported by Bai *et al.* (Scheme 3.1).[289] Subsequently, it was coupled to dibromo-porphyrin **2.39** under Suzuki-Miyaura reaction conditions as outlined in Chapter 2. Purification of product **3.8** proved to be tedious due to the formation of multiple reaction products and presumably interactions between the products and free BODIPY starting material, which made their

separation difficult. Isolation of pure **3.8** in a 24% yield was accomplished after silica gel column chromatography using different solvent systems (dichloromethane (DCM)/methanol (MeOH) and *n*-hexane/ethyl acetate).

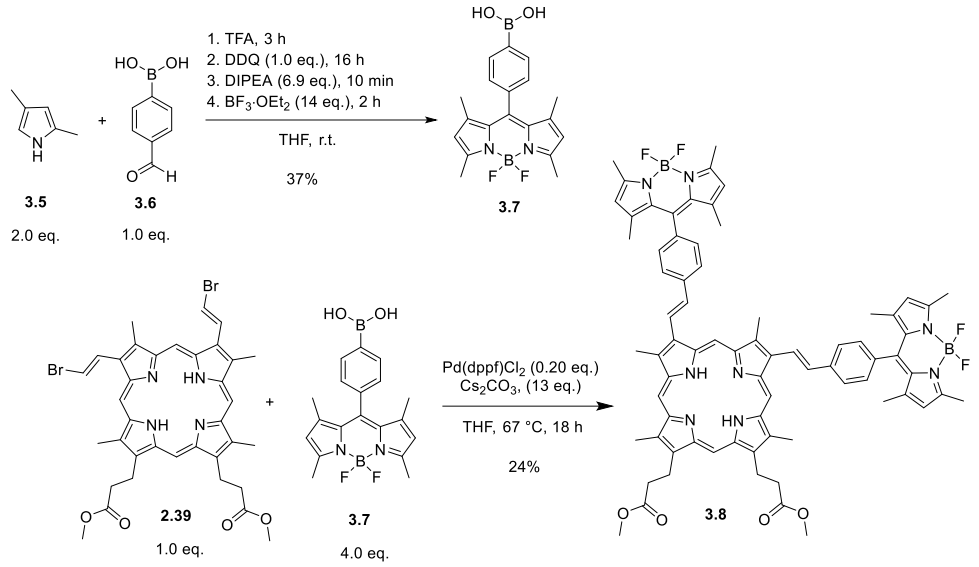

Scheme 3.1. Synthesis of BODIPY **3.6** *via* an acid-catalysed condensation reaction and subsequent Suzuki coupling with di-brominated PPIX-DME **2.39** to give the porphyrin-BODIPY triad **3.8**.

The optical properties of the triad were studied using ultraviolet-visible (UV-Vis) and fluorescence spectroscopy. At first, the single components PPIX-DME **1.23** and BODIPY **3.7** were analysed. PPIX-DME was chosen for these measurements instead of di-brominated PPIX-DME **2.39** since halogen substituents are known to quench fluorescence due to their enhanced intersystem crossing rates.[290] The absorption spectrum of PPIX-DME showed the characteristic Soret band maximum at 409 nm as well as four Q bands with maxima at 507, 543, 579 and 633 nm. When excited at 409 nm, an intense porphyrin emission was observed with the main maximum at 633 nm and a less intense emission band at 701 nm (Figure 3.4a). The 4-phenylboronic acid-substituted BODIPY **3.7** displayed one major absorption band with a maximum at 503 nm. Excitation close to the maximum at 493 nm resulted in intense emission with a maximum at 511 nm, which showcases the characteristic small Stoke‘s shift of BODIPY dyes (Figure 3.4b). The porphyrin-BODIPY triad **3.8** possessed absorption features of the two single components: The Soret absorption band of the porphyrin moiety at 409 nm and its three Q bands at 554 nm, 584 nm and 640 nm. The absorption band of the BODIPY moiety was observed at 503 nm. It overlapped with the porphyrin unit’s first Q band. Upon excitation of the conjugate at 409 nm corresponding to the Soret band of the porphyrin moiety, characteristic porphyrin emission with maxima at 642 nm and 711 nm was detected. The same was observed when **3.8** was

excited in the Q band of the porphyrin moiety at 554 nm. Interestingly, when irradiated at 493 nm in the main absorption band of the BODIPY unit, the same emission pattern with maxima at 642 nm and 712 nm was obtained. The characteristic emission band of the BODIPY moieties was not observed. This pointed towards excitation energy transfer from the BODIPY units to PPIX-DME, resulting in sensitised PPIX-DME fluorescence while the BODIPY's emission was quenched. This finding suggests that triad **3.8** cannot function as an ideal theranostic probe since the emission from the BODIPY moiety cannot be exploited for imaging purposes. Therefore, other ways of producing fluorescent BODIPY-porphyrin conjugates were investigated.

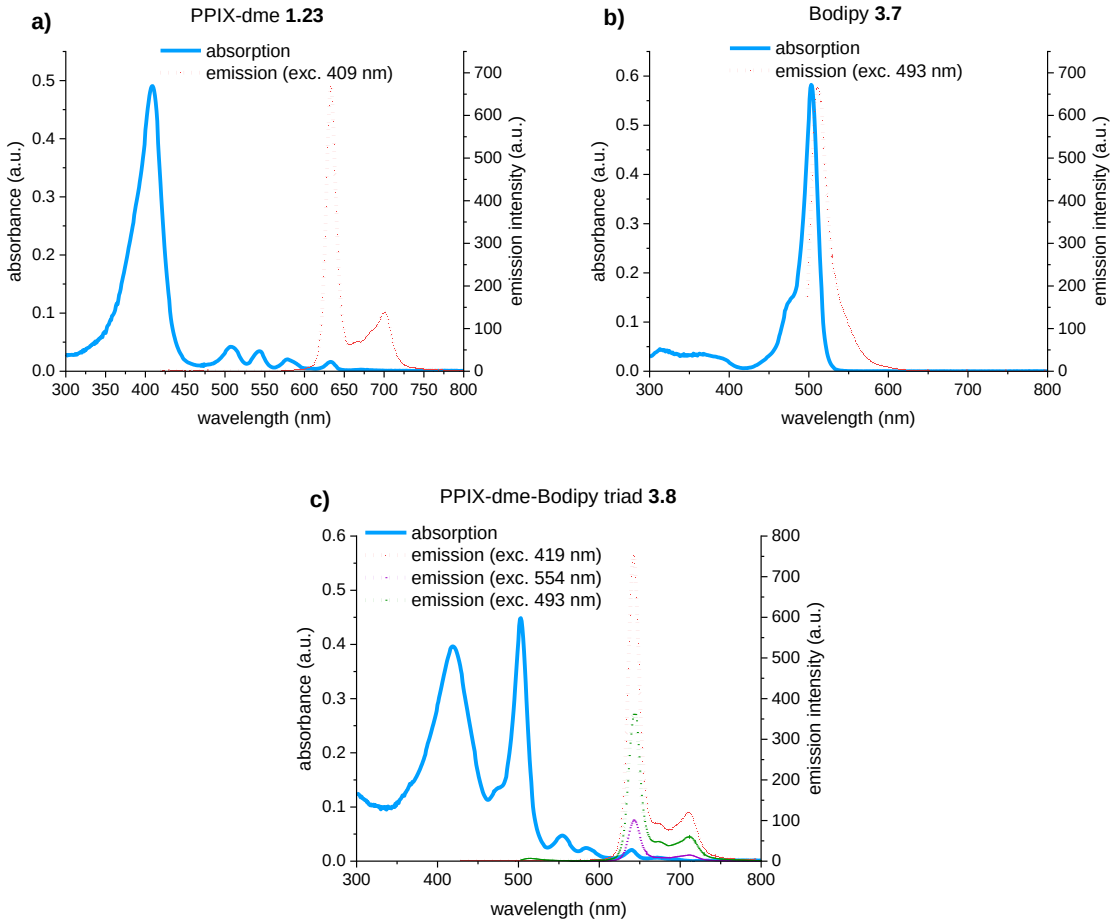

Figure 3.4. Absorption and emission spectra **a)** of free PPIX-DME **1.23**, **b)** free BODIPY **3.7** and **c)** the conjugate of PPIX-DME and BODIPY **3.8** recorded in DCM. Emission spectra were recorded upon excitation in the Soret band (409 nm, 419 nm) or Q band (554 nm) of the porphyrin or porphyrin moiety as well as upon irradiation in the main BODIPY absorption band at 493 nm.

3.3.2 Synthesis of a Sn(IV) Protoporphyrin IX Dimethyl Ester Complex with Axially Ligated BODIPY Units

In search of a different approach towards a dual-function PPIX-DME-BODIPY conjugate, publications detailing the synthesis and spectroscopic properties of axially linked porphyrin-fluorophore complexes were reviewed. In 2002, Kumar *et al*. described the synthesis of dyads, triads and tetrads in which anthracene moieties are bound to a Sn(IV) porphyrin either covalently at the meso positions and/or *via* axial ligation to the central metal (Figure 3.5).[291] Sn(IV) porphyrins can coordinate two additional ligands on either side of the porphyrin plane. They are known to have a strong affinity for oxygen donor ligands and therefore can be used to construct arrays through metal-ligand coordination.[292] Thus, Kumar *et al.* used 9-anthracenemethanol for ligation *via* the formation of an oxygen-Sn(IV) bond. While in the axially coordinated porphyrin-anthracene complex **3.9** the anthracene fluorescence was mainly retained, in compounds where the anthracene subunits were bound covalently (**3.10** and **3.11**) their fluorescence was strongly quenched by energy transfer of the excited anthracene unit to the Sn(IV) porphyrin (Figure 3.5). The authors suggested that this observation was due to the orientational dependence of energy transfer and that the transfer was strongly favoured in the peripheral arrangement of the porphyrin and anthracene as opposed to the axial arrangement.[291] Using the same concept, Lazarides *et al*. expanded the scope of these Sn(IV) porphyrin coordination complexes with fluorophores using phenol- and benzoic acid-substituted BODIPY dyes as axial ligands (Figure 3.5). The phenolate-linked porphyrin-BODIPY triad **3.12** showed almost no emission upon excitation of the BODIPY moiety. This finding was attributed to energy transfer from the excited BODIPY to the porphyrin unit to form the porphyrin singlet excited state, which is quenched by the subsequent formation of a charge-separated state. On the other hand, excitation of the BODIPY moieties in triad **3.13**, which are coordinated to the porphyrin metal centre *via* benzoate bridges, led to efficient energy transfer from the BODIPY units to the porphyrin. The benzoate moieties did not mediate electron transfer, therefore quenching of the Sn(IV) porphyrin singlet excited state did not occur *via* this pathway and sensitised porphyrin emission was observed.[293]

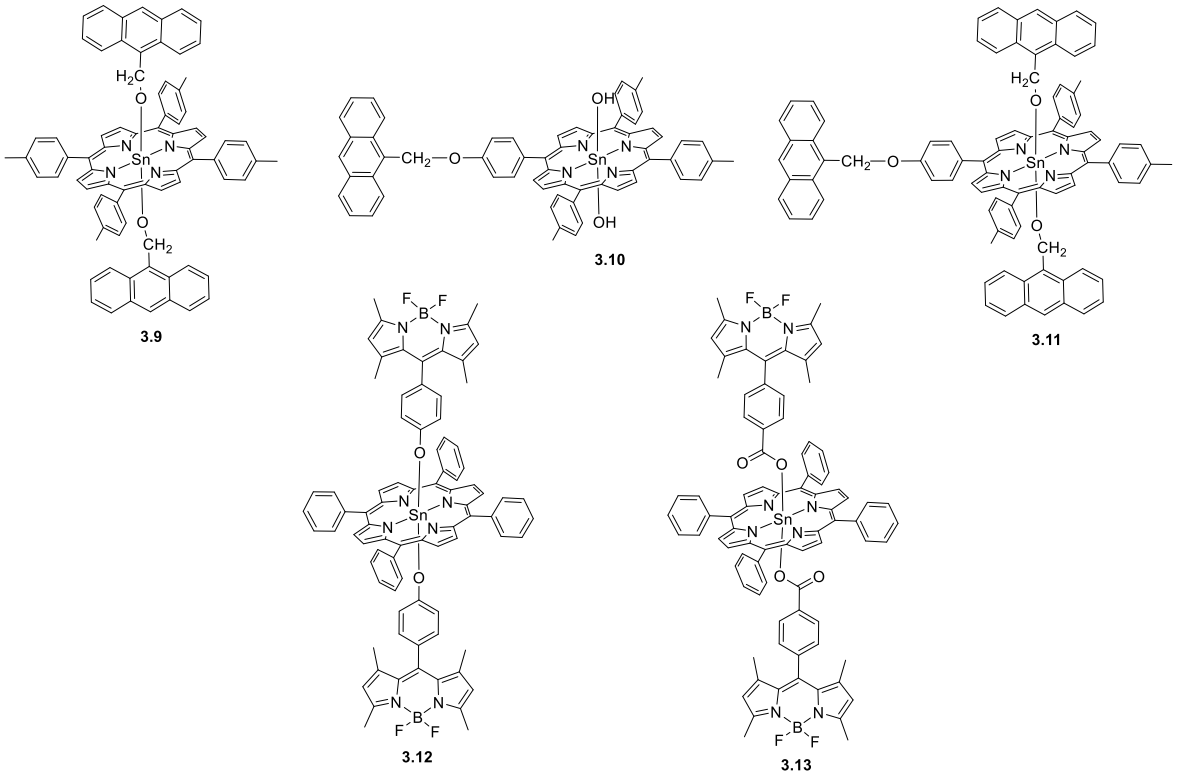

Figure 3.5. Structures of previously synthesised Sn(IV) porphyrin-anthracene[291] and -BODIPY[293] complexes.

It was intended to synthesise axially linked PPIX-DME-BODIPY complexes and to investigate their optical properties. Firstly, the synthesis of a PPIX-DME Sn(IV) complex (Sn(IV)PPIX-DME) was attempted. Initial attempts were made to selectively obtain the dichloro-Sn(IV)PPIX-DME complex but it was found that this compound reacted with water and alcohol residues during the metalation reaction and the work-up, resulting in product mixtures. Hence, the synthesis of the dihydroxo-Sn(IV) porphyrin complex became the focus. The dihydroxo-Sn(IV) porphyrin complex can act as a useful starting material for replacement reactions with alcohols or carboxylates.[294] PPIX-DME **1.23** and $SnCl_2$•$2H_2O$ were dissolved in a mixture of chloroform and ethanol and the mixture was heated at 61 °C for 2.5 h (Scheme 3.2). The reaction of $SnCl_2$ in the presence of ethanol likely resulted in the formation of a mixture of chloro- and ethoxo-complexes of the Sn(IV) porphyrin.[294] An immediate aqueous work-up of the crude solids after the reaction was employed to convert the mixed complexes to the dihydroxo-Sn(IV) complex. The product **3.14** could be isolated in 72% yield.

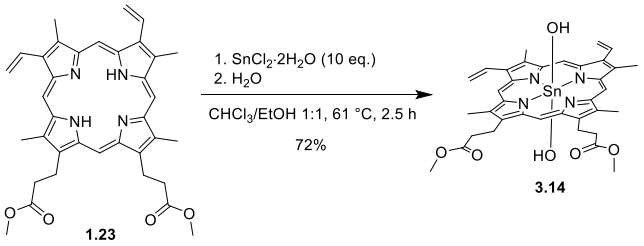

Scheme 3.2. Synthesis of the dihydroxo-Sn(IV)PPIX-DME complex **3.14** from PPIX-DME.

Conversion of dihydroxo-Sn(IV) porphyrin complexes to alkoxo-Sn(IV) complexes can be accomplished if the pK_a value of the hydroxyl substrate is lower than that of water.[294] In a first trial, it was attempted to replace the hydroxo ligands in compound **3.14** with a benzyl alcohol substituted BODIPY **3.16**. The aim was to obtain a BODIPY-PPIX-DME triad with similar photophysical properties as the di(9-anthracenemethanolate)-porphyrin complex **3.9** prepared by Kumar *et al.*, in which almost no quenching of the anthracene-based fluorescence occurred.[291] BODIPY **3.16** was synthesised in a one-pot condensation procedure from 2,4-dimethylpyrrole **3.5** and 4-(hydroxymethyl)benzaldehyde.[295] In the next step, complex formation with Sn(IV)PPIX-DME was attempted. Several literature procedures, which had previously been applied for similar complex formations, were tested.[291,293,295] However, prolonged reflux of the BODIPY-Sn(IV) porphyrin mixture in different solvents (benzene, chloroform and pyridine) did not yield any BODIPY-porphyrin triad **3.16** (Scheme 3.3).

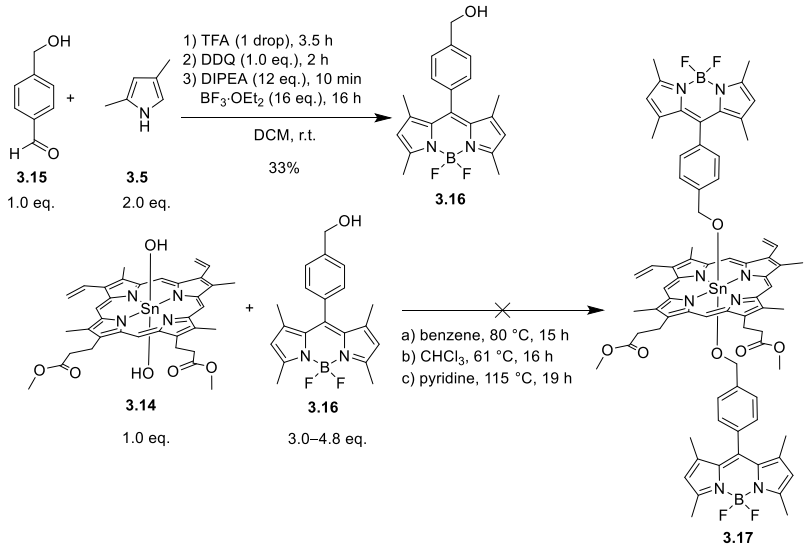

Scheme 3.3. Attempted synthesis of an axially linked Sn(IV)PPIX-DME BODIPY triad **3.17** using a benzylalcohol-substituted BODIPY **3.16**.

It was reasoned that the benzylic hydroxy group of **3.16** does not readily engage in complex formation with Sn(IV)PPIX-DME, possibly due to its relatively large pK_a value compared to

phenylic hydroxy groups. Therefore, it was decided to repeat the reaction, this time using a 4-hydroxyphenyl-substituted BODIPY ligand, similar to that reported by Lazarides *et al*.[293] meso-4-Hydroxyphenyl-substituted BODIPY **3.18** was synthesised according to a literature procedure.[296] A mixture of Sn(IV)PPIX-DME and BODIPY **3.18** was refluxed in benzene for 16 h (Scheme 3.4). TLC analysis on neutral aluminium oxide showed conversion of the starting materials and the appearance of a spot indicating product formation. In contrast, TLC analysis on silica gel showed only starting materials, indicating that hydrolysis of the complex occurred. Hence, aluminium oxide was chosen for the purification of the crude products *via* column chromatography. Triad **3.19** was isolated in 14% yield.

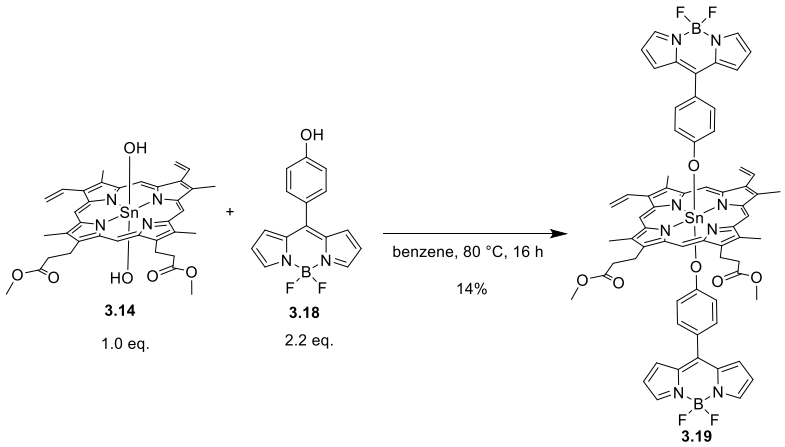

Scheme 3.4. Synthesis of an axially ligated Sn(IV)PPIX-DME-BODIPY triad **3.19** with phenolate bridges mediating the binding to the metal centre.

Optical characterisation of complex **3.19** was carried out using absorption and emission spectroscopy. The Sn(IV)PPIX-DME starting material showed a Soret band with a maximum at 416 nm and only two Q bands at 547 nm and 585 nm. This is characteristic of a metalated porphyrin (Figure 3.6a). Excitation in its Soret band at 417 nm resulted in a fluorescence response with two emission bands at 588 nm and 641 nm. The emission intensity of the Sn(IV) porphyrin was found to be lower than that of the free-base PPIX-DME. BODIPY **3.18** showed a main absorption band at 501 nm and a weaker but broader band at 382 nm, as well as intense emission at 514 nm (Figure 3.6b). The axial coordination complex **3.19** of Sn(IV)PPIX-DME and 4-hydroxyphenyl-substituted BODIPY absorbed at 412 nm, 497 nm, 545 nm and 583 nm, thus the complex essentially displayed the sum of the absorption properties of its single components (Figure 3.6c). Excitation in the porphyrin moiety's Soret band at 412 nm mostly resulted in emission originating from the porphyrin unit with maxima at 586 nm and 641 nm alongside weak emission from the BODIPY moieties at 514 nm. In this case, the emission of the BODIPY units was probably observed due to an overlap of the porphyrin moiety's Soret absorption band with the minor absorption

band of the BODIPY units. When complex **3.19** was irradiated at 487 nm the BODIPY moieties were excited selectively. The main emission at 515 nm stemmed from the BODIPY moieties, while weaker emission originating from the porphyrin was also observed. This suggests that partial energy transfer from the BODIPY units to the porphyrin took place while some BODIPY fluorescence was retained. However, in line with the findings made by Lazarides *et al*., the overall fluorescence of the coordination complex was lower than the emission of free BODIPY **3.18** (Figure 3.6b). They reported on a Sn(IV) porphyrin linked to BODIPY dyes *via* phenolate bridges (compound **3.12**, Figure 3.5), the authors attributed this to quenching by electron transfer and charge separation pathways.[293]

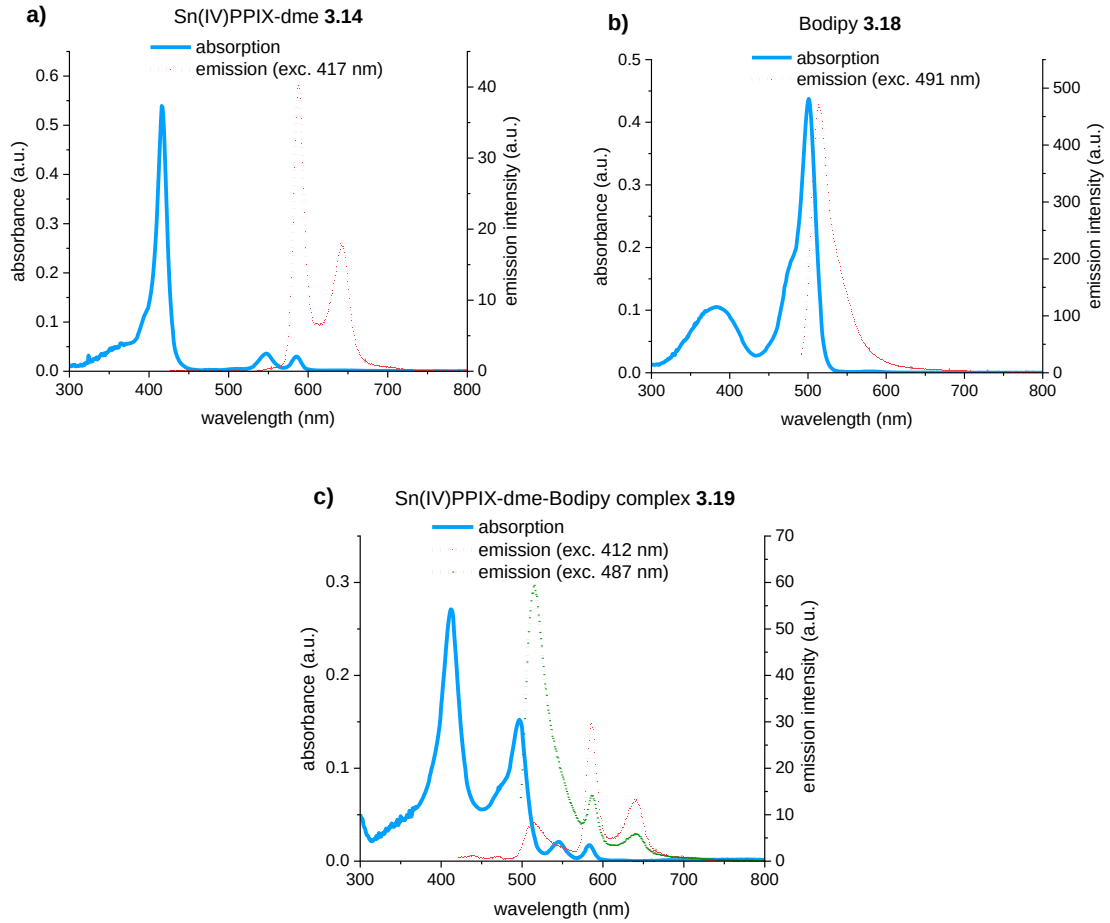

Figure 3.6. Absorption and emission spectra of **a)** free Sn(IV)PPIX-DME **3.14**, **b)** free BODIPY **3.18** and **c)** the axial coordination complex of Sn(IV)PPIX-DME and BODIPY **3.19** recorded in DCM. Emission spectra were recorded upon excitation of the Soret band (417 nm or 412 nm) of the porphyrin or porphyrin moiety, and of the absorption band of the BODIPY moiety (491 nm or 487 nm).

Based on the results of the optical measurements obtained for triad **3.19**, namely its rather weak overall emission, the synthesis of a different triad was attempted with the aim to

minimise energy transfer and electronic interactions between the moieties and to increase the fluorescence of the complex. A new triad with favourable emission properties was designed with an increased distance r between the donor and acceptor moieties to reduce the efficiency E of the resonance energy transfer based on the correlation $E \sim r^{-6}$. A second consideration made was the inclusion of alkyl spacers between the porphyrin and BODIPY units to hamper the electronic communication between the moieties. Hence, it was aimed to introduce a long alkyl chain spacer between Sn(IV)PPIX-DME and BODIPY **3.18**. Previous experiments showed that while the hydroxyl ligands in Sn(IV) porphyrin **3.14** underwent displacement with aryl alcohols (BODIPY **3.18**), the reaction did not proceed with an alkyl-bound hydroxyl group (BODIPY **3.16**). As outlined earlier, this was likely based on the different acidities of aryl and alkyl alcohols. It was assumed that low reactivity would be encountered again if a direct replacement of the hydroxyl ligands in Sn(IV)PPIX-DME with long-chain aliphatic alcohols was attempted.

Another strategy for the attachment of alkoxy ligands was reported for Sb(V) porphyrins. Shiragami *et al*. reacted a dihydroxo-complex of (tetraphenylporphyrinato)antimony(V) with a bomoalkyl-substituted BODIPY to produce an axial coordination complex of an Sb(V) porphyrin with BODIPYs.[297] In this case, nucleophilic substitution of the bromides by the Sb-bound hydroxyl groups was achieved. The same reaction strategy was applied to the dihydroxo-Sn(IV)PPIX-DME complex.

In the first step, 4-hydroxyphenyl-substituted BODIPY **3.18** was appended with a bromoalkyl chain (Scheme 3.5). The reaction of **3.18** with 1,4-dibromobutane and K_2CO_3 in DMF gave alkylated BODIPY **3.20** in 48% yield. For the intended formation of the BODIPY-Sn(IV)PPIX-DME triad **3.21**, the starting materials **3.14** and **3.20** were heated to reflux with K_2CO_3 and 18-crown-6-ether in acetonitrile. Product formation was not observed after 17 h. Different reaction conditions were tested using K_2CO_3 and a catalytic amount of NaI in DMF. Again, no complex formation was detected.

The difficulties in the reactivity as well as the stability encountered with Sn(IV)PPIX-DME complexes prompted investigations into more robust ways to synthesise theranostic porphyrin-BODIPY conjugates.

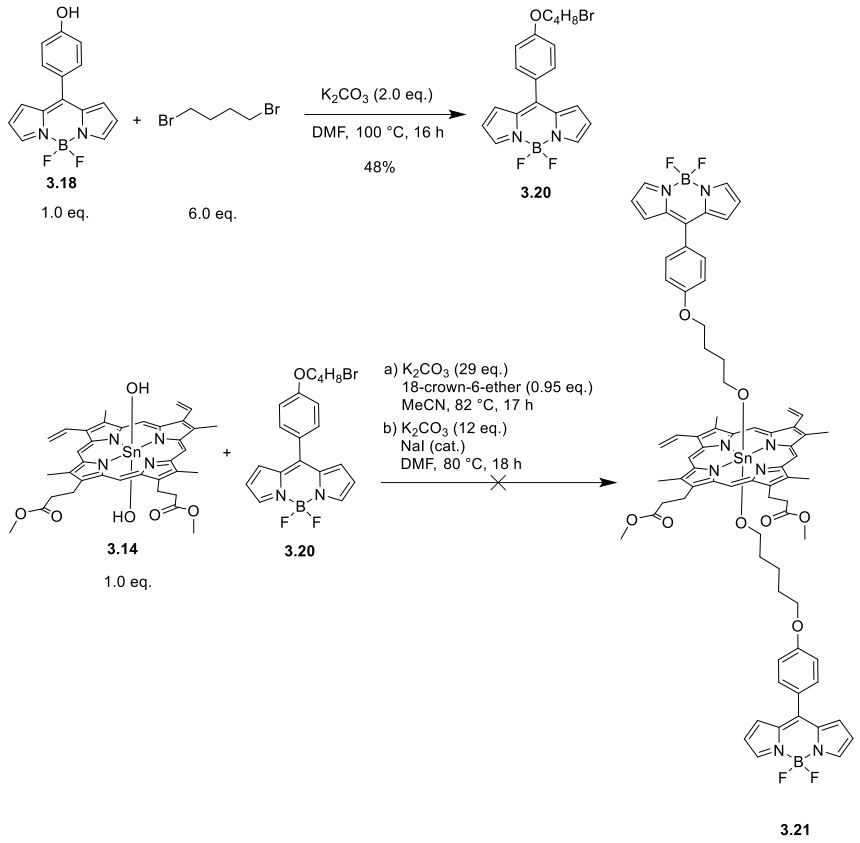

Scheme 3.5. Synthesis of a bromoalkyl-substituted BODIPY derivative **3.20** and attempted alkylation of dihydroxo-Sn(IV)PPIX-DME **3.14**.

3.3.3 Synthesis of Protoporphyrin IX Dimethyl Ester Conjugates with Aza- and Distyryl-BODIPYs

Classic BODIPY dyes typically absorb, roughly speaking, in the spectral window around 500 nm and commonly show small Stokes shifts. However, these properties can be tuned by the adjustment of the substitution pattern or modification of the core.[285,298] One such modification of the BODIPY scaffold, which proved effective in the past is the replacement of the methine (meso) carbon with a nitrogen atom to give so-called „aza-BODIPY“ dyes. This alteration of the structure leads to a decreased HOMO-LUMO gap, hence the absorption and emission of the aza-BODIPY is shifted to the far-red or near-infrared regions.[299] These special properties render aza-BODIPYs interesting candidates for conjugation to porphyrins. More specifically, in a conjugate of PPIX-DME with an aza-BODIPY the efficiency and direction of the excitation energy transfer are anticipated to be different because of the change in the emission/absorption spectral overlap. A few examples of aza-BODIPY-porphyrin dyads and triads have been reported previously. Depending on the nature of the compounds, different observations were made concerning the energy and electron transfer behaviour between the moieties.[300]

Herein, it was aimed to synthesise an aza-BODIPY dye with red-shifted absorption and emission maxima, to append it onto PPIX-DME *via* Pd-catalysed coupling procedures and to investigate its optical properties.

As opposed to classical BODIPY dyes which can be obtained by simple acid-catalysed condensation reactions from aldehydes and pyrroles, the aza-BODIPY needs to be constructed in a stepwise manner. Of the several possible routes to synthesise aza-BODIPYs, the O'Shea and co-workers method was chosen (Scheme 3.6).[299] Chalcone **3.22** was transformed to the nitroketone **3.23** by the Michael addition of nitromethane, followed by condensation of **3.23** with ammonium acetate. Boron insertion into the azadipyrromethene **3.24** was effected by diisopropylethylamine (DIPEA) and boron trifluoride diethyl etherate ($BF_3{\cdot}OEt_2$).

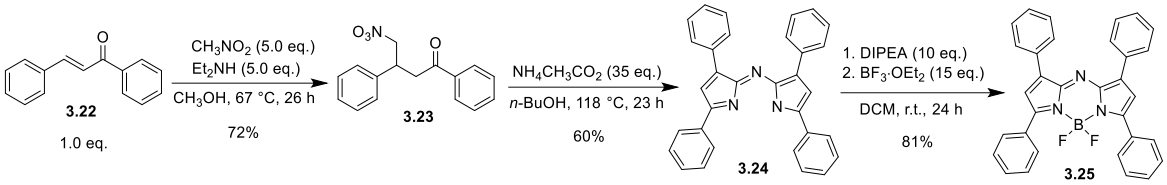

Scheme 3.6. Synthesis of tetraphenyl-substituted aza-BODIPY **3.25** from chalcone **3.22**.

The aza-BODIPY was then functionalised for use in Pd-catalysed coupling reactions by mono-bromination in the β-position using NBS (Scheme 3.7). Stirring of the aza-BODIPY **3.25** solution with 0.9 eq. NBS in a mixture of DCM and DMF at room temperature overnight resulted in the conversion of about 75% of the starting material to the mono-brominated species, while approximately 25% unbrominated starting material remained as determined by ^{1}H NMR spectroscopy. Another 0.40 eq. of NBS was added to the mixture and the reaction was continued for 16 h. The brominated product **3.26** was isolated together with unbrominated starting material (approx. 6%). The mixture could not be separated by chromatography and was used as such for the next step.

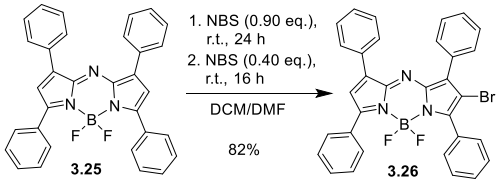

Scheme 3.7. Mono-bromination of aza-BODIPY **3.26**.

Initially, direct Sonogashira coupling of mono-brominated aza-BODIPY **3.26** with acetylene-appended PPIX-DME **2.54** (prepared earlier, see Chapter B) was attempted; however, the conversion of the starting material was found to be low and no product was isolated

(Scheme 3.8). It was assumed that the reaction with ethynylated PPIX-DME **2.54** could not proceed efficiently due to steric hindrance between the porphyrin core and the phenyl rings in the α- and β-positions of the aza-BODIPY scaffold. It was predicted that an additional spacer unit on the porphyrin to move the reactive ethynyl moiety further away from the porphyrin macrocycle could enhance the reactivity. However, when porphyrin **2.47** which carries phenylacetylene moieties on the vinyl groups (prepared earlier, see Chapter B) was reacted with monobromo-aza-BODIPY **3.26** under Sonogashira coupling reaction conditions, product formation was not observed (Scheme 3.8).

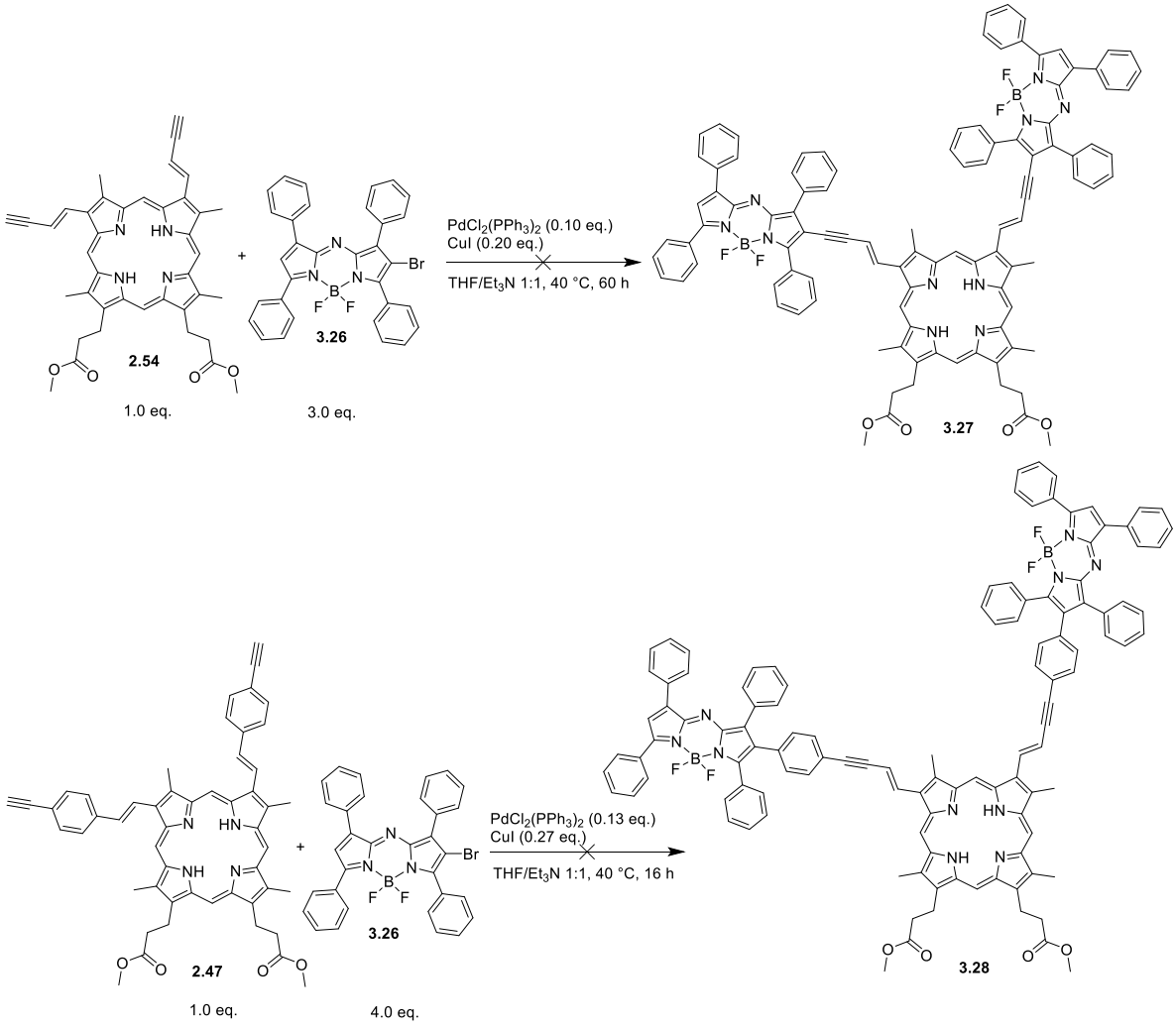

Scheme 3.8. Attempted Sonogashira coupling reactions with two different acetylene-appended PPIX-DME derivatives **2.54** and **2.47** and monobromo-aza-BODIPY **3.26**.

It was reasoned that the reactivity of acetylene-appended protoporphyrin derivatives in this transformation was low and a different approach was taken. Instead, the 4-((trimethylsilyl)ethynyl)phenyl spacer was appended onto the aza-BODIPY core by a Suzuki

coupling reaction of **3.26** with boronic ester **3.29** using $Pd(PPh_3)_4$ as a catalyst and Na_2CO_3 as a base in a mixture of toluene, ethanol and water (Scheme 3.9). The coupling product **3.30** could be isolated in 65% yield. However, it was found that the aza-dipyrrin core had lost the BF_2 unit. Without proceeding with the full characterisation of the coupling product, reinsertion of BF_2 using $BF_3{\cdot}OEt_2$ and removal of the TMS protection group with tetrabutyl ammonium fluoride (TBAF) were carried out to yield an aza-BODIPY dye bearing a free acetylene moiety (**3.32**).

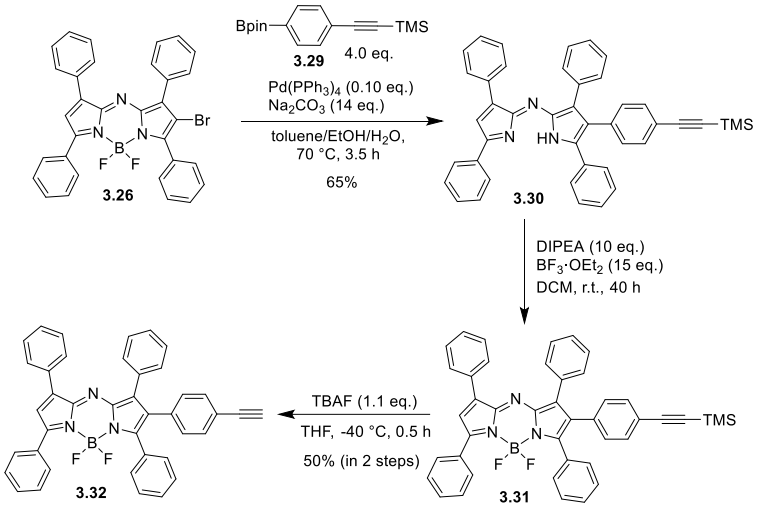

Scheme 3.9. Synthesis of a 4-ethynylphenyl-appended aza-BODIPY derivative (**3.32**).

The Sonogashira coupling precursor was then reacted with dibromo-PPIX-DME **2.39** using the same reaction conditions employed previously for this porphyrin (see Chapter 2) (Scheme 3.10). The formation of coupling products was indicated by the observation of green coloured spots during TLC analysis.

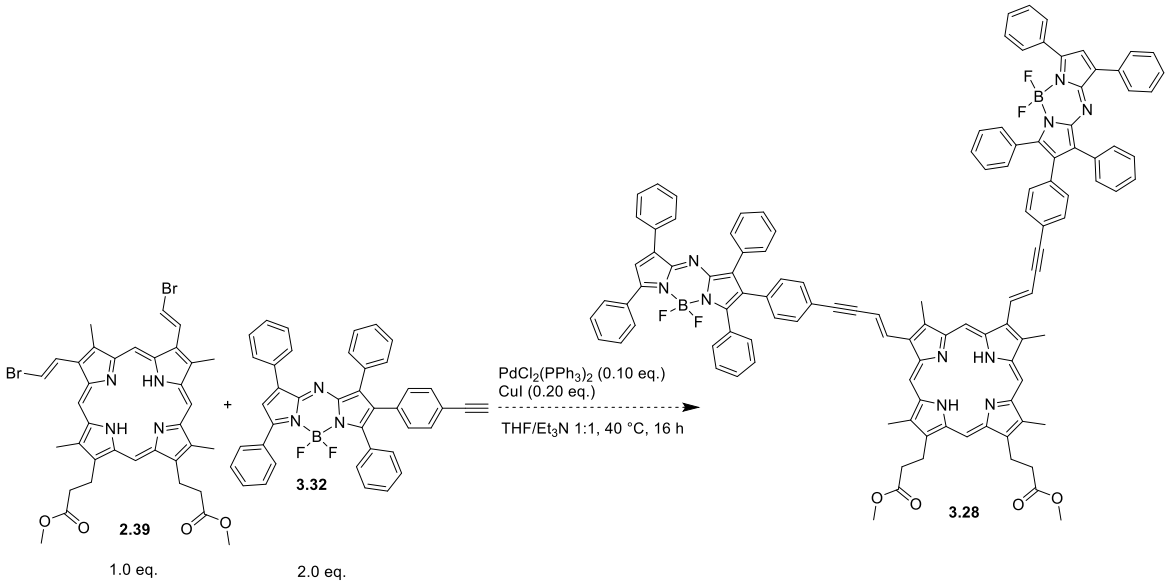

Scheme 3.10. Synthesis of a PPIX-DME-aza-BODIPY triad **3.28** from dibromo-PPIX-DME **2.39** and 4-ethynylphenyl-substituted aza-BODIPY **3.32**.

Isolation of the single product by column chromatography on aluminium oxide proved difficult. The major green fraction was confirmed to be a mixture of mono- and bis-coupled products, **3.33** and **3.34** (Figure 3.7), as indicated by HR-MALDI mass spectrometry. A peak at *m/z* = 1215.4055 corresponds to the mono-coupled product **3.33** in which one bromine moiety remained but the BF_2 unit of the aza-BODIPY was lost. A peak at *m/z* = 1732.7000 is likely due to the bis-coupled product in which one of the two BF_2 units was lost. It is not clear if BF_2 was removed during the Pd-catalysed coupling reaction or during the mass spectrometry measurement.[301]

Although it was shown that coupling products formed in the reaction between aza-BODIPY **3.32** and porphyrin **2.39**, the difficulties in the purification of the products, significant side product formation and tedious preparation of the starting materials prompted us to investigate other possibilities for the preparation of PPIX-DME conjugates with red light-absorbing fluorophores.

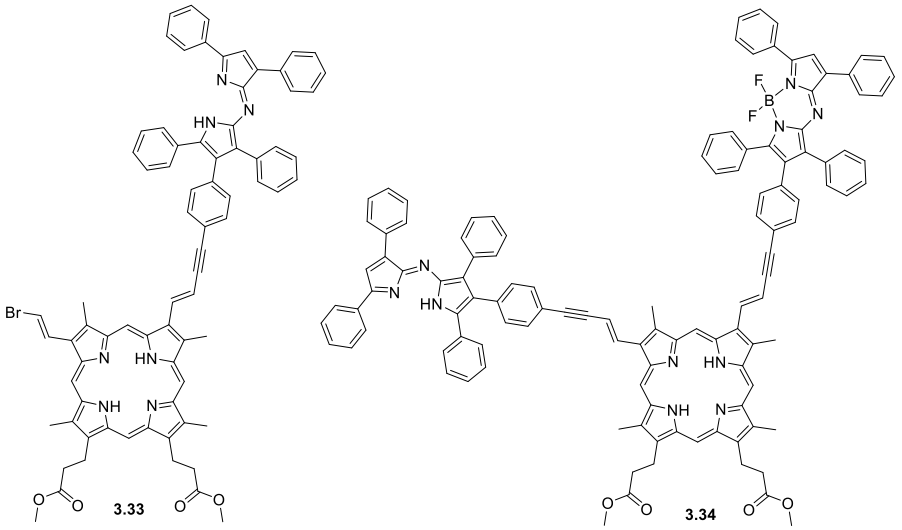

Figure 3.7. Structures **3.33** and **3.34** which are assumed to correspond to the peaks at *m/z* = 1215.4055 and 1732.700 found by HR-MALDI-MS analysis in the major product fraction of the Sonogashira coupling reaction.

Another class of BODIPY dyes whose synthesis and use has been reported more frequently in recent years due to their potential to absorb red light are distyryl-BODIPYs. These compounds were prepared for the first time in 2001 by Rurack *et al*. who condensed α-styrylpyrroles with aldehydes.[302] Later, the synthesis was optimised by Akkaya and co-workers who prepared modified 3,5-dimethyl-substituted BODIPY precursors by a Knoevenagel condensation with aldehydes. The conjugation with styryl moieties shifts the BODIPY dyes‘ absorption maximum beyond 650 nm.[303]

Due to the apparent ease of this transformation, a one-step reaction on a readily available BODIPY precursor, it was decided to attempt the modification of PPIX-DME with distyryl-BODIPYs. A ((trimethylsilyl)ethynyl)phenyl-substituted BODIPY **3.36** was synthesised by a condensation reaction between 2,4-dimethylpyrrole and ((trimethylsilyl)ethynyl)benzaldehyde following a standard procedure (Scheme 3.11).[304] Styryl moieties were appended onto the BODIPY core by Knoevenagel condensation of the methyl groups in the 3- and 5-positions with benzaldehyde (4.0 eq.), piperidine and acetic acid in DMF in a microwave reactor at 150 °C.[305] A mixture of TMS-ethynyl-substituted BODIPY **3.37** (45%) and BODIPY **3.38**, which had lost the TMS protection group (44%) were isolated. The use of a strong base in this reaction mediated the TMS group cleavage. The remaining TMS-protected BODIPY fraction **3.37** was deprotected using TBAF.

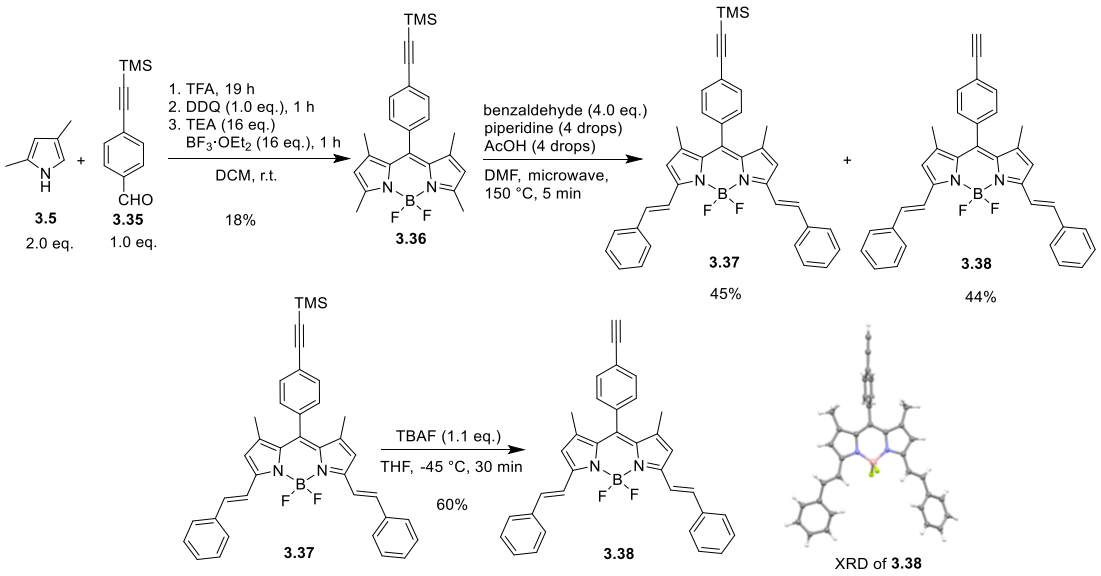

Scheme 3.11. Synthesis of a 4-ethynylphenyl-substituted distyryl-BODIPY **3.38** as a precursor for a Sonogashira coupling reaction. X-ray diffraction (XRD) image of **3.38** in the crystal is shown.

With a sufficient amount of ethynyl-substituted BODIPY precursor **3.38** at hand, a Sonogashira coupling reaction of di-brominated PPIX-DME **2.39** with **3.38** could be performed using $Pd(PPh_3)_2Cl_2$ and CuI as catalysts. Several reaction products were formed. A dark green fraction was isolated by silica gel column chromatography, which was later confirmed to be the bis-coupled product **3.39** by HR-MALDI mass spectrometry. The product was obtained in 17% yield. The ^{1}H NMR spectrum of **3.39**, recorded in different solvents, showed only broad signals, which indicated strong π-π stacking interactions between the molecules.

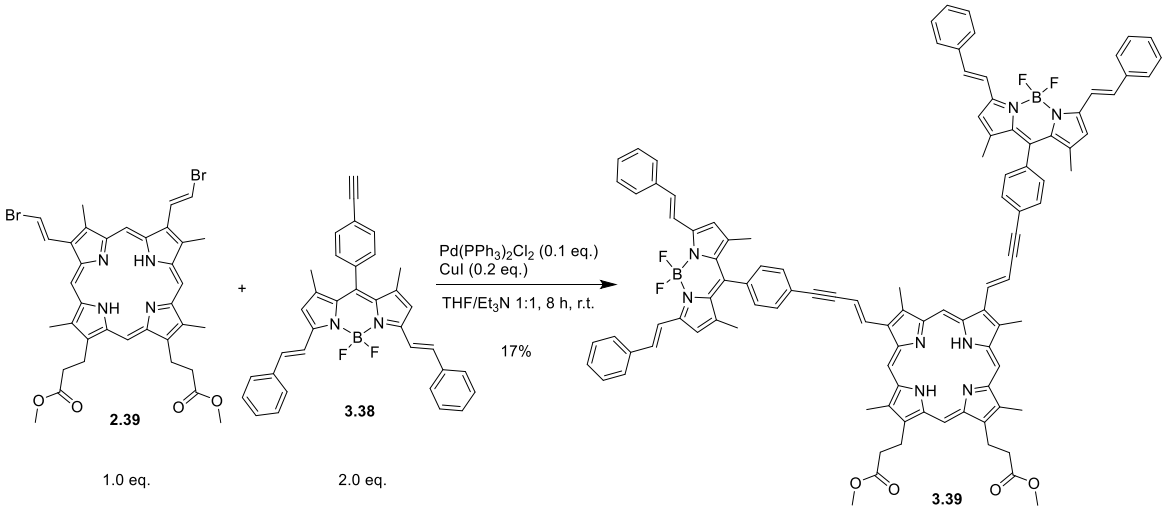

Scheme 3.12. Sonogashira coupling of di-brominated PPIX-DME **2.39** and distyryl-BODIPY **3.38** to give the porphyrin-BODIPY triad **3.39**.

Optical characterisation of the triad **3.39** was carried out using UV-Vis absorption and fluorescence spectroscopy. At first, the absorption spectra of the precursor porphyrin and BODIPY were analysed. PPIX-DME **1.23** showed absorption maxima at 408 nm (Soret band), 508 nm, 542 nm, 579 nm and 633 nm (Q bands). When excited at 408 nm a typical emission spectrum with a main peak at 633 nm and a smaller maximum at 700 nm was obtained (Figure 3.8a). For the distyryl-BODIPY **3.38** absorption maxima were observed at 351, 578 and 629 nm (Figure 3.8b). Taking into account the small Stokes shift typically displayed by BODIPY dyes, **3.38** was irradiated at 610 nm, a slightly lower wavelength than its absorption maximum. This enabled the acquisition of the main emission band in almost full width. The distyryl-BODIPY showed relatively high-intensity emission at 636 nm and 694 nm. The fact that these bands overlapped strongly with the emission of PPIX-DME made differentiating between the porphyrin- and BODIPY-centred emission in the conjugate **3.39** difficult. Therefore, analysis of possible energy transfer processes taking place in the triad could only be based on the emission intensity rather than the location of the emission maxima.

To support the evaluation of the absorption and emission profiles of triad **3.39**, the absorption and fluorescence spectra of a 1:2 mixture of free PPIX-DME and distyryl-BODIPY were analysed (Figure 3.8c). The absorption spectrum of the mixture displayed the sum of the absorption bands observed for the single components. The two lowest energy Q bands of PPIX-DME were covered by the two BODIPY's absorption bands in this region of the spectrum. Excitation of the porphyrin's Soret band at 408 nm resulted in a relatively low-intensity fluorescence with maxima at 633 and 700 nm, indicating that emission mainly originated from the porphyrin. Irradiation with 610 nm light resulted in a 6-

fold increase in emission at 635 nm with another maximum at 693 nm, showing a strong fluorescence response from the BODIPY dye. The weaker fluorescence of the BODIPY in the mixture with PPIX-DME as compared to a solution of the neat BODIPY dye points towards the occurrence of through-space energy transfer to the porphyrin. This process might occur to some extent even under the dilute conditions employed in this study.

The absorption spectrum of the porphyrin-BODIPY triad **3.39** showed the absorption maxima of the BODIPY moieties at 350, 580 and 629 nm as well as the slightly red-shifted Soret band of the porphyrin moiety at 415 nm (Figure 3.8d). On the other hand, no distinct bands corresponding to the Q bands of the PPIX-DME unit were observed. Upon excitation of the Soret band of the porphyrin moiety at 413 nm, relatively strong fluorescence with maxima at 637 nm and 698 nm was detected. The intensity of the first emission maximum was about 3.7 times higher than that of free PPIX-DME (Figure 3.8a) and 3.3 times higher than that of the porphyrin-BODIPY mixture (Figure 3.8c) when the porphyrin Soret band was excited. This pointed towards sensitised BODIPY emission by excitation energy transfer from the porphyrin unit. This finding can be explained by the spectral overlap of the porphyrin's main emission band and the BODIPY's main absorption band, providing a prerequisite for FRET. Electron transfer processes could also have played a role considering that the moieties are in π-conjugation with each other. When the triad **3.39** was excited in the BODIPY moieties' main absorption band at 610 nm, BODIPY emission with maxima at 639 nm and 696 nm was observed. However, this fluorescence was much weaker than what was observed for the free distyryl-BODIPY **3.38** (Figure 3.8b) as well as that of the mixture of porphyrin and distyryl-BODIPY (Figure 3.8c). It can be assumed that energy transfer from the BODIPY to the porphyrin moiety takes place as well. This process is likely to happen due to the spectral overlap of the BODIPY's main emission band and the porphyrin's last Q band as well as the electronic communication between the moieties. Such a phenomenon has been described before as "back-and-forward" or "ping-pong" energy transfer between donor and acceptor moieties.[306] For clarification of the energy transfer mechanisms taking place in the triad, more specialised measurements are required such as transient absorption spectroscopy.

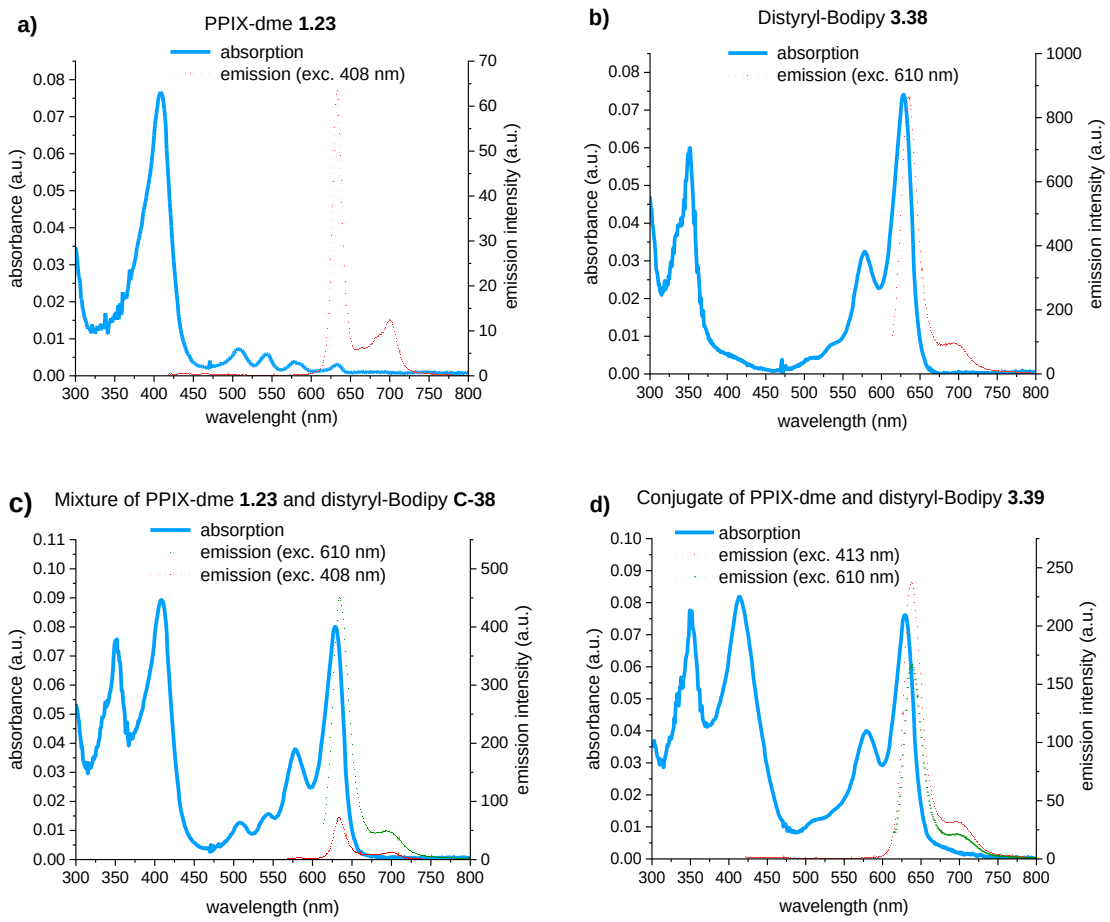

Figure 3.8. Absorption and emission spectra of free PPIX-DME **1.23**, free distyryl-BODIPY **3.38**, a mixture of the two components **1.23** and **3.38** and the conjugate of PPIX-DME and distryryl-BODIPY **3.39** recorded in DCM. Emission spectra were recorded upon excitation of the Soret band (408 nm or 413 nm) of the porphyrin or porphyrin moiety, and upon irradiation of the main BODIPY absorption band (610 nm).

Following the conjugation of distyryl-BODIPY units to PPIX-DME *via* a Sonogashira coupling reaction, it was intended to couple another distyryl-BODIPY derivative to **2.39**. A Suzuki coupling protocol was used. Direct attachment of the BODIPY moieties to the vinyl groups of PPIX-DME *via* Suzuki coupling reactions rather than through ethynyl spacers was expected to result in different torsional angles between the porphyrin and BODIPY planes. This was expected to reduce π-π stacking interactions between the molecules and provide a pathway for characterisation by NMR spectroscopy.

A boronic ester-substituted BODIPY was synthesised based on a literature procedure.[307] In the first step, 4-bromophenyl-substituted BODIPY was formed by a condensation reaction, followed by Pd-catalysed Miyaura borylation (Scheme 3.13).[253a] The subsequent Knoevenagel condensation was found to proceed in a less efficient manner compared to

BODIPY **3.36**. Formation of a mixture of mono- and distyryl-BODIPYs as well as strong interactions between the borylated BODIPYs and the column material complicated the purification process. The di-substituted BODIPY **3.43** was isolated in only 17% yield and impurities remained.

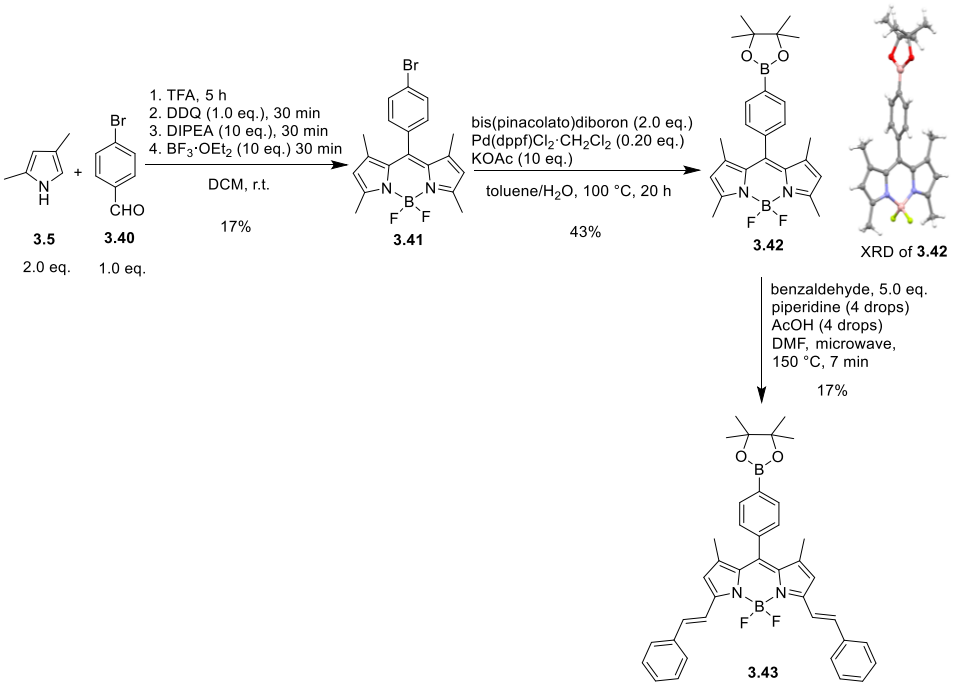

Scheme 3.13. Synthesis of a distyryl-BODIPY with a boronic ester moiety **3.43** as a precursor for Suzuki coupling reactions. X-ray diffraction (XRD) image of **3.42** in the crystal is shown.

Porphyrin **2.39** was reacted with BODIPY **3.43** in THF at 67 °C for 20 h using Pd(dppf)Cl_2 as a catalyst and Cs_2CO_3 as a base (Scheme 3.14). The reaction mostly led to the formation of black decomposition products and coupling products were not isolated. Possibly, deborylation of the BODIPY and polymerisation of the starting materials occurred under the employed reaction conditions.

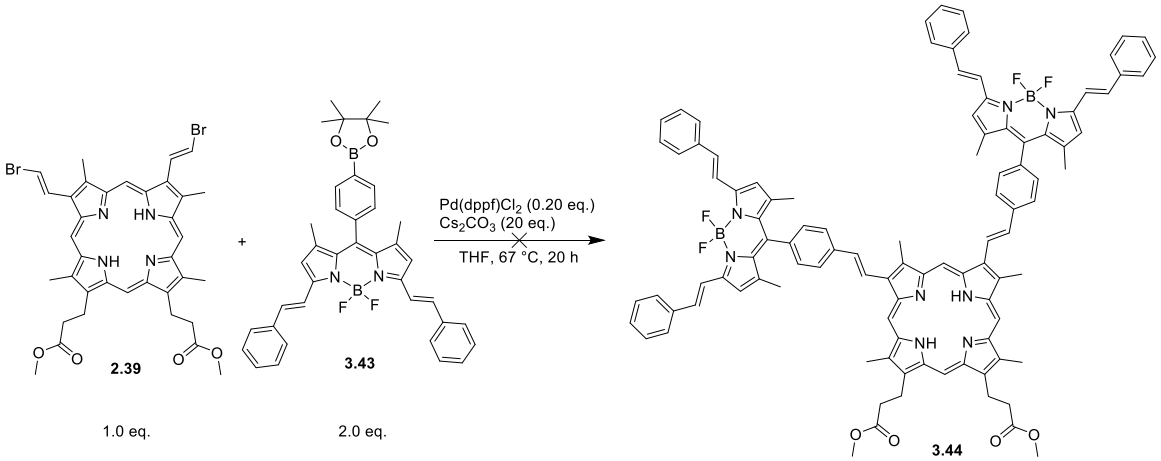

Scheme 3.14. Attempted Suzuki coupling reaction between borylated distyryl-BODIPY **3.43** and di-brominated PPIX-DME **2.39**.

3.4 Conclusion and Outlook

Steps towards the development of theranostic probes were undertaken. The aim of the project was to synthesise PPIX-DME derivatives carrying fluorescent BODIPY moieties. Three different approaches were investigated: The conjugation of a classic BODIPY to the vinyl groups of PPIX-DME, the attachment of BODIPY dyes with red-shifted absorption maxima to a porphyrin and the coordination of hydroxy-substituted BODIPYs to the metal centre of Sn(IV)PPIX-DME. A triad consisting of PPIX-DME and two classic BODIPY moieties (**3.8**) was successfully synthesised by a Suzuki coupling reaction using di-brominated PPIX-DME and a 4-phenylboronic acid-substituted BODIPY. A second porphyrin-BODIPY conjugate, **3.39**, carrying BODIPY moieties with red-shifted absorption and emission maxima was prepared by Sonogashira coupling of di-brominated PPIX-DME and a 4-ethynylphenyl-substituted distyryl-BODIPY. Lastly, a complex of Sn(IV)PPIX-DME with two axially coordinated phenoxide-substituted BODIPYs (**3.19**) was synthesised.

All three triads were characterised by simple spectroscopic methods. Compound **3.8** showed excitation energy transfer from the BODIPY to the porphyrin moiety, resulting in sensitised porphyrin emission and complete quenching of the BODIPY fluorescence. In triad **3.19**, the excitation energy transfer from the BODIPY to the porphyrin moiety was reduced and some BODIPY fluorescence was retained, while the sensitised porphyrin fluorescence was low. The overall emission intensity of this complex was lower than that of the other triads. Presumably, this was due to fluorescence quenching by electronic interactions between the subunits. Lastly, the porphyrin-BODIPY conjugate **3.39** showed the most promising optical properties. The red-shifted absorption and emission of the BODIPY

moieties resulted in excitation energy transfer occurring from the porphyrin to the BODIPY moieties and significant sensitised BODIPY emission. However, due to the spectral overlap of the BODIPY moieties‘ emission and the porphyrin unit’s last Q band, energy transfer from the BODIPY to the porphyrin moiety upon excitation of the BODIPY was also observed. This lowered the overall emission intensity of the conjugate.

In order to further optimise the optical properties of the PPIX-DME-BODIPY triad, modifications to further shift the BODIPY moieties‘ absorption and emission maxima to higher wavelengths, e.g., by introduction of alkenyl groups in the α-positions which carry phenyl rings with electron-donating substituents are required.[308] This way, spectral overlap with the porphyrin moiety’s absorption bands could be circumvented. Another promising approach is the metalation of PPIX-DME to alter the number and position of the porphyrin’s Q bands.

Chapter 4. Synthesis of Di-substituted and Tri-substituted Bicyclo[1.1.1]pentane-Triazoles

The synthesis of functionalised hydrocarbon cages such as bicyclo[1.1.1]pentane (BCP) that can serve as building blocks and molecular tectons for possible applications in medicinal and materials chemistry is an active research interest of our group. Searching for versatile methods for the synthesis of new BCP building blocks and BCP-chromophore arrays it was reflected that the copper-catalysed azide-alkyne cycloaddition ("click" reaction)[259,260] to form 1,2,3-triazole scaffolds can be a very useful tool due to its broad substrate scope, its efficiency and easily available precursors.[309] Hereafter, an overview of selected synthetic procedures towards the synthesis of differently substituted 1,2,3-triazoles is given. Subsequently, our approaches towards appending such triazole scaffolds onto the BCP moiety will be discussed.

4.1 The Utility of Selected 1,3-Dipolar Cycloaddition Reactions

The reaction of a dipolarophile, (alkenes, alkynes or nitriles) with a 1,3-dipolar molecule under formation of a five-membered ring is commonly described as a Huisgen[260] [3+2] cycloaddition reaction. Such 1,3-dipoles are typically heteroallyl or heteropropargyl/heteroallenyl systems, they possess a nucleophilic and electrophilic character at the same time. The 1,3-dipolar cycloaddition is one of the most widely used tools for the synthesis of heterocyclic compounds,[310] especially popular in this respect is the cycloaddition of organic azides and terminal alkynes to synthesise 1,4-di-substituted 1,2,3-triazole rings. While known for a long time, a major drawback of this transformation was its lack of regioselectivity and commonly a mixture of two regioisomers was obtained. In 2002, the groups of Meldal and Sharpless independently reported on the synthesis of 1,2,3-triazoles from azides and alkynes under mild conditions using a Cu(I) catalyst. These reaction conditions gave high yields, were applicable for a range of different substrates and, most importantly, resulted in the formation of only the 1,4-regioisomer.[259,310] Sharpless and co-workers coined the name "click" reaction for this type of transformation based on its simplicity, functional group tolerance, scope, high yields, selectivity and little by-product formation.[261] The ease it provides for the preparation of new molecules has since made the Cu(I)-catalysed "click" reaction find application in a variety of fields, such as bioconjugation chemistry, materials sciences and the synthesis of drugs.[311] "Click" reactions have also proven as useful tools for the modification of porphyrins as well as rigid hydrocarbon linkers and previously have been employed by our research group for these purposes.[249,312]

The reaction mechanism of the Cu-catalysed „click“ reaction starts from Cu(I) as the active species. The presence of Cu in the +1 oxidation state can be ensured by use of Cu(I) salts as catalysts or the use of Cu(II) salts in combination with a reducing agent. A mechanism for the “click“ reaction involving two chemically equivalent Cu atoms which catalyse the reaction cooperatively was postulated by Fokin and coworkers (Scheme 4.1). Bonding of a Cu atom with the π-electrons of the acetylide **4.1** to form complex **4.2** is followed by the formation of a Cu-acetylide σ-bond with a second incoming Cu atom. The so-formed dinuclear Cu-acetylide complex (**4.3**) reversibly coordinates the organic azide **4.4** and the β-carbon of the acetylide attacks at the electrophilic nitrogen of the azide forming the covalently bonded intermediate **4.5**. This intermediate is stabilised by the two proximal degenerate Cu centres. Ring closure occurs *via* formation of another C-N bond while one of the Cu atoms leaves the complex. Exchange of Cu with a proton in the intermediate **4.6** results in the formation of the 5-protiotriazole **4.7**.[313]

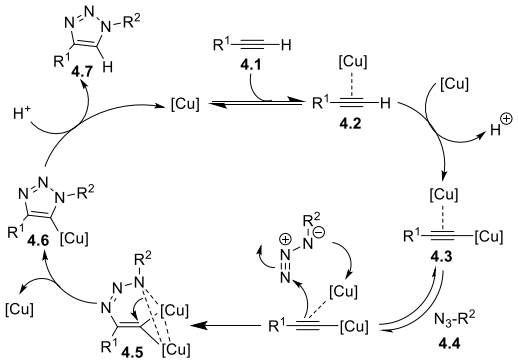

Scheme 4.1. Catalytic cycle for the Cu(I)-catalysed azide-alkyne cycloaddition reaction as proposed by Fokin and coworkers.[313]

Since its discovery in 2002, research in the “click” reaction has drastically increased and the scope of this transformation has been expanded significantly, e.g., a Cu-free strain-promoted cycloaddition of azides and cyclic alkynes was developed which can serve as a biorthogonal reaction.[314] Another synthetic development in this field is the preparation of more highly functionalised triazole cores, i.e., 1,4,5-tri-substituted 1,2,3-triazoles. Such molecules can be produced in one-pot reactions from the respective alkynes and azides. Of special interest are 5-halogentad triazoles – on the one hand they offer a synthetic handle for easy transformations such as transition metal-catalysed coupling reactions, on the other hand these 5-halogenated 1,4,5-tri-substituted triazoles exhibit different interesting properties and potential applications themselves. The 5-iodotriazole **4.8** was found to be an inhibitor of carboanhydrase IX and could be used to inhibit tumour cell proliferation.[315] The iodine substituents in 5-iodotriazoles have also been reported to engage in anion binding

and rotaxanes containing 5-iodotriazole and 5-iodotriazolium moieties have been employed as host systems for selective sensing of halides.[316] Årstad *et al.* synthesised a ^{125}I-radiolabeled 5-iodotriazole tracer molecule containing a rhodamine unit (**4.9**) for dual optical and nuclear imaging *via* a three-component "click" reaction.[317]

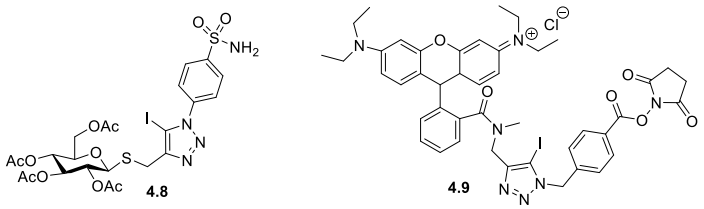

Figure 4.1. Structures of a potential carboanhydrase IX inhibitor (**4.8**)[315] and a dual optical and nuclear labeling reagent (**4.9**),[317] both of which contain an iodotriazole moiety as a crucial functional feature.

Triazoles with halogen substituents in the 5-position are commonly synthesised by the cycloaddition of an iodoalkyne with an azide, or the iodine is introduced by addition or *in situ* generation of an electrophilic iodine species.[318] A variety of procedures has been reported for the Cu-catalysed formation of 5-iodotriazoles by reaction of an azide with a terminal alkyne in the presence of an electrophilic iodine species "I^+" (Scheme 4.2).[318,319] The key step in this transformation is the trapping of the Cu(I) triazolide intermediate with "I^+". The work by Wu *et al.* is an early example of the synthesis of 5-iodotriazoles according to this strategy. ICl (1.0 eq.) was used as a source of electrophilic iodine in combination with CuI (1.0 eq.) as the catalyst for the cycloaddition reaction (Table 4.1, entry a).[319a] The electrophilic iodine species can be generated by addition of an oxidising agent and an iodine source to the Cu(I)-catalysed "click" reaction. This strategy was employed by Zhang and co-workers, among others, who used a slight excess of CuI (1.1 eq.), simultaneously being the catalyst and the iodine source, in combination with DIPEA as a base and NBS (1.2 eq.) as an oxidising agent to convert I^- into an electrophilic iodine species (Scheme 4.2, Table 4.1, entry b).[319d] In a different approach, the alkyne and azide were reacted with a stoichiometric amount of CuI under aerial oxidation while *tert*-butyldimethylsilyl chloride (TBDMSCl) (0.50 eq.) was added as an activator for the oxidative halogenation (Scheme 4.2, Table 4.1, entry c).[319c] Zhu and co-workers employed NaI (4.0 eq.) as the iodine source and $Cu(ClO_4)_2$•2 H_2O (2.0 eq.) as the combined catalyst and oxidant (Scheme 4.2, Table 4.1, entry d).[319e] Addition of tris((1-benzyl-1*H*-1,2,3-triazol-4-yl)methyl)amine (TBTA) (10 mol%) as a ligand promoted the product formation (Scheme 4.2, Table 4.1, entry e).[319b] A similar approach was taken by Årstad and co-workers who strived to produce radioactively labelled 5-[^{125}I]iodotriazoles as tracers for nuclear imaging. They used [^{125}I]NaI in excess as an iodinating agent and a Cu(II) salt ($CuCl_2$, 1.0 eq.) as a bifunctional reagent for oxidation

of I^- and for catalysis of the "click" reaction (Scheme 4.2, Table 4.1, entry f).[317, 319g] Alternatively, 5-iodotriazoles were prepared with CuI (1.0 eq.) and NIS (1.1 eq.) as the source of electrophilic iodine (Scheme 4.2, Table 4.1, entry g).[317, 319g] Zhang *et al*. employed Et_4NI as an iodine source, Selectfluor as an oxidant and CuI as the catalyst for the synthesis of 5-iodotriazoles in aqueous medium (Scheme 4.2, Table 4.1, entry h).[319h]

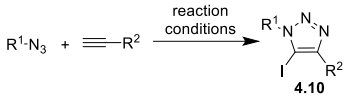

Scheme 4.2. Synthesis of 5-iodo-1,2,3-triazoles from organic azides and terminal alkynes.

Table 4.1. Different reaction conditions applied for the synthesis of tri-substituted 5-iodo-1,2,3-triazoles from terminal alkyne and azide precursors according to Scheme 4.2.

entry	reagents	temp.	solvents	time
a	ICl (1.0 eq.),CuI (1.0 eq.), TEA (1.2 eq.)	25 °C	THF	20 h
b	CuI (1.1 eq.), NBS (1.2 eq.), DIPEA (1.0 eq.)	r.t.	THF	3 h
c	CuI (1.0 eq.), TBDMSCl (0.50 eq.), O_2, DIPEA (1.0 eq.)	r.t.	CH_3CN	18 h
d	NaI (4.0 eq.), $Cu(ClO_4)_2$•2 H_2O (2.0 eq.), TEA or DBU (1.0 eq.)	r.t.	THF or CH_3CN	6–12 h
e	NaI or KI (4.0 eq.), $Cu(ClO_4)_2$•2 H_2O (2.0 eq.), TEA or DBU (1.0 eq.), TBTA (10 mol%)	r.t.	THF or CH_3CN	≤6 h
f	[^{125}I]NaI (excess), CuCl (1.0 eq.), TEA (1.5 eq.)	r.t.–60 °C	CH_3CN/ H_2O 10:1	1.5 h
g	CuI (1.0 eq.), NIS (1.1 eq.), TEA (1.0 eq.)	r.t.	DMF	2–18 h
h	Et_4NI (1.1 eq.), DIPEA (1.2 eq.), Selectfluor (1.2 eq.), CuI (0.10 eq.)	30 °C	H_2O	3 h

A different pathway towards 5-iodotriazoles is the pre-functionalisation of alkynes and use of these halogenated alkynes for the cycloaddition reaction (Scheme 4.3).[320] Sharpless, Fokin and co-workers regioselectively synthesised 5-iodotriazoles from organic azides and 1-iodoalkynes using CuI (5 mol%) as a catalyst and tris((1-*tert*-butyl-1*H*-1,2,3-triazolyl)methyl)amine (TTTA) (5 mol%) as an amine ligand.[321a] García-Álvarez *et al.* applied this methodology to the synthesis of 5-iodotriazoles in aqueous medium and under air, catalysed by a water-soluble Cu(I) complex.[321b]

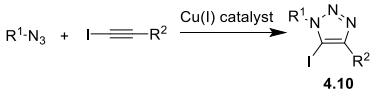

Scheme 4.3. Cu(I)-catalysed synthesis of 5-iodotriazoles from 1-iodoalkynes and organic azides.

5-Iodotriazoles are useful precursors for further functionalisation of the triazole scaffold. While the iodine substituent acts as a synthetic handle for transition metal-catalysed

coupling reactions to produce 1,4,5-tri-substituted triazoles in 2 steps overall, several Cu-catalysed single step one-pot procedures have been reported as well for the same transformations. In this case, the reactions are believed to proceed *via* a Cu(I)-triazolide intermediate which traps an electrophilic reactant. This methodology can yield 5-acetylenated, -arylated or -alkylated triazoles.[320,322] 5-Ethynylated 1,2,3-triazoles can essentially form under "click" conditions when the reaction is carried out in the presence of air and methanol is used as a solvent. Reacting benzyl- or alkyl bromides with NaN_3 and different terminal alkynes under these conditions while using Cu_2O as a catalyst gave 1,4,5-tri-substituted triazoles in moderate to high yields (Scheme 4.4). The reaction mechanism postulated by Alonso *et al.* comprises aerial oxidation of the alkynyl-bound Cu(II)-triazolide complex, followed by reductive elimination under C-C bond formation and recovery of the Cu(I) catalyst (Table 4.2, entry a).[323] A similar approach for a multicomponent one-pot synthesis of 5-alkynylated tri-substituted triazoles was applied by Yang *et al*. who reacted arylboronic acids with terminal alkynes and NaN_3 in a 2:1 mixture of 1,4-dioxane and water using a combination of $CuSO_4$•5 H_2O and CuI as the catalytic system (Scheme 4.4, Table 4.2, entry b).[324]

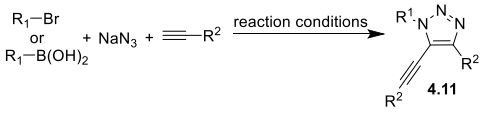

Scheme 4.4. Synthesis of 5-alkynyl triazoles from NaN_3, terminal alkynes and benzyl/alkyl bromides or boronic acids

Table 4.2. Reaction conditions applied for the synthesis of 5-ethynylated 1,2,3-triazoles from NaN_3, terminal alkynes and organobromides or -boronic acids according to Scheme 4.4.

entry	reagents	temp.	solvents	time
a	Cu_2O (0.01 eq.)	r.t.	MeOH	6–24 h
b	CuI (0.10 eq.), $CuSO_4$•5 H_2O (0.20 eq.),	r.t.	H_2O/1,4-dioxane 2:1	16 h

Alternatively, tri-substituted triazoles were prepared from azides and terminal alkynes using a Cu(I) catalyst ($Cu(CH_3CN)_4PF_6$) with *N*,*N*-dimethylethylenediamine as a ligand under aerial oxidation and addition of a co-oxidant, *N*-methoxymorpholine *N*-oxide (NMO) (Scheme 4.5, Table 4.3, entry a).[325] A modified system for the oxidative coupling leading to the formation of 5-alkynylated triazoles was employed by Zhang *et al*. who reacted organic azides and terminal alkynes under aerobic conditions using CuBr and KOH in methanol (Scheme 4.5, Table 4.3, entry b).[326]

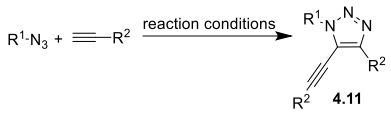

Scheme 4.5. Synthesis of 5-alkynyl triazoles from organic azides and terminal alkynes.

Table 4.3. Reaction conditions applied for the synthesis of 5-ethynylated 1,2,3-triazoles from organic azides and terminal alkynes according to Scheme 4.5.

entry	reagents	temp.	solvents	time
a	$Cu(CH_3CN)PF_6$ (0.20 eq.), *N*,*N*-dimethylethylenediamine (0.20 eq.), NMO (0.10 eq.)	r.t.	DCM	20 min
b	CuBr (0.10 eq.), KOH (2.0 eq.)	60 °C	EtOH	10 h

Multicomponent one-pot reactions which employ haloalkynes next to terminal alkynes and organic azides can result in the formation of structurally even more diverse tri-substituted triazoles by introduction of different substituents to all the three positions. Yamamoto *et al*. employed a combined azide-alkyne cycloaddition with a Sonogashira coupling reaction using a Cu(I) catalyst as well as a latent Pd catalyst to link the three components while minimising the formation of unwanted side products such as diynes (Scheme 4.6). In the first step of the reaction, a 5-iodotriazole is formed by Cu(I)-catalysed cycloaddition of the iodoalkyne and the organic azide, in the second step the latent Pd catalyst is activated by elevating the reaction temperature from room temperature to 85 °C and Sonogashira cross-coupling of the 5-iodotriazole with remaining terminal alkyne is initiated (Table 4.4, entry a).[327] Wang *et al*. circumvented the need of a Pd catalyst in the Cu(I)-catalysed three-component coupling of a bromoalkyne, a terminal alkyne and an organic azide (Scheme 4.6). The first step of the one-pot reaction comprises the cycloaddition reaction resulting in the formation of the Cu(I)-triazolide intermediate. This intermediate is trapped by the electrophilic bromoalkyne and a 5-alkynylated triazole is formed (Table 4.4, entry b).[328]

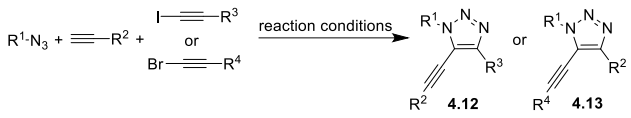

Scheme 4.6. Multicomponent synthesis of 5-alkynyl triazoles from organic azides, terminal alkynes and alkynyl halides.

Table 4.4. Reaction conditions applied for the synthesis of 5-alkynyl 1,2,3-triazoles from organic azides, terminal alkynes and alkynyl halides according to Scheme 4.6.

entry	reagents	temp.	solvents	time
a	CuI (0.05 eq.), tris[(1-benzyl-1H-1,2,3-triazol-4-yl)methyl]amine (0.05 eq.), XPhos-Pd catalyst (0.01 eq.), KOAc (3.0 eq.)	r.t., then 85 °C	THF	15–24 h
b	CuCl (0.2 eq.), LiO^{t}Bu (2.0 eq.),	r.t.	1,2-DCE, 4 Å mol. sieves	12 h

4.2 Objectives

The development of synthetic routes towards bicyclo[1.1.1]pentane (BCP) derivatives is a field of growing interest as has been discussed in Chapter 1.[144,182a] This rigid hydrocarbon scaffold has attracted attention as a linear linker in electron donor-acceptor systems as well as in molecular rods and rotors. Future applications require simple and robust synthetic methods for its modification. Notably, BCP derivatives have promise as bioisosteres for organic moieties, such as phenyl rings, *tert*-butyl groups and alkynes. The BCP moiety can favourably alter physicochemical and pharmacokinetic properties of drug candidate molecules such as its solubility, membrane permeability and metabolic stability as has been discussed earlier.[144a,182d,219a,219d,222b]

The importance of “click“ reactions in medicinal chemistry is constantly growing – this reaction can be used to easily conjugate drug moieties or bio-probes, as a bioorthogonal reaction it can be used for *in situ* transformations in cells and the triazole moiety can act as a bioisostere or pharmacophore itself.[329] Therefore, it is prompting to combine both, BCP and „click“ chemistry and to investigate the utility of “click“ transformations on the BCP scaffold.

So far, such reactions on BCP have been limited to a rather narrow range of small molecule substrates to obtain phenyl-, benzyl- and methyl carboxylate-substituted triazoles.[194,195,197] It is intended to expand the scope of “click“ reactions to more versatile substrates. This

includes broadening the range of accessible BCP-triazoles to derivatives with complex chromophoric substituents, such as porphyrins, BODIPYs, and pyrene. Such BCP-appended dye moieties could potentially find application in bioimaging as well as in materials sciences.

The scope of BCP functionalisation reactions is then aimed to be expanded to cycloaddition reactions which incorporate an additional functional group in the triazole scaffold. It is intended to focus on single-step one-pot procedures to achieve such transformations. Firstly, a protocol for the synthesis of different BCP 5-iodotriazoles will be implemented. The further functionalisation of the 5-iodo-position of these derivatives by Pd-catalysed coupling reactions will be tested. Secondly, a simple procedure for the synthesis of 5-alkynylated BCP triazoles by a one-pot reaction is aimed to be devised. The structural features and intermolecular interactions of different BCP triazole scaffolds will be analysed. This can lay a foundation for envisaging possible interactions of the BCP scaffold with biomolecules.

4.3 Functionalisation of Bicyclo[1.1.1]pentane by "Click" Reactions

"Click" reactions on BCP derivatives have been reported previously for a small number of substrates by the groups of Adsool and Grygorenko.[194,195,197] The first protocol reported for such a Cu(I)-catalysed "click" reaction on BCP used 1-azido-3-iodo-BCP as a starting material (**1.92**).[194] This precursor can conveniently be prepared following a procedure by Hossain *et al*. by *in situ* generation of IN_3 from ICl and NaN_3 and subsequent reaction with [1.1.1]propellane (Scheme 4.7).[189b]

Scheme 4.7. Synthesis of 1-azido-3-iodo-BCP from [1.1.1]propellane, NaN_3 and ICl according to a procedure by Hossain *et al*.[189b]

This azide **1.92** was converted to the 1,2,3-triazole by reaction with phenylacetylene, using CuI as a catalyst and TEA as a base. The 4-phenyltriazole **4.14** was isolated with a yield of 89% (Figure 4.2).[194] Later, the substrate scope was expanded to include ethoxyethyne and methyl propiolate as ethynyl components (**4.15**–**4.19**).[195,197] A different approach towards BCP triazoles is the use of 1-ethynyl-BCP as the starting material which was reacted with benzyl azides (**4.20**–**4.21**).[197]

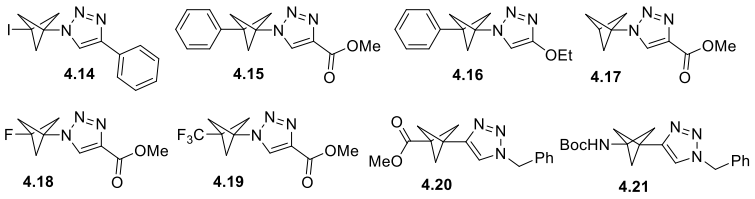

Figure 4.2. Selected BCP-triazoles which have been prepared from azido-BCP or ethynyl-BCP precursors, respectively.

In this study, 1-azido-3-iodo-BCP was chosen as the starting material due to its relatively easy preparation from [1.1.1]propellane in a single step. [1.1.1]Propellane was synthesised based on a procedure by Knochel and co-workers[200d] and subsequently converted to 1-azido-3-iodo-BCP as shown in Scheme 4.7.[189b] In numerous repetitions, the synthesis of [1.1.1]propellane typically gave yields around 30%. The conversion to 1-azido-3-iodo-BCP usually proceeded with yields around 25%. The moderate yields for the conversion to the BCP azide can partially be explained by the formation of considerable amounts of 1,3-diiodo-BCP as a side product. In addition, the starting material as well as the product are not particularly stable at room temperature and it can be assumed that some decomposition in the reaction mixture occurred.

Intending to use the 1-azido-3-iodo-BCP for “click“ reactions with chromophores bearing different electronic properties, suitable ethynyl-substituted starting materials had to be prepared. Three molecules with different photophysical properties, BODIPY, pyrene, and porphyrin dyes, were chosen as substrates for the cycloaddition reaction. 8-(4-Ethynylphenyl)-4,4-difluoro-1,3,5,7-tetramethyl-4-bora-3a,4a-diaza-*s*-indacene (**4.24**),[304] 1-ethynylpyrene (**4.27**)[330] and (5-(4-ethynylphenyl)-10,20-bis(4-methylphenyl)-15-phenylporphyrinato))zinc(II) (**4.34**)[181] were synthesised according to literature procedures (Scheme 4.8). The A_2BC-type porphyrin **4.35** was synthesised *via* a modular approach by acid-catalysed condensation of dipyrromethane **4.28** with 4-methylbenzaldehyde to obtain A_2B_2 porphyrin **4.29**, which was substituted with a phenyl group in one meso-position by reaction with phenyllithium (PhLi), H_2O and 2,3-dichloro-5,6-dicyano-*p*-benzoquinone (DDQ). This was followed by meso-iodination, zinc insertion, Suzuki coupling and deprotection of the TMS-ethynyl moiety to give the alkynyl-substituted precursor porphyrin **4.34**.

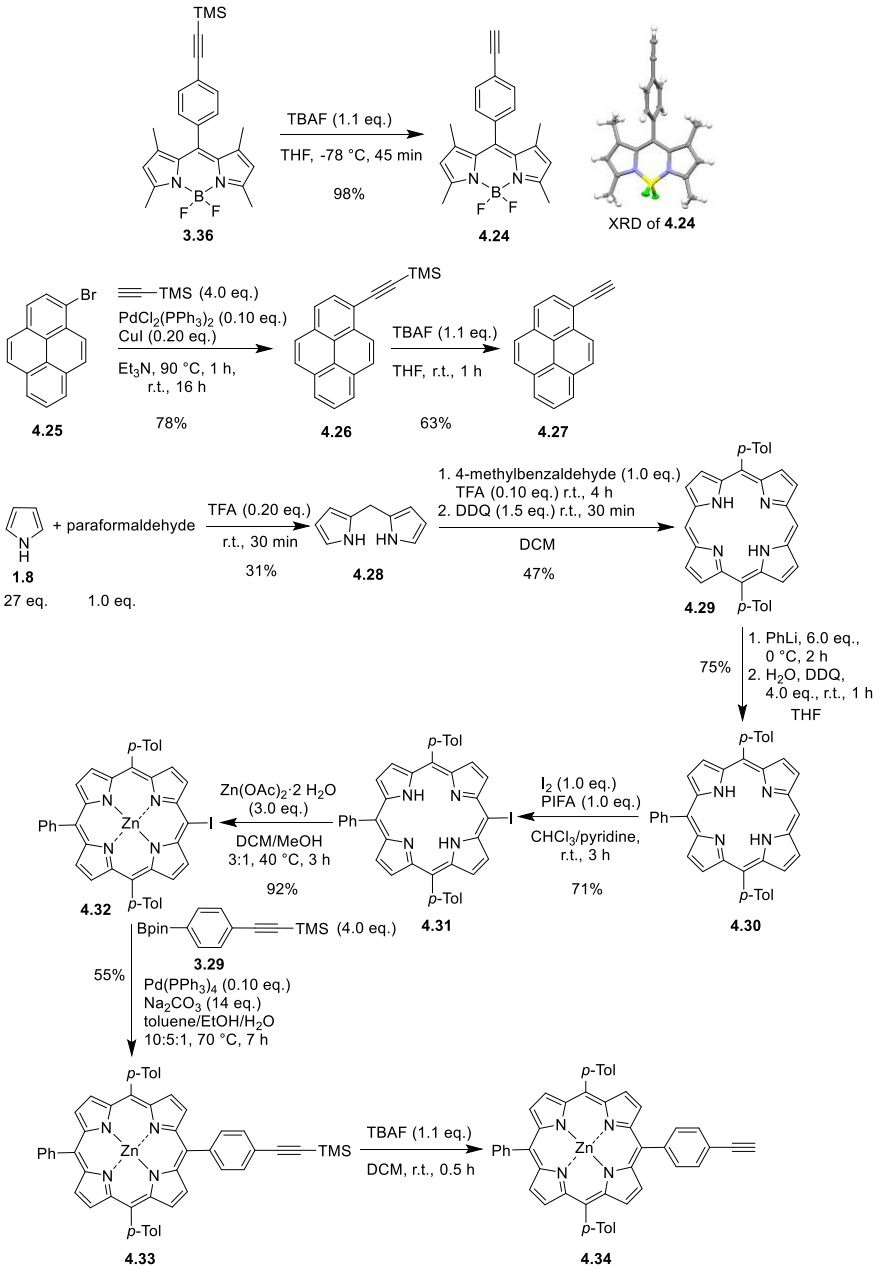

Scheme 4.8. Synthesis of ethynyl-BODIPY, -pyrene, and -porphyrin precursors for Cu-catalysed "click" reactions. XRD image of **4.24** in the crystal is shown.

In a first attempt, the isolated BCP azide **1.92** was subjected to a "click" reaction with ethynylphenyl-substituted BODIPY **4.24** using previously reported reaction conditions.[194,195,197] A solution of **1.92** in THF was stirred with TEA (1.5 eq.), CuI (0.10 eq.) and BODIPY **4.24** (1.0 eq.) for 16 h. The reaction yielded the 1,2,3-triazole product **4.36** in 82% (Scheme 4.9). In the reaction of BCP **1.92** with alkynyl-porphyrin **4.34**, 5-protio-1,2,3-triazole **4.38** was formed in a good yield of 79% as well. On the other hand, the reaction of **1.92** with 1-ethynylpyrene **4.27** gave a much lower yield of 10% of **4.39**. It has been observed in the past that alkynes with electron-withdrawing groups react more efficiently in

Cu(I)-catalysed azide-alkyne cycloadditions, probably due to the higher acidity of the alkynyl proton, hence more facile deprotonation in the reaction.[331] 1-Ethynylpyrene as a molecule with a large π-electron system possibly shows lower reactivity in the cycloaddition and might undergo more side reactions instead.

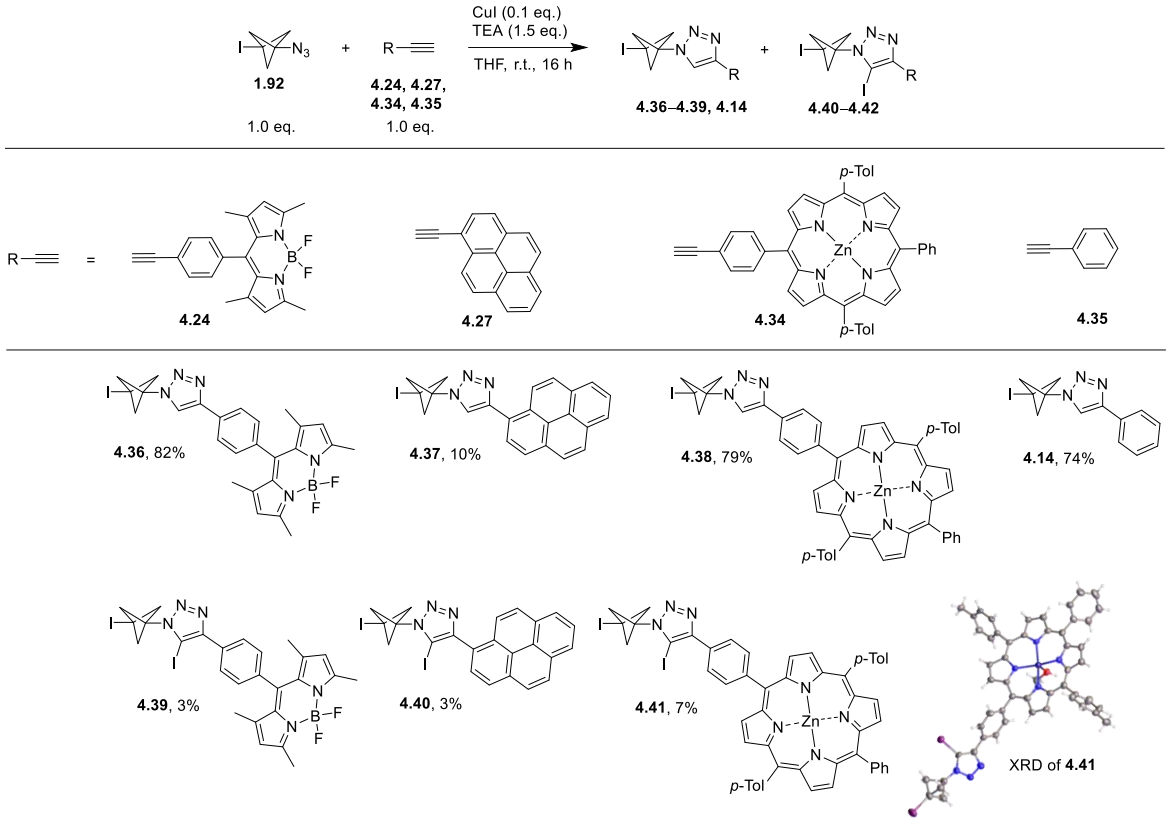

Scheme 4.9. Cu-catalysed azide-alkyne cycloaddition reaction on 1-azido-3-iodo-BCP **1.92** with different alkynes to give 5-protio-1,2,3-triazoles as main products and 5-iodo-1,2,3-triazoles as side products. XRD image of **4.41** in the crystal is shown.

In each of these three reactions the formation of small amounts (3-7%) of a side product was observed. The reproducibility was tested with the BODIPY substrate **4.24** and the side product was found to form in each repetition of the reaction. The “click“ reaction was repeated with phenylacetylene **4.35** as a simple substrate. In this case, only formation of the expected 5-protio-1,2,3-triazole product **4.14** in 74% was observed. No other side products could be isolated.

It was decided to investigate this peculiar side reaction more in-depth. The ^{1}H NMR spectra of the three side products isolated from the “click“ reactions with alkynyl-BODIPY, -porphyrin, and -pyrene all showed the characteristic peaks of the BCP moiety between

2.56–3.15 ppm as well as all the signals corresponding to the chromophoric units but no signals for the proton in the 5-position of the triazole ring. Representative spectra of the 5-protiotriazole **4.36** and the side product **4.39** are shown in Figure 4.3.

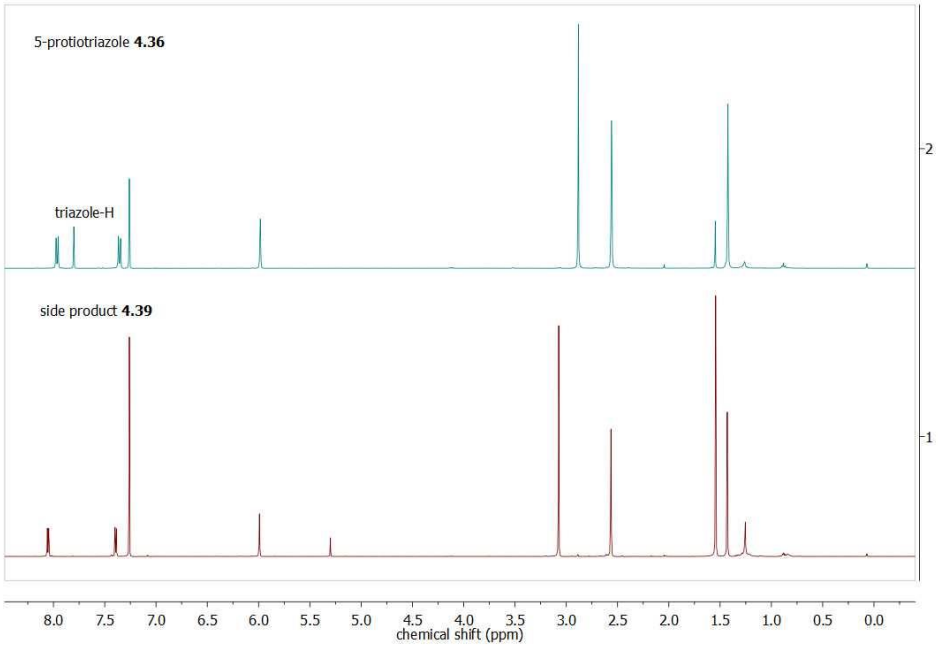

Figure 4.3. Comparison of the ^{1}H NMR spectra of the 5-protiotriazole **4.36** and the side product **4.39**. Spectra were recorded in $CDCl_3$.

This first led to the assumption that a direct substitution of the azide moiety on the BCP with the ethyne had taken place. However, no typical signals indicative of an alkynyl unit could be found in the ^{13}C NMR spectra of the compounds and mass spectrometry measurements suggested that the products still contained a nitrogen fragment. Eventually, a crystal of side product **4.40** could be obtained and X-ray structural analysis revealed this compound as a 5-iodotriazole scaffold (Figure 4.4).

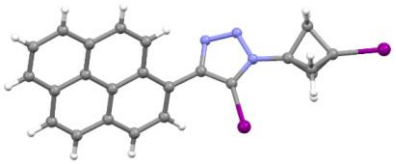

Figure 4.4. Representative view of the molecular structure of compound **4.40** in the crystal. The crystal structure shows a 1,4,5-tri-substituted 1,2,3-triazole scaffold and confirms the presence of an iodine substituent in the 5-position of the triazole ring. Atomic displacement shown at 50% probability level.

A porphyrin with an ethynyl moiety directly appended at the meso position (**4.43**) was synthesised according to a published procedure.[181] This porphyrin was subjected to a

"click" reaction under the same conditions as above (Scheme 4.10). The formation of several products was observed but after purification by silica gel column chromatography and analysis by ^{1}H NMR spectroscopy, no signal indicating the presence of the BCP moiety could be found in any of the isolated fractions. The lack of triazole formation in this reaction presumably was due to the fact that the precursor porphyrin bore the ethynyl-moiety directly at the meso-position, exerting a considerable steric hindrance for reaction with the azide unit on the BCP bridgehead carbon. It was concluded that a spacer group between the bulky porphyrin and the ethynyl moiety is required for the porphyrin to take part in the „click" reaction.

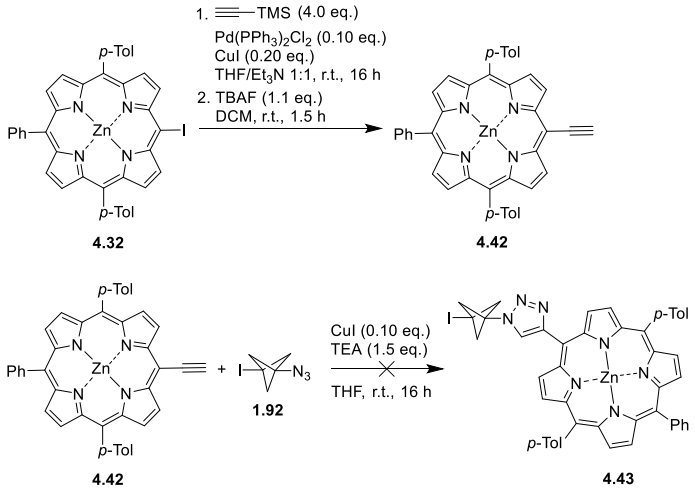

Scheme 4.10. Synthesis of a meso-ethynyl-substituted porphyrin **4.42** and attempted "click" reaction with **1.92** which did not result in the formation of the desired triazole product **4.43**.

4.4 Synthesis of BCP-5-Iodotriazoles

The repeated formation of BCP 5-iodo-1,2,3-triazoles in reactions with different substrates led us to investigate this side reaction in more depth. A survey of the literature revealed that the synthesis of 5-iodo-1,2,3-triazoles *via* 1,3-dipolar cycloaddition reactions can be achieved by two different routes as discussed in section **4.1**. Either a terminal alkyne can be used in combination with an electrophilic iodine species which is added as such or generated *in situ* or an iodoalkyne is employed as a starting material.[318,320] In a few cases, the formation of small amounts of 5-iodo-1,2,3-triazoles as side products in "click" reactions was observed under conditions similar to the ones employed by us.[332]

The formation of 5-iodo-1,2,3-triazoles is likely affected by the presence of residual oxygen in the reaction mixture which facilitates oxidation of I^- to an electrophilic iodine species. To confirm this assumption, different reaction conditions were screened using ethynyl-BODIPY

4.24 as a substrate. This compound was chosen as the starting material because of its relatively easy availability and since its coloured reaction products can more easily be separated by column chromatography. BCP **1.92** was reacted with BODIPY **4.24** under air or argon atmosphere, respectively, and using varying amounts of CuI as a catalyst (Table 4.5). The yields of the 5-iodotriazole and 5-protiotriazole products formed were determined by ^{1}H NMR using dibromomethane as an internal standard. It was noted that reactions carried out under air gave slightly higher yields (about 4%) of the 5-iodotriazole product than the respective reactions which were carried out under argon atmosphere. This supported the assumption that atmospheric oxygen is involved in the formation of electrophilic iodine species. Secondly, an increase in the amount of CuI used to 0.20, 0.30 and 1.0 eq. led to an enhanced 5-iodotriazole formation because under these reaction conditions CuI acts as the iodine source. Using 1.0 eq. of CuI and carrying out the reaction under air led to an elevated yield of 5-iodo-1,2,3-triazole **4.39** of 33% along with 22% of the 5-protio-1,2,3-triazole **4.36** as determined by ^{1}H NMR spectroscopy. However, the increased amounts of CuI used and exposure of the reaction mixture to air led to the formation of a considerable amount of a butadiyne-linked BODIPY dimer from a Glaser coupling reaction[250] and limited the yield of **4.39**. Intending to enhance the formation the new BCP-5-iodotriazole building blocks, a literature procedure was applied, using CuI (1.0 eq) in combination with an oxidant, NBS (1.2 eq.), and a base, *N*,*N*-diisopropylethylamine (DIPEA) (1.0 eq.).[319d] Compound **4.39** was formed in a good yield of 69% under these conditions.

Table 4.5. Screening of reaction conditions for the formation of 5-protio-1,2,3-triazole **4.36** and 5-iodo-1,2,3-triazole **4.39** from precursors **1.92** and **4.24**.[a] All reactions were carried out with **1.92** (28.7 µmol) and **4.24** (28.7 µmol) in THF (0.67 mL) for 16 h. [b] For reactions carried out under argon atmosphere the solvent was deoxygenated by purging with argon for 15 min. [c] Yield obtained from ^{1}H NMR with an internal standard.

entry	conditions	atmosph.[b]	yield[c] of 4.46	yield[c] of 4.42
1	CuI (0.2 eq.), TEA (1.5 eq.)	argon	11%	80%
2	CuI (0.3 eq.), TEA (1.5 eq.)	argon	13%	71%
3	CuI (0.2 eq.), TEA (1.5 eq.)	air	15%	54%
4	CuI (0.3 eq.), TEA (1.5 eq.)	air	17%	54%
5	CuI (1.0 eq.), TEA (3.8 eq.)	air	33%	22%
6	CuI (1.0 eq.), DIPEA (1 eq.), NBS (1.2 eq.)	argon	69%	6%

These reaction conditions proved to be promising for the synthesis of different BCP-5-iodo-1,2,3-triazoles in improved yields. Thus, the substrates used previously for “click“ reactions were now reacted under modified conditions aiming to promote the formation of 5-

iodotriazoles over 5-protiotriazole formation. Improved, however quite low, yields of the 5-iodotriazoles were achieved with the BODIPY (**4.24**, 10%), porphyrin (**4.34**, 19%) and pyrene (**4.27**, 17%) substrates as well as with phenylacetylene (**4.35**, 7%) (Scheme 4.11). Only when 4-ethynylpyridine (**4.44**) was used as a substrate, the 5-iodotriazole product formed in a good yield of 66%. Probably steric as well as electronic factors influence the efficiency of the reaction. In the case of the reaction with **4.34** a large amount of ethynylporphyrin starting material (59%) was recovered, indicating that the cycloaddition reaction itself did not proceed efficiently under these conditions. Presumably, this is due to the steric hindrance imposed by the porphyrin macrocycle. On the other hand, the electron-rich substrates 1-ethynylpyrene and 1-phenylacetylene underwent homocoupling to a larger extent. Liu and co-workers reported an efficient homocoupling of terminal alkynes under very similar conditions using CuI, NBS and DIPEA in the absence of an azide substrate. They stated that the diyne formation was not dependent on the presence of oxygen.[333] This implies that the reaction conditions employed also promoted alkyne-alkyne homocoupling which competed with the formation of cycloaddition products. Surprisingly, only a small amount of 5-iodotriazole product **4.39** could be isolated from the reaction with BODIPY **4.24** as opposed to the good yields determined by ^{1}H NMR spectroscopy which were observed in the test reaction under the same conditions (Table 4.5, entry 6). It is likely that this was due to difficulties with purification of the reaction products. Firstly, they were found to stick to silica gel, hence some compound might have been lost which did not elute completely. Secondly, separation of the 5-iodotriazole product **4.39** from the 5-protiotriazole side product **4.36,** which also formed in this reaction, was more difficult when a larger amount of 5-iodotriazole was produced. Again, the steric bulk of the BODIPY moiety could cause reduced formation of **4.39** comprising a large iodine atom in the 5-position of the triazole ring which might be accommodated less readily than the proton in **4.36**.

In contrast to the other substrates used for this reaction, 4-ethynylpyridine is electron-poor. On the one hand, such substrates have been reported to easily undergo Cu(I)-catalysed alkyne-azide cycloaddition reactions.[181] On the other hand, a similar alkyne, 3-etynylpyridine, was observed to be less reactive in Glaser coupling reactions.[334] Its electronics combined with its low steric demand might account for the considerably higher yield which 4-ethynylpyridine gives in the formation of 5-iodotriazoles as compared to the other substrates.

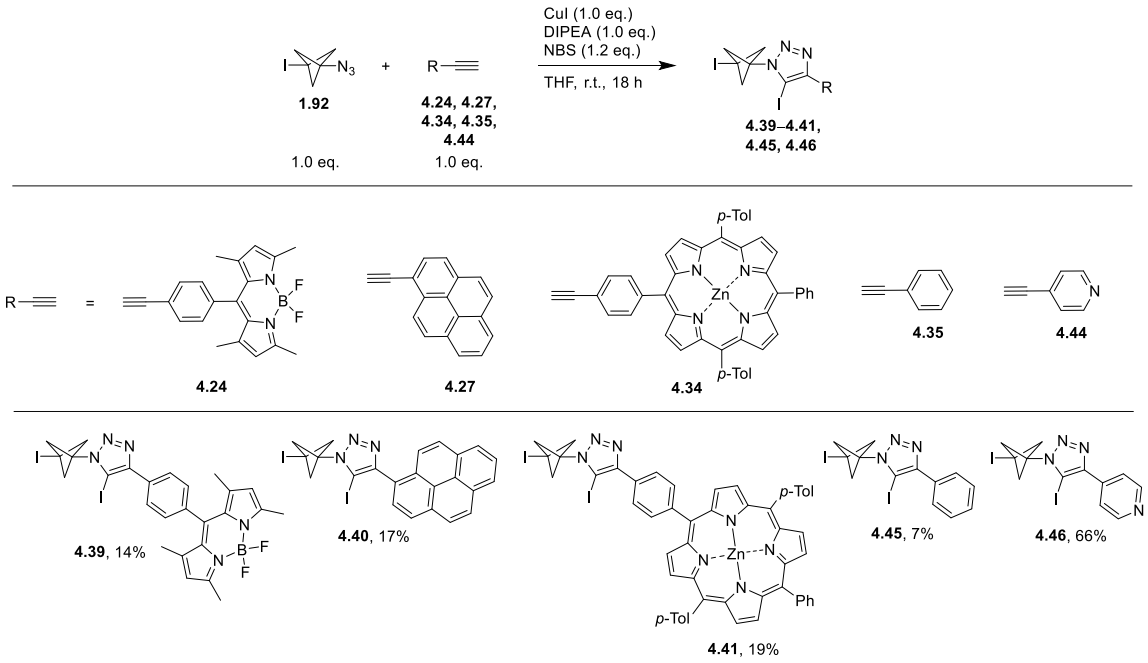

Scheme 4.11. Synthesis of 5-iodo-1,2,3-triazoles from **1.92**.

4.5 Synthesis of 5-Alkynylated BCP-Triazoles

The 5-iodo of the triazole ring is a useful synthetic handle for subsequent functionalisation with a second moiety yielding tweezer-like 1,4,5-tri-substituted 1,2,3-triazoles. Such scaffolds can likewise be synthesised by several single-step procedures from the respective azide and different precursors such as terminal alkynes.[320,322] 1,4,5-Tri-substituted 1,2,3-triazoles have been reported as compounds with promising biological activities in various fields.[335] Hence, we investigated the reactivity of 1-azido-3-iodo-BCP to produce 1,4,5-tri-substituted 1,2,3-triazoles. 5-Alkynylated triazoles can be obtained in one-pot reactions using only copper salts as catalysts in the presence of oxygen or oxidants such as *N*-methylmorpholine-*N*-oxide.[320,322,323,325] The reaction proceeds *via* a triazolide intermediate with copper(I) bound in the 5-position of the triazole ring that undergoes C-C bond formation with a free terminal acetylene.[322] Another approach to 5-alkynyl 1,2,3-triazoles is the use of 5-halogenated precursors or their *in situ* generation followed by Pd-catalysed Sonogashira coupling reaction.[327,335b,336] Surprisingly, when we directly used 1-azido-3-iodo-BCP in a Sonogashira reaction with 1-ethynylpyrene using $Pd(PPh_3)_2Cl_2$ (0.10 eq.) and CuI (0.20 eq.) formation of the 1,4,5-tri-substituted triazole **4.50** in 7% yield was observed (Scheme 4.12). Apparently, the reaction conditions mediated the azide-alkyne 1,3-dipolar cycloaddition and C-C bond formation reaction in the 5-position of the triazole ring in a single step. One such example of the formation of a 1,4,5-tri-substituted 1,2,3-triazole from azide and alkyne starting materials as a side product in Sonogashira coupling reactions was

reported in the literature and it was proposed that the 5-alkynylation reaction is copper-mediated.[337]

The scope of the unprecedented reaction was tested using different alkynyl-substrates as reactants (Scheme 4.12). With phenylacetylene the 1,4,5-tri-substituted 1,2,3-triazole product **4.52** was obtained in 10% yield while, using 4-ethynylpyridine, 27% of the tri-substituted product **4.53** formed. The 5-protio-1,2,3-triazole **4.56** was also formed and isolated in 31% yield. None of the desired reaction products could be isolated in pure form when **1.92** was reacted with 4-ethynylaniline (**4.47**) and 4-ethynylphenylboronic acid pinacol ester (**4.48**), respectively.

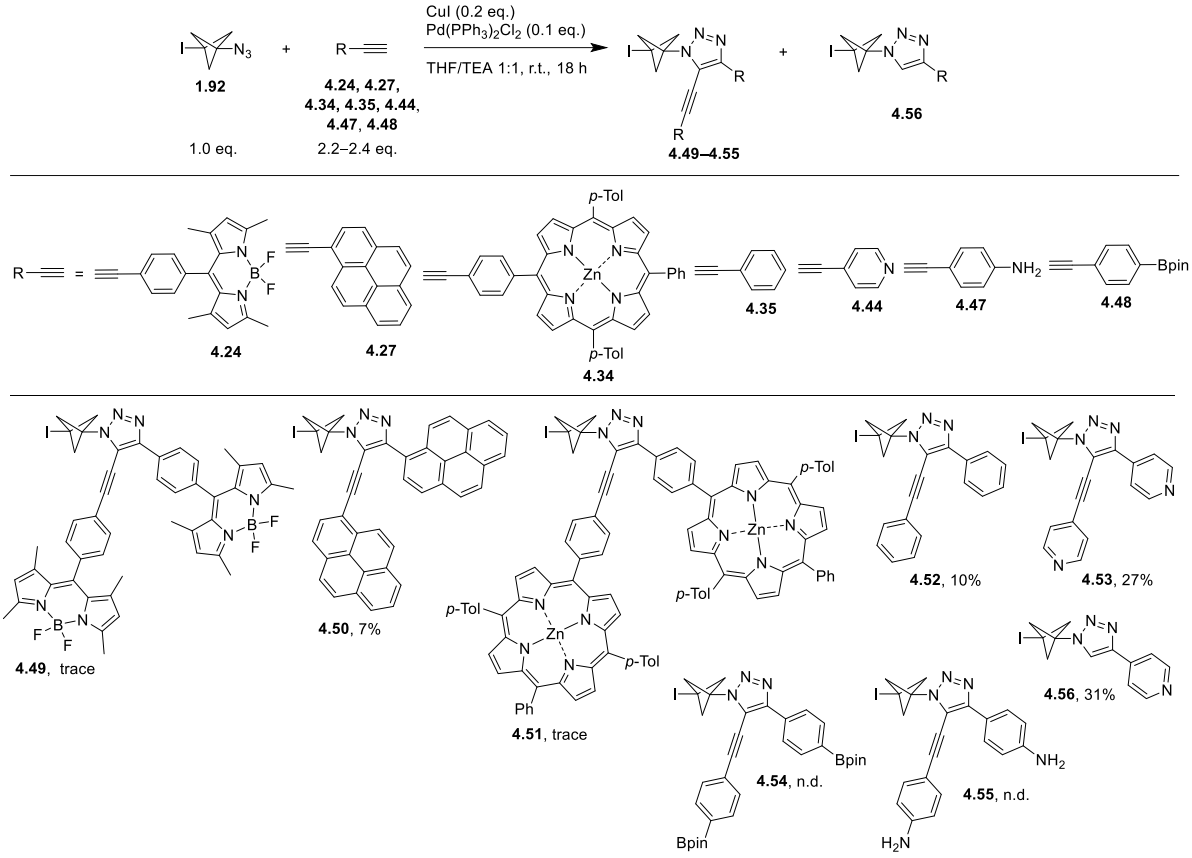

Scheme 4.12. Synthesis of 5-alkynylated 1,2,3-triazoles from **1.92**. n. d. – not determined

We saw potential in using this reaction for the one-pot synthesis of BCP-bound chromophore tweezers and reacted **1.92** with alkynyl-substituted BODIPY **4.24** and porphyrin **4.34**. In both cases, complex mixtures of reaction products formed. Several ways to purify the product mixtures were attempted, such as column chromatography on silica gel or aluminium oxide as well as preparative silica gel TLC. However, the compounds

interacted strongly with the different column materials resulting in poor separation, only allowing for the isolation of trace amounts of the respective 1,4,5-tri-substituted 1,2,3-triazoles **4.49** and **4.51**.

To explain the differences in yields for the various substrates, similar considerations can be made as for the reactions to form 5-iodotriazoles. In general, the formation of large amounts of homocoupled butadiyne products was observed. The addition of Pd(0) or Pd(II) salts as co-catalysts can make the homocoupling of acetylenes more efficient[338] and the overall low yields of the one-pot cycloaddition/coupling reaction are largely attributed to the competing homocoupling reaction. Again, the best yields were observed for smaller substrates and electron-poor acetylenes, i.e. the reaction with 4-ethynylpyridine which yielded the tweezer product **4.53** in 27%. The 5-protiotriazole **4.56** formed in this reaction as a significant side product in 31%.

Due to the low yield for large chromophoric moieties in the one-pot cycloaddition-coupling reaction, a sequential approach was tested. However, when 5-iodo-1,2,3-triazole **4.39** was reacted with ethynyl-substituted BODIPY **4.24** under Sonogashira coupling conditions only the BODIPY dimer **4.57** was obtained along with unreacted starting material **4.39** (Scheme 4.13). Apparently, the 5-position of the 5-iodotriazole **4.39** is not very reactive under Sonogashira coupling reaction conditions and homocoupling of the ethynyl-BODIPY starting material is the preferred reaction. The low reactivity of **4.39** towards **4.24** can possibly be explained by steric hindrance of the two bulky reactants.

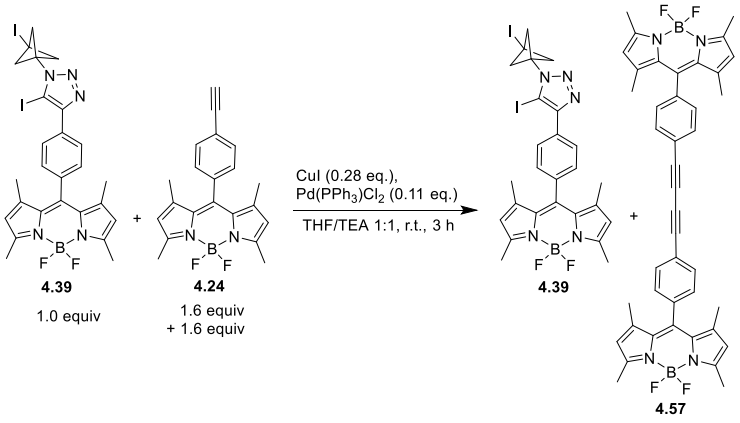

Scheme 4.13. Attempted synthesis of the 5-alkynylated triazole **4.49** in a stepwise manner.

In another attempt to establish a protocol for the stepwise functionalisation of **4.39** the iodotriazole was reacted under Suzuki-Miyaura coupling conditions. As a proof of concept, **4.39** was reacted with the sterically less demanding 4-carboxymethoxyphenylboronic acid pinacol ester **4.58** (Scheme 4.14). The use of a boronic acid pinacol ester instead of an

acetylene substrate circumvents consumption of the starting material by homocoupling. The 1,4,5-tri-substituted 1,2,3-triazole product **4.59** formed in the Suzuki reaction was confirmed by mass spectrometry (Figure 4.4). Even though the boronic ester starting material could not be removed entirely from the product during purification, hence its yield could not be determined, the results indicate that Suzuki coupling could be a useful tool for the stepwise assembly of 1,4,5-tri-substituted BCP triazoles.

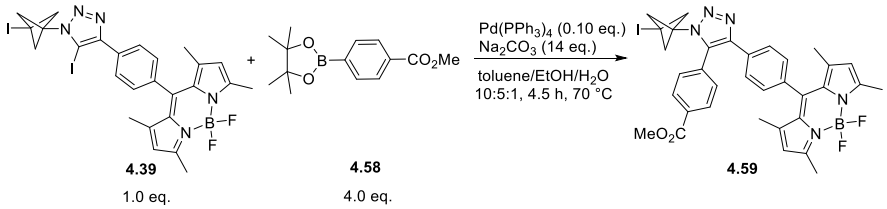

Scheme 4.14. Attempted Suzuki coupling reaction on 5-iodotriazole **4.39**.

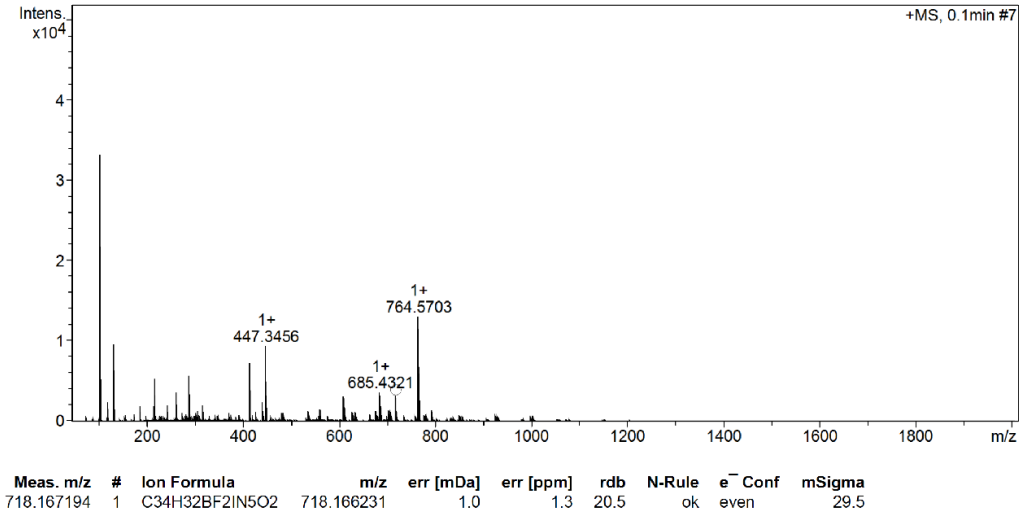

Meas. m/z	#	Ion Formula	m/z	err [mDa]	err [ppm]	rdb	N-Rule	e⁻ Conf	mSigma
718.167194	1	C34H32BF2IN5O2	718.166231	1.0	1.3	20.5	ok	even	29.5

Figure 4.4. HR-ESI-MS spectrum of **4.59**, calc. *m/z* $[M+H]^+$ = 718.1662; found 718.1672 (positive mode).

To investigate the dependence of the 5-alkynylation reaction on Pd, we carried out one reaction with 4-ethynylpyridine under the reported conditions but without addition of a Pd(II) catalyst. No formation of product **4.53** was observed, indicating that Pd is required for the 5-alkynylation reaction to take place. One possible reaction mechanism could be the .formation of a 5-iodotriazole as a reaction intermediate and subsequent Sonogahira coupling reaction between the aryl iodide and remaining terminal alkyne. However, this mechanistic route seems unlikely based on several indications. One of them is that, when a Pd/Cu-catalysed Sonogashira coupling was attempted using the 5-iodotriazole **4.39** as a starting material no formation of the tri-substituted triazole product **4.53** was observed at all (Scheme 4.13). By contrast, in the one-pot cycloaddition/coupling reaction using BODIPY

4.24 and BCP **1.92** as starting materials, the formation of a small amount of compound **4.53** was observed (Scheme 4.12). A second factor which contradicts the hypothesis of a 5-iodotriazole intermediate formation is that only catalytic amounts of CuI (0.20 eq.) as the iodine source were used and that no oxidant was added which should generally result in the formation of only trace amounts of 5-iodotriazoles. Hence, it is more likely that the one-pot cycloaddition/coupling reaction proceeds through a transmetalation of the Cu-triazolide intermediate **4.6** (Scheme 4.1) with a Pd species. Pd might also play a role in the pre-activation of the terminal alkyne which attacks at the 5-position of the triazole.[339] Detailed studies are ongoing to shed more light on this reaction mechanism.

4.6 Structural Analysis of BCP-Triazoles

The structures of BODIPY **4.24** and BCP compounds **4.36**, **4.14**, **4.40**, **4.41**, **4.45**, **4.46**, **4.52**, **4.53**, **4.56** were determined by single crystal X-ray diffraction analysis. We focused on the identification of prominent non-covalent interactions. Such interactions are of great importance in nature, where they determine the 3D structure of biomacromolecules and mediate ligand-receptor interactions.[340] Considering that the BCP moiety attracts growing interest as a bioisostere in drug candidates[182d,219a,219d,222b] it is pivotal to study the effects of the bioisosteric replacement on the weak interactions with molecules in the surroundings. The engineering of crystals with tuned non-covalent interactions is also of growing interest for the design of functional materials.[341] In the case of BCP-triazoles some interesting non-covalent interactions were observed for the different types of molecules. Halogen bonding[342] governs the molecular packing in several structures. Prominent interactions that were identified are I···N,[343] I···I [343c,344] I···H,[345] as well as N···H[346] contacts resulting in the arrangement of molecules in 2D sheets or 3D networks, respectively.

The crystal structure of 5-protio-1,2,3-triazole-substituted BCP **4.36** shows an intermolecular I···π interaction between I1 and a pyrrole ring of the dipyrromethene unit at a distance of 3.472 Å and with an angle of 175.3° (Figure 4.5). Examples of interactions between iodocarbons and the π-electrons of aromatic rings are not very abundant in the literature.[347] I···π interactions were found likewise in the crystal of **4.14** (Figure 4.5).

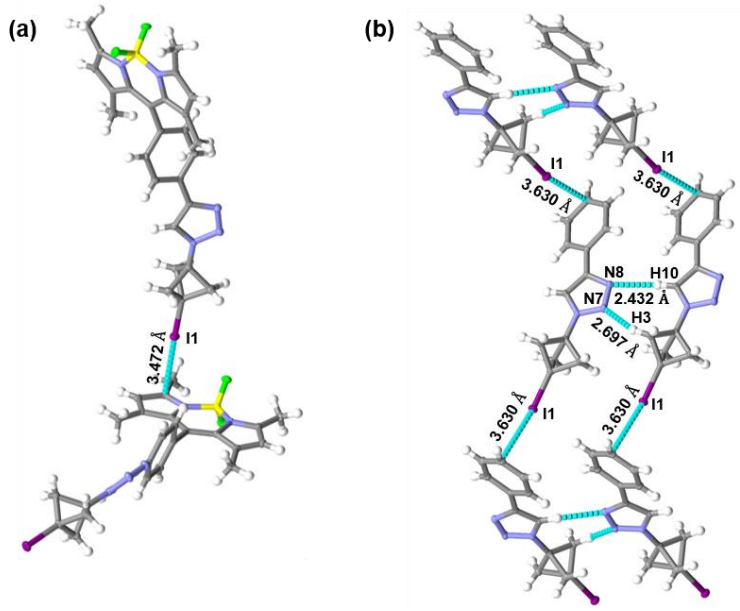

Figure 4.5. Non-covalent interactions in the crystal structures of (a) BCP **4.36** and (b) BCP **4.14**.

BCP **4.14** exhibits an intermolecular I···π contact between I1 and the phenyl ring at a distance of 3.630 Å and with an angle of 161.6°. It connects the molecules in a zig-zag pattern. Additional intermolecular nitrogen-hydrogen interactions[346] between N7 and H3 as well as N8 and H10, cause head-to-head packing of adjacent molecules. Several 1-iodo-3-triazolyl-BCP compounds were found to form I···N bonds in the solid state.[343] In the crystal structure of compound **4.40**, molecules in one layer interact *via* non-covalent bonds between I2 and N8 of the triazole rings at a distance of 2.848 Å and with an angle of 177.3°, in accordance with published data for C-I···N interactions.[343] The pyrene moieties are packed in a staggered manner. π···π-Interactions between the pyrene units of two adjacent layers at an inter-plane distance of 3.612 Å causes formation of a stack (Figure 4.6a). Additional I···I halogen bonds[343c,344] (I2···I2 = 3.879 Å) as well as I···H contacts[345] (I2···H20 = 3.071 Å; I1···H18 = 3.063 Å) effect the 3D network formation (Figure 4.6b).

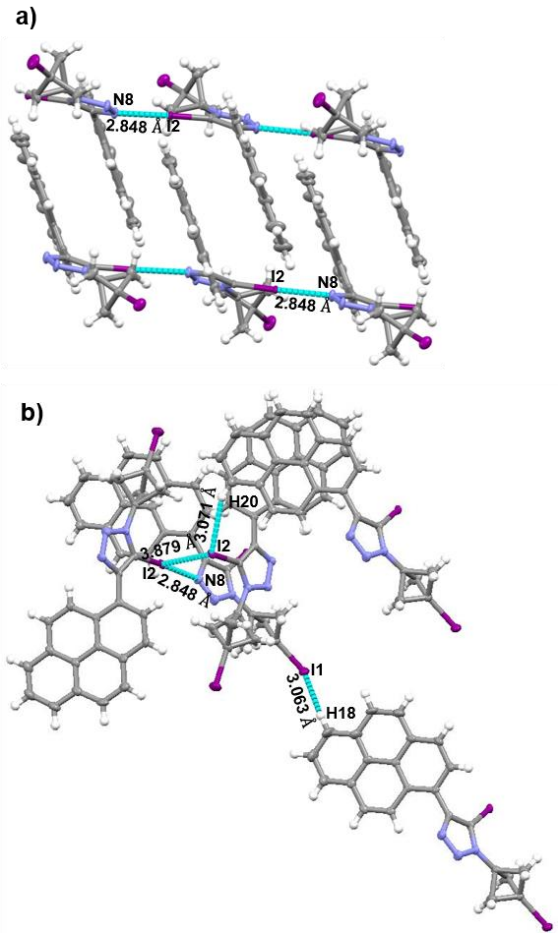

Figure 4.6. Two different views of the packing of BCP **4.40** molecules in the crystal showing (a) the π-stacking and (b) the halogen contacts (solvent in the void omitted for clarity).

BCP **4.46** differs from BCP **4.45** only by having a pyridine in place of a phenyl substituent in the 4-position of the triazole ring. In BCP **4.45** a halogen bond between triazolo-nitrogen N8 and triazolo-iodine I2 at a distance of 2.897 Å fixes the molecules in a head-to-head packing pattern (Figure 4.7a). In BCP **4.46** halogen bonding between I1 and pyridyl-nitrogen N13 becomes the dominant interaction over iodine-hydrogen bonding (Figure 4.7b). The non-covalent I1···N13 bond is formed at a distance of 3.184 Å and with an angle of 176.0°. In parallel, the nucleophilic site of I1 forms a type II halogen bond with the electrophilic end of I2 at a distance of 3.721 Å and with angles of 172.2° and 89.1°, which is in the expected range for this type of interaction.[343c,344] In combination with an additional N6···H14 contact this results in an offset packing of parallel sheets.

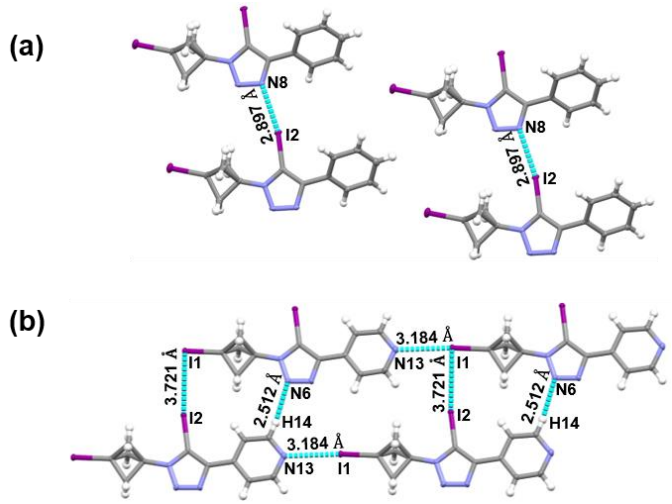

Figure 4.7. Non-covalent interactions in the crystal structures of (a) BCP **4.45** and (b) BCP **4.46**.

Looking at the crystal structures of the 5-protiotriazoles BCP **4.14** and BCP **4.56** it is again observed that replacement of a phenyl ring with a pyridyl moiety results in an iodine-nitrogen interaction (I1···N15 = 3.630 Å) (Figure 4.8b) which dominates over the iodine-π interaction (I1··· π = 3.630 Å) observed for the phenyl containing sample (Figure 4.8a). In both compounds bonds are formed between triazolo-hydrogen and triazolo-nitrogen (N8···H10 = 2.432 Å and N9···H11 = 2.482 Å) which mediate the formation of parallel sheets.

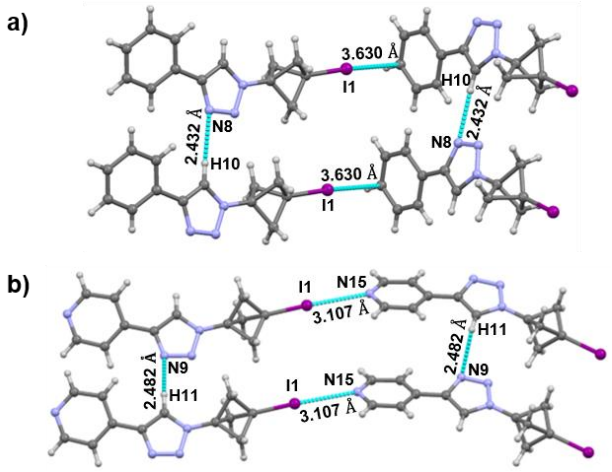

Figure 4.8. Non-covalent interactions in the crystal structures of (a) BCP **4.14** and (b) BCP **4.56**.

Crystal structures of the phenyl- and pyridyl-substituted BCP tweezer compounds **4.52** and **4.53** were compared as well. BCP **4.52** molecules are arranged in layers that are interconnected by intermolecular iodine-hydrogen (I1···H19 = 2.999 Å) and nitrogen-hydrogen (N9···H21 = 2.703 Å) contacts (Figure 4.9a). The planes of the 4-phenyl moieties of molecules in different layers are tilted at 45.5° towards each other (Figure 4.9b).

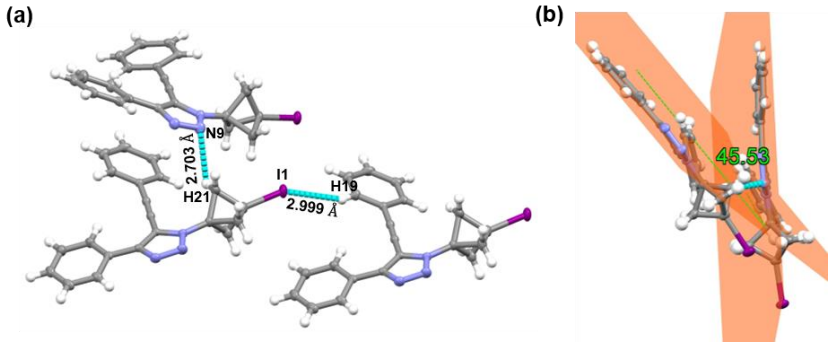

Figure 4.9. (a) Non-covalent interactions in the crystal structure of BCP **4.52** and (b) tilt angle between the molecular planes of the phenyl moieties in the 4-position of the triazole ring (C1-C6).

In the crystal structure of compound **4.53** additional hydrogen bonds are formed by the two pyridine moieties. Pyridyl-nitrogen N22 forms a bifurcated interaction with pyridyl-hydrogens H18 and H21 of an adjacent tweezer molecule (N22···H18 = 2.573 Å; N22···H21 = 2.646 Å) (Figure 4.10a). The formation of bifurcated hydrogen interactions of pyridine-type compounds has been previously observed in solid state and in solution.[348] Additional hydrogen contacts occur between triazolo-nitrogen N7 and BCP hydrogen H3 at a distance of 2.609 Å as well as between pyridyl-nitrogen N16 and BCP hydrogen H2 at 2.639 Å. In combination with an I···π interaction between I1 and a pyridine ring at 3.583 Å distance this leads to the formation of layers in which the individual molecules are arranged in a head-to-tail packing fashion. The planes of the 4-pyridyl moieties in these different layers are tilted at 63.4° towards each other (Figure 4.10b).

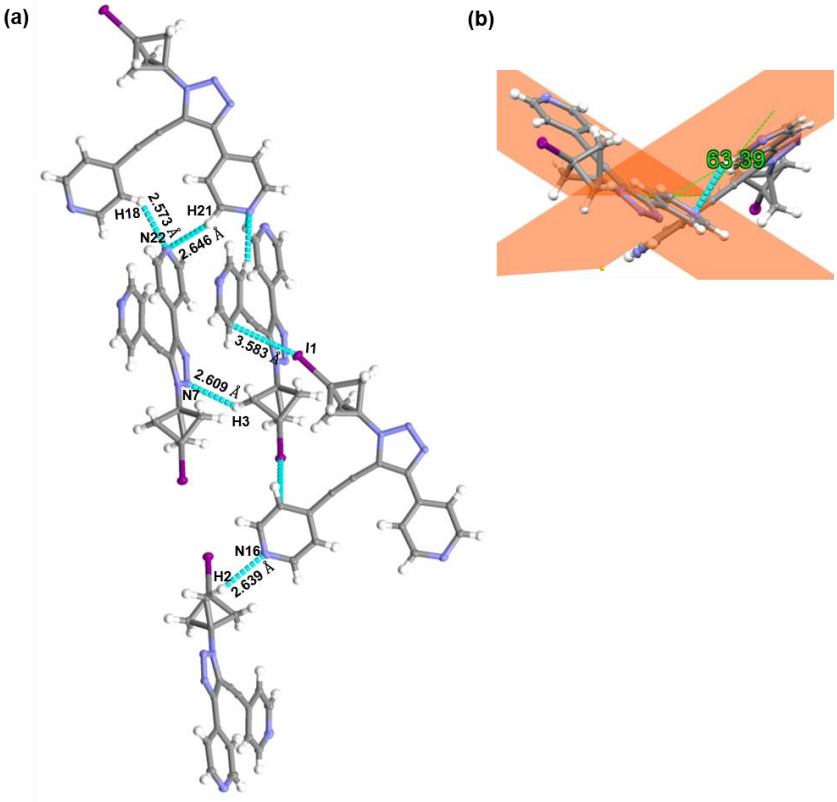

Figure 4.10. (a) Non-covalent interactions in the crystal of BCP **4.53** and (b) tilt angle between the molecular planes of the pyridyl moieties in the 4-position of the triazole ring (C19, C20, C21, N22, C23, C24).

4.7 Conclusion and Outlook

In conclusion, three different means to synthesise new BCP-triazole building blocks using 1,3-dipolar cycloaddition reactions were explored. Molecules with iodine substituents in the 5-position of the triazole ring were obtained in moderate to good yields. Iodine in this position is a useful synthetic handle for further functionalisation as well as a site for molecular interaction. BCPs substituted with 5-alkynylated 1,2,3-triazoles were also synthesised in a one-step cycloaddition/Pd-catalysed coupling reaction to yield molecular tweezer compounds. X-ray analysis revealed notable intermolecular interactions of some of the synthesised derivatives in the solid state. Particularly noteworthy are different non-covalent interactions involving iodine moieties, indicating intermolecular binding capabilities of this class of molecules.

Previously, 5-iodotriazole have been reported as scaffolds in drugs and optical imaging agents as well as in halide sensors.[9-11] At the same time, the BCP unit is under scrutiny as a bioisostere for phenyl, acetylene and *tert*-butyl moieties in drug molecules.[24] The compounds produced herein combine both these prominent moieties and therefore have

promise for potential applications in medicinal chemistry. For further investigations in this field, the improvement of the reaction yields to enable the bulk synthesis of the reported derivatives will be of major interest. While different protocols for 5-iodotriazole formation were tested and the reaction conditions could be optimised for a specific substrate, for some other substrates only low to moderate yields could be achieved. If time permitted, more reaction protocols could be tested on different substrates to further increase the selectivity and reduce the formation of side products. Optimisation studies in this area are ongoing.

Preliminary results suggest Suzuki coupling reactions to be a promising tool for the easy functionalisation of 5-iodotriazoles at the 5-position. This protocol could reduce the formation of side products and enable for the incorporation of larger moieties at the 5-position. This will be useful to obtain triazoles with BODIPY and/or porphyrin substituents in both the 4- and 5-position, compounds which could not be isolated in sufficient amounts from the one-pot cycloaddition/coupling reactions. From a structural point of view, appending substituents directly to the 5-position of the triazole ring without an ethynyl linker unit in between would result in an altered angle between the substituents in the 4- and 5-position and therefore possibly in a different molecular interaction profile.

An especially interesting finding is the formation of 5-alkynylated triazoles in a one-pot cycloaddition/coupling reaction. Complete elucidation of the reaction mechanism in this case could lay the cornerstone for further optimization of the reaction conditions used in order to improve the yields. In addition, as a part of successive investigations, a larger range of substrates will be screened to study the influence of electron-rich/electron-poor substituents.

The synthetic approaches presented herein merge BCP- with “click“-chemistry and do not only provide access to generic 1,4-di-substituted but also to 1,4,5-tri-substituted triazoles which offer new potential applications in the fields of medicinal chemistry and materials sciences.

Chapter 5. Synthesis of Bicyclo[1.1.1]pentane-Linked Porphyrin Arrays as Excitation Energy Transfer Model Systems

Tetrapyrroles are the central components of energy and electron transfer processes in nature. This includes hemes as prosthetic groups of cytochromes which are involved in the electron transport chain as well as chlorophylls and bacteriochlorophylls as pigments of the photosynthetic reaction centres and antenna complexes.[147] General aspects of the oxygenic photosynthesis process were outlined in Chapter 1. Chromophore arrays with tetrapyrroles as energy acceptor and/or donor units can be used to gain better insight in the electron and energy transfer processes taking place in nature and there are numerous reports on the synthesis of such model systems and studies on the communication between the donor and acceptor moieties.[146,349] We envisioned the synthesis of chromophore arrays bridged by bicyclo[1.1.1]pentane as a non-conjugated rigid hydrocarbon. This linker bears the potential of arranging moieties in a defined geometry and at a fixed distance while inhibiting undesired electronic communication between them. After giving a general introduction to the properties of bridged porphyrin arrays, our endeavours to synthesise a library of BCP-linked chromophore arrays will be presented.

5.1 Introduction to Bridged Porphyrin Array Systems

When designing donor-acceptor arrays, several factors need to be taken into consideration, including the electronic properties of the donor and acceptor moieties in the ground state and the excited state, the distance between them as well as their mutual orientation and the nature of the bridging unit between the moieties.[146a] Multiporphyrin arrays have been used to study the influence of these factors on the electronic communication between the chromophores.[349b] In our work we mainly focused on the synthesis of bisporphyrins, hence classic examples of bisporphyrin systems and how energy transfer properties of such donor-acceptor dyads can be modulated will be discussed hereafter.

Electronic communication in bisporphyrins is dependent on the mutual orientation between the porphyrins as well as the orientation of the moieties in respect to the linker unit. This is controlled by the torsional angles between the porphyrins and the linker unit and by how freely the moieties can rotate around the centre axis. The linker can show various degrees of electronic coupling with the porphyrin units. The extent of electronic coupling is partly determined by the dihedral angles between the porphyrins and the linker. Certain dihedral angles favour an overlap of their frontier molecular orbitals (FMOs), thus the linker's ability to act as a mediator for electronic communication between the porphyrin units. Weak

electronic coupling between the porphyrin donor and acceptor moieties ensures that both units mostly retain their individual properties. Lindsey and co-workers studied the electronic communication and energy transfer rates upon photoexcitation in diarylethynyl-linked dimers of Zn(II)porphyrin and free base porphyrin **5.1**, **5.2**, and **5.3** (Figure 5.1) where the Zn(II) porphyrin acted as the energy donor due to its lower oxidation potential. The researchers found that with the diarylethyne linker, the electronic properties of the individual porphyrin units were mostly retained while electronic coupling was still sufficient to enable energy and electron transfer. The diarylethyne unit was described as a “semi-rigid” linker which allows for rotation of the porphyrin units around the acetylene in solution.[150] In addition, the porphyrin moieties can rotate around the phenyl rings of the linker which allowed for rapid energy transfer ((24 ps)$^{-1}$) within the dyad **5.1** from Zn(II) porphyrin to free base porphyrin. In contrast, when methyl groups were introduced in the ortho positions of the linker phenyl rings in **5.2**, the energy transfer rate was decreased to (115 ps)$^{-1}$ because rotation towards coplanarity was hindered. This prevented efficient overlap of the porphyrin and linker orbitals.[150,350]

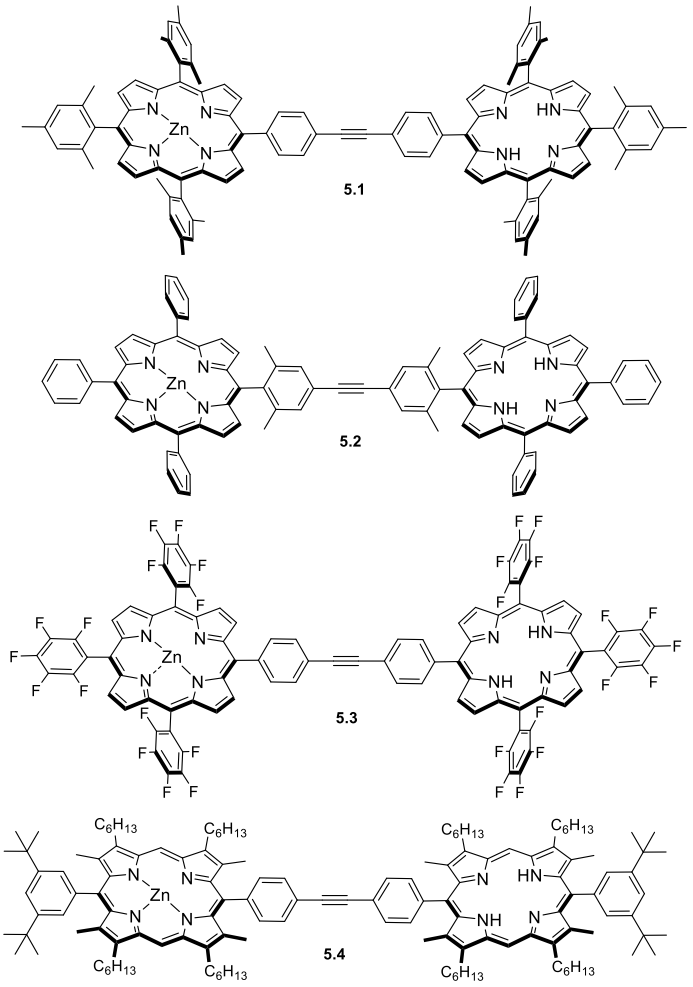

Figure 5.1. Zn(II)-free base porphyrin dimers with electron-donating (**5.1**) and electron-withdrawing (**5.3**) meso substituents, a dimer which shows restricted rotation around the linker unit (**5.2**) and a β-substituted dimer (**5.4**).

Besides orientation factors, modulation of the donor and acceptor units' FMOs can influence the extent of electronic communication. The localisation of the highest occupied molecular orbital (HOMO) in porphyrins depends on the porphyrin's substitution pattern. In the meso-aryl substituted Zn(II)-free base porphyrin heterodimer **5.1**, the a_{2u} orbital is the porphyrin's HOMO which means that significant electron density is located on the meso-carbons while the β-positions comprise nodal points (Figure 5.2). Hence, the linker attachment site on the porphyrin determines the degree of electronic communication between the macrocycles. On the other hand, in the Zn(II)-free base porphyrin heterodimer **5.3** where six meso-positions are substituted with electron-withdrawing pentafluorophenyl moieties the a_{1u} orbital becomes the HOMO, resulting in substantial electron density at the β-positions and nodal points at the meso carbons(Figure 5.2).[350]

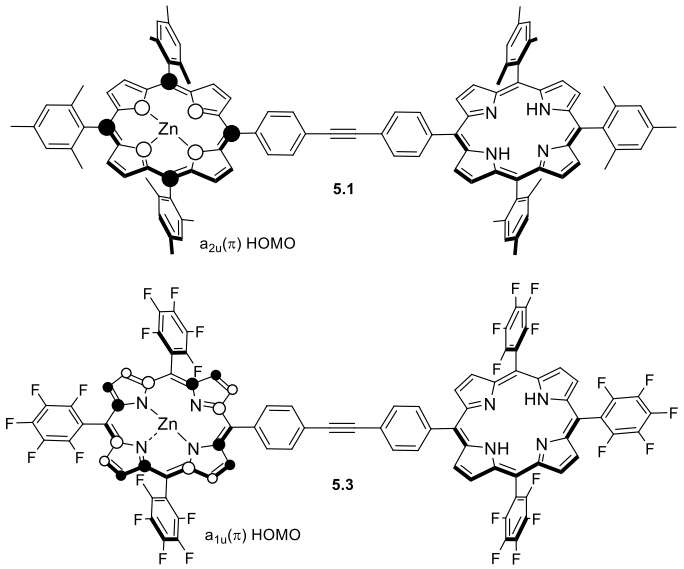

Figure 5.2. Frontier molecular orbitals indicated on the Zn(II) porphyrin moieties of the dimers **5.1** and **5.3**. In the case of dimer **5.1** with electron-donating mesityl-substituents in the meso positions the a_{2u} orbital is the HOMO while in case of dimer **5.3** with electron-withdrawing pentafluorophenyl-substituents in the meso-positions the a_{1u} orbital is the HOMO.[350]

While the substitution of six meso-positions with pentafluorophenyl units in **5.2** resulted in a reordering of the a_{2u} and a_{1u} orbitals, more gradual changes can be achieved by the introduction of a smaller number of pentafluorophenyl groups. For example, it was found that in (5,10,15,20-tetraphenylporphyrinato)zinc(II) the a_{2u} orbital is stabilised by 0.85 kcal/mol relative to the a_{1u} orbital for each pentafluorophenyl unit introduced. Hence, in (5-(pentafluorophenyl)-10,15,20-triphenylporphyrinato)zinc(II) the a_{2u} orbital is the HOMO while in the respective porphyrins with two pentafluorophenyl units the a_{1u} and a_{2u} orbitals are nearly degenerate. Substitution of three or four phenyl rings with pentafluorophenyl moieties results in such strong stabilisation of the a_{2u} orbital that its energy falls below the a_{1u} orbital.[351] The role which the porphyrin substitution plays for orbital energies can also be seen in another example. While for the Zn(II)-free base porphyrin dimer **5.1** a fast energy transfer [$(24\ ps)^{-1}$] from the excited Zn(II) porphyrin donor to the free base porphyrin acceptor was observed, in the β-substituted Zn(II)-free base porphyrin dimer **5.4** (Figure 5.1) the energy transfer rate was much lower [$(417\ ps)^{-1}$]. It was assumed that this observation was based on lower intramolecular electronic communication in the dimer originating from a different location of the HOMOs. In the fully meso-substituted dimer **5.1** the a_{2u} orbital is the HOMO which results in substantial electron density on the meso carbons. In contrast, in molecule **5.4** with alkyl substituents in the β-positions the a_{1u} orbital becomes the HOMO with main electron density located on the β-carbons, thus electronic communication through the linker in the meso position is minimised.[350,352]

As stated in Chapter 1, the electron transfer efficiency generally depends on the distance between donor and acceptor moieties. The distance dependency of the electron transfer can be described by its exponential decay constant β. β is typically large for two units bridged by alkyl linkers and lower for π-conjugated linkers such as alkenyl- or aryl-bridges but in this case strongly depends on the dihedral angles between the aryl rings (see Chapter 1).[148,149] For porphyrin dimers containing π-conjugated linkers such as phenylene, ethynylene, and phenylene vinylene bridges the through-bond electronic coupling between the donor and acceptor moieties was found to have a larger contribution than the through-space transfer. The distance dependence of the energy transfer was rather low in these conjugated dimers.[352,353] The transfer rates were determined to depend more strongly on the nature and the geometry of the linker unit.[353]

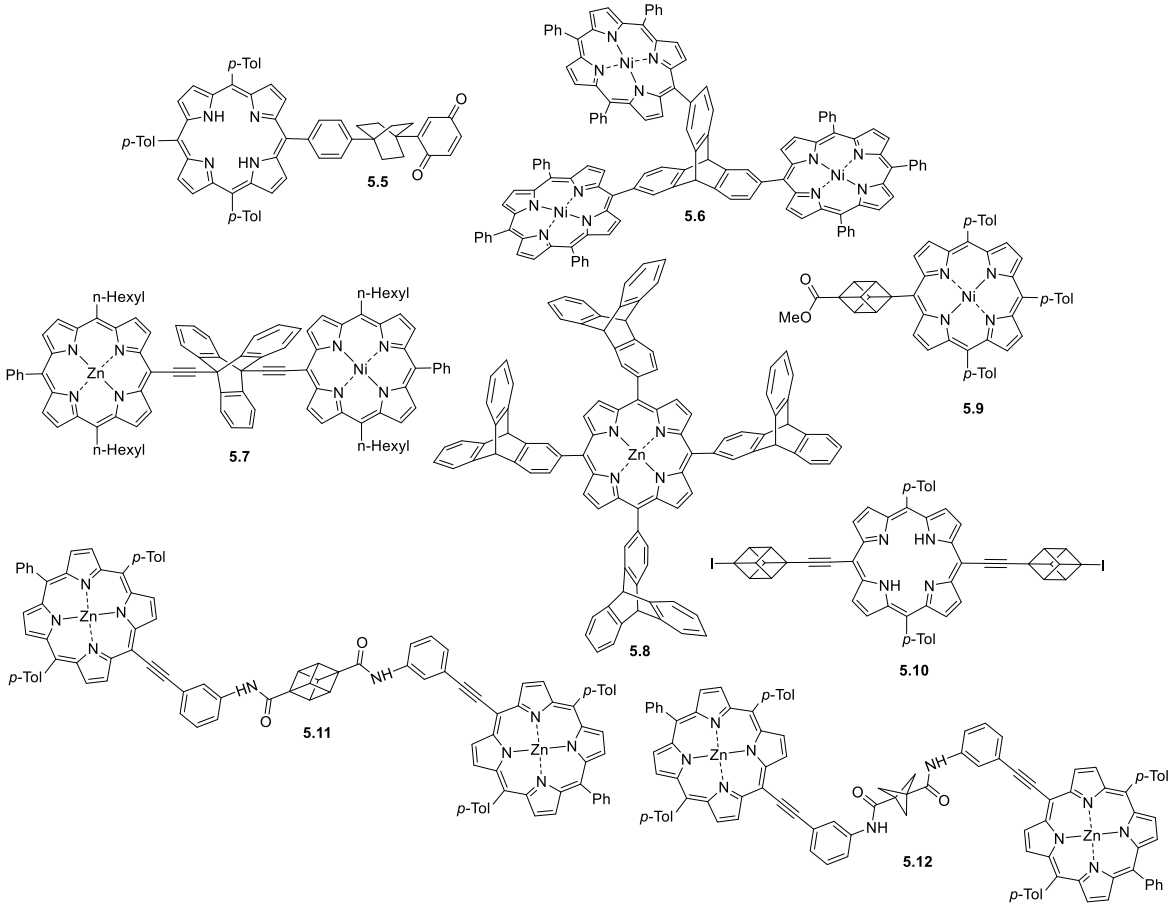

Figure 5.3. Selected examples of bicyclo[2.2.2]octane- (**5.5**),[354a] triptycene- (**5.6**-**5.8**),[355c, 355e, 355f] cubane- (**5.9**-**5.11**)[356a,181] and bicyclo[1.1.1]pentane- (**5.12**)[181] linked porphyrins.

Rigid hydrocarbon linkers are being studied as possible mediators or resistors, respectively, for electron transfer between two excitable moieties. Three main properties make them interesting compounds to act as such linker units: They are rigid, they align substituents in a linear manner and they are non-conjugated, thus hamper undesired electronic

communication.[144] Despite these favourable properties, only a few examples of porphyrin-rigid linker arrays have been reported (Figure 5.3). This is likely due to the limited synthetic accessibility of such derivatives. Several bicyclo[2.2.2]octane (BCO)-linked porphyrin systems (representative example **5.5**) have been synthesised and studied as photosynthetic mimics.[144a,354] Bolton *et al*. observed less efficient photo-induced electron transfer in a BCO-linked porphyrin-quinone dyad **5.5** compared to a similar triptycene-linked dyad which had been reported earlier. In addition, a ground state interaction between the moieties in **5.5** was not detected, in contrast to a comparable flexibly linked porphyrin-quinone dyad.[354a] Several triptycene-porphyrin arrays have been reported as well (representative examples **5.6**–**5.8**).[355] Prior to the work presented herein, to the best of our knowledge there are only two reports on cubane- and one report on BCP-linked porphyrin arrays (representative examples **5.9**–**5.11** and **5.12**).[356a,181] In the previously prepared BCP-linked porphyrin arrays, the BCP and porphyrin units were connected *via* amide bonds which imparted structural flexibility and rendered these molecules unsuitable for energy transfer studies.[181]

Among these linker molecules, the linker with the shortest non-bonding C-C distance of 1.85 Å is bicyclo[1.1.1]pentane (BCP).[144,164] Hence, of all the hydrocarbon linkers, BCP shows an inter-carbon distance value closest to the one of the triple bond with 1.19 Å.[144a,357] While the ethyne unit is a conjugating linker and substituents can rotate around it, BCP is rigid and non-conjugating. At the same time, there is evidence for residual electronic communication through the BCP cage.[358] Therefore, BCP appears as a suitable linker for the study of energy transfer processes by holding its substituents in a defined geometry and at a specific distance. In addition, it is predicted that the BCP linker separates the substituents electronically so that the properties of the single moieties are retained while it can still allow for some electronic communication.

The most ideal case of such a linker system is one where the donor and acceptor moieties are directly bound to the bridgehead positions of the BCP scaffold. However, the direct carbon-carbon bond formation on the BCP bridgehead positions can be complicated since they are not easily accessible to conventional Pd-catalysed coupling reactions and the substrate scope for known bridgehead modifications is limited. Therefore, the easier to functionalise bis-1,3-(4-iodophenyl)bicyclo[1.1.1]pentane molecule was used as the starting material for the synthesis of BCP-chromophore arrays.

5.2 Objectives

In the course of this work, it is aimed to prepare BCP-linked chromophore dyads as possible probes for studies of excitation energy transfer through the BCP scaffold. Herein, the focus is on the development of synthetic approaches towards functionalisation of a 1,3-diphenyl-BCP linker unit with photoactive groups. It is aimed to synthesise a library of dyads with different photophysical and structural properties whose influence on energy transfer efficiencies are to be evaluated in follow-up studies (Figure 5.4). Different parameters are will be altered: Energy donor and acceptor moieties with varying electronic and photophysical properties will be employed and the overall geometry of the dyads will be varied by usage of different linking units.

Porphyrins are intended to serve as energy acceptor units. Their electronic properties will be tuned by the incorporation of electron-donating phenyl and electron-withdrawing pentafluorophenyl moieties as meso-substituents and by the insertion of different metals in the core, e.g., Zn(II), Ni(II) and Cu(II).

BODIPY and pyrene are targeted as energy donor moieties. Furthermore, it is aimed to synthesise a porphyrin dimer with a (15-(pentafluorophenyl)-10,20-diphenylporphyrinato)zinc(II) acceptor unit and a (10,15,20-triphenylporphyrinato)zinc(II) donor moiety.

Different reaction types will be utilised for the attachment of the donor and acceptor chromophores to the 1,3-diphenyl-BCP unit. Coupling of the chromophores to the linker will be achieved by incorporating ethyne spacer units (Sonogashira coupling reactions) or by attachment without additional spacers (Suzuki coupling reaction). The different attachment modes are expected to influence the overlap of the chromophore and linker orbitals and therefore the electronic coupling through the linker.[359]

Lastly, a synthetic route will be tested to synthesise porphyrin arrays in which the porphyrin macrocycle is connected to BCP without any phenyl spacers. With this approach it is intended to shorten the length of the linker between the donor and acceptor moieties.

The overall goal of this study is to prepare a library of BCP-linked porphyrin arrays with energy donor-acceptor properties. In secondary studies, these molecules can be used to investigate excitation energy transfer processes between moieties which are non-conjugated and arranged in a defined geometry.

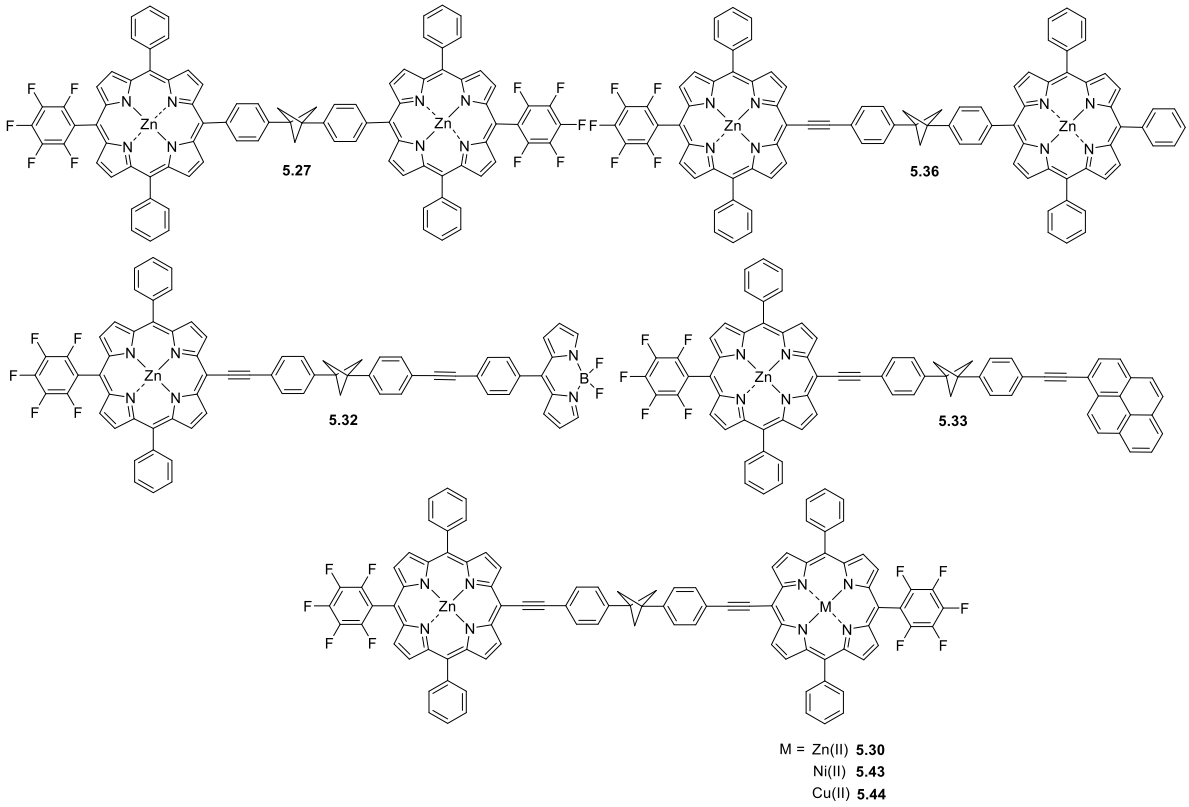

Figure 5.4. Target BCP-linked dyads comprising a (15-(pentafluorophenyl)-10,20-diphenylporphyrinato)zinc(II) moiety to be prepared in this study.

5.3 Strategic Synthesis of Diphenyl-BCP-Linked Donor-Acceptor Dyads

For the synthesis of BCP-linked donor-acceptor dyads, various starting materials had to be synthesised first, including porphyrins and the BCP linker. As the central linker unit for all dyads 1,3-diphenyl-BCP was employed. The use of this compound had previously been reported by de Meijere *et al*. to link an anthracene fluorophore with three different photochromic units in close proximity while not allowing for significant π-conjugation between the units. Efficient resonance energy transfer was found to take place between the moieties. Bis-1,3-(4-iodophenyl)bicyclo[1.1.1]pentane served as the starting material for Sonogashira and Negishi coupling reactions with the chromophores.[173]

Herein, bis-1,3-(4-iodophenyl)bicyclo[1.1.1]pentane **5.15** was synthesised by Dr. Nitika Grover according to the literature procedure by reaction of [1.1.1]propellane **1.66** with phenylmagnesium bromide and subsequent Negishi coupling with bromobenzene (Scheme 5.1).[173] The following iodination in both 4-positions of the phenyl rings afforded di-iodinated BCP **5.15**. This molecule constitutes a suitable starting material for the attachment of moieties by Pd-catalysed coupling reactions.

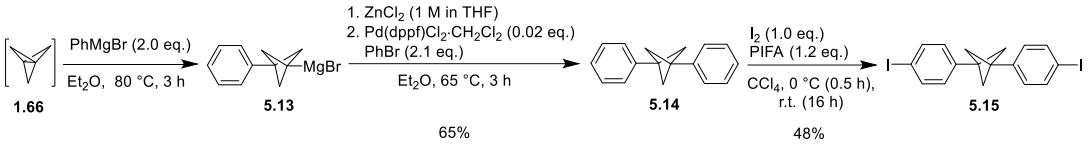

Scheme 5.1. Synthesis of bis-1,3-(4-iodophenyl)bicyclo[1.1.1]pentane **5.15** from [1.1.1]propellane **1.66** by Grignard and Negishi reactions followed by iodination.

Our intention was to use a porphyrin with one pentafluorophenyl meso-substituent, (5-(pentafluorophenyl)-10,20-diphenylporphyrinato)zinc(II) as the general acceptor unit in BCP-linked donor-acceptor dyads. Based on previous findings by Ginia *et al*., it was anticipated that in this compound the a_{2u} orbital will remain as the HOMO while being significantly stabilised at the same time, making this porphyrin unit a good electron acceptor.[351] (5-(Pentafluorophenyl)-10,20-diphenylporphyrinato)zinc(II) is a porphyrin of the A_2BC type. Porphyrins of this kind can be synthesised either by mixed condensation reactions from pyrrole and aldehydes or in a stepwise manner from dipyrromethane (DPM) precursors. Since mixed condensations typically result in the formation of product mixtures and tedious separations, the stepwise approach was preferred. Following a synthetic strategy developed by Lindsey and co-workers, meso-pentafluorophenyl-substituted DPM (**5.19**) was reacted with ethylmagnesium bromide, followed by addition of benzoyl chloride to yield a mixture of 1-mono- and 1,9-di-acylated dipyrromethanes (Scheme 5.2).[360] The 1,9-di-acylated product (**5.20**) was isolated by column chromatography and subsequently reduced to the dicarbinol-DPM **5.21** which was used without further purification. TFA-catalysed condensation of **5.21** with meso-free DPM **5.22** yielded 5-(pentafluorophenyl)-10,15-diphenylporphyrin **5.23**.

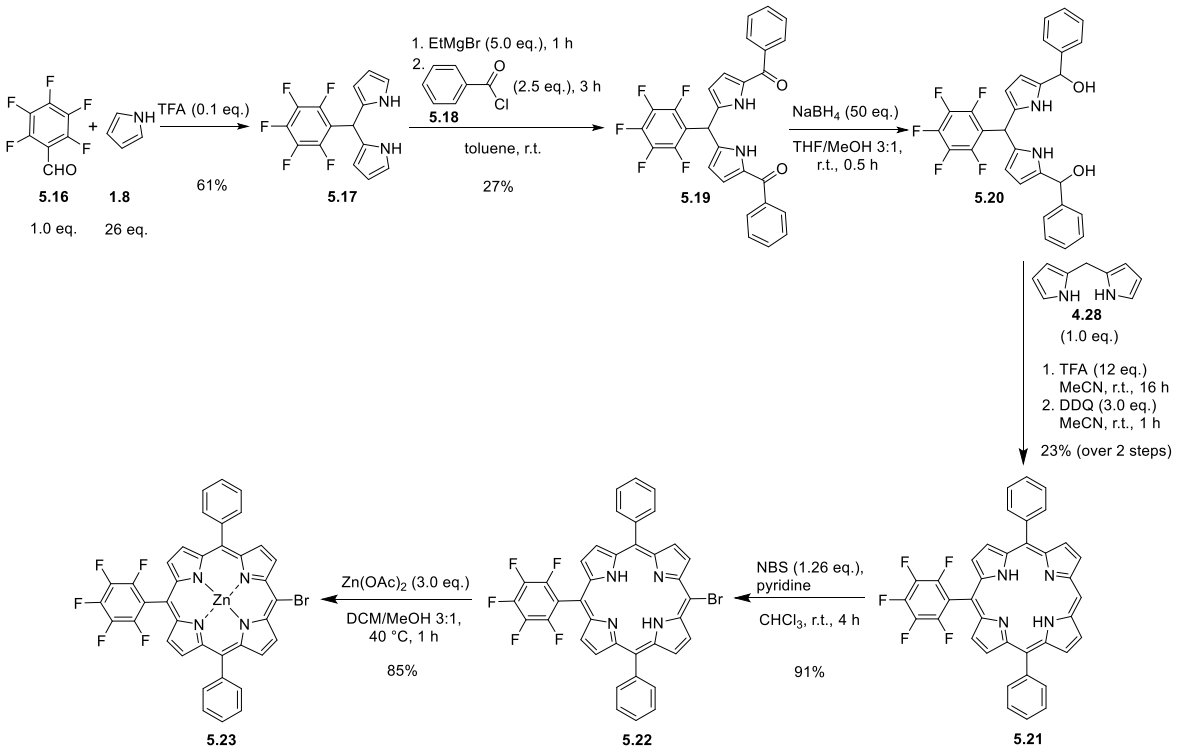

Scheme 5.2. Multistep synthesis of brominated pentafluorophenyl-substituted porphyrin **5.23**.

A halogenation in the free meso-position of **5.21** was intended to enable subsequent attachment of functional groups such as trimethylsilylacetylene (TMS-acetylene) or a boronic acid pinacol ester, respectively. In a first trial, iodination of **5.21** was attempted using I_2 and PIFA in the presence of pyridine in chloroform. No conversion of the starting material was observed after 3 h. Presumably, the change in the energy of the porphyrin's HOMO due to pentafluorophenyl substitution led to less reactivity of **5.21** towards electrophilic iodination in the meso position. As a result, it was decided to attempt bromination of the meso position instead. Based on a procedure by Takanami *et al*., published for a similar pentafluorophenyl-substituted porphyrin, Zn(II) was inserted into the macrocycle first by using $Zn(OAc)_2$.[361] This was followed by attempted bromination with NBS (1.5 eq.) in chloroform. However, complete degradation of the porphyrin macrocycle occurred under these conditions. A different synthetic route was tested instead, where the free base porphyrin was used as the starting material for bromination. **5.21**, dissolved in chloroform, was stirred with 1.1 eq. NBS at r.t. (Scheme 5.2). Some pyridine (about 8.0 eq.) was added to the reaction mixture to prevent degradation of the porphyrin. The reaction was monitored by TLC analysis and another 0.16 eq. NBS were added after 3 h, resulting in complete conversion of the starting material after 4 h. The mono-brominated product **5.22** could be isolated in 91%.

For the purpose of preparing BCP-linked porphyrin-fluorophore dyads, zinc(II) insertion into the porphyrin was envisioned to protect the macrocycle from core metalation during Pd- and Cu-catalysed coupling reactions. Zinc was chosen as a metal because Zn(II) porphyrins are photoactive and their fluorescence properties can be used to detect energy transfer processes. The insertion was effected by reaction with $Zn(OAc)_2$ (3.0 eq.) in a mixture of DCM and methanol to give Zn(II) porphyrin **5.25** (Scheme 5.2).

This brominated porphyrin was used as a precursor for functionalisation with a boronic acid pinacol ester *via* Miyaura borylation. Reaction of **5.23** with pinacolborane (20 eq.) under catalysis by $Pd(PPh_3)_2Cl_2$ (0.20 eq.) and triethylamine (TEA) (20 eq.) in 1,2-DCE gave meso-borylated porphyrin **5.24** in 58% yield (Scheme 5.3). This precursor for Suzuki coupling reactions was complemented by preparation of a precursor for Sonogashira coupling reactions. Bromo-porphyrin **5.23** was reacted with TMS-acetylene (3.8 eq.), $Pd(PPh_3)_2Cl_2$ (0.10 eq.) and CuI (0.20 eq.) in a mixture of THF and TEA. After isolation of TMS-acetylene-substituted porphyrin **5.25**, deprotection with TBAF (1.1 eq.) gave ethynyl-porphyrin **5.26** in 65% overall yield (Scheme 5.3).[37b]

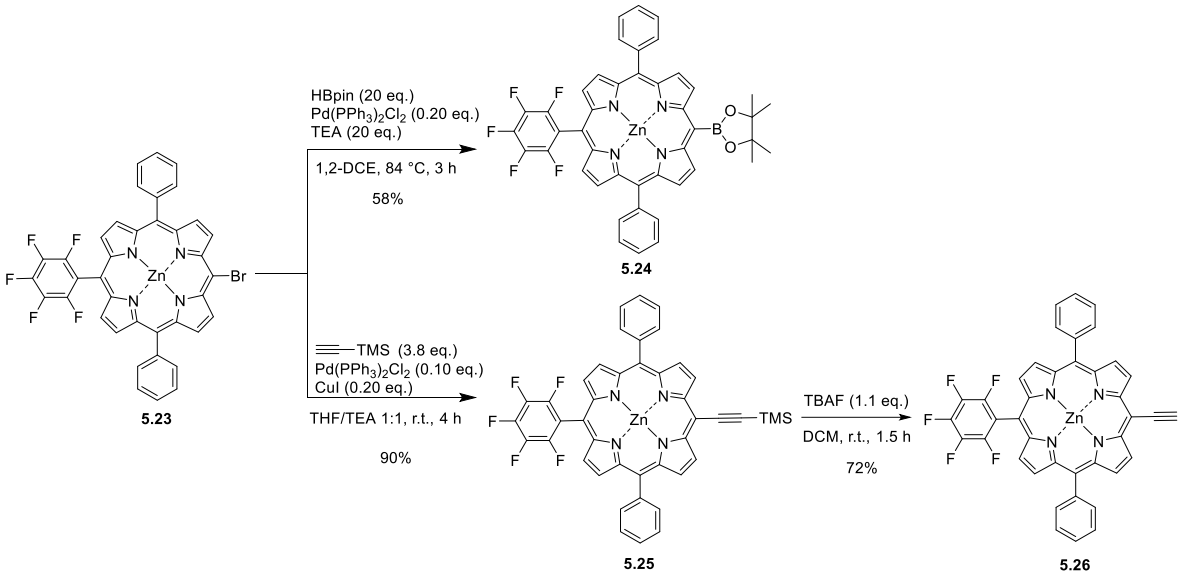

Scheme 5.3. Synthesis of borylated and ethynylated porphyrin precursors **5.24** and **5.26** for Suzuki and Sonogashira coupling reactions.

With the functionalised porphyrins **5.24** and **5.26** at hand, Pd-catalysed coupling reactions with the bis-1,3-(4-iodophenyl)bicyclo[1.1.1]pentane linker (**5.16**) could be carried out. In initial studies, a single porphyrin moiety was tried to be coupled to **5.16** *via* a Suzuki reaction to obtain BCP-appended porphyrin monomers. This was attempted by reaction of 1 eq. of the porphyrin with 1 eq. of the linker. However, it was observed that under the relatively harsh reaction conditions typically employed for Suzuki couplings, the iodine substituent on

the side of the linker which had not undergone a coupling reaction was lost. Hence, no further coupling reaction to append a second moiety onto the BCP linker could be carried out. On the other hand, when 2.0 eq. of borylated porphyrin **5.24** were reacted with 1.0 eq. of the bis-1,3-(4-iodophenyl)bicyclo[1.1.1]pentane linker using $Pd(PPh_3)_4$ and K_2CO_3 in DMF, the symmetric BCP-linked porphyrin dimer **5.27** could be obtained in 46% yield (Scheme 5.4). The formation of a trace amount of monomer **5.28** was also detected by high resolution mass spectrometry (HRMS) measurements.

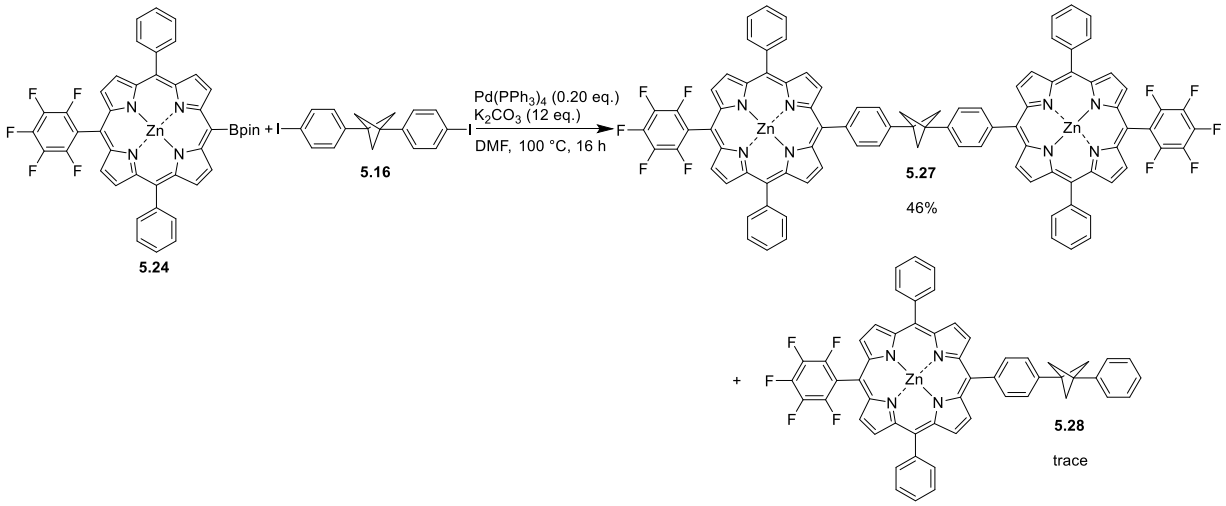

Scheme 5.4. Synthesis of the symmetrical BCP-linked porphyrin dimer **5.29** by a Suzuki coupling reaction.

However, for the synthesis of unsymmetric dyads a different synthetic strategy had to be employed. When the linker **5.16** was reacted with 1.4 eq. of ethynyl-substituted porphyrin **5.26** under Sonogashira coupling conditions using $Pd(PPh_3)_2Cl_2$ (0.11 eq.) and CuI (0.21 eq.) as catalysts in a mixture of THF and TEA the BCP-appended porphyrin monomer **5.29** could be isolated in 35% yield (Scheme 5.5). In this compound the iodine moiety on the uncoupled side of the linker unit stayed intact, owing to the milder reaction conditions. This allowed for further functionalisation of **5.29** by Pd-catalysed coupling reactions. The bis-coupled compound, BCP-linked porphyrin dimer **5.30**, was also formed as a minor product in 8% yield.

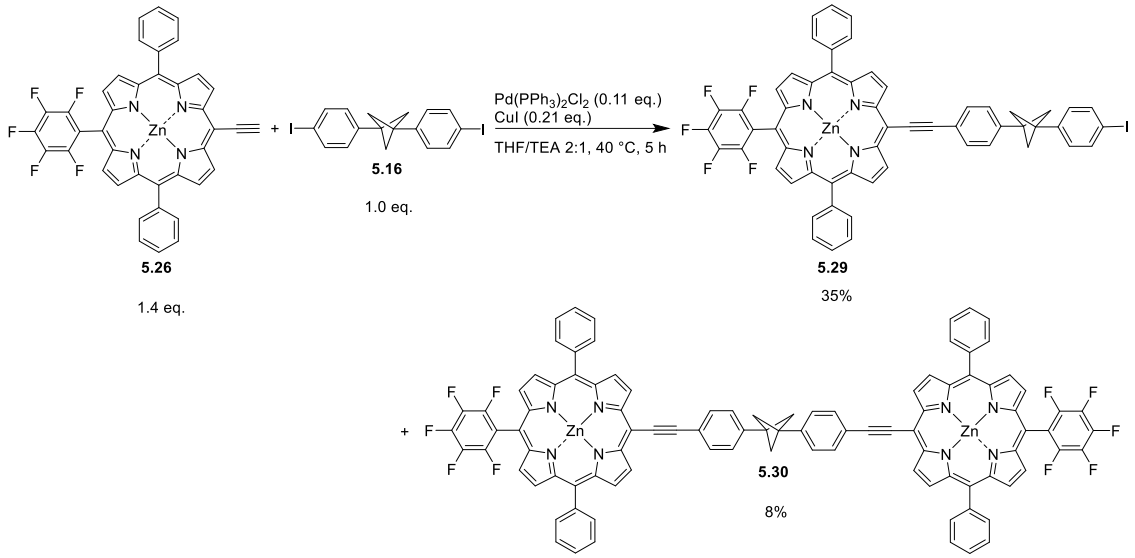

Scheme 5.5. Synthesis of BCP-appended porphyrin monomer **5.29** in which the iodine moiety on the uncoupled side of the linker unit was retained.

Compound **5.29** was subsequently used for the synthesis of unsymmetric BCP-linked dyads as donor-acceptor systems. As coupling substrates, ethynyl-substituted BODIPY and pyrene dyes were chosen since these fluorophores are well-known as energy donor moieties in conjunction with porphyrin acceptors.[362] In addition, a (10,15,20-triphenylporphyrinato)zinc(II) moiety was aimed to be introduced which was anticipated to act as an energy donor moiety for the (15-(pentafluorophenyl)-10,20-diphenylporphyrinato)zinc(II) unit. The ethynyl-substituted BODIPY and pyrene precursors were prepared following literature procedures.[363,330] Subsequently, they were reacted with monomer **5.29** under Sonogashira coupling conditions (Scheme 5.6). The reaction of **5.29** with 4-ethynylphenyl-substituted BODIPY **5.31** (1.4 eq.) under catalysis by $Pd(PPh_3)_2Cl_2$ (0.2 eq.) and CuI (0.3 eq.) proceeded smoothly and yielded the porphyrin- BODIPY dyad **5.32** in 74% after 5 h reaction time. When **5.29** was reacted with 1-ethynylpyrene **4.27** (1.4 eq.) under the same reaction conditions, formation of a considerable amount of the homo-coupled butadiyne-linked pyrene dimer was observed by TLC analysis. Therefore, more 1-ethynylpyrene was added to the reaction in batches of 0.70 eq. and 0.35 eq. after 4.5 h and 5.5 h, respectively, until after 6 h complete conversion of starting material **5.29** was determined. The porphyrin-pyrene dyad **5.33** was isolated in 58% yield.

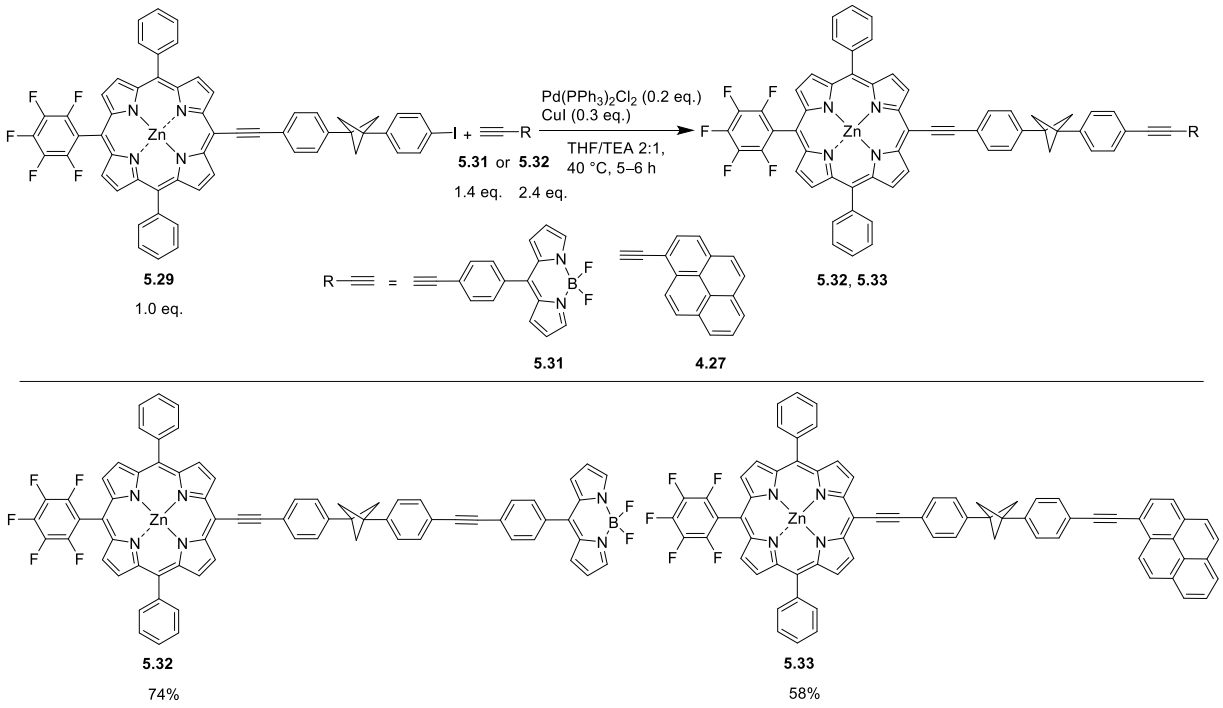

Scheme 5.6. Synthesis of BCP-linked porphyrin-BODIPY (**5.32**) and porphyrin-pyrene (**5.33**) dyads *via* Sonogashira coupling reactions on porphyrin monomer **5.29**.

A BCP-linked porphyrin-porphyrin dyad comprising a (15-(pentafluorophenyl)-10,20-diphenylporphyrinato)zinc(II) moiety on one side and a (10,15,20-triphenylporphyrinato)zinc(II) moiety on the other side was synthesised by a Suzuki coupling reaction (Scheme 5.7). In this case, the Suzuki protocol was chosen over Sonogashira reaction conditions because it was observed in previous experiments that Sonogashira reactions with ethynyl-substituted porphyrins resulted in the formation of a large amount of homo-coupled porphyrin dimer side products. The butadiynyl-linked porphyrin dimers can be difficult to separate from the BCP-linked porphyrin dimers by column chromatography, thus reducing the overall yield of the isolated product. Hence, boronic acid pinacol ester-substituted porphyrin **5.34** was synthesised as a precursor for a Suzuki coupling reaction according to a literature procedure.[355a] The coupling reaction of **5.34** with the BCP-appended porphyrin monomer **5.29** in DMF using $Pd(PPh_3)_4$ (0.2 eq.) as a catalyst and K_2CO_3 (12 eq.) as a base yielded the porphyrin dimer **5.35** in 51% yield.

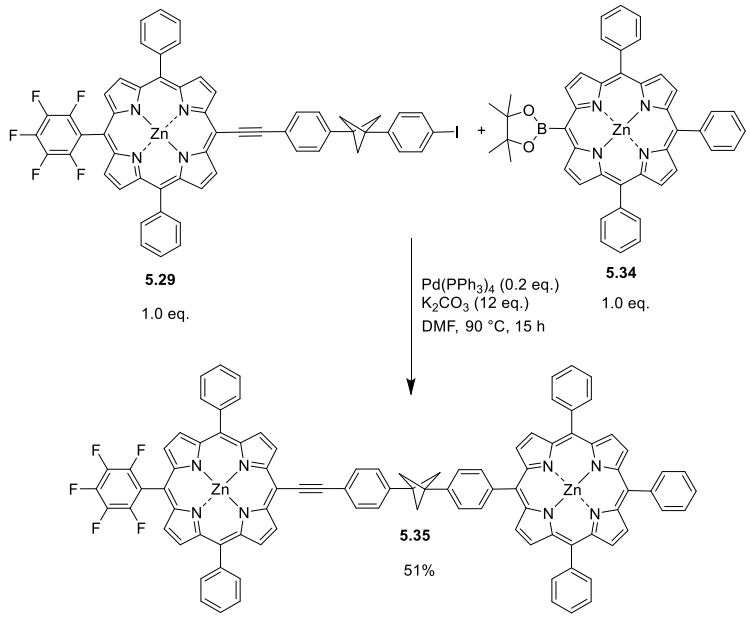

Scheme 5.7. Synthesis of a dyad comprising a (15-(pentafluorophenyl)-10,20-diphenylporphyrinato)zinc(II) moiety and a (10,15,20-triphenylporphyrinato)zinc(II) moiety (**5.35**).

Furthermore, we were interested in synthesising BCP-linked porphyrin dimers containing two different metal centres for future studies of the electronic communication between the different metalloporphyrins. The relative ease of their synthetic preparation rendered Ni(II) and Cu(II) porphyrins as admirable candidates for the synthesis of such dyads. In a series of Zn(II), Ni(II) and Cu(II) metalated tetraphenylporphyrins (Zn(II)TPP, Ni(II)TPP and Cu(II)TPP), Zn(II)TPP is the easiest to oxidise, its first oxidation potential being 0.84 V, while higher potentials were measured for Cu(II)TPP (0.97 V) and Ni(II)TPP (1.02 V).[364] When constructing BCP-linked Zn(II)-Cu(II) and Zn(II)-Ni(II) porphyrin dimers it can therefore be anticipated that the Zn(II) porphyrin moiety can act as a donor while the Ni(II) and Cu(II) porphyrin moieties can act as acceptors for electron transfer.

Using the previously prepared zinc(II) porphyrin monomer **5.29** as a starting material, 15-(pentafluorophenyl)-10,20-diphenylporphyrin moieties containing Cu(II) or Ni(II) metal centres, respectively, were intended to be appended on **5.29** (Scheme 5.8). The metalloporphyrin substrates for coupling reaction with **5.29** were prepared by Cu(II) and Ni(II) insertion into brominated porphyrin **5.23** using $Cu(OAc)_2$ (3.0 eq.) in a mixture of DCM and methanol (conditions a, Scheme 5.8) or $Ni(acac)_2$ (4.0 eq.) in toluene (conditions b, Scheme 5.8). The Cu(II) and Ni(II) porphyrins **5.36** and **5.37** were isolated in 93% and quantitative yield, respectively. Ethynyl moieties were appended onto **5.36** and **5.37** *via* Sonogashira coupling reactions and subsequent deprotection under the conditions employed previously for the equivalent Zn(II) porphyrins **5.23** and **5.25**. The ethynyl-

substituted Cu(II) and Ni(II) porphyrin complexes **5.40** and **5.41** were obtained in 84% and 76% yield over two steps, respectively.

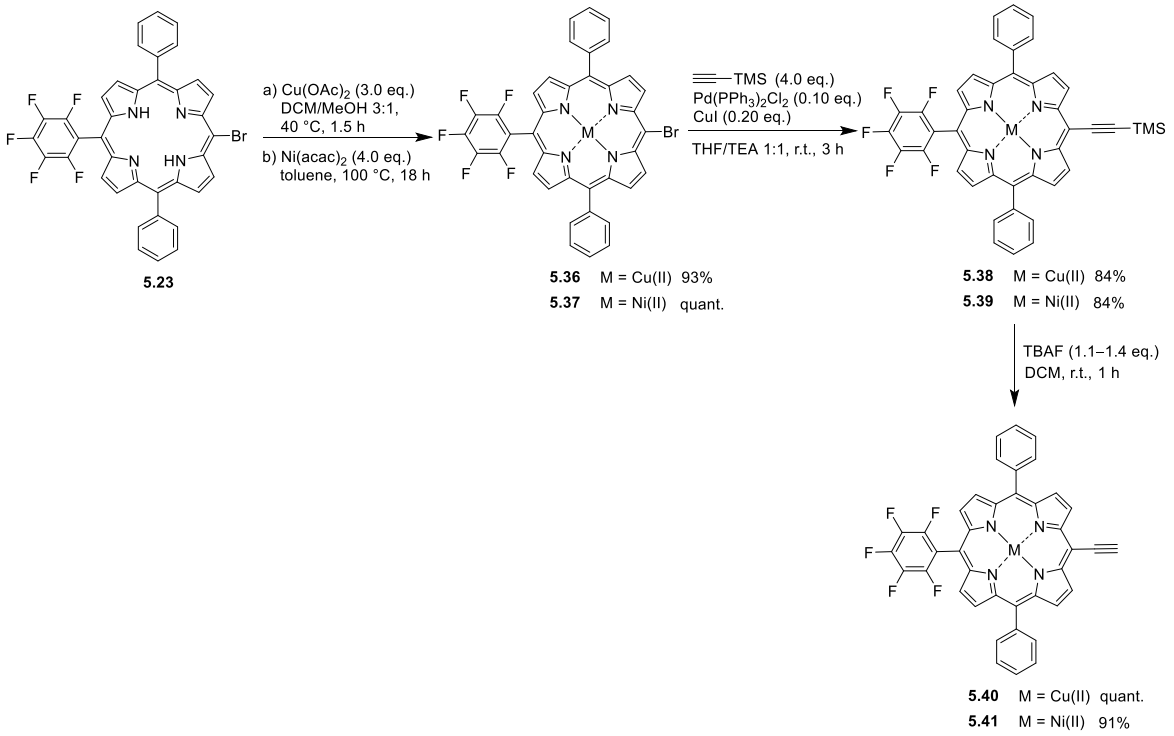

Scheme 5.8. Synthesis of Cu(II) and Ni(II) complexes of 5-ethynyl-10,20-diphenyl-15-pentafluorophenylporphyrin **5.40** and **5.41**.

The ethynylated Cu(II) and Ni(II) porphyrins were reacted with BCP-appended Zn(II) porphyrin monomer **5.29** under Sonogashira coupling reaction conditions using $Pd(PPh_3)_2Cl_2$ (0.2 eq.) and CuI (0.3 eq.) in a mixture of THF and TEA (conditions a and b, Scheme 5.9). The purification of both, the Zn(II)-Cu(II) and Zn(II)-Ni(II) dyads **5.42** and **5.43**, by silica gel column chromatography was complicated by similar polarities of the desired products and the Zn(II) porphyrin starting material **5.29** as well as the side products from homo-coupling reactions. **5.42** and **5.43** were isolated in 48% and 22% yield, respectively.

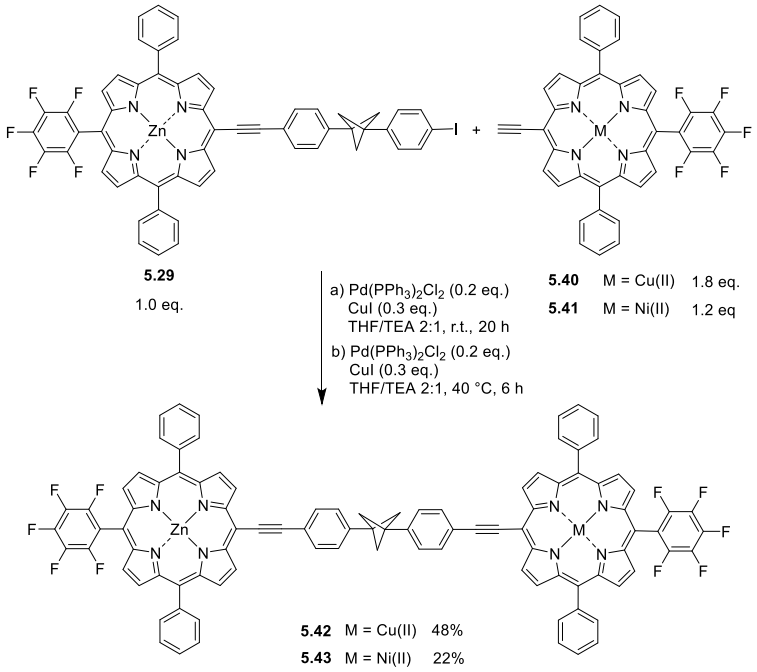

Scheme 5.9. Synthesis of BCP-linked Zn(II)-Cu(II) (conditions a) and Zn(II)-Ni(II) (conditions b) dyads **5.42** and **5.43** by Sonogashira coupling reactions.

In order to evaluate the influence of the BCP linker unit on energy/electron transfer processes in the dyads synthesised herein, a porphyrin dimer (**5.45**) with similar structural properties but a conjugated linker unit was aimed to be synthesised. A phenyl ring was incorporated into the linker in place of the BCP moiety to impart weak electronic coupling between the porphyrin units while the overall geometry of the dyad should be retained. A comparison of the conjugated reference dyad **5.45** with BCP-linked porphyrin dimer **5.27** can be made to determine the impact of the non-conjugated BCP linker on the photophysical properties of the dimer.

The synthesis of **5.45** was achieved by a Suzuki coupling reaction of the previously prepared borylated porphyrin **5.24** with commercially available 4,4''-dibromo-*p*-terphenyl **5.44** using $Pd(PPh_3)_4$ (0.20 eq.) and K_2CO_3 (12 eq.) in DMF (Scheme 5.10). The *p*-terphenyl-linked Zn(II) porphyrin dimer **5.45** was isolated in 33% yield.

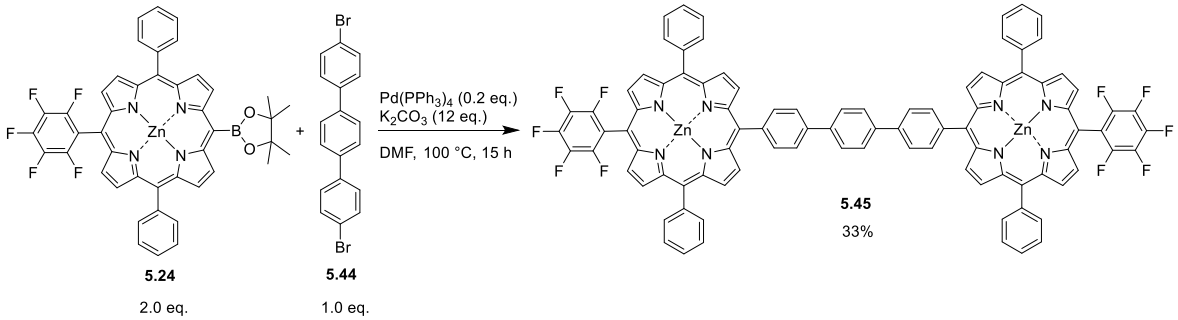

Scheme 5.10. Synthesis of *p*-terphenyl-linked Zn(II) porphyrin dimer **5.45** by a Suzuki coupling reaction.

In parallel to the series of dyads with a (15-(pentafluorophenyl)-10,20-diphenylporphyrinato)zinc(II) moiety, a series of BCP-linked dyads containing a (10,15,20-triphenylporphyrinato)zinc(II) moiety or (15-phenyl-10,20-di(4-methylphenyl)porphyrinato)zinc(II), respectively, was synthesised by Dr. Nitika Grover (Figure 5.5). The energy transfer efficiencies through the BCP linker in both series will be analysed as part of up-coming studies.

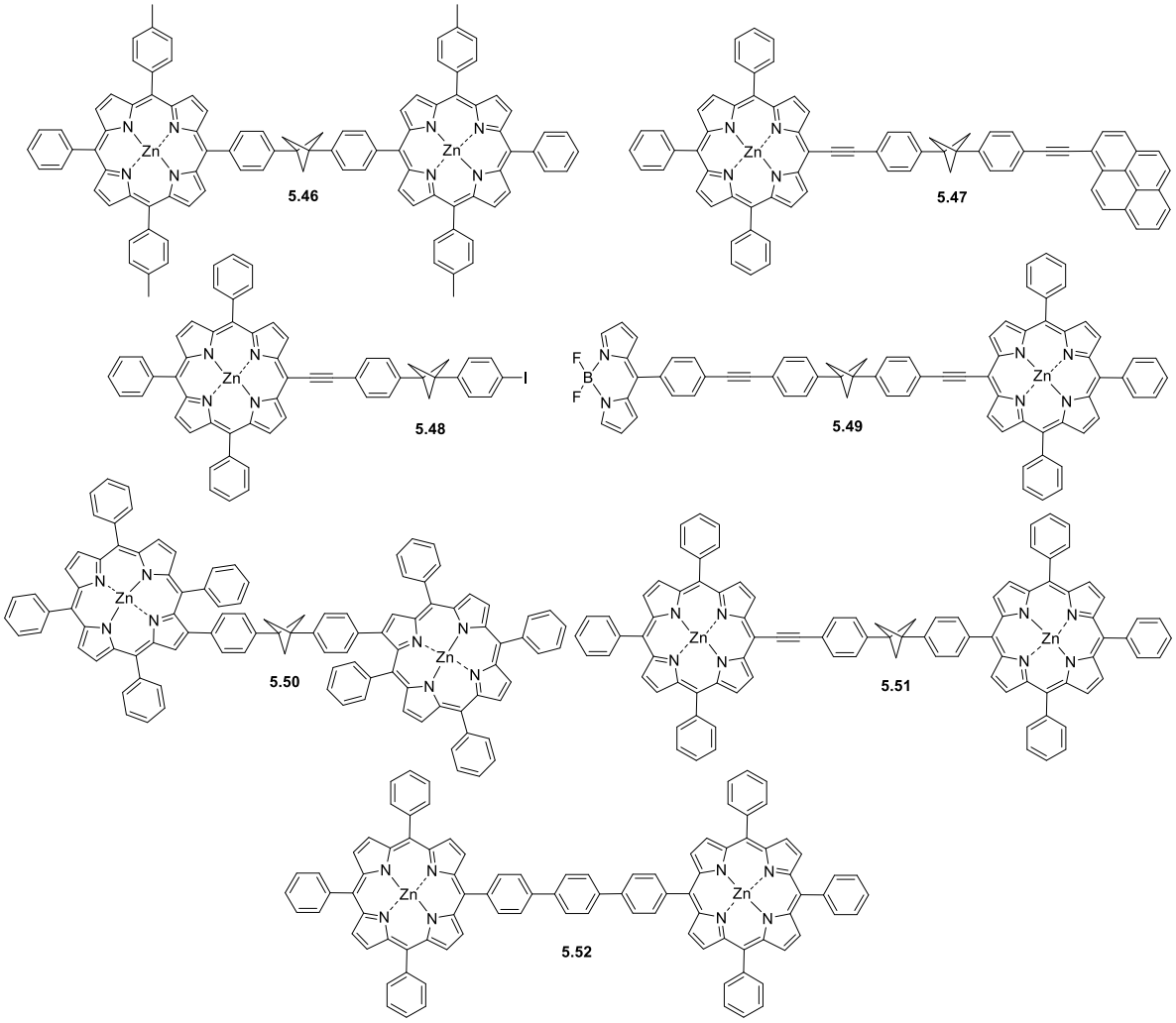

Figure 5.5. Series of dyads synthesised by Dr. Nitika Grover in which the pentafluorophenyl unit has been replaced by a phenyl or 4-methylphenyl substituent.

The bis-1,3-(4-iodophenyl)bicyclo[1.1.1]pentane linker **5.16** represents a synthetically readily accessible molecule which can be functionalised in a facile and versatile manner, e.g. by Pd-catalysed coupling reactions. That is why this linker unit proved to be very useful for the synthesis of two BCP-linked dyad series as discussed above.

It is known that in meso-phenyl-substituted porphyrins the phenyl rings are not co-planar with the porphyrin macrocycle; depending on the porphyrin substitution and the central metal ions and their ligands in metalloporphyrin derivatives the torsional angle between the meso-phenyl and the macrocycle planes can range from 30° to 90°.[14a] As stated before, the rotation of the phenyl rings relative to the porphyrin core determines the overlap of their FMOs.[150,350,353b,353c] In the diphenyl-BCP linked dyads, through-bond energy transfer processes are influenced by dihedral angles between the phenyl rings of the linker unit and the substituents. Furthermore, energy transfer processes are generally affected by the

relative orientation of the donor and acceptor moieties as well as the distance between them.[146a,365]

Therefore, the synthesis of a porphyrin arrays in which the BCP unit is directly attached to the meso-position of the porphyrin was targeted. However, this was anticipated to be challenging due to limitations in performing Pd-catalysed coupling reactions on the BCP bridgehead positions.

An alternative idea arose from the stepwise synthesis of porphyrin **5.23**, namely the assembly of a porphyrin from BCP-functionalised dipyrromethane (DPM) building blocks. The crucial step in this synthesis is the conjugation of the BCP unit onto the DPM fragment. In the method developed Lindsey and co-workers, the modification of the α-positions of DPM is accomplished by the treatment of DPM with ethylmagnesium bromide and subsequent reaction with an acyl chloride to obtain mono- or di-acylated DPM.[360] Hence, preparation of a BCP-acyl chloride as a reactant for the DPM modification is desirable. The use of a Grignard reagent for the DPM acylation reaction necessitates that the BCP precursor contains only one carbonyl group, otherwise side reactions can occur. Ethyl 3-arylbicyclo[1.1.1]pentane-carboxylates have been prepared by Knochel and co-workers by applying Grignard chemistry on [1.1.1]propellane.[200c] In the first step, reaction of [1.1.1]propellane with an arylmagnesium bromide reagent generates a BCP Grignard reagent **5.53** (Scheme 5.11). This reaction is equivalent to the first step of the synthesis of the bis-1,3-(4-iodophenyl)bicyclo[1.1.1]pentane linker **5.16**. The BCP Grignard reagent is converted *in situ* to the ester **5.54** by reaction with ethyl chlorformate.

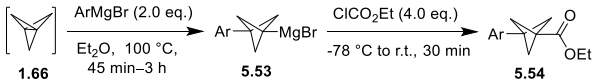

Scheme 5.11. Synthesis of ethyl 3-arylbicyclo[1.1.1]pentane-1-carboxylates after a procedure by Knochel and co-workers.[200c]

Conversion of BCP carboxylic esters to carboxylic acids and then to the acyl chlorides is required to obtain the precursors for the DPM modification. This can be achieved by, first, base-catalysed deprotection of the ester and subsequent transformation with oxalyl chloride.[181] Based on these known synthetic routes, a retrosynthetic plan was constructed for the synthesis of BCP-substituted porphyrin **5.55** as shown in Scheme 5.12.

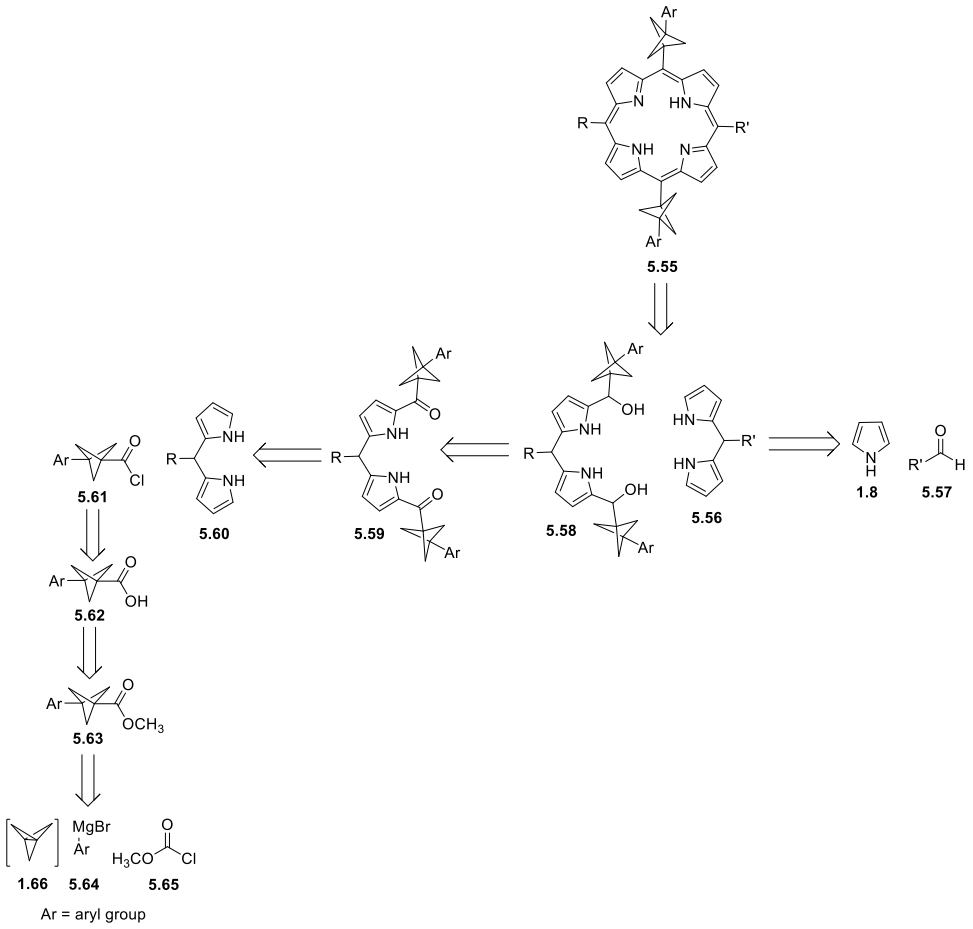

Scheme 5.12. Retrosynthetic analysis for the synthesis of a meso-BCP-substituted porphyrin **5.55**.

To test the viability of the planned synthetic route, it was decided to first synthesise methyl 3-phenylbicyclo[1.1.1]pentane-carboxylate **5.66** as the simplest 3-arylated BCP ester. If this synthesis would prove to be successful, different aryl groups such as anthracene or pyrene residues could later be attempted to be introduced at the BCP bridgehead position *via* Grignard reactions. BCP **5.66** was synthesised according to the literature procedure with the difference that methyl chloroformate was used as the carboxylating agent (Scheme 5.13).[200c] The product **5.66** could be isolated in 34% yield. Subsequent deprotection was effected by stirring a solution of **5.66** with NaOH (2.0 eq.) in a mixture of THF and methanol at r.t. for 16 h. 3-Phenylbicyclo[1.1.1]pentane-1-carboxylic acid **5.67** was isolated in 75% yield (Scheme 5.13).[197]

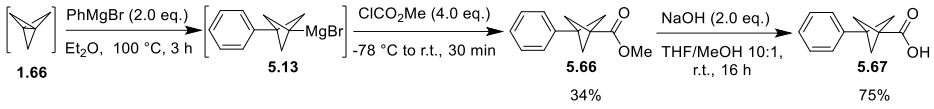

Scheme 5.13. Synthesis of 3-phenylbicyclo[1.1.1]pentane-1-carboxylic acid **5.67** from [1.1.1]propellane.

Carboxylic acid **5.67** was intended to be converted to the acyl chlroide according to a literature procedure and then to be reacted *in situ*.[181] **5.67** was dissolved in DCM and under addition of a few drops of DMF to ensure complete dissolution. Oxalyl chloride (1.2 eq.) was added dropwise at 0 °C, then the reaction mixture was heated to 40 °C for 2 h (Scheme 5.14). In the meantime, a DPM was pre-functionalised by treatment with ethylmagnesium bromide (5.0 eq.) in toluene and stirring for 1 h. meso-Pentafluorophenyl-substituted DPM **5.17** was chosen as the DPM precursor because it would impart beneficial properties to the final porphyrin macrocycle such as a low-lying HOMO and good energy acceptor abilities as well as, based on previous observations, a higher tendency to crystallise.

The solution of the *in situ* generated BCP acyl chloride was transferred to the DPM-containing reaction mixture and the solution was stirred at r.t. for 3 h (Scheme 5.14). After purification of the reaction mixture no di-acylated DPM **5.69** could be isolated. However, the formation of a considerable amount of mono-acylated DPM **5.70** was observed. When the reaction was repeated the same results were obtained – no formation of the di-substituted product was observed but the mono-substituted DPM could be isolated in 25% yield.

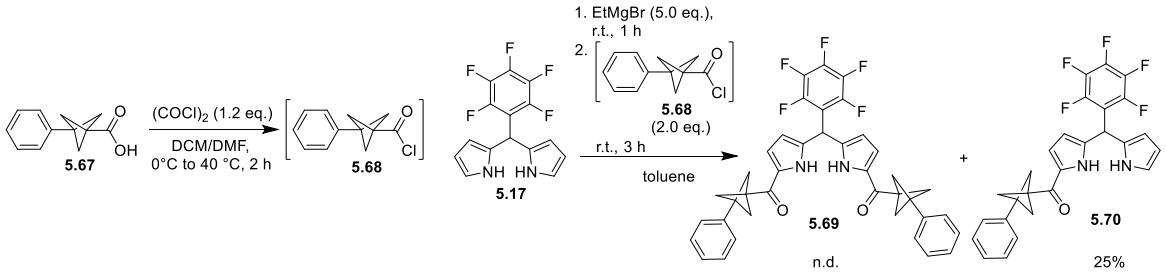

Scheme 5.14. Synthesis of an α-BCP-substituted DPM **5.70** from 3-phenylbicyclo[1.1.1]pentane-1-carboxylic acid and meso-pentafluorophenyl-DPM precursors.

Although the desired compound **5.69** could not be obtained, formation of the mono-substituted product **5.70** in a sufficient amount led us to attempt a porphyrin synthesis with this compound instead. Lindsey and co-workers reported that after reduction of the ketone to an alcohol, self-condensation of α-mono-substituted DPMs is possible to give A_2B_2-type porphyrins.[366] Following this procedure, compound **5.70** was reduced using $NaBH_4$ (25 eq.)

in THF/methanol (Scheme 5.15). The solid isolated from this reaction was used without further purification for a porphyrin condensation reaction. The condensation was effected by addition of TFA (3.3 eq.) to a solution of the starting material in acetonitrile. After 16h, DDQ (2.0 eq.) was added and the mixture was left to stir for 1 h before the reaction mixture was neutralised using TEA. Silica gel column chromatography of the crude products afforded *trans*-BCP-substituted porphyrin **5.72** in 5% yield.

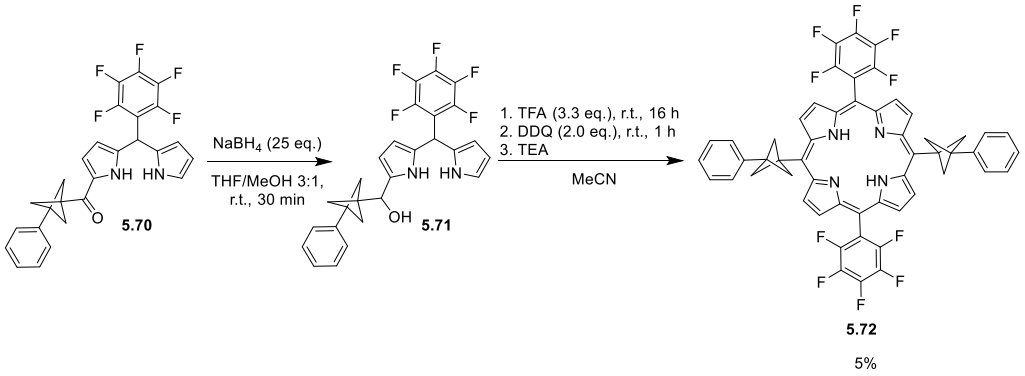

Scheme 5.15. Synthesis of a *trans*-A_2B_2 porphyrin comprising two BCP units directly appended to the meso positions.

The synthesis of porphyrin **5.72** served as a proof-of-concept that a meso-BCP-substituted porphyrin could be synthesised following the synthetic route we had envisioned. The next obvious goal was to change the substituent on the 3-position of the BCP scaffold to a moiety which can act as an energy donor. This would enable for the study of the shortest non-conjugated interaction of a donor and an acceptor moiety which are connected by a linear rigid linker. First, it was aimed to append anthracene onto the BCP bridgehead.

Intending to follow the same reaction sequence as employed earlier for the synthesis of methyl 3-phenylbicyclo[1.1.1]pentane-carboxylate **5.66**, it was attempted to generate anthracen-9-ylmagnesium bromide and to react it with [1.1.1]propellane, followed by treatment with methyl chloroformate. However, this reaction sequence did not yield any of the desired product **5.76** (Scheme 5.16). This was attributed to inefficient formation of the anthracene Grignard reagent under the conditions employed.

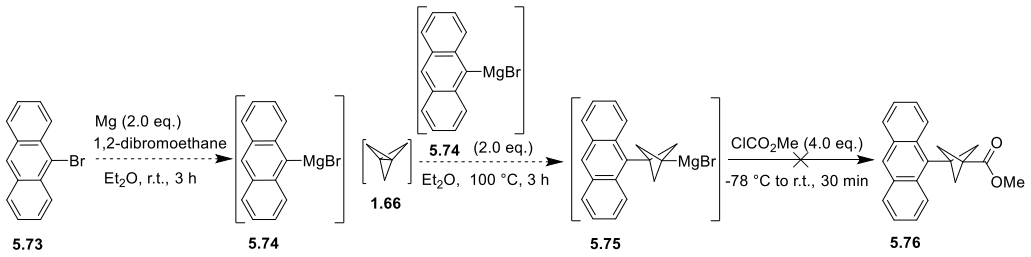

Scheme 5.16. Attempted synthesis of methyl 3-(anthracen-9-yl)bicyclo[1.1.1]pentane-carboxylate **5.76** *via* Grignard chemistry and carboxylation with methyl chloroformate.

A different approach was taken instead by trying to introduce a substituent in the 3-position of the BCP scaffold which carries a synthetic handle for late-stage functionalisation reactions. The 4-((trimethylsilyl)ethynyl)phenyl moiety was chosen for this purpose since it can be used as a functional group for Sonogahsira coupling reactions. The reaction sequence to prepare methyl 3-(4-((trimethylsilyl)ethynyl)phenyl)bicyclo[1.1.1]pentane-1-carboxylate **5.80** was carried out in the standard way and the product was isolated in 12% yield (Scheme 5.17). Unfortunately, due to time constraints this compound could not be reacted further. However, it could be demonstrated that the preparation of BCP-carboxylates carrying synthetic handles in the 3-position can be a viable approach towards the synthesis of BCP-substituted porphyrins which can be modified by late stage functionalisation reactions.

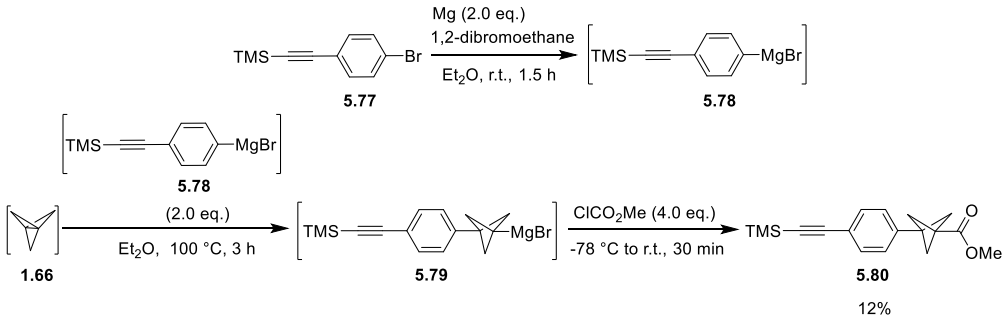

Scheme 5.17. Synthesis of 3-(4-((trimethylsilyl)ethynyl)phenyl)bicyclo[1.1.1]pentane-carboxylate **5.80**.

5.4 Crystallographic Analysis of BCP-Porphyrin Arrays

The compounds **5.21**, **5.23**, **5.27**, **5.29**, **5.32**, **5.36** and **5.45** were analysed by X-ray spectroscopy. A crystal of a side product from the borylation of **5.23** was obtained as well and it was found to be the de-brominated Zn(II) porphyrin **5.81** (Figure 5.6).

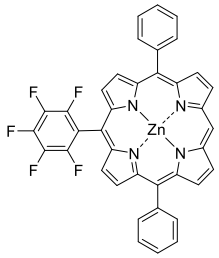

5.81

Figure 5.6. Structure of Zn(II) porphyrin **5.81** which was isolated as a side product from the borylation of **5.23**.

The molecular structures of the precursor porphyrins **5.21**, **5.23**, **5.36** and **5.81** are represented in Figure 5.7. While the out-of-plane structure of Zn(II) porphyrin **5.81** is dominated by a moderate ruffle distortion, the two brominated compounds **5.23** and **5.36** show a saddle shape.[55a,367]

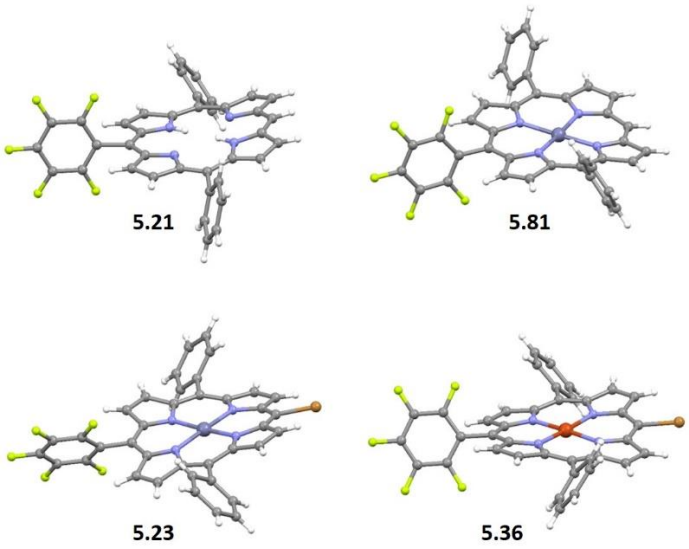

Figure 5.7. Representative views of the molecular structures of **5.21**, **5.81**, **5.23** and **5.36** in the crystals with atomic displacement shown at 50% probability level. Solvents omitted for clarity.

When looking at the crystal structures of the BCP-containing compounds **5.29**, **5.32**, **5.27** and **5.45**, the analysis of torsional angles between the porphyrin and phenyl planes as well as the phenyl rings of the linker was of special interest. As discussed previously, the rotation between the conjugated moieties determines the overlap between interacting molecular orbitals. The geometry of the molecules in the solid state can give a clue towards understanding intramolecular energy transfer processes in the dyads.

In the crystal structure of porphyrin-BCP monomer **5.29** a twist of φ_2 = 40.40(17)° between the two phenyl rings of the linker (ring 1 and ring 2) (Figure 5.8) is observed. Ring 1 is

rotated by φ_1 = 42.96(2)° towards the porphyrin plane, which is slightly larger than the 35° angle reported by Anderson and co-workers for phenyl rings attached to porphyrins *via* ethynyl spacers.[359]

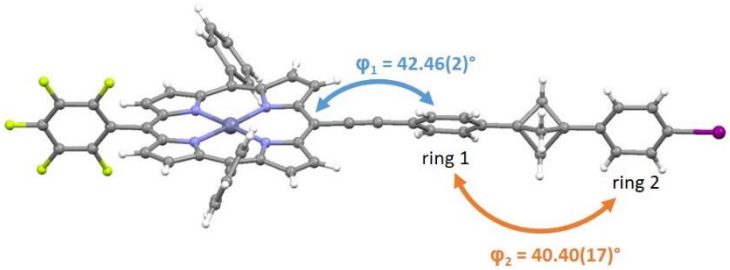

Figure 5.8. View of the molecular structure of **5.29** in the crystal with atomic displacement shown at 50% probability level. Solvents omitted for clarity. Torsional angles φ between the porphyrin and the phenyl ring planes are indicated.

In contrast to the monomer **5.29**, in the BCP-linked porphyrin-BODIPY dyad **5.32** the molecule takes on a more planar geometry with the twist angles between the phenyl rings of the linker unit and between the linker and its substituents becoming smaller (Figure 5.9). An almost coplanar conformation with a twist angle of only φ_1 = 5.25(16)° is observed between the porphyrin plane and ring 1 of the diphenyl-BCP linker. The angle between the meso-phenyl substituent of the BODIPY (ring 3) and phenyl ring 2 of the BCP linker which are connected by an ethynyl unit is also comparably small with φ_3 = 10.26(19)°. The phenyl rings 1 and 2 of the BCP linker unit are less twisted than in **5.29** at an angle of φ_2 = 27.29(19)°.

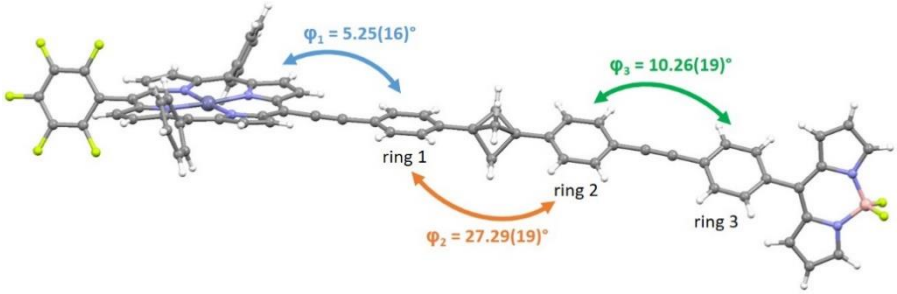

Figure 5.9. Representative view of the molecular structure of **5.32** in the crystal with atomic displacement shown at 50% probability level. Solvents omitted for clarity. Torsional angles φ between the porphyrin and the phenyl ring planes are indicated.

Interestingly, the phenyl rings 1 and 2 of the BCP linker in compound **5.27** are completely coplanar (φ_2 = 0.00(0)°) (Figure 5.10). This results in a linear geometry of the dyad where the two porphyrin substituents are also in plane with each other. As expected, the direct

linkage of the porphyrins to the phenyl moieties of the linker results in a large dihedral angle between the porphyrin and the phenyl planes of φ_1 = 74.55(3)°.[359]

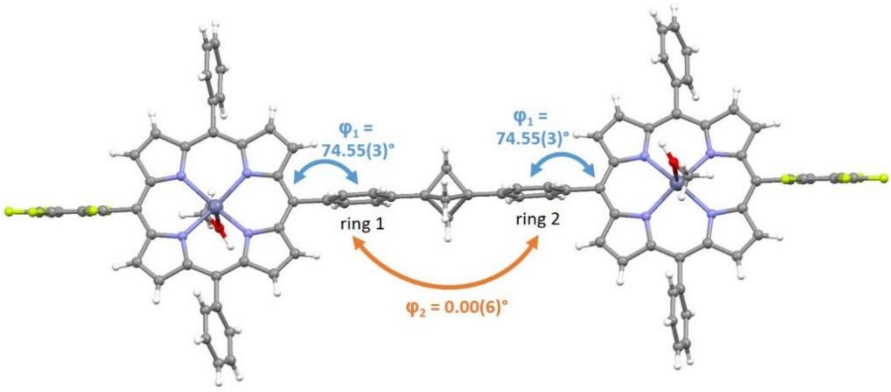

Figure 5.10. Representative view of the molecular structure of **5.27** in the crystal with atomic displacement shown at 50% probability level. Solvents omitted for clarity. Torsional angles φ between the porphyrin and the phenyl ring planes are indicated.

The reference compound **5.45** which comprises a triphenyl linker unit between the two porphyrin moieties shows a linear geometry in the solid state which is very similar to the one of **5.27** (Figure 5.11). The two phenyl rings 1 and 3 adjacent to the porphyrin moieties are coplanar (φ_2 = 0.00(2)°). The plane-to-plane angle between the central phenyl ring 2 of the linker and the outer phenyl rings 1 and 3 is φ_3 = 27.52(12)°. The porphyrin moieties are rotated at an angle of φ_1 = 79.18(3)° towards adjacent phenyl rings 1 and 3.

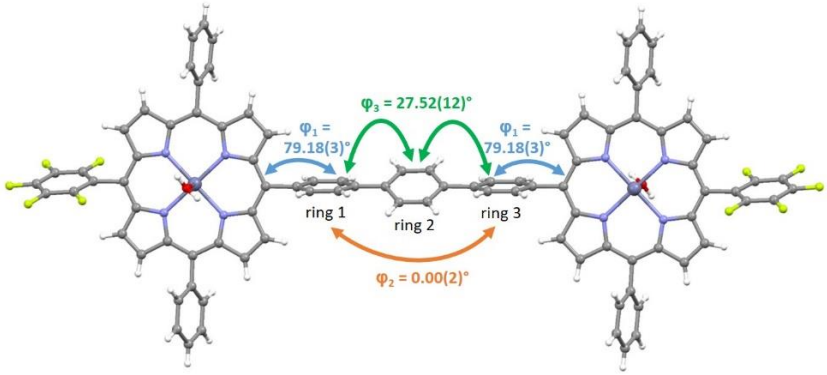

Figure 5.11. Representative view of the molecular structure of **5.45** in the crystal with atomic displacement shown at 50% probability level. Solvents omitted for clarity. Torsional angles φ between the porphyrin and the phenyl ring planes are indicated.

The crystal structures of **5.27**, **5.29**, **5.32** and **5.45** suggest that these molecules are good models for the study of energy transfer processes since different connecting units between the moieties cause varying dihedral angles in the dyads. The BCP-linked dyad **5.27** and the triphenyl-linked reference dyad **5.45** both show a linear geometry and therefore suggest

that they can be directly compared when studying excitation energy transfer processes through the linker unit.

Besides intramolecular steric and electronic factors, the geometries observed in the solid state can partially be attributed to packing interactions in the crystal. Therefore, the molecular geometries in the crystal can only give indications about the compounds‘ geometries in solution. Solution state measurements such as transient absorption spectroscopy are additionally required to complement the results obtained from X-ray crystallography studies.

5.5 Conclusion and Outlook

Herein, the BCP unit was incorporated in different donor-acceptor dyads with the electron-deficient 15-(pentafluorophenyl)-10,20-diphenylporphyrin acceptor moieties. As donor moieties, BODIPY and pyrene fluorophores as well as 10,15,20-triphenylporphyrin were employed. BCP-linked bisporphyrins with two different metal centres, Zn-Cu and Zn-Ni, were prepared as well. The synthesis of dyads was achieved by Sonogashira and Suzuki coupling reactions on bis-1,3-(4-iodophenyl)bicyclo[1.1.1]pentane. The yields of the isolated products were commonly good but lower for some substrates. The yields also depended on the degree of competing side reactions such as Glaser homo-couplings taking place and on challenges encountered in the separation of different reaction products.

Varying sizes of the linker, achieved by incorporation of additional ethynyl spacers, resulted in different overall geometries of the dyads in the solid state as confirmed by X-ray crystallographic analysis of some of the prepared derivatives. A series of BCP-linked donor-acceptor dyads equivalent to the ones described herein but comprising a 10,15,20-triphenylporphyrin instead of a 15-(pentafluorophenyl)-10,20-diphenylporphyrin acceptor unit was synthesised in parallel by Dr. Nitika Grover. With this library of BCP-linked dyads at hand, it will be possible to study the impact of geometric as well as electronic factors on excitation energy transfer processes through the BCP linker unit. For the investigation of these processes it is envisioned to perform theoretical (density functional theory (DFT) calculations) and experimental (singlet and triplet excited state quantum yields, singlet excited state lifetime, transient absorption spectroscopy) analyses with the compounds synthesised.

Furthermore, a synthetic route towards the preparation of porphyrin moieties directly bound to the bridgehead carbon of BCP without an additional phenyl spacer was implemented. This was achieved by mono-acylation of the α-position of a dipyrromethane with a BCP acyl

chloride, reduction and self-condensation of the DPM to yield a 5,15-bis-BCP-substituted porphyrin, proving the concept that meso-BCP-substituted porphyrins are accessible in this manner. In future, this strategy could be used for the synthesis of BCP-linked porphyrin-based donor-acceptor dyads by introducing different substituents at the 3-position of the BCP-1-acyl chloride, followed by DPM modification and condensation.

The compounds synthesised herein can serve as model systems for the study of energy and electron transfer processes between molecular units, which are arranged in a defined spatial manner and are not π-conjugated. Such systems can serve as mimics of multichromophoric arrays in nature and help towards the understanding of natural processes involving energy transfer cascades.

Chapter 6. Experimental Section

6.1 General Methods and Instrumentation

Reagents and solvents were of analytical grade and commercially acquired. Unless stated otherwise, they were used without further purification. Anhydrous DCM was obtained by distillation from P_2O_5 and stored over activated molecular sieves. Anhydrous 1,2-dichloroethane, DMF, benzene, THF, TEA, diethyl ether and acetonitrile were commercially acquired and used as such. Larger amounts of THF were obtained from an automated solvent purification system where the solvent was dried by passing it through aluminium oxide under nitrogen. Air- and moisture-sensitive reactions were performed under inert argon atmosphere using “Schlenk“ techniques. Reactions at elevated temperatures were carried out using a hot plate with an oil bath as a heat source. Flash column chromatography was carried out using silica gel 60 (230-400 mesh; *Sigma-Aldrich*) or aluminium oxide (neutral, activated with 6% H_2O, Brockman Grade III, particle size 0.05–0.15 mm; *Aldrich*). Mobile phases are described as (v/v). Analytical thin-layer chromatography (TLC) was performed on precoated 60 F254 silica gel plates (0.2 mm thick; *Merck*) or on precoated 60 F254 neutral aluminium oxide plates and visualised by UV irradiation on a Shimadzu Multispec-1501 (*Merck*). All melting points are uncorrected and were measured using a Stuart SMP10 melting point apparatus. NMR spectra were recorded using a Bruker Advance III 400 MHz, a Bruker DPX400 400 MHz and an Agilent 400 spectrometer for ^{1}H (400.13 MHz), $^{13}C\{^{1}H\}$ (100.61 MHz), $^{19}F\{^{1}H\}$ (376.60 MHz) and ^{11}B (128.40 MHz) NMR spectra and a Bruker Ultrashield 600 spectrometer was utilised for ^{1}H (600.13 MHz) and $^{13}C\{^{1}H\}$ (150.90 MHz) NMR spectra. All NMR experiments were performed at room temperature. Chemical shifts δ are given in ppm and referenced to the solvent residual signals: $CDCl_3$ (δ_H = 7.26 ppm, δ_C = 77.0 ppm), CD_3OD (δ_H = 3.31 ppm, δ_C = 49.0 ppm), $(CD_3)_2SO$ (δ_H = 2.50 ppm, δ_C = 39.5 ppm), C_4D_8O (δ_H = 3.58, 1.73 ppm, δ_C = 67.57, 25.37 ppm). The assignment of the signals was confirmed by 2D spectra (COSY, TOCSY, HSQC, HMBC). MALDI mass spectra were acquired using a Q-Tof Premier Waters Maldi mass spectrometer in positive or negative mode with *trans*-2-[3-(4-*tert*-butylphenyl)-2-methyl-2-propenylidene]malononitrile as the matrix. ESI mass spectra were recorded in positive or negative modes using a Micromass time of flight mass spectrometer (TOF) interfaced to a Waters 2960 HPLC or a Bruker microTOF-Q III spectrometer interfaced to a Dionex UltiMate 3000 LC. APCI experiments were conducted on a Bruker microTOF-Q III spectrometer interfaced to a Dionex UltiMate 3000 LC. Photophysical measurements were carried out in DCM, DMSO or THF. UV-visible (UV-Vis) absorption measurements were

performed using a Specord 250 spectrophotometer from Analytik Jena (1 cm path length quartz cell). Fluorescence spectra were recorded using an Agilent Cary Eclipse Fluorescence Spectrophotometer. IR spectra were acquired on a PerkinElmer Spectrum 100 FT-IR instrument.

6.2 Chapter 2 – Methods Development for the Functionalisation of Protoporphyrin IX Dimethyl Ester

General Procedure A – Metal Insertions in Protoporphyrin IX Dimethyl Ester (**1.23**)

Protoporphyrin dimethyl ester (PPIX-DME) **1.23** was synthesised from protoporphyrin disodium salt following a standard procedure.[240]

Porphyrin metal complexes were prepared using a modified literature procedure.[241] Porphyrin **1.23** was dissolved in a DCM/MeOH 3:1 mixture, the respective metal salt (3.0–5.3 eq.) was added and the solution was stirred at 40 °C until complete consumption of the starting material was confirmed by UV-Vis spectroscopy. The solvent was removed *in vacuo*, the residue was dissolved in DCM and washed with saturated aqueous $NaHCO_3$ solution**,** H_2O and brine. If necessary, the product was purified by silica gel column chromatography (SiO_2, DCM/MeOH 100:0.5, v/v).

The protoporphyrin IX dimethyl ester metal complex was dissolved in a THF/MeOH 1:1 mixture and KOH (8.0 eq.), dissolved in H_2O (5% of the reaction mixture volume), was added. The solution was stirred at 66 °C for 18 h. The solvent was *in vacuo*, the residue was dispersed in a small amount of H_2O and dilute aqueous HCl was added until the solution became acidic (pH 5). A precipitate formed which was collected by suction filtration and washed with H_2O and *n*-hexane.

General Procedure B – Suzuki coupling Reactions on (*E*,*E*)-3^2,8^2-Dibromo-protoporphyrin dimethyl ester 2.39

Compound **2.39** and Cs_2CO_3 (13–20 eq.) were dried under high vacuum for 1 h. Anhydrous THF was added under argon and the solution was purged with argon for 20 min. The appropriate boronic acid or boronic acid pinacol ester (4.0–20 eq.) and $Pd(dppf)Cl_2$ (20 mol%) were added and the mixture was purged with argon for another 5 min. The reaction mixture was then heated to 66 °C for 15–63 h. The solvent was removed *in vacuo* and the residue redissolved in DCM. This was washed sequentially with saturated aqueous $NaHCO_3$ solution, deionised H_2O, and brine. The organic layer was dried over $MgSO_4$, the

solvent was removed *in vacuo* and the residue was purified as indicated in the respective section.

General Procedure C – Sonogashira coupling Reactions on (*E*,*E*)-3^2,8^2-Dibromo-protoporphyrin dimethyl ester 2.39

Compound **2.39**, $Pd(PPh_3)_2Cl_2$ (10 mol%), CuI (20 mol%) and, if solid, the ethynyl substrate (4.0 eq.) were dried under high vac. for 30 min. To a separate sealed tube, anhydrous THF and anhydrous TEA were added in a 1:1 ratio under argon, followed by, if liquid, the ethynyl substrate (4.0 eq.). The mixture was purged with argon for 15 min and then transferred to the reaction vessel *via* a syringe. The reaction was then stirred at 25–40 °C for 16 h. The solvent was removed *in vacuo* and the residue was purified as indicated in the respective section.

(Protoporphyrinato)zinc(II) (**1.48**)[368]

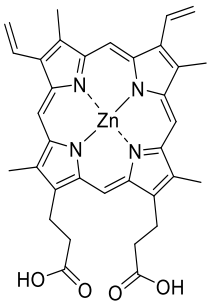

1.48

Compound **1.23** (58.0 mg, 98.2 µmol) was reacted with $Zn(OAc)_2 \cdot 2\ H_2O$ as outlined in general procedure A to give (protoporphyrinato dimethyl ester)zinc(II) (**1.27**) as purple powder (60.0 mg, 92.0 µmol, 93%). For hydrolysis of the methyl ester groups, **1.27** was reacted with KOH (41.0 mg, 0.734 mmol) to yield **1.48** as a purple powder (49.0 mg, 78.1 µmol, 85%); ^{1}H NMR (600 MHz, DMSO-d_6, 25 °C): δ = 3.16 (t, *J* = 7.6 Hz, 4 H, 2x α-carbonyl-C*H*$_2$), 3.61 (s, 3 H, C*H*$_3$), 3.63 (s, 3 H, C*H*$_3$), 3.75 (s, 3 H, C*H*$_3$), 3.76 (s, 3 H, C*H*$_3$), 4.33 (t, $^3J_{H,H}$ = 6.2 Hz, 4 H, 2x β-carbonyl-C*H*$_2$), 6.15 (dd, *J* = 11.5 Hz, 1.3 Hz, 1 H, β-vinyl-H), 6.15 (dd, *J* = 11.4, 1.3 Hz, 1 H, β-vinyl-H), 6.41 (dd, *J* = 17.8 Hz, 1.3 Hz, 1 H, β-vinyl-H), 6.42 (dd, *J* = 17.8 Hz, 1.3 Hz, 1 H, β-vinyl-H), 8.52 (dd, *J* = 17.8, 11.6 Hz, 1 H, α-vinyl-H), 8.54 (dd, *J* = 17.8, 11.6 Hz, 1 H, α-vinyl-H), 10.17 (s, 1 H, meso-H), 10.18 (s, 1 H, meso-H), 10.19 (s, 1 H, meso-H) and 10.27 (s, 1 H, meso-H) ppm; ^{13}C{^{1}H} NMR (151 MHz, DMSO-d_6, 25 °C): δ = 11.4, 12.7, 21.7, 37.7, 97.3, 97.4, 97.7, 98.1, 119.6, 131.0, 131.0, 140.0, 140.1, 146.0, 146.5, 147.2, 147.5, 147.7, 147.8, 148.0, 148.3 and 174.4 ppm; UV-Vis (DMSO) λ_{max} [log(ε/M^{-1} cm^{-1})] = 423 [5.48], 548 [4.33], 585 [4.31] nm; HRMS (MALDI): *m/z* calcd. for $[C_{34}H_{32}N_4O_4Zn]$ $[M]^+$: 624.1715; found 624.1737.

(Protoporphyrinato)copper(II) (**2.31**)[368]

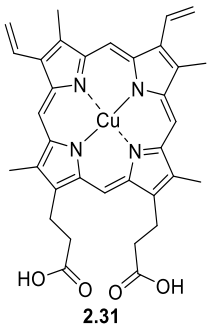

2.31

Compound **1.23** (60.0 mg, 98.2 µmol) was reacted with $Cu(OAc)_2$ (91.0 mg, 0.500 mmol) as outlined in general procedure **A** to give (protoporphyrinato dimethyl ester)copper(II) (**2.29**) as purple powder (53.0 mg, 81.3 µmol, 80%). For hydrolysis of the methyl ester groups, **2.29** was reacted with KOH (36.0 mg, 0.642 mmol) to yield **2.31** as a purple powder (33.0 mg, 52.9 µmol, 65%); UV-Vis (DMSO) λ_{max} [log(ε/M^{-1} cm^{-1})] = 409 [5.31], 534 [4.08], 572 [4.32] nm; HRMS (MALDI): *m/z* calcd. for $[C_{34}H_{32}N_4O_4Cu]$ $[M]^+$: 623.1720; found 623.1718.

(Protoporphyrinato)silver(II) (**2.32**)[369]

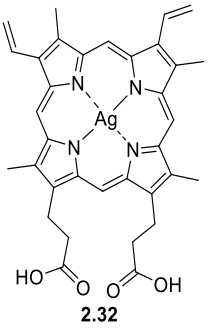

2.32

Compound **1.23** (60 mg, 98.2 µmol) was reacted with Ag(OAc) (102 mg, 0.611 mmol) as outlined in general procedure **A** to give (protoporphyrinato dimethyl ester)silver(II) (**2.30**) as purple powder (42.0 mg, 60.3 µmol, 59%). For hydrolysis of the methyl ester groups, **2.30** was reacted with KOH (27.0 mg, 0.483 mmol) to yield **2.32** as purple powder (18.0 mg, 26.9 µmol, 45%); UV-Vis (DMSO) λ_{max} [log(ε/M^{-1} cm^{-1})] = 417 [5.21], 534 [4.07], 569 [4.19] nm; HRMS (MALDI): *m/z* calcd. for $[C_{34}H_{32}N_4O_4Ag]$ $[M]^+$: 667.1475; found 667.1492.

(*E*,*E*)-3²,8²-Dibromo-protoporphyrin dimethyl ester (**2.39**)

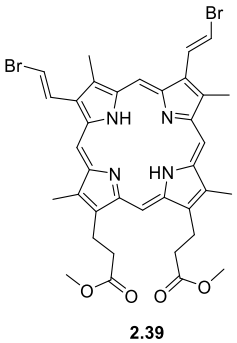

2.39

In a 100 mL 3-necked round-bottomed flask with attached reflux condenser, compound **1.23** (100 mg, 0.169 mmol) was dissolved in $CHCl_3$ (40 mL). Pyridinium bromide perbromide (119 mg, 0.372 mmol) was added and the reaction mixture was stirred at 61 °C for 3 h. The mixture was cooled to room temperature and washed with saturated aqueous $Na_2S_2O_3$ solution, deionised H_2O and brine. The organic layer was dried over $MgSO_4$, filtered and the solvent was removed *in vacuo*. The crude product was purified by column chromatography (SiO_2, DCM/EtOAc 40:1, v/v) and the solvents were removed *in vacuo* to give **2.39** as a purple powder (106 mg, 0.142 mmol, 84%); M.p. >300 °C; R_f = 0.71 (SiO_2, DCM/EtOAc 40:1, v/v); ^{1}H NMR (400 MHz, $CDCl_3$, 25 °C): δ = –4.82 (br s, 2H, N*H*), 2.70 (s, 3H, C*H*$_3$), 3.20 (s, 3H, C*H*$_3$), 3.21–3.29 (m, 4H, C*H*$_2$), 3.40 (s, 3H, C*H*$_3$), 3.48 (s, 3H, C*H*$_3$), 3.70 (s, 6H, C*H*$_3$), 4.25–4.36 (m, 4H, C*H*$_2$), 6.89 (d, *J* = 14.0, 1H, β-vinyl-H), 6.90 (d, *J* = 14.0, 1H, β-vinyl-H), 7.88 (d, *J* = 14.0 Hz, 1H, α-vinyl-H), 8.04 (d, *J* = 14.0 Hz, 1H, α-vinyl-H), 8.70 (s, 1H, meso-H), 9.31 (s, 1H, meso-H), 9.51 (s, 1H, meso-H), 9.82 (s, 1H,

meso-H) ppm; $^{13}C\{^{1}H\}$ NMR (101 MHz, $CDCl_3$, 25 °C): δ = 11.7, 11.7, 12.3, 12.8, 21.9, 29.9, 37.0, 37.0, 51.9, 96.2, 96.4, 96.7, 97.0, 110.0, 110.1, 130.2, 173.6 ppm; UV-Vis (DCM) λ_{max} [log(ε/M^{-1} cm^{-1})] = 410 [5.13], 508 [4.06], 544 [4.00], 578 [3.76], 632 [3.66] nm; HRMS (APCI): *m/z* calcd. for $[C_{36}H_{37}Br_2N_4O_4]$ $[M+H]^+$: 747.1176; found 747.1177.

(*E*,*E*)-3^2,8^2-Bis(4-methylphenyl)-protoporphyrin dimethyl ester (**2.41**)

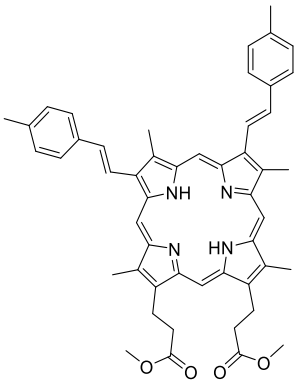

2.41

Compound **2.39** (28.0 mg, 37.5 µmol), Cs_2CO_3 (245 mg, 0.751 mmol), 4-tolylboronic acid (102 mg, 0.751 mmol) and Pd(dppf)Cl_2 (5.50 mg, 7.51 µmol) were reacted in anhydrous THF (15 mL) for 18 h in accordance with general procedure **B**. The crude product was purified by column chromatography (SiO_2, DCM/MeOH eluent of increasing polarity up to DCM/MeOH 100:0.175, v/v) and the solvents were removed *in vacuo* to yield **2.41** as a purple powder (25.0 mg, 32.4 µmol, 86%); M.p. = 294–296 °C; R_f = 0.56 (SiO_2, DCM/MeOH 80:1, v/v); ^{1}H NMR (400 MHz, $CDCl_3$, 25 °C): δ = –4.18, (br s, 2H, N*H*), 2.55 (s, 6H, CH_3), 3.22 (t, *J* = 7.8 Hz, 4H, CH_2), 3.36 (s, 3H, CH_3), 3.44–3.47 (m, 9H, CH_3), 3.68 (s, 6H, CH_3), 4.29 (t, *J* = 7.5 Hz, 2H, CH_2), 4.29 (t, *J* = 7.5 Hz, 2H, CH_2), 7.39–7.44 (m, 4H, Ar-H), 7.47 (d, *J* = 16.4 Hz, 1H, β-vinyl-H), 7.54 (d, *J* = 16.4 Hz, 1H, β-vinyl-H), 7.76 (d, *J* = 7.9 Hz, 2 H, Ar-H), 7.81 (d, *J* = 7.9 Hz, 2H, Ar-H), 8.21 (d, *J* = 16.4 Hz, 1H, α-vinyl-H), 8.35 (d, *J* =16.4 Hz, 1H, α-vinyl-H), 9.66 (s, 1H, meso-H), 9.67 (s, 1H, meso-H), 9.81 (s, 1H, meso-H), 9.86 (s, 1H, meso-H) ppm; $^{13}C\{^{1}H\}$ NMR (101 MHz, $CDCl_3$, 25 °C): δ = 11.6, 11.7, 12.8, 12.9, 21.6, 21.9, 37.0, 51.9, 95.8, 96.7, 97.0, 97.3, 120.8, 121.0, 126.8, 129.8, 129.8, 134.7, 134.8 135.7, 135.8, 137.9, 138.0, 173.7 ppm; UV-Vis (DCM) λ_{max} [log(ε/M^{-1} cm^{-1})] = 414 [4.51], 513 [3.46], 553 [3.53], 582 [3.27], 639 [3.18] nm; HRMS (MALDI): *m/z* calcd. for $[C_{50}H_{50}N_4O_4]$ $[M^+]$: 770.3832; found 770.3866.

(*E*,*E*)-3^2,8^2-Bis(4-methoxyphenyl)-protoporphyrin dimethyl ester (**2.42**)[42b]

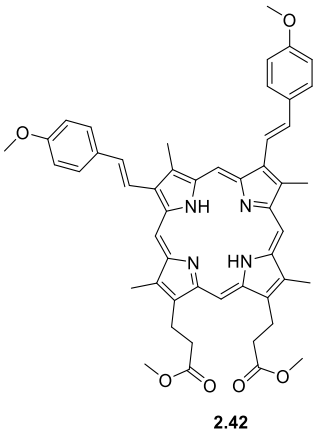
2.42

Compound **2.39** (20.0 mg, 26.7 µmol), Cs_2CO_3 (174 mg, 0.534 mmol), 2-(4-methoxyphenyl)-4,4,5,5-tetramethyl-1,3,2-dioxaborolane (81.2 mg, 0.534 mmol) and Pd(dppf)Cl_2 (3.90 mg, 5.34 µmol) were reacted in anhydrous THF (5 mL) for 17 h in accordance with general procedure **B**. The crude product was passed through a plug of grade III neutral aluminium oxide using DCM for elution and then further purified by column chromatography (SiO_2, DCM). The solvent was removed *in vacuo* to yield compound **2.42** as a purple solid (13.6 mg, 16.9 µmol, 63%); M.p. = 248–250 °C (lit. 252–255 °C);[42b] R_f = 0.23 (SiO_2, DCM/MeOH 100:0.25, v/v). ^{1}H NMR (400 MHz, $CDCl_3$ + TFA-d, 25 °C): δ = –3.28 (br s, 1H, N*H*), –3.10 (s, 1H, N*H*), 3.11–3.19 (m, 4H, CH_2), 3.62 (s, 3H, CH_3), 3.63 (s, 3H, CH_3), 3.64 (s, 3H, CH_3), 3.67 (s, 3H, CH_3), 3.74 (s, 3H, CH_3), 3.78 (s, 3H, CH_3), 3.98 (s, 3H, CH_3), 3.98 (s, 3H, CH_3), 4.41–4.51 (m, 4H, CH_2), 7.17–7.12 (m, 4H, Ar-H), 7.54 (d, *J* = 16.4 Hz, 1H, β-vinyl-H), 7.58 (d, *J* = 16.4 Hz, 1H, β-vinyl-H), 7.91–7.86 (m, 4 H, Ar-H), 8.36 (d, *J* = 16.4 Hz, 1H, α-vinyl-H), 8.39 (d, *J* = 16.4 Hz, 1H, α-vinyl-H), 10.63 (s, 1H, meso-H), 10.69 (s, 1H, meso-H), 10.76 (s, 1H, meso-H), 10.87 (s, 1H, meso-H) ppm; ^{13}C{^{1}H} NMR (101 MHz, $CDCl_3$ + TFA-d, 25 °C): δ = 12.0, 12.1, 13.1, 21.6, 21.7, 35.5, 35.6, 52.7, 55.8, 98.7, 99.0, 99.6, 100.2, 114.9, 116.9, 129.1, 130.2, 137.5, 137.5, 138.8, 139.0, 139.0, 139.1, 140.0, 140.3, 142.6, 142.7, 160.8, 160.8, 174.9 ppm; UV-Vis (DCM) λ_{max} [log(ε/M^{-1} cm^{-1})] = 414 [5.10], 516 [4.07], 554 [4.16], 583 [3.91], 640 [3.80] nm; HRMS (MALDI): *m/z* calcd. for [$C_{50}H_{50}N_4O_6$] [M]$^+$: 802.3730; found 802.3766.

(*E*,*E*)-3^2,8^2-Bis(4-formylphenyl)-protoporphyrin dimethyl ester (**2.43**)

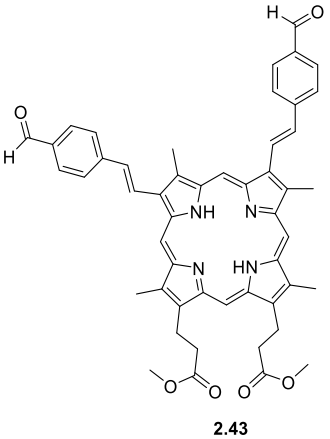
2.43

Compound **2.39** (60.0 mg, 80.2 µmol), Cs_2CO_3 (523 mg, 1.60 mmol), 4-formylphenylboronic acid (240 mg, 1.60 mmol) and Pd(dppf)Cl_2 (11.7 mg, 16.0 µmol) were reacted in anhydrous THF (50 mL) for 15 h in accordance with general procedure **B**. The crude product was purified by column chromatography (SiO_2, DCM/MeOH/TEA eluent of increasing polarity up to DCM/MeOH/TEA 100:0.375:0.5, v/v/v) and the solvents were removed *in vacuo*. Recrystallisation from DCM/*n*-hexane gave **2.43** as a purple powder (43.0 mg, 53.8 µmol, 67%); M.p. >300 °C; R_f = 0.29 (SiO_2, DCM/MeOH 80:1, v/v); ^{1}H NMR (600 MHz, $CDCl_3$, 25 °C): δ = –4.00 (br s, 2H, N*H*), 3.24 (t, *J* = 7.7 Hz, 2H,

CH_2), 3.25 (t, *J* = 7.7 Hz, 2H, CH_2), 3.27 (s, 3H, CH_3), 3.43 (s, 6H, CH_3), 3.50 (s, 3H, CH_3), 3.67–3.68 (m, 6H, CH_3), 4.30 (t, *J* = 7.7 Hz, 2H, CH_2), 4.32 (t, *J* = 7.7 Hz, 2H, CH_2), 7.38 (d, *J* = 16.4 Hz, 1H, β-vinyl-H), 7.43 (d, *J* = 16.4 Hz, 1H, β-vinyl-H), 7.83 (d, *J* = 7.7 Hz, 2H, Ar-H), 7.88 (d, *J* = 7.7 Hz, 2H, Ar-H), 8.00–8.04 (m, 4H, Ar-H), 8.27 (d, *J* = 16.4 Hz, 1H, α-vinyl-H), 8.37 (d, *J* = 16.4 Hz, 1H, α-vinyl-H), 9.56 (s, 1H, meso-H), 9.74 (s, 1H, meso-H), 9.76 (s, 1H, meso-H), 9.90 (s, 1H, meso-H), 10.12 (s, 1H, C*H*O) and 10.33 (s, 1H, C*H*O) ppm; $^{13}C\{^1H\}$ NMR (151 MHz, $CDCl_3$, 25 °C): *δ* = 11.8, 13.0, 13.3, 14.3, 21.9, 29.8, 36.9, 51.9, 96.4, 96.9, 97.4, 97.5, 125.1, 127.1, 130.6, 133.1, 133.2, 135.7, 144.1, 173.6, 191.8 ppm; UV-Vis (DCM) λ_{max} [log(ε/M^{-1} cm^{-1})] = 424 [4.38], 515 [3.48], 555 [3.52], 585 [3.31], 641 [3.20] nm; HRMS (MALDI): *m/z* calcd. for [$C_{50}H_{46}N_4O_6$] [M^+]: 798.3417, found 798.3403.

(*E*,*E*)-3^2,8^2-Bis(4-methoxycarbonylphenyl)-protoporphyrin dimethyl ester (**2.44**)[42b]

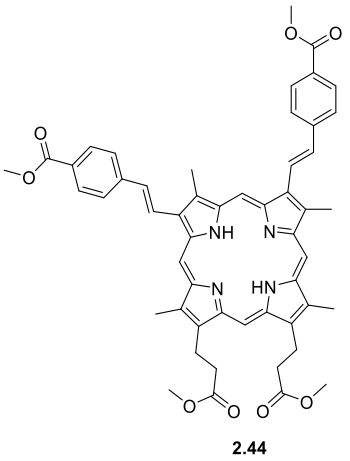

2.44

Compound **2.39** (20.0 mg, 26.7 µmol), Cs_2CO_3 (174 mg, 0.534 mmol), 3-methoxycarbonylphenylboronic acid pinacol ester (140 mg, 0.534 mmol) and Pd(dppf)Cl_2 (3.90 mg, 5.34 µmol) were reacted in anhydrous THF (13 mL) for 63 h in accordance with general procedure **B**. The crude product was passed through a plug of silica gel (DCM/MeOH, 100:1) and then further purified by preparative TLC (DCM/MeOH 100:0.5). The solvents were removed *in vacuo* and compound **2.44** was obtained as a purple solid (11.2 mg, 13.0 µmol, 49%); M.p. > 300 °C (lit. 187–189 °C);[42b] R_f = 0.24 (SiO_2, DCM/MeOH 100:1, v/v); ^1H NMR (400 MHz, $CDCl_3$, 25 °C): *δ* = –4.35 (br s, 2H, N*H*), 3.03 (s, 3H, CH_3), 3.24–3.16 (m, 7H, CH_2, CH_3), 3.34 (s, 3 H, CH_3), 3.39 (s, 3H, CH_3), 3.67 (s, 6H, CH_3), 4.06 (s, 3H, CH_3), 4.06 (s, 3H, CH_3), 4.20–4.27 (m, 4H, CH_2), 7.18 (d, *J* = 16.4 Hz, 1H, β-vinyl-H), 7.31 (d, *J* = 16.4 Hz, 1H, β-vinyl-H), 7.69 (d, *J* = 8.0 Hz, 2H, Ar-H), 7.79 (d, *J* = 8.0 Hz, 2H, Ar-H), 7.98 (d, *J* = 16.4 Hz, 1H, α-vinyl-H), 8.24–8.16 (m, 5H, Ar-H, α-vinyl-H), 9.21 (s, 1H, meso-H), 9.49 (s, 1H, meso-H), 9.57 (s, 1H, meso-H), 9.76 (s, 1H, meso-H) ppm; $^{13}C\{^1H\}$ NMR (101 MHz, $CDCl_3$, 25 °C): *δ* = 11.6, 11.7, 12.8, 12.9, 21.8, 36.9, 51.9, 52.4, 96.1, 96.7, 97.0, 97.2, 123.9, 124.0, 126.5, 126.5, 129.2, 129.3, 130.4, 130.4, 133.0, 133.2, 142.6, 142.6, 167.1, 167.2, 173.6 ppm; UV-Vis (DCM) λ_{max} [log(ε/M^{-1} cm^{-1})] = 424 [5.25], 517 [4.25], 555 [4.34], 585 [4.09], 641 [3.97] nm; HRMS (MALDI): *m/z* calcd. for [$C_{52}H_{50}N_4O_8$] [$M]^+$: 858.3629; found 858.3652.

(*E*,*E*)-3^2,8^2-Bis(anthracen-9-yl)-protoporphyrin dimethyl ester (**2.45**)[42b]

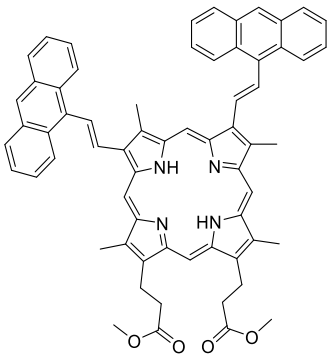

2.45

Compound **2.39** (47.0 mg, 62.8 µmol), Cs_2CO_3 (409 mg, 1.26 mmol), 9-anthracenylboronic acid (279 mg, 1.26 mmol) and Pd(dppf)Cl_2 (9.20 mg, 12.6 µmol) were reacted in anhydrous THF (20 mL) for 18 h in accordance with general procedure **B**. The crude product was purified by column chromatography (SiO_2, DCM/MeOH eluent of increasing polarity up to DCM/MeOH 100:0.2, v/v) and the solvents were removed *in vacuo*. Recrystallisation from DCM/MeOH yielded **2.45** as a purple powder (35.0 mg, 36.6 mmol, 59%); M.p. = 153 °C (lit. 145–148 °C);[42b] R_f = 0.65 (SiO_2, DCM/MeOH 80:1, v/v); ^{1}H NMR (400 MHz, $CDCl_3$, 25 °C): δ = –3.58 (br s, 1H, N*H*), 3.24 (t, *J* = 7.8 Hz, 2H, CH_2), 3.29 (t, *J* = 7.8 Hz, 2H, CH_2), 3.45 (s, 3H, CH_3), 3.60 (s, 3 H, CH_3), 3.64 (s, 3 H, CH_3), 3.67 (s, 3 H, CH_3), 3.70 (s, 3H, CH_3), 3.75 (s, 3H, CH_3), 4.29–4.34 (m, 2H, CH_2), 4.34–4.39 (m, 2H, CH_2) 7.56–7.64 (m, 8H, Ar-H), 8.11–8.19 (m, 6H, Ar-*H*), 8.20–8.29 (m, 2H, α-vinyl-H), 8.57 (s, 2H, Ar-H), 8.71–8.79 (m, 4H, Ar-H, β-vinyl-H), 9.99 (s, 1H, meso-H), 10.04 (s, 1H, meso-H), 10.08 (s, 1H, meso-H), 10.14 (s, 1H, meso-H) ppm; ^{13}C{^{1}H} NMR (151 MHz, $CDCl_3$, 25 °C): δ = 11.3, 11.5, 12.0, 12.3, 14.0, 21.7, 21.8, 29.9, 36.9, 37.0, 51.9, 51.9 96.0, 96.9, 97.0, 97.3, 125.3, 125.3, 125.5, 125.5, 126.0, 126.1, 126.6, 126.6, 127.3, 128.9, 128.9, 129.5, 131.7, 131.7, 133.5, 134.1, 173.7, 173.7, 183.2 ppm; UV-Vis (DCM) λ_{max} [log(ε/M^{-1} cm^{-1})] = 416 [4.50], 512 [3.53], 548 [3.49], 580 [3.31], 635 [3.11] nm; HRMS (MALDI): *m/z* calcd. for [$C_{64}H_{54}N_4O_4$] [M$^+$]: 942.4145, found 942.4162.

(*E*,*E*)-3^2,8^2-Bis(1-methylindol-5-yl)-protoporphyrin dimethyl ester (**2.46**)

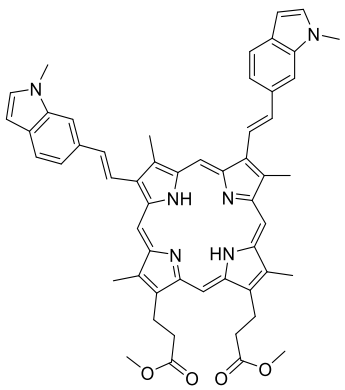

2.46

Compound **2.39** (20.0 mg, 26.7 µmol), Cs_2CO_3 (174 mg, 0.534 mmol), 1-methyl-1H-indol-5-boronic acid (137 mg, 0.534 mmol) and Pd(dppf)Cl_2 (3.90 mg, 5.34 µmol) were reacted in anhydrous THF (5 mL) for 15 h in accordance with general procedure **B**. The crude product was passed through a plug of grade III neutral aluminium oxide using DCM for elution and then further purified by column chromatography (aluminium oxide, DCM/*n*-hexane 1:1, 3:2, v/v). The product containing fraction was passed through a pad of silica gel using DCM and DCM/MeOH (100:0.3, v/v) to remove any remaining boronic acid. The solvents were removed *in vacuo* and compound **2.46** was isolated as a purple solid (6.90 mg, 8.13 µmol, 30%); M.p. > 300 °C; R_f = 0.18 (SiO_2, DCM);

^{1}H NMR (400 MHz, $CDCl_3$ + TFA-d, 25 °C): δ = –3.85 (br s, 1H, N*H*), 3.26 (t, *J* = 7.7 Hz, 4H, CH_2), 3.56 (s, 6H, CH_3), 3.62 (s, 3 H, CH_3), 3.65 (s, 3H, CH_3), 3.68 (s, 6H, CH_3), 3.91 (s, 6H, CH_3), 4.32–4.40 (m, 4H, CH_2), 6.67–6.69 (m, 2H, Ar-H), 7.16–7.18 (m, 2H, Ar-H), 7.53 (d, *J* = 8.4 Hz, 2H, Ar-H), 7.79 (d, *J* = 16.3 Hz, 1H, β-vinyl-H), 7.82 (d, *J* = 16.3 Hz, 1H, β-vinyl-H), 7.88–7.94 (m, 2H, Ar-H), 8.14 (d, *J* = 6.1 Hz, 2H, Ar-H), 8.46 (d, *J* =16.4 Hz, 1H, α-vinyl-H), 8.53 (d, *J* = 16.4 Hz, 1H, α-vinyl-H), 9.89 (s, 1H, meso-H), 9.92 (s, 1H, meso-H), 10.07 (s, 1H, meso-H), 10.13 (s, 1H, meso-H) ppm; ^{13}C{^{1}H} NMR (101 MHz, $CDCl_3$ + TFA-d, 25 °C): δ =11.8, 11.9, 13.1, 13.2, 22.0, 33.2, 37.1, 51.9, 96.0, 96.9, 97.5, 97.9, 101.8, 109.9, 119.2, 119.3, 120.1, 120.6, 129.2, 129.8, 130.3, 130.3, 137.0, 173.8 ppm; UV-Vis (DCM) λ_{max} [log(ε/M^{-1} cm^{-1})] = 413 [5.20], 515 [4.19], 556 [4.27], 582 [4.09], 641 [3.94], 675 [3.74] nm; HRMS (MALDI): *m/z* calcd. for [$C_{54}H_{52}N_6O_4$] $[M]^+$: 848.4050; found 848.4059.

(*E*,*E*)-3^2,8^2-Bis(4-ethynylphenyl)-protoporphyrin dimethyl ester (**2.47**)

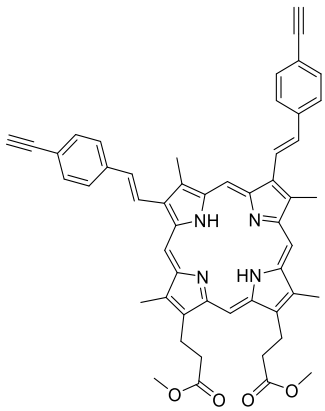

2.47

Compound **2.39** (50.0 mg, 66.8 µmol) and K_3PO_4 (284 mg, 1.34 mmol) were dried under high vacuum for 1 h. Anhydrous THF (20 mL) was added and the solution was purged with argon for 30 minutes. 4-[(Trimethylsilyl)ethynyl]phenylboronic acid pinacol ester (201 mg, 0.668 mmol) and $Pd(PPh_3)_4$ (7.70 mg, 6.68 µmol) were added, the solution was purged with argon for 10 minutes and the mixture was heated to 66 °C for 15 h. The solvent was removed *in vacuo* and the residue was purified by column chromatography (SiO_2, DCM/MeOH 100:0.25, v/v). A mixture of TMS-protected and partially deprotected porphyrins (28.4 mg, 32.2 µmol) was isolated. This mixture was used for the subsequent deprotection step. The residue was dissolved in anhydrous DCM (15 mL) and a 1 M solution of tetrabutylammonium fluoride (TBAF) in THF (54 µL, 54.0 µmol) was added under argon. The mixture was stirred at room temperature for 15 min and subsequently passed through a plug of grade III neutral aluminium oxide and eluted with DCM. Removal of the solvents *in vacuo* and recrystallisation from DCM/MeOH yielded **2.47** as a purple powder (16.7 mg, 21.1 µmol, 32%); M.p. = 168 °C dec.; R_f = 0.38 (aluminium oxide, DCM/*n*-hexane 3:1, v/v); ^{1}H NMR (600 MHz, $CDCl_3$ + TFA-d, 25°C): δ = 3.11–3.19 (m, 4H, CH_2), 3.26 (s, 1H, acetylene-H), 3.27 (s, 1H, acetylene-H), 3.58 (s, 3H, CH_3), 3.59 (s, 3H, CH_3), 3.60 (s, 3H, CH_3), 3.65 (s, 3H, CH_3), 3.69 (s, 3H, CH_3), 3.76 (s, 3H, CH_3), 4.37–4.46 (m, 4H, CH_2), 7.50–7.60 (m, 2H, β-vinyl-H), 7.68–7.74 (m, 4H, Ar-H), 7.83–7.90 (m, 4H, Ar-H), 8.48 (d, *J* = 16.2 Hz, 1H, α-vinyl-H), 8.49 (d, *J* = 16.2 Hz, 1H, α-vinyl-H), 10.54 (s, 1H, meso-H), 10.56 (s, 1H, meso-H),10.64 (s, 1H, meso-H), 10.81 (s, 1H, meso-H) ppm; ^{13}C{^{1}H} NMR

(151 MHz, $CDCl_3$, 25°C): δ = 12.2, 12.2, 13.2, 13.2, 21.8, 21.9, 35.6, 35.7, 52.0, 79.1, 83.6, 98.9, 99.1, 100.0, 112.1, 115.0, 120.7, 123.0, 123.0, 127.3, 133.0, 136.6, 136.8, 136.9, 137.1, 137.5, 138.0, 138.0, 139.7, 139.7, 140.6, 140.7, 141.1, 142.1, 142.1, 142.4, 142.5, 143.0, 173.1 ppm; UV-Vis (DCM): λ_{max} [log(ε/M^{-1} cm^{-1})] = 421 [5.24], 515 [4.23], 555 [4.29], 584 [4.07], 640 [3.99], 671 [3.79] nm; HRMS (MALDI): *m/z* calcd. for [$C_{52}H_{46}N_4O_4$] $[M]^+$: 790.3519; found 790.3531.

(*E*,*E*)-3^2,8^2-Bis(4,4,5,5-tetramethyl-1,3,2-dioxaborolan-2-yl)-protoporphyrin dimethyl ester (**2.51**)

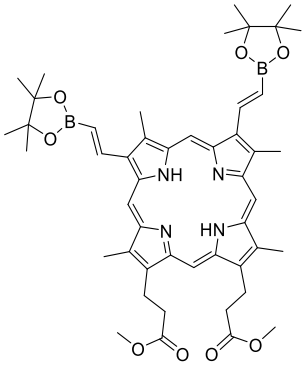

2.51

Compound **2.39** (20.0 mg, 26.7 µmol) and $Pd(PPh_3)_2Cl_2$ (3.8 mg, 5.34 µmol) were dried under high vac. for 30 min. Anhydrous 1,2-dichloroethane (1 mL), TEA (70 µL, 0.534 mmol) and pinacolborane (80 µmL, 0.534 mmol) were added under argon and the solution was purged with argon for 10 min. The reaction mixture was heated to 84 °C for 3 h. The solvent was removed *in vacuo* and the crude product was purified by column chromatography (SiO_2, DCM/EtOAc 20:1, v/v). Removal of the solvents *in vacuo* followed by recrystallisation from DCM/*n*-hexane yielded **2.51** as a purple powder (10.7 mg, 12.7 mmol, 48%); M.p. > 300 °C; R_f = 0.28 (SiO_2, DCM/EtOAc 20:1, v/v); ^{1}H NMR (600 MHz, $CDCl_3$, 25 °C): δ = –3.96 (br s, 1H, N*H*), 1.57 (s, 24H, boryl-C*H*$_3$), 3.20–3.29 (m, 4H, C*H*$_2$), 3.54 (s, 3H, C*H*$_3$), 3.61 (s, 3H, C*H*$_3$), 3.64 (s, 3H, C*H*$_3$), 3.67 (s, 3H, C*H*$_3$), 3.70 (s, 3H, C*H*$_3$), 3.75 (s, 3H, C*H*$_3$), 4.29–4.39 (m, 4H, C*H*$_2$), 6.86 (d, *J* = 18.6, 1H, β-vinyl-H), 6.88 (d, *J* = 18.6, 1H, β -vinyl-H), 8.99 (d, *J* = 18.6, 1H, α-vinyl-H), 9.02 (d, *J* = 18.6, 1H, α-vinyl-H), 9.86 (s, 1H, meso-H), 9.90 (s, 1H, meso-H), 10.12 (s, 1H, meso-H), 10.16 (s, 1H, meso-H) ppm; ^{13}C{^{1}H} NMR (151 MHz, $CDCl_3$, 25 °C): δ = 11.7, 12.0, 13.3, 13.6, 21.9, 22.0, 25.2, 4.0, 51.9, 83.9, 96.0, 97.4, 97.6, 98.5, 142.7, 142.8, 173.7, 173.7 ppm; UV-Vis (DCM) λ_{max} [log(ε/M^{-1} cm^{-1})] = 416 [5.34], 512 [4.29], 548 [4.27], 581 [4.01], 636 [3.92] nm; HRMS (MALDI): *m/z* calcd. for [$C_{48}H_{60}B_2N_4O_8$] $[M]^+$: 842.4597, found 842.4633.

(*E*,*E*)-3^2,8^2-Bis(trimethylsilylethynyl)-protoporphyrin dimethyl ester (**2.53**)

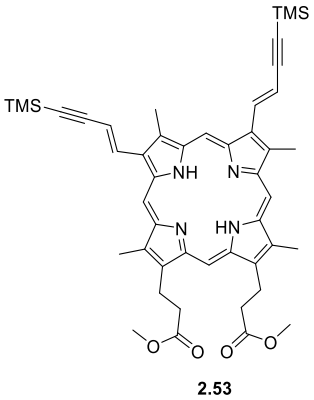

2.53

Compound **2.39** (152 mg, 0.203 mmol), (trimethylsilyl)acetylene (0.11 mL, 0.800 mmol), $PdCl_2(PPh_3)_2$ (19.0 mg, 27.1 µmol) and CuI (9.60 mg, 39.9 µmol) were reacted in a mixture of THF (2.5 mL) and TEA (2.5 mL) for 15 h in accordance with general procedure **B**. The crude product was purified by column chromatography (SiO_2, DCM/MeOH eluent of increasing polarity from 100:0.1 to 100:0.5, v/v) and the solvents were removed *in vacuo* to yield **2.53** as a purple powder (178 mg, 0.200 mmol, 98%); M.p. > 300 °C; R_f = 0.37 (SiO_2, DCM/MeOH 100:0.1, v/v); ^{1}H NMR (400 MHz, $CDCl_3$ + TFA-d, 25 °C): δ = 0.39 (s, 18H, TMS-CH_3), 3.10–3.18 (m, 4H, CH_2), 3.56 (s, 6H, CH_3), 3.64 (s, 3H, CH_3), 3.64 (s, 3H, CH_3), 3.71 (s, 3H, CH_3), 3.72 (s, 3H, CH_3), 4.38–4.46 (m, 4H, CH_2), 6.72 (d, J = 16.3 Hz, 2H, β-vinyl-H), 6.72 (d, J = 16.4 Hz, 2H, β-vinyl-H), 8.40 (d, J = 16.4 Hz, 2H, α-vinyl-H), 10.53 (s, 1H, meso-H), 10.57 (s, 1H, meso-H), 10.61 (s, 1H, meso-H), 10.87 (s, 1H, meso-H) ppm; ^{13}C{^{1}H} NMR (101 MHz, $CDCl_3$ +TFA-d, 25 °C): δ = 0.0, 12.1, 12.3, 13.2, 13.4, 21.8, 35.5, 35.5, 52.1, 98.9, 99.2, 99.6, 100.1, 102.2, 102.3, 103.9, 120.9, 121.0, 132.4, 132.4, 135.5, 135.8, 137.5, 137.8, 138.8, 138.9, 140.3, 173.4 ppm; UV-Vis (DCM) λ_{max} [log(ε/M^{-1} cm^{-1})] = 420 [5.71], 517 [4.60], 553 [4.69], 584 [4.65], 641 [4.25] nm; HRMS (MALDI): *m/z* calcd. for [$C_{46}H_{54}N_4O_4Si_2$] [M]$^+$: 782.3684, found 782.3682.

(*E*,*E*)-3^2,8^2-Bisethynyl-protoporphyrin dimethyl ester (**2.54**)

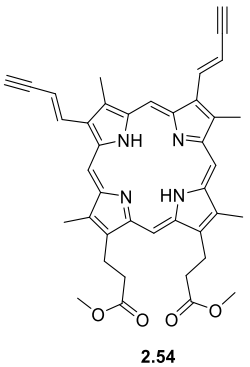

2.54

Compound **2.53** (59.2 mg, 75.6 µmol) was dissolved in anhydrous DCM (30 mL) under argon, a 1 M solution of TBAF in THF (0.17 mL, 0.170 mmol) was added and the mixture was stirred for 20 min at room temperature. The reaction mixture was washed with water (2 ×) and brine (1 ×), the organic layer was dried over $MgSO_4$, filtered and the solvent was removed *in vacuo* to give **2.54** as a purple powder (41.1 mg, 64.9 µmol, 86%); M.p. > 300 °C; R_f = 0.25 (SiO_2, DCM); ^{1}H NMR (400 MHz, $CDCl_3$ + TFA-d, 25 °C): δ = 3.10–3.18 (m, 4H, CH_2), 3.54 (br s, 2H, acetylene-H), 3.56 (s, 3H, CH_3), 3.57 (s, 3H, CH_3), 3.63 (s, 3H, CH_3), 3.64 (s, 3H, CH_3), 3.72 (s, 3H, CH_3), 4.37–4.46 (m, 4H, CH_2), 6.65–6.71 (m, 2H, β-vinyl-H), 8.46 (d, J = 16.4 Hz, 1H, α-vinyl-H), 8.47 (d, J = 16.4 Hz, 1H, α-vinyl-H), 10.50 (s, 1H, meso-H), 10.56 (s, 1H, meso-H), 10.59 (s, 1H, meso-H), 10.87 (s, 1H, meso-H) ppm; ^{13}C{^{1}H} NMR (101 MHz, $CDCl_3$ + TFA-d, 25 °C): δ = 12.1, 12.2, 13.2, 13.3, 21.8, 35.5, 35.6, 52.0, 82.6, 83.3, 83.4, 98.8, 99.3, 99.6, 100.0, 119.5, 119.6, 133.6, 134.9, 135.2,

137.4, 137.8, 138.6, 138.7, 140.0, 140.2, 140.3, 140.8, 141.6, 141.7, 142.4, 142.7, 142.8, 143.1, 173.1 ppm; UV-Vis (DCM) λ_{max} [log(ε/M^{-1} cm^{-1})] = 417 [5.69], 515 [4.61], 550 [4.65], 582 [4.61], 640 [4.24] nm; HRMS (MALDI): *m/z* calcd. for [$C_{40}H_{38}N_4O_4$] $[M]^+$: 638.2893; found 638.2924.

(*E*,*E*)-3^2,8^2-Bis(4-phenylethynyl)-protoporphyrin dimethyl ester (**2.55**)

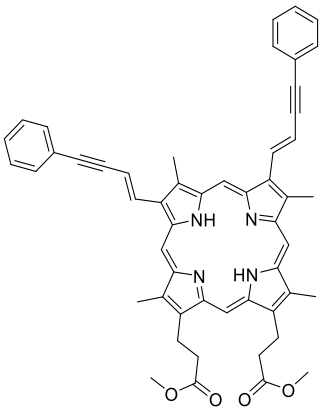

2.55

Compound **2.39** (15.0 mg, 20.0 µmol), phenylacetylene (10 µL, 91.2 µmol), $PdCl_2(PPh_3)_2$ (1.4 mg, 2.00 µmol) and CuI (0.80 mg, 4.01 µmol) were reacted in a mixture of THF (2.5 mL) and TEA (2.5 mL) for 3 h in accordance with general procedure D-B. The solvents were removed *in vacuo* and the crude solids were passed through a plug of silica gel (DCM/MeOH 100:0.2). After removal of the solvents *in vacuo*, compound **2.55** was obtained as a purple powder (15.3 mg, 19.3 µmol, 97%); M.p. > 300 °C; R_f = 0.37 (aluminium oxide, DCM); ^{1}H NMR (400 MHz, $CDCl_3$ + TFA-d, 25 °C): δ = 3.11–3.18 (m, 4H, CH_2), 3.58 (s, 6H, CH_3), 3.65 (s, 3H, CH_3), 3.66 (s, 3H, CH_3), 3.76 (s, 3H, CH_3), 3.77 (s, 3H, CH_3), 4.47–4.40 (m, 4H, CH_2), 6.95 (d, *J* = 16.2 Hz, 1H, β-vinyl-H), 6.97 (d, *J* = 16.2 Hz, 1H, β-vinyl-H), 7.44–7.48 (m, 6H, Ar-H), 7.72–7.67 (m, 4H, Ar-*H*), 8.46 (d, *J* = 16.2 Hz, 1H, α-vinyl-H), 8.47 (d, *J* = 16.2 Hz, 1H, α-vinyl-H), 10.60 (s, 2H, meso-H), 10.68 (s, 1H, meso-H) and 10.88 (s, 1H, meso-H) ppm; $^{13}C\{^1H\}$ NMR (151 MHz, $CDCl_3$ + TFA-d, 25 °C): δ = 12.1, 12.3, 13.2, 13.4, 21.8, 35.5, 35.5 52.2, 90.0, 90.0, 96.4, 96.4, 98.9, 99.3, 99.6, 100.1, 121.2, 121.3, 122.9, 128.8, 129.3, 131.3, 132.1, 132.1, 135.9, 136.3, 137.5, 137.8, 138.9, 139.0, 140.4, 140.4, 173.6 ppm; UV-Vis (DCM) λ_{max} [log(ε/M^{-1} cm^{-1})] = 422 [5.59], 518 [4.55], 556 [4.64], 586 [4.56], 642 [4.28] nm; HRMS (MALDI): *m/z* calcd. for [$C_{52}H_{46}N_4O_4$] $[M^+]$: 790.3528; found 790.3519.

(*E*,*E*)-3^2,8^2-Bis(4-methoxycarbonylphenylethynyl)-protoporphyrin dimethyl ester (**2.56**)

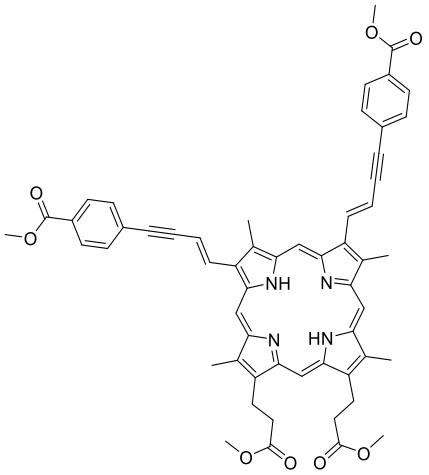

2.56

Compound **2.39** (20.0 mg, 26.7 µmol), methyl 4-ethynylbenzoate (17.0 mg, 0.107 mmol), $Pd(PPh_3)_2Cl_2$ (3.90 mg, 2.67 µmol) and CuI (1.0 mg, 5.34 µmol) were reacted in a mixture of anhydrous THF (0.5 mL) and TEA (0.5 mL) for 22 h in accordance with general procedure **C**. The crude product was passed through a plug of silica gel (DCM, DCM/MeOH 100:1, v/v). The crude product was further purified by column chromatography (1. aluminium oxide, DCM/*n*-hexane 1:1, 3:2, v/v, and DCM/MeOH 100:0.5, v/v, and 2. SiO_2, DCM, DCM/MeOH 100:0.5, 100:1, v/v) and the solvents were removed *in vacuo* to yield compound **2.56** as a purple powder (8.50 mg, 9.37 µmol, 35%); M.p. > 300 °C; R_f = 0.16 (SiO_2, DCM/MeOH 100:1, v/v); ^{1}H NMR (400 MHz, $CDCl_3$ + TFA-d, 25 °C): δ = 3.11–3.19 (m, 4H, CH_2), 3.59 (s, 6H, CO_2CH_3), 3.66 (s, 6H, CH_3), 3.78 (s, 3 H, CH_3), 3.78 (s, 3H, CH_3), 4.00 (s, 6H, CH_3), 4.40–4.48 (m, 4H, CH_2), 6.96 (d, *J* = 16.2 Hz, 1H, β-vinyl-H), 6.98 (d, *J* = 16.2 Hz, 1H, β-vinyl-H), 7.75 (d, *J* = 8.1 Hz, 2H, Ar-H), 7.76 (d, *J* = 8.1 Hz, 2H, Ar-*H*), 8.13 (d, *J* = 8.1 Hz, 4H, Ar-*H*), 8.51 (d, *J* = 16.2 Hz, 1H, α-vinyl-H), 8.52 (d, *J* = 16.2 Hz, 1H, α-vinyl-H), 10.61 (s, 1H, meso-H), 10.64 (s, 1H, meso-H), 10.70 (s, 1H, meso-H), 10.91 (s, 1H, meso-H) ppm; ^{13}C{^{1}H} NMR (101 MHz, $CDCl_3$ + TFA-d, 25 °C): δ = 12.1, 12.2, 13.2, 13.4, 21.7, 35.5, 35.5, 52.4, 52.9, 91.6, 95.2, 98.6, 99.0, 99.4, 99.7, 120.6, 127.8, 130.0, 132.1, 132.1, 132.3, 135.8, 136.1, 138.0, 139.3, 140.6, 167.5, 174.0 and 174.0 ppm; UV-Vis (DCM) λ_{max} [log(ε/M^{-1} cm^{-1})] = 429 [4.85], 520 [3.89], 559 [3.98], 587 [3.76], 644 [3.65] nm; HRMS (MALDI): *m/z* calcd. for [$C_{56}H_{50}N_4O_8$] [M]$^+$: 906.3629; found 906.3612.

(*E*,*E*)-3^2,8^2-Bis(2-(1-(3-bromophenyl)-1*H*-1,2,3-triazol-4-yl))-protoporphyrin dimethyl ester (**2.65**)

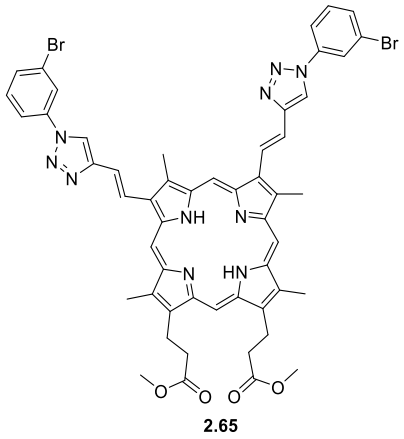

2.65

1-Azido-3-bromobenzene was synthesised according to a procedure by Matoba *et al*.[264] Compound **2.54** (14.8 mg, 23.1 µmol), sodium ascorbate (17.4 mg, 87.9 µmol) and $CuSO_4$•$5H_2O$ (15.2 mg, 60.8 µmol) were dissolved in anhydrous DMF (3 mL), 1-azido-3-bromobenzene (18.4 mg, 92.9 µmol) was added and the reaction mixture was stirred at 25 °C for 25 h. Then the reaction mixture was heated up to 100 °C for 1 h. The solvent was removed *in vacuo*, the crude solids were dissolved in a mixture of 0.6% MeOH in DCM and passed through an aluminium oxide pad to give the Cu(II) porphyrin complex **2.62**. Metalloporphyrin **2.62** was dissolved in a mixture of chloroform (4 mL) and concentrated sulfuric acid (0.4 mL) and stirred at 0 °C for 7 min. Colour change from green to dark brown indicated completion of the demetallation reaction. The mixture was diluted with chloroform, washed with 5% aqueous $NaHCO_3$ solution (2 ×) and water (2 ×). The combined aqueous layers were extracted with chloroform (1 ×). The combined organic layers were dried over $MgSO_4$, filtered and the solvent was removed *in vacuo*. The solids were dissolved in 0.5% MeOH in DCM and passed through an aluminium oxide pad to and the solvents were removed *in vacuo* to give **2.65** as a purple powder (11.7 mg, 11.3 µmol, 49%); M.p. = 260–267 °C; ^{1}H NMR (400 MHz, $CDCl_3$ + TFA-d, 25 °C): δ = 10.89 (s, 1H, meso-H), 10.65 (s, 1H, meso-H), 10.63 (s, 1H, meso-H), 10.58 (s, 1H, meso-H), 8.88 (d, *J* = 16.4 Hz, 1H, α-vinyl-H), 8.86 (d, *J* = 16.2 Hz, 1H, α-vinyl-H), 8.25 (s, 1H, triazole-H), 8.21 (s, 1H, triazole-H), 8.03 (s, 1H, Ar-H), 7.99 (s, 1H, Ar-H), 7.80–7.72 (m, 2H, Ar-H), 7.68 (br s, 1H, Ar-H), 7.66 (br s, 1H, Ar-H), 7.53 (d, *J* = 16.2 Hz, 1H, β-vinyl-H), 7.50 (d, *J* = 17.2 Hz, 1H, β-vinyl-H), 7.52 – 7.45 (m, 2H, Ar-H), 4.46–4.37 (m, 4H, CH_2), 3.74 (s, 3H, CH_3), 3.64(s, 3H, CH_3), 3.58 (s, 3H, OCH_3), 3.58 (s, 3H, OCH_3), 3.56 (s, 3H, CH_3), 3.55 (s, 3H, CH_3), 3.18–3.12 (m, 4H, CH_2) ppm; ^{13}C{^{1}H} NMR (101 MHz, $CDCl_3$ + TFA-d, 25 °C): δ = 173.1 (2 ×) 146.5, 146.4, 143.0, 142.5, 142.3, 142.0, 141.9, 141.1, 140.5, 140.2, 138.9, 138.6, 137.8, 137.7, 137.6, 137.3, 136.2, 135.8, 132.5, 131.4, 127.8, 127.4, 123.8, 123.7, 122.7, 122.6, 120.5, 120.4, 119.1, 115.5, 112.6, 100.3, 99.3 (2 ×), 99.1, 52.1, 35.6, 35.5, 29.9, 21.8, 13.3, 13.2, 12.1 ppm; HRMS (MALDI): *m/z* calcd. for [$C_{52}H_{46}N_{10}O_4Br_2Na$] [M+Na]$^+$: 1055.1968; found 1055.2018.

(*E*,*E*)-3^2,8^2-Bis(2-(1-(4-bromophenyl)-1*H*-1,2,3-triazol-4-yl))-protoporphyrin dimethyl ester (**2.66**)

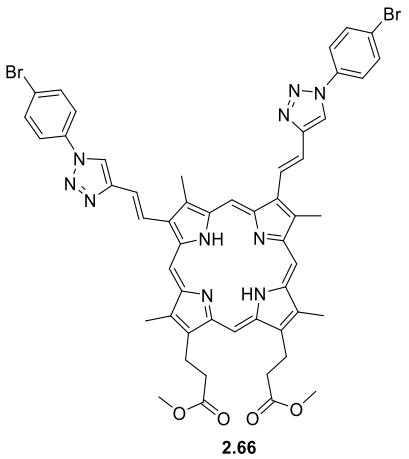

2.66

1-Azido-4-bromobenzene was synthesised according to a procedure by Matoba *et al*.[264] Compound **2.54** (20.0 mg, 28.5 µmol), sodium ascorbate (21.8 mg, 0.110 mmol) and $CuSO_4$•$5H_2O$ (14.7 mg, 58.8 µmol) were dissolved in anhydrous DMF (3 mL), 1-azido-3-bromobenzene (26.1 mg, 0.132 mmol) was added and the reaction mixture was stirred at 25 °C for 25 h. Then the reaction mixture was heated up to 100 °C for 1 h. The solvent was removed *in vacuo*, the crude solids were dissolved in a mixture of 0.6% MeOH in DCM and passed through an aluminium oxide pad to give the Cu(II) porphyrin complex **2.63**. Metalloporphyrin **2.63** was dissolved in a mixture of chloroform (4 mL) and concentrated sulfuric acid (0.4 mL) and stirred at 0 °C for 7 min. Colour change from green to dark brown indicated completion of the demetallation reaction. The mixture was diluted with chloroform, washed with 5% aqueous $NaHCO_3$ solution (2 ×) and water (2 ×). The combined aqueous layers were extracted with chloroform (1 ×). The combined organic layers were dried over $MgSO_4$, filtered and the solvent was removed *in vacuo*. The solids were dissolved in 0.5% MeOH in DCM and passed through an aluminium oxide pad. The solvents were removed *in vacuo* and **2.66** was obtained as a purple powder (12.7 mg, 12.3 µmol, 43%); M.p. > 300 °C; ^{1}H NMR (600 MHz, $CDCl_3$ + TFA-d, 25 °C): δ = 10.90 (s, 1H, meso-H), 10.73 (s, 1H, meso-H), 10.68 (s, 1H, meso-H), 10.59 (s, 1H, meso-H), 8.92 (d, *J* = 16.6 Hz, 1H, α-vinyl-H), 8.90 (d, *J* = 15.8 Hz Hz, 1H, α-vinyl-H), 8.33 (s, 1H, triazole-H), 8.29 (s, 1H, triazole-H), 7.76 (br s, 8H, Ar-H), 7.56 (d, *J* = 15.4 Hz, 1H, β-vinyl-H), 7.54 (d, *J* = 15.6 Hz, 1H, β-vinyl-H), 4.47–4.39 (m, 4H, CH_2), 3.77 (s, 3H, CH_3), 3.66 (s, 6H, CH_3), 3.60 (s, 3H, CH_3), 3.58 (s, 3H, OCH_3), 3.57 (s, 3H, OCH_3), 3.18–3.13 (m, 4H, CH_2) ppm; ^{13}C{^{1}H} NMR (101 MHz, $CDCl_3$ + TFA-d, 25 °C): δ = 173.3 (2 ×), 146.3, 143.1, 142.6, 142.3, 142.0, 141.9, 141.1, 140.4, 140.3, 139.1, 138.7, 138.2, 137.6, 136.2, 135.8, 135.6, 133.4, 127.7, 127.4, 123.5, 123.0, 122.2, 120.7, 120.6, 115.7, 112.8, 109.9, 100.5, 99.4, 99.3, 99.1, 52.1, 35.6, 35.5, 29.9, 21.8, 13.2, 13.1, 12.2, 12.1 ppm; UV-Vis (DCM): λ_{max} (log ε) = 417 [5.52], 514 [4.50], 552 [4.55], 583 [4.36], 640 [4.25] nm; HRMS (MALDI): *m/z* calcd. for [$C_{52}H_{47}N_{10}O_4Br_2$] $[M+H]^+$: 1033.2134; found 1033.2148.

((*E*,*E*)-3²,8²-Bis(trimethylsilylethynyl)-protoporphyrinato dimethyl ester)zinc(II) (**2.67**)

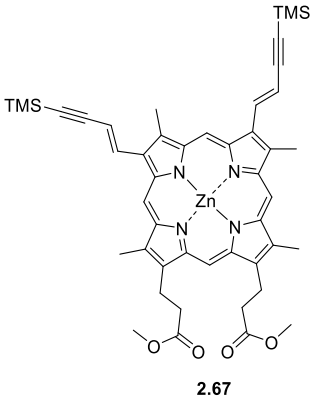

2.67

Compound **2.53** (25.0 mg, 31.9 µmol) was dissolved in CH_2Cl_2 (9 mL) and $ZnOAc_2•2H_2O$ (21.0 mg, 95.8 µmol) dissolved in MeOH (3 mL) was added. The mixture was heated to 40 °C for 1.5 h. Additional $ZnOAc_2•2H_2O$ (7.00 mg, 31.9 µmol) was added and the mixture was heated to 40 °C for 1 h more. The solvent was removed *in vacuo* and the residue was purified by column chromatography (aluminium oxide, DCM/*n*-hexane 1:1, 2:1, v/v, DCM/MeOH, 100:0.3, v/v). After removal of the solvents *in vacuo*, **2.67** was obtained as a green solid (19.9 mg, 23.5 µmol, 74%); M.p. > 300 °C; R_f = 0.62 (SiO_2, DCM/MeOH 100:0.25, v/v); ^{1}H NMR (600 MHz, $CDCl_3$, 25 °C): δ = 0.57 (s, 18H, TMS-C*H*$_3$), 2.15 (s, 3H, C*H*$_3$), 2.61 (s, 3H, C*H*$_3$), 2.95–3.03 (m, 7H, C*H*$_3$, C*H*$_2$), 3.11 (s, 3H, C*H*$_3$), 3.70 (s, 3H, C*H*$_3$), 3.73 (s, 3H, C*H*$_3$), 3.82–3.91 (br m, 4H, C*H*$_2$), 5.93 (d, *J* = 14.9 Hz, 1H, β-vinyl-H), 6.05 (d, *J* = 14.9 Hz, 1H, β-vinyl-H), 6.95–7.18 (br m, 2H, α-vinyl-H, meso-H), 7.59 (d, *J* = 13.7 Hz, 1H, α-vinyl-H), 8.09 (s, 1H, meso-H), 8.36 (s, 1H, meso-H) and 8.70 (s, 1H, meso-H) ppm; ^{13}C{^{1}H} NMR (151 MHz, $CDCl_3$, 25 °C): δ = 0.6, 11.2, 11.5, 12.0, 12.4, 21.6, 36.9, 36.9, 51.9, 95.3, 95.7, 96.2, 97.2, 97.2, 106.3, 106.4, 110.7, 111.0, 132.6, 132.8, 134.7, 135.2, 135.3, 136.0, 136.5, 136.9, 137.9, 138.1, 142.7, 143.9, 144.4, 145.0, 146.2, 146.6, 146.6, 147.0, 173.6, 173.6 ppm; UV-Vis (DCM) λ_{max} [log(ε/M^{-1} cm^{-1})] = 426 [5.59], 549 [4.52], 590 [4.78] nm; HRMS (MALDI): *m/z* calcd. for [$C_{46}H_{52}N_4O_4Si_2Zn$] [M]$^+$: 844.2819; found 844.2797.

((*E*,*E*)-3²,8²-Bisethynyl-protoporphyrinato dimethyl ester)zinc(II) (**2.57**)

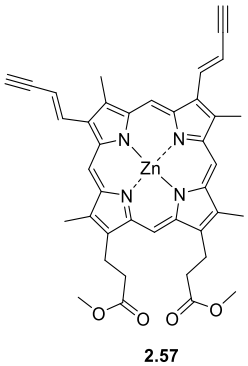

2.57

Compound **2.67** (31.8 mg, 37.5 µmol) was dissolved in anhydrous DCM (20 mL) under argon, a 1 M solution of TBAF in THF (90 µL, 90.0 µmol) was added and the mixture was stirred for 50 min at room temperature. The reaction mixture was passed through a plug of grade III neutral aluminium oxide (DCM/MeOH, 100:0.2, v/v) and the solvents were removed *in vacuo* to give **2.57** as a green solid (25.9 mg, 36.9 µmol, 98%); M.p. > 300 °C; R_f = 0.41 (SiO_2, DCM/MeOH 100:0.25, v/v); ^{1}H NMR (600 MHz, THF-d_8, 25 °C): δ = 3.24–3.29 (m, 4H, C*H*$_2$), 3.57 (s, 3H, C*H*$_3$), 3.57 (s, 6H, C*H*$_3$), 3.60 (s, 6H, C*H*$_3$), 3.68 (s, 3 H, C*H*$_3$), 3.81–3.79 (m, 2H, acetylene-H), 4.34–4.40 (m, 4H, C*H*$_2$), 6.79 (d, *J* = 16.5 Hz, 2H, β-vinyl-H), 8.63–8.73 (m, 2H, α-vinyl-H), 9.95 (s, 3H, meso-H), 9.99 (s, 1H, meso-H) ppm; ^{13}C{^{1}H} NMR (151 MHz, $CDCl_3$, 25 °C): δ = 11.8, 11.8, 13.5, 13.5, 22.8, 37.9, 51.7, 81.1, 81.2, 85.4, 97.8, 97.9, 98.6, 98.8, 112.0, 112.0, 135.7, 136.0, 137.7, 138.1, 138.5,

138.7, 138.8, 140.6, 140.7, 146.9, 147.9, 148.3, 148.8, 149.6, 149.6, 149.7, 150.1, 173.8 ppm; UV-Vis (THF) λ_{max} [log(ε/M^{-1} cm^{-1})] = 431 [5.43], 555 [4.43], 594 [4.54] nm; HRMS (MALDI): *m/z* calcd. for [$C_{40}H_{36}N_4O_4Zn$] $[M]^+$: 700.2028; found 700.2049.

((*E*,*E*)-3^2,8^2-Bis(2-(1-(3-bromophenyl)-1*H*-1,2,3-triazol-4-yl))-protoporphyrinato dimethyl ester)zinc(II) (**2.68**)

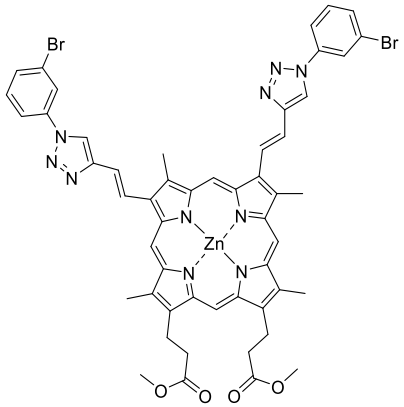

2.68

1-Azido-3-bromobenzene was synthesised according to a procedure by Matoba *et al*.[264] Compound **2.57** (24.5 mg, 34.8 µmol), sodium ascorbate (27.5 mg, 0.139 mmol) and $CuSO_4$•$5H_2O$ (19.0 mg, 76.1 µmol) were dissolved in anhydrous DMF (5 mL), 1-azido-3-bromobenzene (34.8 mg, 0.175 mmol) was added and the reaction mixture was heated to 100 °C for 5 h. EtOAC was added and the mixture was washed with saturated aqueous $NaHCO_3$ solution (3 ×). The organic layer was dried over $MgSO_4$, filtered and the solvent was removed *in vacuo*. The residue was purified by column chromatography (SiO_2, DCM, DCM/MeOH 100:2, v/v). The collected product was dissolved in a minimal amount of DCM, a few drops of pyridine were added and the solution was layered with methanol. A precipitate formed that was collected by suction filtration and washed with methanol. Compound **2.68** was obtained as a purple powder (10.7 mg, 9.74 µmol, 28%); M.p. = 259–264 °C; R_f = 0.27 (aluminium oxide, DCM/MeOH 100:1, v/v); ^{1}H NMR (600 MHz, DMSO-d_6, 25 °C): δ = 3.28–3.31 (m, 4H, CH_2), 3.59 (s, 3H, CH_3), 3.60 (s, 3H, CH_3), 3.64 (s, 3H, CH_3), 3.65 (s, 3H, CH_3), 3.88 (s, 3H, CH_3), 3.91 (s, 3H, CH_3), 4.34–4.40 (m, 4H, CH_2), 7.69 (t, *J* = 8.1 Hz, 2H, Ar-H), 7.81 (d, *J* = 8.0 Hz, 2H, Ar-H), 7.86 (d, *J* = 15.9 Hz, 2H, β-vinyl-H), 8.15 (d, *J* = 7.7 Hz, 2H, Ar-H), 8.34–8.38 (m, 2H, Ar-H), 9.13–9.22 (m, 2H, α-vinyl-H), 9.58 (s, 1H, triazole-H), 9.59 (s, 1H, triazole-H), 10.08 (s, 1H, meso-H), 10.21 (s, 1H, meso-H), 10.27 (s, 1H, meso-H), 10.39 (s, 1H, meso-H) ppm; ^{13}C{^{1}H} NMR (151 MHz, DMSO-d_6, 25 °C): δ = 11.4, 11.5, 13.3, 13.4, 21.4, 36.8, 51.3, 97.0, 97.1, 97.9, 98.0, 119.2, 119.2, 120.4, 120.4, 121.2, 121.3, 122.6, 122.7, 122.7, 124.6, 124.7, 131.5, 132.1, 135.4, 135.6, 136.8, 137.1, 137.6, 137.7, 137.9, 139.4, 139.6, 146.2, 146.8, 147.4, 147.7, 147.8, 147.8, 147.9, 148.0, 148.1, 148.4 and 173.1 ppm; UV-Vis (THF) λ_{max} [log(ε/M^{-1} cm^{-1})] = 431 [5.16], 555 [4.18], 594 [4.36] nm; HRMS (MALDI): *m/z* calcd. for [$C_{52}H_{44}Br_2N_{10}O_4Zn$] $[M]^+$: 1094.1205; found 1094.1213.

6.3 Chapter 3 – Synthesis of Protoporphyrin IX Dimethyl Ester-Fluorophore Triads

(*E*,*E*)-3^2,8^2-Bis(1,3,5,7-tetramethyl-8-(phen-4-ylene)-4,4-difluoro-4-bora-3a,4a-diaza-s-indacene)-protoporphyrin dimethyl ester (**3.8**)

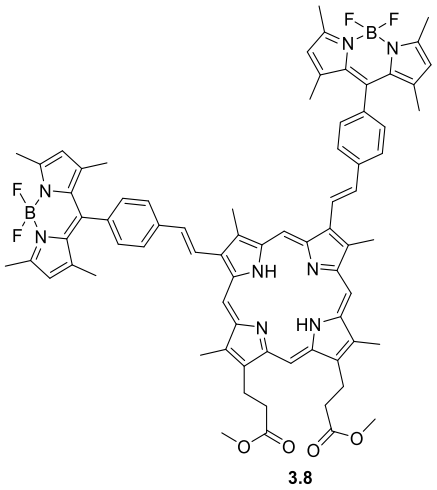

3.8

1,3,5,7-tetramethyl-8-(4-phenylboronic acid)-4,4-difluoro-4-bora-3a,4a-diaza-*s*-indacene (**3.7**) was synthesised according to a literature procedure.[289] Compound **2.39** (25.0 mg, 33.4 µmol), Cs_2CO_3 (145 mg, 0.445 mmol), 1,3,5,7-tetramethyl-8-(4-phenylboronic acid)-4,4-difluoro-4-bora-3a,4a-diaza-*s*-indacene (**3.7**) (49.2 mg, 0.134 mmol) and Pd(dppf)Cl_2 (4.9 mg, 6.68 µmol) were reacted in anhydrous THF (10 mL) for 18 h in accordance with general procedure **B** in section **6.2**. The crude product was purified by column chromatography (SiO_2, *n*-hexane/EtOAc 2:1, 1:1, v/v) and the solvents were removed *in vacuo* to give **3.8** as light-red crystals (10.0 mg, 8.10 µmol, 24%); M.p. = 244 °C dec.; R_f = 0.51 (SiO_2, EtOAc/*n*-hexane 1:1, v/v); ^{1}H NMR (600 MHz, $CDCl_3$, 25°C): δ = –3.71 (br s, 2H, N*H*), 1.65 (s, 6H, CH_3), 1.66 (s, 6H, CH_3), 2.63 (s, 12H, CH_3), 3.28 (t, *J* = 7.7 Hz, 4H, CH_2), 3.60 (s, 3H, CH_3), 3.61 (s, 3H, CH_3), 3.67 (s, 6H, CH_3), 3.76 (s, 3H, CH_3), 3.77 (s, 3H, CH_3), 4.36–4.40 (m, 4H, CH_2), 6.08 (s, 4H, pyrrolic-H), 7.53–7.50 (m, 4H, Ar-H), 7.80 (d, *J* = 16.4 Hz, 1H, β-vinyl-H), 7.79 (d, *J* = 16.4 Hz, 1H, β-vinyl-H), 8.09 (d, *J* = 7.8 Hz, 4H, Ar-H), 8.75 (d, *J* = 16.5 Hz, 1H, α-vinyl-H), 8.76 (d, *J* = 16.4 Hz, 1H, α-vinyl-H), 9.99 (s, 1H, meso-H), 10.00 (s, 1H, meso-H), 10.16 (s, 1H, meso-H), 10.17 (s, 1H, meso-H) ppm; ^{13}C{^{1}H} NMR (151 MHz, $CDCl_3$, 25°C): δ = 11.7, 11.8, 13.3, 13.4, 14.7, 14.9, 21.8, 36.9, 51.8, 96.4, 97.2, 97.3, 97.8, 121.4, 122.9, 127.4, 128.8, 131.6, 134.0, 134.6, 138.9, 141.6, 143.2, 155.7, 173.6 ppm; ^{19}F{^{1}H} NMR (377 MHz, $CDCl_3$, 25°C): δ = –146.13 ppm (q, *J* = 32.6 Hz);^{11}B NMR (128 MHz, $CDCl_3$, 25°C): δ = 0.88 ppm (t, *J* = 33.3 Hz); UV-Vis (DCM): λ_{max} [log(ε/M^{-1} cm^{-1})] = 419 [5.86], 502 [5.91], 553 [4.96], 583 [4.66], 639 [4.60] nm; HRMS (MALDI): *m/z* calcd. for [$C_{74}H_{72}B_2F_4N_8O_4$] [M]$^+$: 1234.5799; found 1234.5824.

(Bishydroxy)(protoporphyrinato dimethyl ester)tin(IV) (**3.14**)

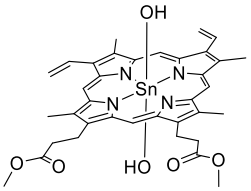

3.14

In a 100 mL RBF, protoporphyrin IX dimethyl ester **1.23** (90.0 mg, 0.152 mmol) was dissolved in $CHCl_3$ (27 mL). $SnCl_2 \cdot 2H_2O$ (342 mg, 1.52 mmol), dissolved in EtOH (27 mL), was added and the mixture was refluxed for 2.5 h. The solvent was removed *in vacuo* and the residue was dissolved in DCM and washed with H_2O (4 ×) and brine (1 ×). The organic layer was dried over $MgSO_4$, filtered and the solvent was removed *in vacuo* to give **3.14** as pink powder (81.7 mg, 0.110 mmol, 72%); M.p. > 300 °C; R_f = 0.30 (DCM/MeOH 100:6.25); ^{1}H NMR (400 MHz, $CDCl_3$, 25 °C): δ = 3.42 (t, *J* = 7.6 Hz, 2H, CH_2), 3.43 (t, *J* = 7.4 Hz, 2H, CH_2), 3.62 (s, 3H, CH_3), 3.63 (s, 3 H, CH_3), 3.80 (s, 3 H, CH_3), 3.82 (s, 3 H, CH_3), 3.86 (s, 3H, CH_3), 3.88 (s, 3H, CH_3), 4.56 (t, *J* = 7.2 Hz, 2H, CH_2), 4.57 (t, *J* = 7.2 Hz, 2H, CH_2), 6.38 (d, *J* = 4.7 Hz, 1H, β-vinyl-H), 6.40 (d, *J* = 4.7 Hz, 1H, β-vinyl-H), 6.53 (d, *J* = 17.8 Hz, 1H, β-vinyl-H), 6.55 (d, *J* = 17.9 Hz, 1H, β-vinyl-H), 8.34 (dd, *J* = 17.2, 4.9 Hz, 1H, α-vinyl-H), 8.37 (dd, *J* = 17.4, 4.7 Hz, 1H, α-vinyl-*H*), 10.63 (s, 1H, meso-H), 10.71 (s, 1 H, meso-H), 10.71 (s, 1 H, meso-H), 10.77 (s, 1 H, meso-H) ppm; ^{13}C{^{1}H} NMR (151 MHz, $CDCl_3$, 25 °C): δ = 12.1, 13.0, 13.0, 22.0, 22.0, 36.6, 36.6, 52.0, 97.8, 97.9, 98.2, 98.2, 98.7, 98.7, 99.2, 124.0, 124.0, 129.4, 129.5, 138.3, 138.7, 139.1, 139.2, 139.4, 139.6, 141.0, 143.2, 143.4, 144.3, 144.3, 144.4, 144.4, 144.6, 144.9, 173.5 ppm; UV-Vis (DCM) λ_{max} [log(ε/M^{-1} cm^{-1})] = 418 [5.44], 547 [4.26], 585 [4.18] nm; HRMS (MALDI): *m/z* calcd. for [$C_{36}H_{38}N_4O_6Sn$] $[M+H]^+$: 743.1886; found 743.1469.

(Bis(8-(4-phenolate)-4,4-difluoro-4-bora-3a,4a-diaza-*s*-indacene))(protoporphyrinato dimethyl ester)tin(IV) (**3.19**)

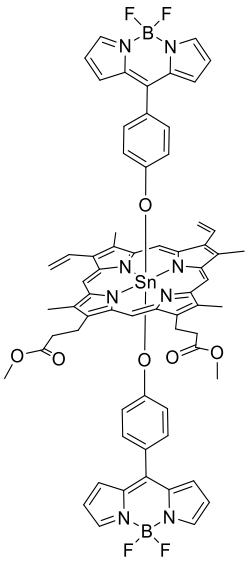
3.19

8-(4-Phenyl)-4,4-difluoro-4-bora-3a,4a-diaza-*s*-indacene (**3.18**) was synthesised according to a literature procedure.[296] In a 50 mL RBF, (Bishydroxy)(protoporphyrinato dimethyl ester)tin(IV) (**3.14**) (15.0 mg, 20.2 µmol) and 8-(4-phenyl)-4,4-difluoro-4-bora-3a,4a-diaza-*s*-indacene (**3.18**) (12.6 mg, 44.5 µmol) were dissolved in anhydrous benzene (8 mL) and the reaction mixture was stirred at 80 °C for 16 h under argon. The solvent was removed *in vacuo* and the crude product was purified by column chromatography (aluminium oxide, DCM). After removal of the solvents *in vacuo* **3.19** was obtained as dark orange crystals (3.50 mg, 3.06 µmol, 14%); M.p. = 287 °C; R_f = 0.26 (aluminium oxide, DCM). ^{1}H NMR (400 MHz, $CDCl_3$, 25 °C): δ = 1.65 (d, *J* = 8.5 Hz, 4H, Ar-H), 3.36 (t, *J* = 7.3 Hz, 2H, CH_2), 3.38 (t, *J* = 7.3 Hz, 2H, CH_2), 3.64 (s, 3H, CH_3), 3.64 (s, 3H, CH_3), 3.77 (s, 3H, CH_3), 3.81 (s, 3H, CH_3), 3.84 (s, 3H, CH_3), 3.86 (s, 3H, CH_3), 4.56 (t, *J* = 7.3 Hz, 2H, CH_2), 4.58 (t, *J* = 7.3 Hz, 2H, CH_2), 5.78 (d, *J* = 8.4 Hz, 4H, Ar-H), 6.35 (d, *J* = 3.7 Hz, 4H, β-pyrrolic-H), 6.38–6.43 (m, 2H, β-vinyl-H), 6.44 (dd, *J* = 4.1, 1.6, 4H, β-pyrrolic-H), 6.51 (d, *J* = 17.9 Hz, 2H, β-vinyl-H), 6.54 (d, *J* = 17.8 Hz, 2H, α-vinyl-H), 7.76 (s, 4H, α-pyrrolic-H), 8.35 (dd, *J* = 17.8, 10.8 Hz, 1H, α-vinyl-H), 8.38 (dd, *J* = 17.8, 10.8 Hz, 1H, α-vinyl-H), 10.52 (s, 1H, meso-H), 10.59 (s, 1H, meso-H), 10.67 (s, 1H, meso-H), 10.70 (s, 1H, meso-H) ppm; ^{13}C{^{1}H} NMR (151 MHz, $CDCl_3$, 25 °C): δ = 12.2, 13.1, 21.9, 36.7, 52.1, 98.6, 98.7, 99.1, 99.7, 115.5, 117.5, 117.6, 118.4, 122.4, 124.2, 124.3, 129.3, 129.3, 129.8, 130.7, 131.4, 132.6, 134.3, 138.3, 138.6, 139.0, 139.2, 139.4, 139.5, 141.3, 142.1, 143.6, 144.2, 144.5, 145.2, 145.3, 145.4, 145.4, 145.6, 146.0, 148.4, 159.0, 173.3 ppm; UV-Vis (DCM): λ_{max} [log(ε/M^{-1} cm^{-1})] = 412 [4.51], 497 [4.26], 545 [3.39], 586 [3.31] nm; No HRMS spectrum of **3.19** could be obtained due to instability of the material under the tried conditions (MALDI).

8-(4-(4-Bromobutoxy)phenyl)-4,4-difluoro-4-bora-3a,4a-diaza-*s*-indacene (**3.20**)

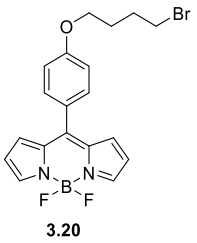

3.20

8-(4-Phenyl)-4,4-difluoro-4-bora-3a,4a-diaza-*s*-indacene[296] (**3.18**) (30.0 mg, 0.105 mmol) and K_2CO_3 (33.0 mg, 0.239 mmol) were dissolved in anhydrous DMF (2 mL) and dibromobutane (90 µL, 0.630 mmol) was added. The solution was heated to 100 °C for 16 h under argon. The solvent was removed *in vacuo* and the crude product was purified by column chromatography (SiO_2, DCM/MeOH, 100:0.1, v/v) twice. Removal of the solvents *in vacuo* yielded **3.20** as orange crystals (21.0 mg, 50.1 µmol, 48%); R_f = 0.70 (SiO_2, DCM); ^{1}H NMR (400 MHz, $CDCl_3$, 25 °C): δ = 2.07–1.98 (m, 2H, CH_2), 2.08–2.16 (m, 2H, CH_2), 3.52 (t, *J* = 6.5 Hz, 2H, CH_2), 4.11 (t, *J* = 5.9 Hz, 2H, CH_2), 6.55 (d, *J* = 2.7 Hz, 2H, β-pyrrolic-H), 6.97 (d, $^3J_{HH}$ = 3.6 Hz, 2H, β-pyrrolic-H), 7.03 (d, *J* = 8.5 Hz, 2H, Ar-H), 7.54 (d, *J* = 8.5 Hz, 2H, Ar-H), 7.92 (s, 2H, α-pyrrolic-H) ppm. ^{13}C{^{1}H} NMR (151 MHz, $CDCl_3$, 25 °C): δ = 27.9, 29.5, 33.4, 67.3, 114.6, 118.4, 126.5, 131.5, 132.6, 135.0, 143.6, 147.5, 161.5 ppm; ^{11}B NMR (128 MHz, $CDCl_3$, 25 °C): δ = 0.30 (t, J = 28.9 Hz) ppm; ^{19}F{^{1}H} NMR (377 MHz, $CDCl_3$, 25 °C): δ = -145.14 (q, J = 28.8 Hz) ppm; UV-Vis (DCM) λ_{max} [log(ε/M^{-1} cm^{-1})] = 399 [3.55], 499 [4.18] nm; HRMS (ESI): *m/z* calcd. for [$C_{19}H_{18}BBrF_2N_2O$] $[M+H]^+$: 419.0750; found 419.0740.

4-Bromo-3,3',5,5'-tetraphenyl-*ms*-aza-2,2'- dipyrromethene difluoroborate (**3.26**)

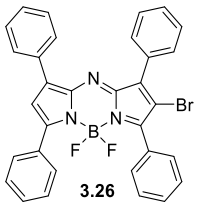

3.26

3,3',5,5'-Tetraphenyl-*ms*-aza-2,2'- dipyrromethene difluoroborate (**3.25**) was prepared as reported previously.[299] 3,3',5,5'-Tetraphenyl-*ms*-aza-2,2'- dipyrromethene difluoroborate (**3.25**) (320 mg, 0.643 mmol) was dissolved in a DCM/DMF 1:1 mixture (32 mL) and NBS (103 mg, 0.580 mmol) dissolved in DCM (6 mL) was added dropwise to the reaction mixture. The solution was stirred for 24 h at room temperature. The reaction mixture was diluted with DCM and washed with H_2O (5 ×) and brine (1 ×). The organic layer was dried over $MgSO_4$, filtered and the solvent was removed *in vacuo*. ^{1}H NMR analysis in $CDCl_3$ revealed the presence of about 25% starting material next to the brominated product. The residue was dissolved in a 1:1 mixture of DCM and DMF (32 mL) and NBS (46 mg, 0.260 mmol) dissolved in DCM (4 mL) was added dropwise to the reaction mixture. The solution was stirred for 16 h. After an aqueous workup as described above the crude product was purified by column chromatography (SiO_2, DCM/*n*-hexane 2:1, v/v) and the solvents were removed *in vacuo*. ^{1}H NMR analysis of the product in $CDCl_3$ indicated the presence of 6% starting material. Separation of the two compounds by column chromatography could not be achieved. **3.26** was obtained as a blue solid (303 mg, 0.526 mmol, 82%); M.p. = 249–251 °C dec.; R_f = 0.31 (SiO_2, *n*-hexane/DCM 2:1, v/v); ^{1}H NMR (400 MHz, $CDCl_3$,

25 °C): δ = 7.12 (s, 1H, pyrrolic-H), 7.45–7.42 (m, 3H, Ar-H), 7.56–7.48 (m, 9H, Ar-H), 7.82–7.78 (m, 2H, Ar-H), 7.97–7.94 (m, 2H, Ar-H), 8.05–8.02 (m, 2H, Ar-H), 8.10–8.06 (m, 2H, Ar-H) ppm; $^{13}C\{^{1}H\}$ NMR (151 MHz, $CDCl_3$, 25 °C): δ = 120.0, 128.1, 128.2, 128.9, 128.9, 129.4, 129.5, 129.9, 130.2, 130.2, 130.5, 130.6, 131.0, 131.3, 131.7, 131.9, 141.1, 143.2, 146.1, 147.0, 155.3, 162.8 ppm; UV-Vis (DCM) λ_{max} [log(ε/M^{-1} cm^{-1})] = 489 [4.05], 645 [4.94] nm; HRMS (MALDI): *m/z* calcd. for [$C_{32}H_{21}BN_3F_2Br$] $[M]^+$: 575.0980; found 575.0978.

4-(4-Ethynylphenyl)-3,3',5,5'-tetraphenyl-*ms*-aza-2,2'-dipyrromethene difluoroborate (3.32)

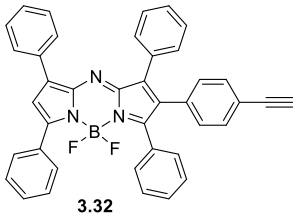

3.32

In a 10 mL Schlenk tube, **3.26** (50.0 mg, 86.8 µmol) and 4-[(trimethylsilyl)ethynyl]phenylboronic acid (156 mg, 0.521 mmol) were dissolved in a mixture of anhydrous toluene (3 mL) and EtOH (1.5 mL) and the solution was purged with argon for 20 min. In a separate vial, Na_2CO_3 was dissolved in H_2O (0.6 mL) and the solution was purged with argon for 10 min. The base solution was transferred to the Schlenk tube, followed by $Pd(PPh_3)_4$, and the mixture was purged with argon for another 5 min. The solution was heated to 70 °C for 3.5 h and then stirred at r.t. for 16 h. The reaction mixture was diluted with DCM and washed with water (3 ×) and brine (1 ×). The organic layer was dried over $MgSO_4$, filtered and the solvent was removed *in vacuo*. Column chromatography (SiO_2, DCM/*n*-hexane 1:1, v/v) and removal of the solvents *in vacuo* afforded deborylated 4-(4-(trimethylsilylethynyl)phenyl)-3,3',5,5'-tetraphenyl-*ms*-aza-2,2'-dipyrromethene **3.30**. In a RBF, the solids were dissolved in anhydrous DCM (8 mL), *N*,*N*-diisopropylethylamine (0.15 mL, 0.852 mmol) was added and the mixture was stirred at r.t. under argon for 1 h. Boron trifluoride diethyl etherate (0.16 mL, 1.287 mmol) was added and the mixture was stirred at r.t. under argon for 40 h. The solvents were removed *in vacuo*, the crude solids were dissolved in a *n*-hexane/EtOAc 1:1 (v/v) mixture and passed through a pad of SiO_2. After removal of the solvents *in vacuo*, 4-(4-((trimethylsilyl)ethynyl)phenyl)-3,3',5,5'-tetraphenyl-*ms*-aza-2,2'-dipyrromethene difluoroborate **3.31** was obtained. In a RBF, the solids were dissolved in anhydrous THF (5 mL) and the solution was cooled to -40 °C using and EtOH/$N_{2(l)}$ bath. A 1 M solution of tetrabutylammonium fluoride (TBAF) in THF (80 µL, 80 µmol) was added under argon and the solution was stirred at -40 °C for 0.5 h. The reaction mixture was diluted with DCM and washed with water (2 ×). The organic layer was dried over $MgSO_4$, filtered and the solvent was removed *in vacuo*. The crude solids were purified by column chromatography (SiO_2, DCM/*n*-hexane 1:3, 1:2, v/v) and the solvents were removed *in vacuo* to afford **3.32** as a blue solid (25.6 mg, 42.9 µmol, 33%); M.p. = 222–224 °C; R_f = 0.23 (SiO_2, DCM/*n*-hexane

1:2, v/v); ^{1}H NMR (600 MHz, $CDCl_3$, 25 °C): δ = 3.08 (s, 1H, acetylene-H), 6.91 (d, *J* = 8.3 Hz, 2H, Ar-H), 7.08 (s, 1H, pyrrolic-H), 7.27–7.38 (m, 8H, Ar-H), 7.41–7.43 (m, 3H, Ar-H), 7.45–7.48 (m, 7H, Ar-H), 8.00–8.03 (m, 2H, Ar-H), 8.08–8.11 (m, 2H, Ar-H) ppm; ^{13}C{^{1}H} NMR (151 MHz, $CDCl_3$, 25 °C): δ = 77.9, 83.7, 119.4, 121.0, 128.0, 128.1, 128.8, 128.8, 129.5, 129.8, 129.8, 129.8, 129.9, 130.0, 130.6, 130.6, 130.7, 131.3, 131.4, 131.4, 131.7, 132.1, 132.2, 132.4, 133.7, 140.9, 144.7, 144.9, 146.6, 157.8, 161.2 ppm; ^{11}B NMR (128 MHz, $CDCl_3$, 25 °C) δ = 0.74 (t, *J* = 30.2 Hz) ppm; ^{19}F{^{1}H} NMR (377 MHz, $CDCl_3$, 25 °C) δ = -131.75 (q, *J* = 30.2 Hz) ppm; UV-Vis (DCM) λ_{max} [log(ε/M^{-1} cm^{-1})] = 282 [4.24], 287 [4.24], 501 nm [3.87], 652 [4.72] nm; HRMS (ESI): *m/z* calcd. for $[C_{40}H_{27}BN_3F_2]$ $[M+H]^+$: 598.2267; found 598.2251.

8-(4-Ethynylphenyl)-4,4-difluoro-1,7,-dimethyl-3,5-distyrenyl-bora-3a,4a-diaza-*s*-indacene (3.38)

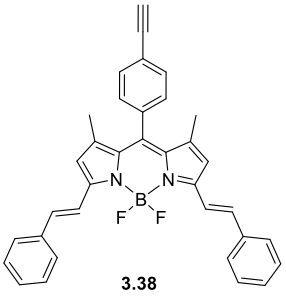

3.38

8-(4-Ethynylphenyl)-4,4-difluoro-1,3,5,7-tetramethyl-4-bora-3a,4a-diaza-*s*-indacene **3.36** was prepared according to a literature procedure.[304] BODIPY **3.36** (50 mg, 0.119 mmol) was added to a microwave tube and the vessel was evacuated and purged with argon three times. Anhydrous DMF (3 mL) was added and the solution purged with argon for 10 minutes. Benzaldehyde (49 µL, 0.476 mmol), piperidine (4 drops) and acetic acid (4 drops) were added to the mixture and the solution was purged with argon for another 5 min. The mixture was placed in the microwave with 1 minute pre-stirring followed by 5 minutes irradiation at 150 °C. The solvent was removed *in vacuo* and the crude product was purified by silica gel column chromatography (*n*-hexane/EtOAc 20:1). Removal of the solvents *in vacuo* afforded 8-(4-((trimethylsilyl)ethynyl)phenyl)-4,4-difluoro-1,7,-dimethyl-3,5-distyrenyl-bora-3a,4a-diaza-*s*-indacene **3.37** and 8-(4-ethynylphenyl)-4,4-difluoro-1,7,-dimethyl-3,5-distyrenyl-bora-3a,4a-diaza-*s*-indacene **3.38** (27.3 mg, 52.1 µmol, 44%) as a blue solid. 8-(4-((Trimethylsilyl)ethynyl)phenyl)-4,4-difluoro-1,7,-dimethyl-3,5-distyrenyl-bora-3a,4a-diaza-*s*-indacene **3.37** was added to a 10 mL Schlenk tube and the reaction vessel was evacuated and purged with argon three times. Anhydrous THF (4 mL) was added and the solution was purged with argon for 5 min. A 1 M solution of TBAF in THF (0.044 mL, 44 µmol) was added and the solution was stirred in a cold bath of ethanol and liquid nitrogen at -40 °C for 30 min. DCM was added and the mixture was washed with H_2O (2 ×). The organic layer was dried over $MgSO_4$, filtered and the solvent was removed *in vacuo*. The crude product was purified by passing it through a pad of SiO_2 (DCM/*n*-hexane 1:1, v/v) and the solvents were removed *in vacuo* to give **3.38** (12.7 mg, 0.0242 mmol, 60%);

M.p. > 300 °C; R_f = 0.65 (SiO_2, DCM/*n*-hexane 2:1, v/v); ^{1}H NMR (400 MHz, $CDCl_3$, 25 °C): δ = 1.48 (s, 6H, C*H*$_3$), 3.20 (s, 1H, acetylene-H), 6.66 (s, 2H, pyrrolic-H), 7.27 (d, *J* = 16.3 Hz, 2H, α-vinyl-H), 7.30–7.35 (m, 4H, Ar-H), 7.41 (t, *J* = 7.3 Hz, 4H, Ar-H), 7.63–7.66 (m, 6H, Ar-H), 7.74 (d, *J* = 16.3 Hz, 2H, β-vinyl-H) ppm; ^{13}C{^{1}H} NMR (101 MHz, $CDCl_3$, 25 °C): δ = 15.0, 78.8, 83.1, 118.2, 119.4, 123.2, 127.8, 128.8, 129.0, 129.2, 133.0, 133.3, 135.9, 136.7, 136.7, 142.2, 153.1 ppm; ^{11}B NMR (128 MHz, $CDCl_3$, 25 °C) δ = 1.14 (t, *J* = 33.7 Hz) ppm; ^{19}F{^{1}H} NMR (377 MHz, $CDCl_3$, 25 °C) δ = -138.15 (q, *J* = 33.3 Hz) ppm; UV-Vis (DCM) λ_{max} [log(ε/M^{-1} cm^{-1})] = 352 [3.76], 578 [3.51], 610 [3.53], 629 [3.87] nm; HRMS (APCI): *m/z* calcd. for $C_{35}H_{27}BF_2N_2$ [M]$^-$: 542.2235, found 524.2245.

(*E*,*E*)-3^2,8^2-Bis(1,7-dimethyl-3,5-distyrenyl-8-(4-phenylethynyl)-4,4-difluoro-4-bora-3a,4a-diaza-s-indacene)-protoporphyrin IX dimethyl ester (3.39)

In a 10 mL Schlenk tube, compound (*E*,*E*)-3^2,8^2-bisbromo-protoporphyrin IX dimethyl ester (28.5 mg, 38.1 µmol) was dried under vacuum and the reaction vessel evacuated and purged with argon three times. Anhydrous THF (2.4 mL) and Et_3N (2.4 mL) were added and the solution was purged with argon for 10 min. $PdCl_2(PPh_3)_2$ (2.65 mg, 3.60 µmol) and CuI (1.425 mg, 7.48 µmol) were added to the solution and the mixture was degassed for another 5 min. 8-(4-Ethynylphenyl)-4,4-difluoro-1,7,-dimethyl-3,5-distyrenyl-bora-3a,4a-diaza-*s*-indacene (**3.38**) (40 mg, 76.1 µmol) was added to the reaction vessel. The solution was stirred for 8 h at room temperature. The solvent was removed *in vacuo* and the crude product was purified by silica gel column chromatography (DCM/*n*-hexane, 1:1). After removal of the solvents *in vacuo* the title compound was obtained as a dark green solid (10.5 mg, 6.40 µmol, 17%); M.p. > 300 °C; R_f = 0.65 (DCM/*n*-hexane, 4:1, v/v); UV-Vis (DCM) λ_{max} [log(ε/M^{-1} cm^{-1})] = 350 [4.18], 413 [4.20], 511 [3.37], 579 [3.88], 629 [4.19] nm; HRMS (MALDI): *m/z* calcd. for $C_{116}H_{86}B_2F_4N_{10}O_4$ [M]+: 1781.6956; found 1781.6997.

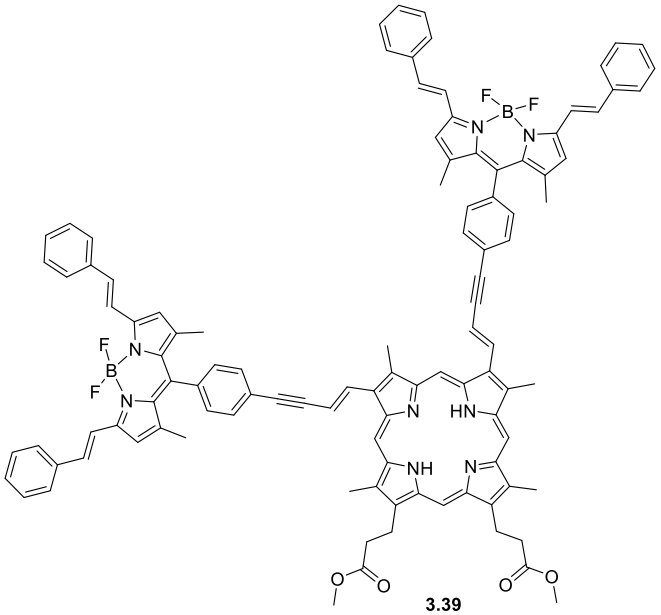

3.39

NMR spectra of **3.39** were recorded in different solvents ($CDCl_3$ + TFA-d, toluene-d_8, DMSO-d_6 and acetone-d_6) but conclusive data was not attainable because of stacking

interactions between the molecules in the sample and strong peak broadening in the spectra.

8-(4-(4,4,5,5-Tetramethyl-1,3,2-dioxaborolan-2-yl)phenyl))-4,4-difluoro-1,7,-dimethyl-3,5-distyrenyl-bora-3a,4a-diaza-*s*-indacene

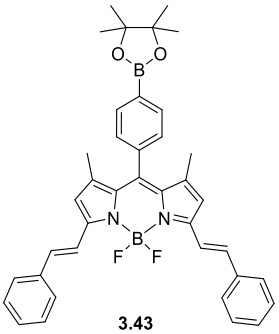

3.43

8-(4-(4,4,5,5-Tetramethyl-1,3,2-dioxaborolan-2-yl)phenyl))-1,3,5,7-tetramethyl-4,4-difluoro-4-bora-3a,4a-diaza-*s*-indacene (**3.42**) was synthesised according to a literature procedure.[307] Compound **3.42** (58.6 mg, 0.136 mmol) was added to a microwave tube and the vessel evacuated and purged with argon three times. Anhydrous DMF (4.8 mL) was added and the solution was purged with argon for 10 minutes. Benzaldehyde (0.069 mL, 0.0679 mmol), piperidine (5 drops) and acetic acid (5 drops) were added to the mixture and the solution further deoxygenated. The mixture was placed in the microwave with 1 min pre-stirring followed by 7 min irradiation at 150 °C. Solvent was removed *in vacuo*. The crude product was purified by column chromatography (SiO_2, DCM/*n*-hexane 1:1, v/v) followed by preparative TLC (SiO_2, *n*-hexane/EtOAc 5:1, v/v). The solvents were removed *in vacuo* to give compound **3.43** as a blue solid (14.3 mg, 22.9 µmol, 17%). Compound **3.43** was not fully characterised because impurities could not be removed entirely. The product was used as such for the next reaction. ^{1}H NMR (400 MHz, $CDCl_3$, 25 °C) δ = 1.40 (s, 12H, boryl-CH_3), 1.45 (s, 6H, *β*-CH_3), 6.64 (s, 2H, pyrrolic-H), 7.26 (d, *J* = 16.1 Hz, 2H, vinyl-H), 7.29–7.37 (m, 4H, Ar-H), 7.40 (t, *J* = 7.5 Hz, 4H, Ar-H), 7.61–7.67 (m, 4H, Ar-H), 7.75 (d, *J* = 16.2 Hz, 2H, vinyl-H), 7.93 (d, *J* = 7.7 Hz, 2H, Ar-H) ppm; ^{11}B NMR (128 MHz, $CDCl_3$, 25 °C) δ = 1.15 (t, *J* = 33.5 Hz) ppm; ^{19}F{^{1}H} NMR (377 MHz, $CDCl_3$, 25 °C) δ = -138.18 (q, *J* = 67.4, 33.1 Hz) ppm; HRMS (APCI): m/z calcd. for $C_{39}H_{38}B_2F_2N_2O_2$ $[M]^-$: 626.3087; found 626.3100.

6.4 Chapter 4 – Synthesis of Di-substituted and Tri-substituted Bicyclo[1.1.1]pentane-Triazoles

The precursors 1-azido-3-iodobicyclo[1.1.1]pentane **1.92**,[189b] 8-(4-ethynylphenyl)-4,4-difluoro-1,3,5,7-tetramethyl-4-bora-3a,4a-diaza-*s*-indacene **4.24**,[304] 1-ethynylpyrene **4.27**,[330] and [5-(4-ethynylphenyl)-10,20-bis(4-methylphenyl)-15-phenylporphyrinato]zinc(II) **4.34**[181] were synthesised according to literature procedures. For some reactions, a mixture of 1-azido-3-iodobicyclo[1.1.1]pentane **1.92** and 1,3-diiodobicyclo[1.1.1]pentane was used. To rule out the possibility that the use of this mixture

as a starting material for “click” reactions has an effect on the product formation, a test “click” reaction with neat 1-azido-3-iodo-BCP **1.92** and BODIPY **4.24** was performed under the conditions of general procedure **D**. The 5-iodo-1,2,3-triazole product **4.39** was isolated with a yield of 6%, alongside the 5-protio-1,2,3-triazole product **4.36** with a yield of 71%. This product distribution was comparable to the results obtained when a mixture of 1-azido-3-iodobicyclo[1.1.1]pentane and 1,3-diiodobicyclo[1.1.1]pentane was used, indicating that use of the mixture had no influence on the product formation.

General Procedure **D** *for the Synthesis of 5-Protio-1,2,3-triazoles* **4.36**, **4.37**, **4.38**, **4.14**. 1,2,3-Triazoles were synthesised by adapting a literature procedure.[194,195] A microwave vial equipped with a rubber septum was evacuated and refilled with argon (3 ×). **1.92** (1.0 eq.) dissolved in anhydrous THF was added to the vial, followed by TEA (1.5 eq.). The mixture was purged with argon for 10 min. CuI (0.10 eq.) and the ethynyl substrate (1.0 eq.) were added and purging with argon was continued for 5 min. The mixture was stirred under argon at room temperature in the dark for 16 h. The solvent was removed *in vacuo*, the residue was dry-loaded onto silica gel and purified by column chromatography.

General Procedure **E** *for the Synthesis of 5-Iodo-1,2,3-triazoles* **4.39**, **4.40**, **4.41**, **4.45**, **4.46**. A modified literature procedure was used for the synthesis of 5-iodo-1,2,3-triazoles.[319d] A microwave vial equipped with a rubber septum was evacuated and refilled with argon (3×). **1.92** (1.0 eq.) dissolved in anhydrous THF was added to the vial, followed by DIPEA (1.0 eq.). The mixture was purged with argon for 10 min. CuI (1.0 eq.), the ethynyl substrate (1.0 eq.) and, at the end, NBS (1.2 eq.) were added and and purging with argon was continued for 5 min. The reaction mixture was stirred under argon at room temperature in the dark for 18 h. The solvent was removed *in vacuo*, the residue was dry-loaded onto silica gel and purified by column chromatography.

General Procedure **F** *for the Synthesis of 5-Alkynylated 1,2,3-Triazoles* **4.49**–**4.53**. An oven-dried Schlenk tube equipped with a rubber septum was evacuated and refilled with argon (3 ×). **1.92** (1.0 eq.) dissolved in anhydrous THF was added to the tube, followed by the same amount of anhydrous TEA. The ethynyl substrate (2.2–2.4 eq.) was added and the mixture was purged with argon for 15 min. CuI (0.20 eq.) and $Pd(PPh_3)_2Cl_2$ (0.10 eq.) were added and purging with argon was continued for 5 min. The reaction mixture was stirred under argon at room temperature in the dark for 18 h. The solvent was removed *in vacuo*. The residue was dissolved in EtOAc or DCM and passed through a plug of silica gel. Subsequently, the crude mixture was dry-loaded onto silica gel and further purified by column chromatography.

Screening of Reaction Conditions for the Formation of 5-Protio-1,2,3-triazole **4.36** *and 5-Iodo-1,2,3-triazole* **4.39***.* Five reactions were carried out with **1.92** (6.7 mg, 28.7 µmol, 1.0 eq.) and **4.24** (10.0 mg, 28.7 µmol, 1.0 eq.) and varying amounts of reagents in 0.67 mL anhydrous THF based on general procedure **F**: **I)** CuI (1.1 mg, 5.78 µmol, 0.2 eq.), TEA (6 µL, 43.0 µmol, 1.5 eq.), under argon atmosphere according to general procedure A. **II)** CuI (1.6 mg, 8.4 µmol, 0.3 eq.), TEA (6 µL, 43.0 µmol, 1.5 eq.), under argon atmosphere according to general procedure **F**. **III)** CuI (1.1 mg, 5.78 µmol, 0.2 eq.), TEA (6 µL, 43.0 µmol, 1.5 eq.), the solvent was not deoxygenated and the reaction was carried out under air. **IV)** CuI (1.6 mg, 8.4 µmol, 0.3 eq.), TEA (6 µL, 43.0 µmol, 1.5 eq.), the solvent was not deoxygenated and the reaction was carried out under air. **V)** CuI (5.5 mg, 28.9 µmol, 1.0 eq.), TEA (15 µL, 108 µmol, 3.8 eq.), the solvent was not deoxygenated and the reaction was carried out under air. One reaction was carried out based on general procedure **E** with **1.92** (6.7 mg, 28.7 µmol, 1.0 eq.) and **4.24** (10.0 mg, 28.7 µmol, 1.0 eq.) in 0.67 mL THF: **VI)** CuI (5.5 mg, 28.9 µmol, 1.0 eq.), DIPEA (5 µL, 28.7 µmol, 1.0 eq.), NBS (6.1 mg, 34.2 µmol, 1.2 eq.) under argon atmosphere according to general procedure **E**. All reactions were left to stir for 16 h in the dark and the solvent was removed *in vacuo*. For reactions **I**−**IV** the crude solids were completely dissolved in $CDCl_3$ (~0.5 mL), the internal standard dibromomethane (20 µL) was added and ^{1}H NMR spectra of the four samples were recorded. For reactions **V** and **VI** a lower solubility was observed due to side product formation. Therefore, the crude solids were dissolved in $CHCl_3$ (1 mL), aliquots of this solution (30 µL) were mixed in NMR tubes with dibromomethane (10 µL) and $CDCl_3$ (~0.5 mL) and the ^{1}H NMR spectra were recorded. The total amounts of compounds **4.36** and **4.39** in the reaction mixtures were calculated based on the intensity of their BCP bridge proton signals at 2.87 ppm and 3.07 ppm relative to the intensity of the signal of dibromomethane at 4.93 ppm.

1-(3-Iodobicyclo[1.1.1]pentan-1-yl)-4-(8-(4-phenyl)-4,4-difluoro-1,3,5,7-tetramethyl-4-bora-3a,4a-diaza-s-indacene)-1*H*-1,2,3-triazole (**4.36**).

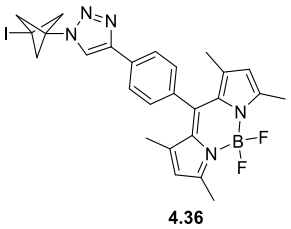
4.36

1-Azido-3-Iodobicyclo[1.1.1]pentane (**1.92**) (13.5 mg, 57.4 µmol), 8-(4-ethynylphenyl)-4,4-difluoro-1,3,5,7-tetramethyl-4-bora-3a,4a-diaza-*s*-indacene (**4.24**) (20 mg, 57.4 µmol), CuI (1.1 mg, 5.78 µmol) and TEA (12 µL, 86.1 µmol) were reacted in THF (0.7 mL) in accordance with general procedure **D**. Column chromatography (SiO_2, *n*-hexane/EtOAc gradient 20:1 to 5:1, v/v) followed by removal of the solvents *in vacuo* afforded compound **4.36** as orange crystals (27.5 mg, 47.2 µmol, 82%); M.p. = 140–174 °C dec.; R_f = 0.26 (SiO_2, *n*-hexane/EtOAc 5:1, v/v); ^{1}H NMR (400 MHz, $CDCl_3$, 25 °C): δ = 1.42 (s, 6H, CH_3), 2.56 (s, 6H, CH_3), 2.88 (s, 6H, CH_2), 5.98 (s, 2H, pyrrolic-H), 7.36 (d, *J* = 8.1 Hz, 2H, Ar-H), 7.80 (s, 1H, triazole-H), 7.96 (d, *J* = 8.1 Hz, 2H, Ar-H) ppm; ^{13}C{^{1}H} NMR (101 MHz, $CDCl_3$, 25 °C): δ = -3.0, 14.7, 54.8, 62.0, 118.5, 121.5, 126.6, 128.8, 131.1, 131.5, 135.2, 141.2, 143.2, 147.1, 155.8 ppm; ^{19}F{^{1}H} NMR (377 MHz, $CDCl_3$, 25 °C): δ = -146.29 (q, *J* = 32.7 Hz) ppm; ^{11}B NMR (128 MHz, $CDCl_3$, 25 °C): δ = 0.77 (t, *J* = 33.3 Hz) ppm; UV-Vis (DCM) λ_{max} [log(ε/M^{-1} cm^{-1})] = 349 [3.89], 474 sh, 504 [4.96]; HRMS (APCI): *m/z* calcd. for [$C_{26}H_{26}BF_2IN_5$] $[M+H]^+$: 584.1293; found 584.1303.

1-(3-Iodobicyclo[1.1.1]pentan-1-yl)-4-(1-pyrenyl)-1*H*-1,2,3-triazole (**4.37**).

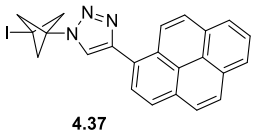
4.37

1-Azido-3-iodobicyclo[1.1.1]pentane (**1.92**) (20.6 mg, 87.6 µmol), 1-ethynylpyrene (**4.27**) (20 mg, 87.6 µmol), CuI (1.7 mg, 8.93 µmol) and TEA (19 µL, 0.138 mmol) were reacted in THF (2 mL) in accordance with general procedure **D**. Column chromatography (SiO_2, *n*-hexane/EtOAc gradient 50:1 to 10:1, v/v) followed by removal of the solvents *in vacuo* afforded compound **4.37** as a white solid (4.2 mg, 9.10 µmol, 10%); M.p. = 201–214 °C dec.; R_f = 0.16 (SiO_2, *n*-hexane/EtOAc 10:1, v/v); ^{1}H NMR (600 MHz, $CDCl_3$, 25 °C): δ = 2.97 (s, 6H, CH_2), 7.90 (s, 1H, triazole-H), 8.02–8.05 (t, *J* = 7.6 Hz, 1H, Ar-H), 8.11 (m, 3H, Ar-H), 8.20–8.23 (m, 4H, Ar-H), 8.65 (d, *J* = 9.2 Hz, 1H, Ar-H) ppm. ^{13}C{^{1}H} NMR (151 MHz, $CDCl_3$, 25 °C): δ = -2.7, 29.9, 53.6, 54.9, 62.2, 121.2, 124.8, 124.9, 124.9, 125.0, 125.2, 125.4, 125.7, 126.3, 127.4, 127.5, 128.1, 128.5, 128.9, 131.0, 131.5, 131.6, 147.7 ppm; UV-Vis (DCM) λ_{max} [log(ε/M^{-1} cm^{-1})] = 273 sh, 283 [4.61], 353 [4.51]; HRMS (ESI): *m/z* calcd. for [$C_{23}H_{17}IN_3$] $[M+H]^+$: 462.0462; found 462.0463.

1-(3-Iodobicyclo[1.1.1]pentan-1-yl)-4-(5-(4-phenyl)-10,20-(4-methylphenyl)-15-phenylporphyrinato)zinc(II)-1*H*-1,2,3-triazole (**4.38**).

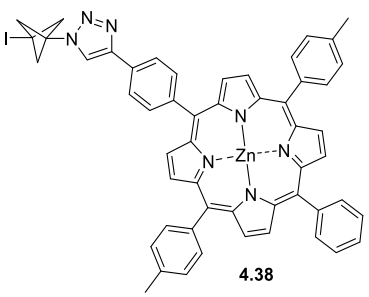

4.38

1-Azido-3-iodobicyclo[1.1.1]pentane (**1.92**) (8.0 mg, 34.0 µmol), [5-(4-ethynylphenyl)-10,20-bis(4-methylphenyl)-15-phenylporphyrinato)]zinc(II) (**4.34**) (25 mg, 34.2 µmol), CuI (0.6 mg, 3.15 µmol) and TEA (6 µL, 43.0 µmol) were reacted in THF (1.3 mL) in accordance with general procedure **D**. Column chromatography (SiO_2, *n*-hexane/EtOAc gradient 20:1 to 10:1, v/v) followed by removal of the solvents *in vacuo* afforded compound **4.38** as purple crystals (23.2 mg, 24.0 µmol, 79%); M.p. > 300 °C; R_f = 0.22 (SiO_2, *n*-hexane/EtOAc 5:1, v/v); ^{1}H NMR (600 MHz, $CDCl_3$, 25 °C): δ = 2.71 (s, 6H, CH_3), 2.97 (s, 1H, CH_2), 7.56 (d, *J* = 7.7 Hz, 4H, Ar-H), 7.73–7.79 (m, 3H, Ar-H), 7.96 (s, 1H, triazole-H), 8.11 (d, *J* = 7.8 Hz, 4H, Ar-H), 8.16 (d, J = 8.0 Hz, 2H, Ar-H), 8.22–8.24 (m, 2H, Ar-H), 8.28 (d, *J* = 8.0 Hz, 2H, Ar-H), 8.95 (d, *J* = 4.6 Hz, 2H, β-H), 8.97–9.00 (m, 6H, β-H); ^{13}C{^{1}H} NMR (151 MHz, $CDCl_3$, 25 °C): δ = -2.7, 21.7, 54.9, 62.1, 118.4, 120.4, 121.3, 121.5, 124.2, 126.7, 127.5, 127.6, 129.5, 131.8, 132.1, 132.2, 132.3, 134.5, 134.6, 135.1, 137.3, 140.0, 143.0, 143.2, 147.9, 150.1, 150.4, 150.5, 150.6 ppm; UV-Vis (DCM) λ_{max} [log(ε/M^{-1} cm^{-1})] = 406 sh, 423 [6.98], 551 [5.56], 592 [4.96] nm; HRMS (ESI): *m/z* calcd. for [$C_{53}H_{39}IN_7Zn$] $[M+H]^+$: 964.1598; found 964.1599.

1-(3-Iodobicyclo[1.1.1]pentan-1-yl)-4-phenyl-1*H*-1,2,3-triazole (**4.14**).[194]

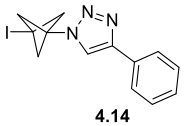

4.14

1-Azido-3-iodobicyclo[1.1.1]pentane (**1.92**) (25 mg, 0.106 mmol), phenylacetylene (**4.35**) (12 µL, 0.106 mmol), CuI (2.0 mg, 10.6 µmol) and TEA (22 µL, 0.159 mmol) were reacted in THF (3 mL) in accordance with general procedure **D**. Column chromatography (SiO_2, *n*-hexane/EtOAc gradient 200:1 to 10:1, v/v) followed by removal of the solvents *in vacuo* afforded compound **4.14** as a white solid (26.5 mg, 78.6 µmol, 74%). Characterisation data is in accordance with the literature;[194] R_f = 0.24 (SiO_2, *n*-hexane/EtOAc 10:1, v/v); ^{1}H NMR (600 MHz, $CDCl_3$, 25 °C): δ = 2.87 (s, 6H, CH_2), 7.32–7.36 (m, 1H, Ar-H), 7.40–7.44 (m, 2H, Ar-H), 7.80–7.82 (m, 2H, Ar-H) ppm; HRMS (ESI): *m/z* calcd. for [$C_{13}H_{13}IN_3$] $[M+H]^+$ 338.0149; found 338.0150.

1-(3-Iodobicyclo[1.1.1]pentan-1-yl)-4-(8-(4-phenyl)-4,4-difluoro-1,3,5,7-tetramethyl-4-bora-3a,4a-diaza-*s*-indacene)-5-iodo-1*H*-1,2,3-triazole (**4.39**).

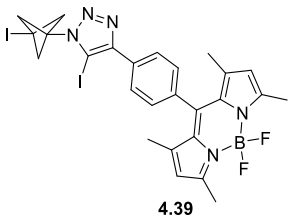
4.39

1-Azido-3-Iodobicyclo[1.1.1]pentane (**1.92**) (6.8 mg, 28.7 µmol), 8-(4-ethynylphenyl)-4,4-difluoro-1,3,5,7-tetramethyl-4-bora-3a,4a-diaza-*s*-indacene (**4.24**) (10.0 mg, 28.7 µmol), CuI (5.5 mg, 28.9 µmol), NBS (6.1 mg, 34.3 µmol) and DIPEA (5 µL, 28.7 µmol) were reacted in THF (2 mL) in accordance with general procedure **E**. Column chromatography (SiO_2, *n*-hexane/ DCM gradient 2:1 to 1:1, v/v) followed by removal of the solvents *in vacuo* afforded compound **4.39** as an orange solid (2.8 mg, 3.95 µmol, 14%); M.p. = 212–236 °C dec.; R_f = 0.33 (SiO_2, *n*-hexane/EtOAc 5:1, v/v); ^{1}H NMR (600 MHz, $CDCl_3$, 25 °C): δ = 1.43 (s, 6H, CH_3), 2.56 (s, 6H, CH_3), 3.07 (s, 6H, CH_2), 5.99 (s, 2H, pyrrolic-H), 7.39 (d, *J* = 8.2 Hz, 2H, Ar-H), 8.05 (d, *J* = 8.2 Hz, 2H, Ar-H) ppm; ^{13}C{^{1}H} NMR (151 MHz, $CDCl_3$, 25 °C): δ = -1.7, 14.7, 14.8, 56.9, 62.4, 73.1, 121.5, 128.4, 128.5, 130.8, 131.5, 135.6, 141.1, 143.2, 149.9, 155.9 ppm; ^{19}F{^{1}H} NMR (377 MHz, $CDCl_3$, 25 °C): δ = -146.28 (q, *J* = 33.0 Hz) ppm. ^{11}B NMR (128 MHz, $CDCl_3$, 25 °C): δ = 0.78 (t, *J* = 33.3 Hz) ppm; UV-Vis (DCM) λ_{max} [log(ε/M^{-1} cm^{-1})] = 348 [4.08], 477 sh, 504 [5.10] nm; HRMS (ESI): *m/z* calcd. for [$C_{26}H_{23}BF_2I_2N_5$] [M-H]$^-$: 708.0114; found 708.0097.

1-(3-Iodobicyclo[1.1.1]pentan-1-yl)-4-(1-pyrenyl)-5-iodo-1*H*-1,2,3-triazole (**4.40**).

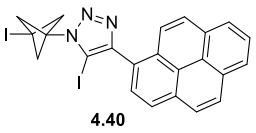
4.40

1-Azido-3-iodobicyclo[1.1.1]pentane (**1.92**) (11.2 mg, 47.8 µmol), 1-ethynylpyrene (**4.27**) (11.8 mg, 47.8 µmol), CuI (9.1 mg, 47.8 µmol) and TEA (19 µL, 0.138 mmol) NBS (10.2 mg, 57.3 µmol) and DIPEA (9 µL, 51.7 µmol) were reacted in 2 mL THF in accordance with general procedure **E**. Column chromatography (SiO_2, *n*-hexane/EtOAc gradient 200:1 to 40:1, v/v), removal of the solvents *in vacuo* and trituration with *n*-hexane and toluene afforded compound **4.40** as a yellow solid (4.8 mg, 8.17 µmol, 17%); M.p. = 196–201 °C dec.; R_f = 0.24 (SiO_2, *n*-hexane/EtOAc 10:1, v/v); ^{1}H NMR (400 MHz, $CDCl_3$, 25 °C): δ = 3.15 (s, 6H, CH_2), 8.02–8.07 (m, 2H, Ar-H), 8.09 (s, 2H, Ar-H), 8.10–8.17 (m, 2H, Ar-H), 8.20–8.27 (m, 3H, Ar-H) ppm; ^{13}C{^{1}H} NMR (101 MHz, $CDCl_3$, 25 °C): δ = -1.5, 53.6, 56.9, 62.5, 124.2, 124.6, 124.7, 125.1, 125.3, 125.6, 125.7, 126.4, 127.5, 128.3, 128.4, 128.5, 129.9, 131.0, 131.4, 132.1, 152.3 ppm; UV-Vis (DCM) λ_{max} [log(ε/M^{-1} cm^{-1})] = 271 sh, 281 [4.67], 336 sh, 348 [4.52] nm; HRMS (ESI): m/z calcd. for [$C_{23}H_{16}I_2N_3$] [M+H]+: 587.9428; found 587.9434.

1-(3-Iodobicyclo[1.1.1]pentan-1-yl)-4-(5-(4-phenyl)-10,20-(4-methylphenyl)-15-phenylporphyrinato)zinc(II)-5-iodo-1*H*-1,2,3-triazole (**4.41**).

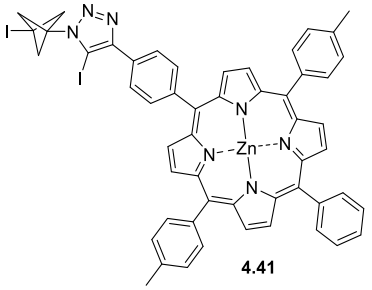

4.41

1-Azido-3-iodobicyclo[1.1.1]pentane (**1.92**) (8.4 mg, 35.6 µmol), [5-(4-ethynylphenyl)-10,20-bis(4-methylphenyl)-15-phenylporphyrinato)]zinc(II) (**4.34**) (26.0 mg, 35.6 µmol), CuI (6.8 mg, 35.7 µmol), NBS (7.6 mg, 42.7 µmol) and DIPEA (5 µL, 28.7 µmol) were reacted in 1.4 mL THF in accordance with general procedure **E**. Column chromatography (SiO_2, *n*-hexane/EtOAc gradient 20:1 to 10:1, v/v) followed by removal of the solvents *in vacuo* afforded compound **4.41** as purple crystals (7.5 mg, 6.87 µmol, 19%); M.p. = 262–282 °C dec.; R_f = 0.32 (SiO_2, *n*-hexane/EtOAc 5:1, v/v); ^{1}H NMR (600 MHz, $CDCl_3$, 25 °C): δ = 2.70 (s, 6H, CH_3), 3.15 (s, 6H, CH_2), 4.17 (br s, 2H, pyridine-H), 5.96–6.01 (m, 2H, pyridine-H), 6.70 (t, *J* = 7.4 Hz, 1H, pyridine-H), 7.53 (d, *J* = 7.4 Hz, 4H, Ar-H), 7.70–7.75 (m, 3H, Ar-H), 8.08 (d, *J* = 7.5 Hz, 4H, Ar-H), 8.20 (d, *J* = 7.1 Hz, 2H, Ar-H), 8.24 (d, *J* = 7.8 Hz, 2H, Ar-H), 8.30 (d, *J* = 7.8 Hz, 2H, Ar-H), 8.87 (d, *J* = 4.4 Hz, 2H, β-H), 8.90–8.93 (m, 6H, β-H) ppm; ^{13}C{^{1}H} NMR (151 MHz, $CDCl_3$, 25 °C): δ = -1.3, 21.7, 56.96, 62.5, 72.9, 119.8, 120.9, 121.0, 122.7, 125.7, 126.5, 127.2, 127.3, 128.8, 129.0, 131.1, 131.6, 131.8, 131.9, 132.0, 134.6, 134.7, 134.9, 135.9, 137.0, 139.5, 140.5, 143.6, 144.2, 145.1, 150.0, 150.2, 150.4, 150.4, 150.9 ppm; UV-Vis (DCM) λ_{max} [log(ε/M^{-1} cm^{-1})] = 403 sh, 423 [5.73], 551 [4.31], 592 [3.73] nm; HRMS (APCI): *m/z* calcd. for [$C_{53}H_{38}I_2N_7Zn$] $[M+H]^+$: 1090.0564; found 1090.0537.

1-(3-Iodobicyclo[1.1.1]pentan-1-yl)-4-phenyl-5-iodo-1*H*-1,2,3-triazole (**4.45**).

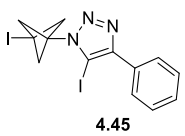

4.45

1-Azido-3-iodobicyclo[1.1.1]pentane (**1.92**) (11.2 mg, 47.8 µmol), phenylacetylene (**4.35**) (6 µL, 54.6 µmol), CuI (9.1 mg, 47.8 µmol), NBS (10.2 mg, 57.3 µmol) and DIPEA (9 µL, 51.7 µmol) were reacted in THF (2 mL) in accordance with general procedure **E**. Column chromatography (SiO_2, *n*-hexane/EtOAc gradient 200:1 to 20:1, v/v) followed by removal of the solvents *in vacuo* afforded **4.45** as an off-white solid (1.5 mg, 3.24 µmol, 7%); M.p. = 182 °C dec.; R_f = 0.42 (SiO_2, *n*-hexane/EtOAc 10:1, v/v); ^{1}H NMR (600 MHz, $CDCl_3$, 25 °C): δ = 3.06 (s, 6H, CH_2), 7.41 (t, J = 7.3 Hz, 1H, Ar-H), 7.46 (t, J = 7.6 Hz, 2H, Ar-H), 7.86 (d, *J* = 7.4 Hz, 2H, Ar-H) ppm; ^{13}C{^{1}H} NMR (151 MHz, $CDCl_3$, 25 °C): δ = -1.4, 56.8, 62.4, 72.6, 127.9, 128.7, 128.9, 123.0, 150.8 ppm; HRMS (APCI): *m/z* calcd. for [$C_{13}H_{12}I_2N_3$] $[M+H]^+$: 463.9115; found 463.9118.

1-(3-Iodobicyclo[1.1.1]pentan-1-yl)-4-(4-pyridinyl)-5-iodo-1H-1,2,3-triazole (**4.46**).

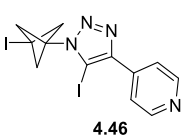
4.46

1-Azido-3-iodobicyclo[1.1.1]pentane (**1.92**) (14.1 mg, 60.0 µmol), 4-ethynylpyridine (**4.44**) (6.2 mg, 60.1 µmol), CuI (11.5 mg, 60.3 µmol), NBS (12.8 mg, 71.9 µmol) and DIPEA (8 µL, 45.9 µmol) were reacted in THF (2 mL) in accordance with general procedure **E**. The crude product was purified by column chromatography (SiO_2, *n*-hexane/EtOAc gradient 5:1 to 2:1, v/v). The isolated product was dissolved in DCM and washed with saturated aqueous $NaHCO_3$ solution (2 ×) and H_2O (1 ×). After removal of the solvents *in vacuo* compound **4.46** was obtained as an off-white solid (18.3 mg, 38.8 µmol, 66%); M.p. = 136–139 °C dec.; R_f = 0.40 (SiO_2, *n*-hexane/EtOAc 1:1, v/v); ^{1}H NMR (600 MHz, $CDCl_3$, 25 °C): δ = 3.07 (s, 6H, CH_2), 7.89 (br d, *J* = 3.7 Hz, 2H, Ar-H), 8.73 (br s, 2H, Ar-H) ppm; ^{13}C{^{1}H} NMR (151 MHz, $CDCl_3$, 25 °C): δ = -1.9, 56.8, 62.4, 73.6, 121.6, 137.6, 147.8, 150.4 ppm; HRMS (ESI): *m/z* calcd. for $[C_{12}H_{11}I_2N_4]$ $[M+H]^+$: 464.9068; found 464.9069.

1-(3-Iodobicyclo[1.1.1]pentan-1-yl)-4-(8-(4-phenyl)-4,4-difluoro-1,3,5,7-tetramethyl-4-bora-3a,4a-diaza-*s*-indacene)-5-(8-(4-phenylethynyl)-4,4-difluoro-1,3,5,7-tetramethyl-4-bora-3a,4a-diaza-*s*-indacene)-1*H*-1,2,3-triazole (**4.49**).

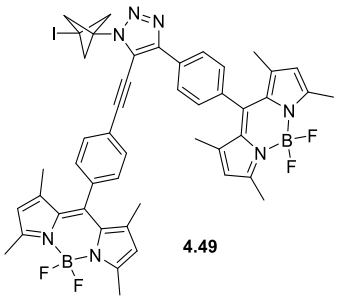
4.49

1-Azido-3-iodobicyclo[1.1.1]pentane (**1.92**) (12.0 mg, 51.1 µmol), 8-(4-ethynylphenyl)-4,4-difluoro-1,3,5,7-tetramethyl-4-bora-3a,4a-diaza-*s*-indacene (**4.24**) (42.0 mg, 121 µmol), CuI (2.1 mg, 11.0 µmol) and $Pd(PPh_3)_2Cl_2$ (3.9 mg, 5.56 µmol) were reacted in a mixture of THF (1 mL) and TEA (1 mL) in accordance with general procedure **F**. Column chromatography (1. SiO_2, *n*-hexane/EtOAc gradient 10:1 to 5:1, v/v; 2. SiO_2, neat DCM and DCM/EtOAc 100:1, v/v) followed by removal of the solvents *in vacuo* afforded compound **4.49** as an orange solid (trace amount); ^{1}H NMR (400 MHz, $CDCl_3$, 25 °C): δ = 1.43 (s, 6H, CH_3), 1.43 (s, 6H, CH_3), 2.54 (s, 6H, CH_3), 2.55 (s, 6H, CH_3), 3.04 (s, 6H, CH_2), 5.97 (s, 2H, pyrrolic-H), 6.00 (s, 2H, pyrrolic-H), 7.41 (dd, *J* = 8.0, 1.8 Hz, 4H, Ar-H), 7.67 (d, *J* = 8.1 Hz, 2H, Ar-H), 8.32 (d, *J* = 8.4 Hz, 2H, Ar-H) ppm; HRMS (MALDI): *m/z* calcd. for $[C_{47}H_{42}B_2F_4IN_7]$ $[M]^+$: 929.2669; found 929.2646.

1-(3-Iodobicyclo[1.1.1]pentan-1-yl)-4-(1-pyrenyl)-5-(1-pyrenylethynyl)-1*H*-1,2,3-triazole (**4.50**)

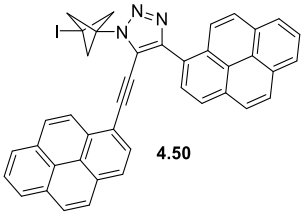

1-Azido-3-iodobicyclo[1.1.1]pentane (**1.92**) (25.0 mg, 0.106 mmol), 1-ethynylpyrene (**4.27**) (57.5 mg, 0.254 mmol), CuI (4.0 mg, 21.2 µmol) and $Pd(PPh_3)_2Cl_2$ (7.4 mg, 10.6 µmol) were reacted in a mixture of THF (0.6 mL) and TEA (0.6 mL) in accordance with general procedure **F**. Column chromatography (1. SiO_2, *n*-hexane/EtOAc 20:1, v/v, 2. SiO_2, *n*-hexane/EtOAc 100:3, v/v) followed by removal of the solvents *in vacuo* afforded compound **4.50** as a light yellow solid (5.4 mg, 7.88 µmol, 7%); M.p. = 200–212 °C dec.; R_f = 0.21 (SiO_2, *n*-hexane/EtOAc 10:1, v/v); ^{1}H NMR (400 MHz, $CDCl_3$, 25 °C): δ = 3.24 (s, 6H, CH_2), 7.33 (d, *J* = 9.1 Hz, 1H, Ar-H), 7.77 (d, *J* = 9.1 Hz, 1H, Ar-H), 7.96–8.12 (m, 7H, Ar-H), 8.15–8.23 (m, 5H, Ar-H), 8.29 (d, *J* = 7.5 Hz, 1H, Ar-H), 8.34 (d, *J* = 7.9 Hz, 1H, Ar-H), 8.49 (d, *J* = 7.9 Hz, 1H, Ar-H), 8.68 (d, *J* = 9.3 Hz, 1H, Ar-H) ppm; ^{13}C{^{1}H} NMR (151 MHz, $CDCl_3$, 25 °C): δ = -1.6, 55.5, 62.6, 80.3, 101.9, 115.2, 119.9, 124.1, 124.4, 124.4, 124.6, 124.7, 124.9, 124.9, 125.3, 125.6, 125.6, 125.7, 126.2, 126.4, 126.6, 127.2, 127.6, 128.1, 128.5, 128.9, 129.1, 129.2, 129.5, 130.8, 131.2, 131.3, 131.5, 132.2, 132.2, 132.4, 149.9 ppm; UV-Vis (DCM) λ_{max} [log(ε/M^{-1} cm^{-1})] = 282 [4.74], 297 sh, 352 [4.77], 374 sh, 398 sh; HRMS (APCI): *m/z* calcd. for $[C_{41}H_{25}IN_3]$ $[M+H]^+$: 686.1088; found 686.1101.

1-(3-Iodobicyclo[1.1.1]pentan-1-yl)-4-(5-(4-phenyl)-10,20-(4-methylphenyl)-15-phenylporphyrinato)zinc(II)-5-(5-(4-phenylethynyl)-10,20-(4-methylphenyl)-15-phenylporphyrinato)zinc(II)-1*H*-1,2,3-triazole (**4.51**).

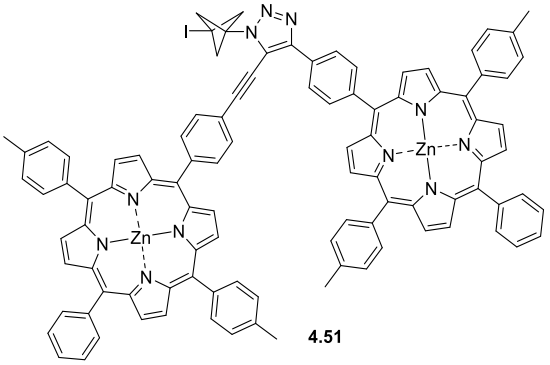

1-Azido-3-iodobicyclo[1.1.1]pentane (**1.92**) (6.4 mg, 27.5 µmol), [5-(4-ethynylphenyl)-10,20-bis(4-methylphenyl)-15-phenylporphyrinato)]zinc(II) (**4.34**) (44.0 mg, 60.3 µmol), CuI (1.0 mg, 5.25 µmol) and $Pd(PPh_3)_2Cl_2$ (2.0 mg, 2.85 µmol) were reacted in a mixture of THF (0.5 mL) and TEA (0.5 mL) in accordance with general procedure **F**. Column chromatography (SiO_2, DCM/*n*-hexane gradient 3:7, 2:3, v/v, neat DCM, DCM/EtOAc 10:1, v/v) and preparative TLC (SiO_2, DCM/*n*-hexane 4:1, v/v) followed by removal of the solvents *in vacuo* afforded compound **4.51** as a purple solid (trace amount); ^{1}H NMR (400 MHz, $CDCl_3$, 25 °C) δ = 2.66 (s, 6H, CH_3), 2.67 (s, 6H, CH_3), 3.27 (s, 6H, CH_2), 7.48–7.53 (m, 4H, Ar-H), 7.70–7.76 (m, 4H, Ar-H), 8.02–8.09 (m, 6H, Ar-H), 8.16–

8.20 (m, 2H, Ar-H), 8.28 (d, *J* = 8.4 Hz, 2H, Ar-H), 8.41 (d, *J* = 8.1 Hz, 2H, Ar-H), 8.69 (d, *J* = 8.3 Hz, 2H, Ar-H), 8.89–8.96 (m, 12H, β-H), 8.99 (d, *J* = 4.9 Hz, 2H, β-H), 9.05 (d, *J* = 4.7 Hz, 2H, β-H) ppm; HRMS (MALDI): *m/z* calcd. for $[C_{101}H_{68}IN_{11}Zn_2]$ $[M]^+$: 1689.3287; found 1689.3296.

1-(3-Iodobicyclo[1.1.1]pentan-1-yl)-4-phenyl-5-(phenylethynyl)-1H-1,2,3-triazole (**4.52**).

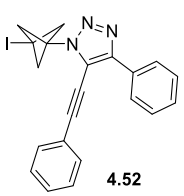

1-Azido-3-Iodobicyclo[1.1.1]pentane (**1.92**) (20 mg, 85.1 µmol), phenylacetylene (**4.35**) (20.9 mg, 0.205 mmol), CuI (3.2 mg, 16.8 µmol) and $Pd(PPh_3)_2Cl_2$ (6.0 mg, 8.55 µmol) were reacted in a mixture of THF (1 mL) and TEA (1 mL) in accordance with general procedure **F**. Column chromatography (SiO_2, *n*-hexane/EtOAc 40:1, v/v) followed by removal of the solvents *in vacuo* afforded compound **4.52** as a white solid (3.8 mg, 8.69 µmol, 10%); M.p. = 173–176 °C; R_f = 0.62 (SiO_2, *n*-hexane/EtOAc 10:1, v/v); ^{1}H NMR (600 MHz, $CDCl_3$, 25 °C): δ = 3.03 (s, 6H, CH_2), 7.38 (t, J = 7.3 Hz, 1H, Ar-H), 7.43–7.50 (m, 5H, Ar-H), 7.55–7.59 (m, 2H, Ar-H), 8.15 (d, J = 7.5 Hz, 2H, Ar-H) ppm; ^{13}C{^{1}H} NMR (151 MHz, $CDCl_3$, 25 °C): δ = -1.7, 55.2, 62.3, 75.6, 102.4, 116.3, 121.4, 126.5, 128.9, 128.9, 129.0, 130.1, 130.1, 131.6, 148.4 ppm; HRMS (ESI): *m/z* calcd. for $[C_{21}H_{17}IN_3]$ $[M+H]^+$: 438.0462; found 438.0456.

1-(3-Iodobicyclo[1.1.1]pentan-1-yl)-4-(4-pyridinyl)-5-(4-pyridinylethynyl)-1,2,3-triazole (**4.53**)

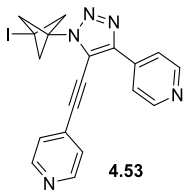

1-Azido-3-iodo[1.1.1]bicyclopentane (**1.92**) (20 mg, 85.0 µmol), 4-ethynylpyridine (**4.44**) (21 mg, 204 µmol), CuI (3.2 mg, 17.2 µmol) and $Pd(PPh_3)_2Cl_2$ (6.0 mg, 8.50 µmol) were reacted in a mixture of THF (0.4 mL) and TEA (0.4 mL) in accordance with general procedure **F**. Column chromatography (SiO_2, *n*-hexane/EtOAc gradient 2:1 to 1:2, v/v) followed by removal of the solvents *in vacuo* afforded compound **4.53** as a white solid (9.9 mg, 22.5 µmol, 27%); M.p. = 159 °C dec.; R_f = 0.19 (SiO_2, *n*-hexane/EtOAc 1:2, v/v); ^{1}H NMR (400 MHz, $CDCl_3$, 25 °C): δ = 3.02 (s, 6H, CH_2), 7.44 (dd, *J* = 4.4, 1.6 Hz, 2H, Ar-H), 8.00 (dd, *J* = 4.6, 1.6 Hz, 2H, Ar-H), 8.73 (dd, *J* = 4.6, 1.6 Hz, 2H, Ar-H), 8.77 (dd, *J* = 4.4, 1.6 Hz, 2H, Ar-H) ppm; ^{13}C{^{1}H} NMR (101 MHz, $CDCl_3$, 25 °C): δ = -2.7, 55.2, 62.3, 78.6, 100.5, 116.9, 120.4, 125.06, 128.8, 137.1, 146.5, 150.6, 150.7 ppm; HRMS (APCI): *m/z* calcd. for $[C_{19}H_{15}IN_5]$ $[M+H]^+$: 440.0367; found 440.0369.

1-(3-Iodobicyclo[1.1.1]pentan-1-yl)-4-(4-pyridinyl)-1*H*-1,2,3-triazole (**4.56**).

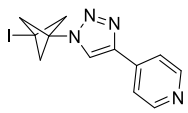
4.56

1-Azido-3-iodobicyclo[1.1.1]pentane (**1.92**) (20 mg, 85.0 µmol), 4-ethynypyridine (**4.44**) (21 mg, 204 µmol), CuI (3.2 mg, 17.2 µmol) and $Pd(PPh_3)_2Cl_2$ (6.0 mg, 8.50 µmol) were reacted in a mixture of THF (0.4 mL) and TEA (0.4 mL) in accordance with general procedure **F**. Column chromatography (SiO_2, *n*-hexane/EtOAc gradient 2:1 to 1:2, v/v) followed by removal of the solvents *in vacuo* afforded compound **4.56** as a white solid (9.0 mg, 26.6 µmol, 31%); M.p. = 216–222 °C (dec.). R_f = 0.33 (SiO_2, *n*-hexane/EtOAc 1:2, v/v); ^{1}H NMR (600 MHz, $CDCl_3$, 25 °C): δ = 2.88 (s, 6H, CH_2), 7.71 (br d, *J* = 3.7 Hz, 2H, Ar-H), 7.85 (s, 1H, triazole-H), 8.69 (s, 2H, Ar-H) ppm; ^{13}C{^{1}H} NMR (151 MHz, $CDCl_3$, 25 °C): δ = -3.2, 54.8, 62.0, 119.5, 120.2, 137.7, 145.4, 150.6 ppm; HRMS (APCI): *m/z* calcd. for $[C_{12}H_{12}IN_4]$ $[M+H]^+$ 339.0101; found 339.0105.

6.5 Chapter 5 – Synthesis of Bicyclo[1.1.1]pentane-Linked Porphyrin Arrays as Excitation Energy Transfer Model Systems

(5-Bromo-10,20-diphenyl-15-pentafluorophenylporphyrinato)zinc(II) (**5.23**)

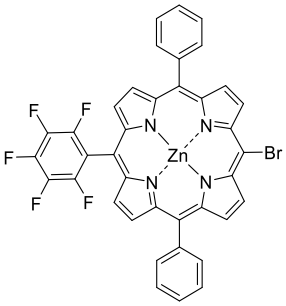
5.23

5-Bromo-10,20-diphenyl-15-pentafluorophenylporphyrin **5.22** was synthesis according to a modified literature procedure.[370] In a round-bottomed flask, 5-bromo-10,20-diphenyl-15-pentafluorophenylporphyrin (**5.22**) (269 mg, 0.380 mmol) was dissolved in DCM (30 mL) and $Zn(OAc)_2{\cdot}2H_2O$ (250 mg, 1.14 mmol), dissolved in MeOH (10 mL), was added. The mixture was stirred at 40 °C for 1 h. The solvent was removed *in vacuo*, the crude solids were dissolved in DCM and passed through a SiO_2 pad, eluting with *n*-hexane/DCM 1:1 (v/v). After removal of the solvents *in vacuo* compound **5.23** was isolated as purple crystals (275 mg, 0.357 mmol, 94%); M.p. = 273 °C; R_f = 0.32 (SiO_2, *n*-hexane/DCM 1:1, v/v); ^{1}H NMR (400 MHz, $CDCl_3$, 25 °C) δ = 7.74–7.82 (m, 6H, Ar-H), 8.16–8.21 (m, 4H, Ar-H), 8.83 (d, 2H, *J* = 4.7 Hz, β-H), 8.98 (dd, 4H, *J* = 6.1, 4.8 Hz, β-H), 9.74 (d, 2H, *J* = 4.7 Hz, β-H) ppm; ^{13}C{^{1}H} NMR (151 MHz, $CDCl_3$, 25 °C): δ = 102.1, 106.6, 117.2, 122.6, 126.9, 128.0, 130.2, 133.6, 134.1, 134.6, 137.6 (d, 2C, J_{CF} = 253.1 Hz), 141.9 (d, 1C, J_{CF} = 250.0 Hz), 142.1, 146.7 (d, 2C, J_{CF} = 237.5 Hz), 149.9, 150.1, 150.8, 151.4 ppm; ^{19}F{^{1}H} NMR (377 MHz, $CDCl_3$, 25 °C): δ = -162.25 (td, 2F, *J* = 23.8, 8.3 Hz), -152.96 (t, 1F, *J* = 20.9 Hz), -137.10 (dd, 2F, *J* = 24.1, 8.2 Hz) ppm; UV-Vis (DCM) λ_{max}

[log(ε/M^{-1} cm^{-1})] = 422 [5.76], 553 [4.34], 592 [3.66] nm; HRMS (MALDI): *m/z* calcd. for $C_{38}H_{18}N_4F_5ZnBr$ $[M]^+$: 767.9926; found 767.9913.

(5-(Trimethylsilyl)ethynyl-10,20-diphenyl-15-pentafluorophenylporphyrinato)zinc(II) (**5.25**)

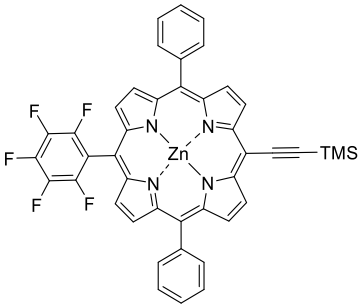

5.25

In a Schlenk tube, (5-bromo-10,20-diphenyl-15-pentafluorophenylporphyrinato)zinc(II) (**5.23**) (200 mg, 0.259 mmol) was dissolved in a mixture of anhydrous THF (3 mL) and anhydrous triethylamine (3 mL) and the mixture was purged with argon for 15 min. $Pd(PPh_3)_2Cl_2$ (18.2 mg, 25.9 µmol) and CuI (9.9 mg, 52.0 µmol) were added and the mixture was purged with argon for 3 min. At the end, trimethylsilylacetylene (0.140 mL, 0.984 mmol) was added and argon was bubbled for another 3 min. The mixture was stirred under argon at r.t. for 4 h. The solvent was removed *in vacuo* and the crude solids were purified by silica gel column chromatography (SiO_2, *n*-hexane/DCM 1:1, v/v). Removal of the solvents *in vacuo* afforded compound (**5.25**) as purple crystals (184 mg, 0.233 mmol, 90%); M.p. > 300 °C; R_f = 0.25 (SiO_2, *n*-hexane/DCM 1:1, v/v); ^{1}H NMR (600 MHz, $CDCl_3$, 25 °C): δ = 0.63 (s, 9H, TMS-C*H*$_3$), 7.76–7.82 (m, 6H, Ar-H), 8.19–8.22 (m, 4H, Ar-H), 8.81 (d, 2H, *J* = 4.6 Hz, β-H), 8.97 (d, 2H, *J* = 4.6 Hz, β-H), 9.00 (d, 2H, *J* = 4.6 Hz, β-H), 9.79 (d, 2H, *J* = 4.6 Hz, β-H); ^{13}C{^{1}H} NMR (151 MHz, $CDCl_3$, 25 °C): δ = 0.5, 101.8, 102.5, 103.0, 107.3, 117.2, 122.7, 126.9, 128.0, 130.1, 131.8, 133.3, 133.6, 134.6, 137.6 (d, 2 C, J_{CF} = 251.7 Hz), 141.9 (d, 1 C, J_{CF} = 253.7 Hz), 146.7 (d, 2 C, J_{CF} = 233.7 Hz), 142.2, 149.3, 150.8, 150.9, 152.7 ppm; ^{19}F{^{1}H} NMR (377 MHz, $CDCl_3$, 25 °C): δ = -162.32 (td, 2F, *J* = 23.8, 8.3 Hz); -153.06 (t, 1F, *J* = 20.9 Hz); -137.15 (dd, 2F, *J* = 24.1, 8.3 Hz) ppm; UV-Vis (DCM) λ_{max} [log(ε/M^{-1} cm^{-1})] = 430 [5.80], 562 [4.36], 603 [4.28] nm; HRMS (APCI): *m/z* calcd. for $C_{43}H_{28}N_4F_5ZnSi$ $[M+H]^+$: 787.1289; found 787.1270.

(5-Ethynyl-10,20-diphenyl-15-pentafluorophenylporphyrinato)zinc(II) (**5.26**)

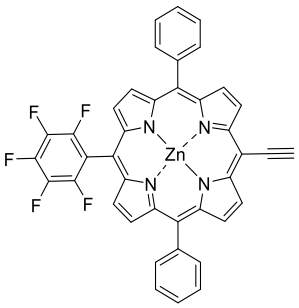

5.26

In a Schlenk flask, (5-(trimethylsilyl)ethynyl-10,20-diphenyl-15-pentafluorophenylporphyrinato)zinc(II) (**5.25**) (146 mg, 0.185 mmol) was dissolved anhydrous DCM (15 mL). A 1 M solution of TBAF in THF (0.21 mL, 0.210 mmol) was added and the mixture was stirred under argon at r.t. for 1.5 h. DCM (20 mL) was added to the reaction mixture and the mixture was washed with water (2 ×) and brine (1 ×). The organic layer was dried over $MgSO_4$, filtered and the solvent was removed *in vacuo*. Column chromatography (SiO_2, *n*-hexane/DCM 1:1, v/v) followed by removal of the solvents *in vacuo* afforded compound (**5.26**) as purple crystals (95 mg, 0.133 mmol, 72%); M.p. > 300 °C; R_f = 0.5 (SiO_2, *n*-hexane/DCM 2:1, v/v); ^{1}H NMR (600 MHz, $CDCl_3$, 25 °C): δ = 3.88 (s, 1H, acetylene-H), 7.74–7.85 (m, 6H, Ar-H), 8.20 (d, 4H, *J* = 6.8 Hz, Ar-H), 8.84 (d, 2H, *J* = 4.5 Hz, β-H), 8.95 (d, 2H, *J* = 4.5 Hz, β-H), 8.99 (d, 2H, *J* = 4.5 Hz, β-H), 9.56 (d, 2H, *J* = 4.5 Hz, β-H) ppm; ^{13}C{^{1}H} NMR (151 MHz, $CDCl_3$, 25 °C): δ = 84.1, 85.7, 99.9, 103.2, 122.6, 126.9, 128.0, 130.2, 131.5, 133.4, 133.7, 134.6, 137.6 (d, 2C, J_{CF} = 253.2 Hz), 142.0 (d, 1C, J_{CF} = 259.6 Hz), 142.2, 146.7 (d, 2C, J_{CF} = 248.9 Hz), 149.3, 150.7, 151.0, 152.6 ppm; ^{19}F{^{1}H} NMR (377 MHz, $CDCl_3$): δ = -162.28 (td, 2F, *J* = 23.9, 8.2 Hz), -152.99 (t, 1F, *J* = 20.9 Hz), -137.13 (dd, 2F, *J* = 24.0, 8.2 Hz) ppm; UV-Vis (DCM) λ_{max} [log(ε/M^{-1} cm^{-1})] = 427 [5.73], 559 [4.32], 598 [4.11] nm; HRMS (APCI): *m/z* calcd. for $C_{40}H_{20}N_4F_5Zn$ $[M+H]^+$: 715.0894; found 715.0883.

(5-(4,4,5,5-Tetramethyl-1,3,2-dioxaborolan-2-yl)-10,20-diphenyl-15-pentafluorophenylporphyrinato)zinc(II) (**5.24**)

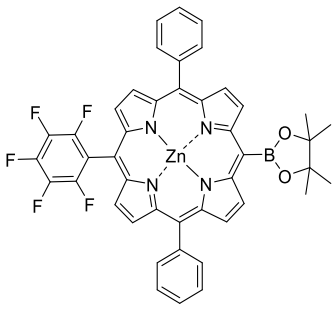

5.24

In a Schlenk tube, (5-bromo-10,20-diphenyl-15-pentafluorophenylporphyrinato)zinc(II) (**5.23**) (95 mg, 0.123 mmol) was dissolved in anhydrous 1,2-dichloroethane (5 mL), triethylamine (0.34 mL, 2.47 mmol) and 4,4,5,5-tetramethyl-1,3,2-dioxaborolane (0.36 mL, 2.47 mmol) were added and the mixture was purged with argon for 15 min. $Pd(PPh_3)_2Cl_2$ (17.3 mg, 24.6 µmol) was added and the mixture was purged with argon for another 5 min. The reaction mixture was stirred under argon at 84 °C for 3 h. The solvent was removed *in vacuo*, the crude solids were dissolved in DCM and passed through a silica gel pad, eluting with DCM. The crude product was further purified by column chromatography (SiO_2, *n*-hexane/DCM 2:1, 1:1, 1:2, v/v) and the solvents were removed *in vacuo* to afford compound

5.24 as pink crystals (58 mg, 70.9 µmol, 58%). M.p. > 300 °C; R_f = 0.42 (SiO_2, *n*-hexane/DCM 1:3, v/v); ^{1}H NMR (400 MHz, $CDCl_3$, 25 °C): δ = 1.87 (s, 12H, boryl-C*H*$_3$), 7.76–7.82 (m, 6H, Ar-H), 8.20–8.27 (m, 4H, Ar-H), 8.90 (d, 2H, *J* = 4.6 Hz, β-H), 9.05 (d, 2H, *J* = 4.7 Hz, β-H), 9.11 (d, 2H, *J* = 4.7 Hz, β-H), 9.94 (d, 2H, *J* = 4.7 Hz, β-H) ppm; ^{13}C{^{1}H} NMR (151 MHz, $CDCl_3$, 25 °C): δ = 25.5, 85.6, 102.7, 117.5, 121.7, 126.8, 127.8, 129.9, 133.3, 133.5, 133.5, 134.7, 137.5 (d, *J* = 247.5 Hz), 141.90 (d, 1C, J_{CF} = 258.1 Hz), 146.7 (d, 2C, J_{CF} = 244.7 Hz), 142.7, 148.7, 150.7, 150.8, 154.3 ppm; ^{19}F{^{1}H} NMR (377 MHz, $CDCl_3$): δ = -162.48 (td, 2F, *J* = 24.0, 8.4 Hz), -153.29 (t, 1F, *J* = 20.9 Hz), -137.08 (dd, 2F, *J* = 24.0, 7.6 Hz) ppm; UV-Vis (DCM) λ_{max} [log(ε/M^{-1} cm^{-1})] = 417 [5.77], 548 [4.34], 584 [3.88] nm; HRMS (APCI): *m/z* calcd. for $C_{44}H_{31}BN_4O_2F_5Zn$ $[M+H]^+$: 817.1754; found 817.1749.

1,3-Bis(4-((15-pentafluorophenyl-10,20-diphenylporphyrinato)zinc(II)-5-yl)phenyl)bicyclo[1.1.1]pentane (**5.27**)

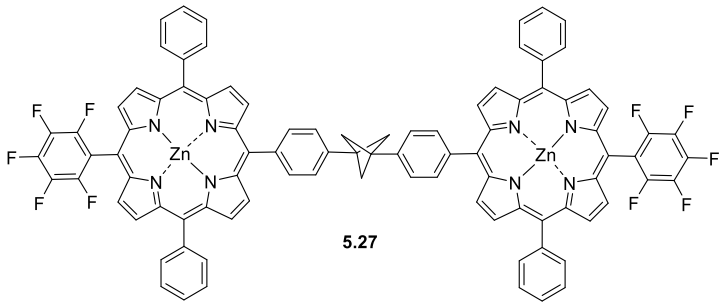

5.27

In a Schlenk tube, [5-(4,4,5,5-Tetramethyl-1,3,2-dioxaborolan-2-yl)-10,20-diphenyl-15-pentafluorophenylporphyrinato]zinc(II) (**5.24**) (58 mg, 70.9 µmol) and 1,3-bis(4-iodophenyl)bicyclo[1.1.1]pentane (16.7 mg, 35.5 µmol) were dissolved in anhydrous DMF (3 mL) and the mixture was purged with argon for 15 min. $Pd(PPh_3)_4$ (8.2 mg, 7.09 µmol) and anhydrous K_2CO_3 (58.7 mg, 0.425 mmol) were added and the mixture was purged with argon for another 5 min. The reaction mixture was stirred under argon at 100 °C for 16 h. The solvent was removed *in vacuo* and crude solids were purified by column chromatography (SiO_2, *n*-hexane/DCM gradient 3:1 to 1:1, v/v). After removal of the solvents *in vacuo*, compound **5.27** was obtained as purple crystals (16.3 µmol, 26 mg, 46%); M.p. > 300 °C; R_f = 0.63 (SiO_2, *n*-hexane/DCM 3:1, v/v); ^{1}H NMR (400 MHz, $CDCl_3$, 25 °C): δ = 2.78 (s, 6H, C*H*$_2$), 7.73–7.66 (m, 16H, Ar-H), 8.20–8.13 (m, 12H, Ar-H), 8.74 (d, *J* = 4.6 Hz, 4H, β-H), 8.84 (d, *J* = 4.7 Hz, 4H, β-H), 8.87–8.95 (m, 8H, β-H) ppm; ^{13}C{^{1}H} NMR (101 MHz, $CDCl_3$, 25 °C): δ = 41.3, 54.7, 121.3, 122.6, 124.3, 126.4, 127.3, 129.3, 131.8, 132.3, 133.2, 134.5, 134.6, 140.1, 141.4, 143.1, 149.4, 150.2, 150.7 ppm; ^{19}F{^{1}H} NMR (377 MHz, $CDCl_3$, 25 °C) δ = -163.26 (td, 2F, *J* = 24.0, 8.4 Hz), -154.31 (t, 1F, *J* = 20.9 Hz), -137.66

(dd, 2F, *J* = 24.0, 7.6 Hz) ppm; UV-Vis (DCM) λ_{max} [log(ε/M^{-1} cm^{-1})] = 423 [5.93], 549 [4.55], 587 (sh) [3.78] nm; HRMS (MALDI): *m/z* calcd. for $C_{93}H_{50}N_8F_{10}Zn_2$ $[M]^+$: 1596.2582; found 1596.2622.

1-(4-((15-Pentafluorophenyl-10,20-diphenylporphyrinato)zinc(II)-5-yl)ethynylphenyl)-3-(4-iodophenyl)bicyclo[1.1.1]pentane (**5.29**)

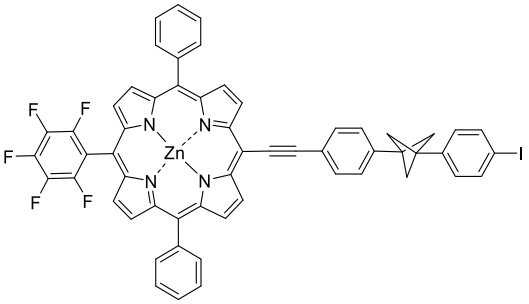

5.29

In a Schlenk tube, (5-ethynyl-10,20-diphenyl-15-pentafluorophenylporphyrinato)zinc(II) (**5.26**) (120 mg, 0.168 mmol) and 1,3-bis(4-iodophenyl)bicyclo[1.1.1]pentane (**5.16**) (79 mg, 0.237 mmol) were dissolved in a mixture of anhydrous THF (6.4 mL) and anhydrous triethylamine (3.2 mL) and argon was bubbled through the mixture for 15 min. $Pd(PPh_3)_2Cl_2$ (17.6 mg, 25.5 µmol) and CuI (9.6 mg, 50.4 µmol) were added and argon was bubbled for another 5 min. The reaction mixture was stirred under argon at 40 °C for 5 h. The solvent was removed *in vacuo* and the crude solids were purified by column chromatography (SiO_2, *n*-hexane/DCM 2:1, 1:1, 2:3, v/v). Removal of the solvents *in vacuo* afforded compound **5.29** as a green solid (61. 4 mg, 57.9 µmol, 35%); M.p. = 276–279 °C dec.; R_f = 0.64 (SiO_2, *n*-hexane/DCM 1:2, v/v); ^{1}H NMR (400 MHz, $CDCl_3$, 25 °C): δ = 2.41 (s, 6H, CH_2), 7.09 (d, 2H, *J* = 7.8 Hz, Ar-H), 7.47 (d, 2H, *J* = 7.8 Hz, Ar-H), 7.68 (d, 2H, *J* = 7.8 Hz, Ar-H), 7.75–7.84 (m, 6H, Ar-H), 7.98 (d, 2H, *J* = 7.7 Hz, Ar-H), 8.20 (d, 4H, *J* = 6.9 Hz, Ar-H), 8.81 (d, 2H, *J* = 4.4 Hz, β-H), 8.97 (d, 2H, *J* = 4.5 Hz, β-H), 9.00 (d, 2H, *J* = 4.5 Hz, β-H), 9.84 (d, 2H, *J* = 4.4 Hz, β-H) ppm; ^{13}C{^{1}H} NMR (101 MHz, $CDCl_3$, 25 °C): δ = 40.8, 41.1, 54.3, 92.1, 92.3, 97.3, 102.5, 102.8, 117.3, 122.3, 122.8, 126.7, 126.9, 128.0, 128.4, 130.0, 131.6, 131.7, 133.2, 133.7, 134.6, 137.4, 137.6 (d, 2C, J_{CF} = 250.4 Hz), 140.5, 141.5, 142.0 (d, 1C, J_{CF} = 232.5 Hz), 142.2, 146.7 (d, 2C, J_{CF} = 250.9 Hz), 149.5, 150.6, 150.8, 152.3 ppm; ^{19}F{^{1}H} NMR (377 MHz, $CDCl_3$, 25 °C): δ = -162.40 – -162.20 (m, 2F), -153.06 (t, 1F, *J* = 20.7 Hz), -137.12 (dd, 2F, *J* = 24.0, 7.2 Hz) ppm; UV-Vis (DCM) λ_{max} [log(ε/M^{-1} cm^{-1})] = 442 [5.68], 567 [4.31], 614 [4.53] nm; HRMS (MALDI): *m/z* calcd. for $C_{57}H_{32}N_4F_5ZnI$ $[M]^+$: 1058.0883; found 1058.0833.

1,3-Bis(4-((15-pentafluorophenyl-10,20-diphenylporphyrinato)zinc(II)-5-yl)ethynylphenyl)bicyclo[1.1.1]pentane (**5.30**)

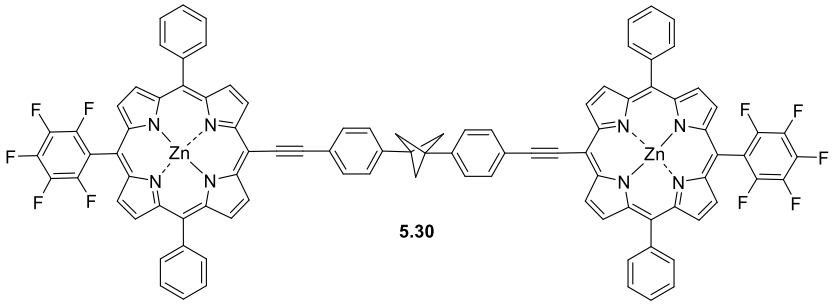

In a Schlenk tube, (5-ethynyl-10,20-diphenyl-15-pentafluorophenylporphyrinato)zinc(II) (**5.26**) (75 mg, 0.105 mmol) and 1,3-bis(4-iodophenyl)bicyclo[1.1.1]pentane (**5.16**) (49.5 mg, 0.105 mmol) were dissolved in a mixture of anhydrous THF (4 mL) and anhydrous triethylamine (2 mL) and argon was bubbled through the mixture for 15 min. $Pd(PPh_3)_2Cl_2$ (11 mg, 15.7 µmol) and CuI (6.0 mg, 31.4 µmol) were added and argon was bubbled for another 5 min. The reaction mixture was stirred under argon at 40 °C for 6.5 h. The solvent was removed *in vacuo* and the crude solids were purified by column chromatography (SiO_2, *n*-hexane/DCM 2:1, 1:1, 2:3, v/v). After removal of the solvents *in vacuo*, 1-(4-((15-pentafluorophenyl-10,20-diphenylporphyrinato)zinc(II)-5-yl)ethynylphenyl)-3-(4-iodophenyl)bicyclo[1.1.1]pentane (**5.29**) (42.1 mg, 39.7 µmol, 38%) and the title compound **5.30** were obtained as purple crystals (13.6 mg, 8.25 µmol, 7.9%); M.p. > 300 °C; R_f = 0.37 (SiO_2, *n*-hexane/DCM 2:1, v/v); ^{1}H NMR (400 MHz, $CDCl_3$ + MeOD, 25 °C): δ = 2.54 (s, 6H, CH_2), 7.54 (d, *J* = 7.8 Hz, 4H, Ar-H), 7.74–7.80 (m, 12H, Ar-H), 8.03 (d, *J* = 7.8 Hz, 4H, Ar-H), 8.21 (d, *J* = 6.2 Hz, 8H, Ar-H), 8.72 (d, *J* = 4.5 Hz, 4H, β-H), 8.89 (d, *J* = 4.6 Hz, 4H, β-H), 8.96 (d, *J* = 4.6 Hz, 4H, β-H), 9.82 (d, *J* = 4.5 Hz, 4H, β-H) ppm; ^{13}C{^{1}H} NMR (101 MHz, $CDCl_3$ + MeOD, 25 °C): δ = 41.2, 54.3, 93.0, 96.5, 101.2, 102.0, 122.2, 122.4, 126.5, 126.7, 127.5, 129.5, 131.0, 131.5, 132.7, 133.1, 134.5, 141.3, 142.7, 149.2, 150.3, 150.6, 152.1 ppm; ^{19}F{^{1}H} NMR (377 MHz, $CDCl_3$ + MeOD, 25 °C): δ = -162.93 – -163.26 (m, 2F), -153.90 – -154.20 (m, 1F), -137.73 (dd, 2F, *J* = 24.0, 6.9 Hz) ppm; UV-Vis (DCM) λ_{max} [log(ε/M^{-1} cm^{-1})] = 444 [6.02], 567 [4.65], 616 [4.89] nm; HRMS (MALDI): *m/z* calcd. for $C_{97}H_{50}N_8F_{10}Zn_2$ $[M]^+$: 1644.2582; found 1644.2594.

1-(4-((15-Pentafluorophenyl-10,20-diphenylporphyrinato)zinc(II)-5-yl)ethynylphenyl)-3-(4-(8-(4-phenylethynyl)-4,4-difluoro-4-bora-3a,4a-diaza-s-indacene)phenyl)bicyclo[1.1.1]pentane (**5.32**)

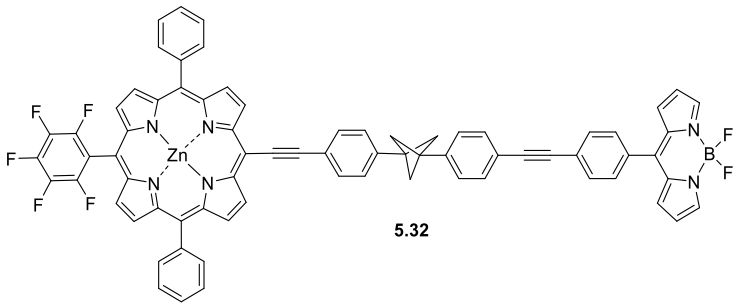

5.32

In a Schlenk tube, 1-(4-((15-pentafluorophenyl-10,20-diphenylporphyrinato)zinc(II)-5-yl)ethynylphenyl)-3-(4-iodophenyl)bicyclo[1.1.1]pentane (**5.29**) (25 mg, 23.6 µmol) was dissolved in a mixture of anhydrous THF (1.3 mL) and anhydrous triethylamine (0.65 mL). argon was bubbled through the mixture for 10 min. $Pd(PPh_3)_2Cl_2$ (3.3 mg, 4.72 µmol) and CuI (1.3 mg, 7.07 µmol) were added and argon was bubbled for 3 min. At the end, 8-(4-phenylethynyl)-4,4-difluoro-4-bora-3a,4a-diaza-s-indacene (**5.31**) (9.6 mg, 33.0 µmol) was added, argon was bubbled for another 3 min and the mixture was stirred under argon at 40 °C for 5 h. The solvent was removed *in vacuo* and the crude solids were purified by column chromatography (SiO_2, *n*-hexane/EtOAc 10:1, 5:1, v/v). Removal of the solvents *in vacuo* afforded compound **5.32** as a turquoise solid (21.4 mg, 17.5 µmol, 74%); M.p. > 300 °C; R_f = 0.35 (SiO_2, *n*-hexane/EtOAc 5:2, v/v); ^{1}H NMR (600 MHz, $CDCl_3$, 25 °C): δ = 2.46 (s, 6H, CH_2), 6.56 (d, 2H, *J* = 2.9 Hz, pyrrolic-H), 6.95 (d, 2H, *J* = 3.9 Hz, pyrrolic-H), 7.36 (d , 2H, *J* = 7.9 Hz, Ar-H), 7.49 (d, 2H, *J* = 7.9 Hz, Ar-H), 7.55–7.59 (m, 4H, Ar-H), 7.70 (d, 2H, *J* = 8.0 Hz, Ar-H), 7.76–7.83 (m, 6H, *J* = 14.4, 7.3 Hz, Ar-H), 7.93 (s, 2H, pyrrolic-H), 7.99 (d, 2H, *J* = 7.9 Hz, Ar-H), 8.21 (d, 4H, *J* = 6.7 Hz, Ar-H), 8.82 (d, 2H, *J* = 4.5 Hz, β-H), 8.97 (d, 2H, *J* = 4.6 Hz, β-H), 8.99 (d, 2H, *J* = 4.5 Hz, β-H), 9.82 (d, 2H, *J* = 4.5 Hz, β-H) ppm; ^{13}C{^{1}H} NMR (151 MHz, $CDCl_3$, 25 °C): δ = 41.2, 41.2, 54.4, 88.5, 92.4, 92.6, 97.3, 102.4, 102.8, 118.8, 121.0, 122.3, 122.7, 126.5, 126.5, 126.8, 126.9, 128.0, 130.0, 130.7, 131.5, 131.7, 131.7, 131.8, 133.2, 133.5, 133.7, 134.6, 134.9, 141.5, 141.8, 142.2, 144.4, 146.6, 149.5, 150.8, 152.2 ppm; ^{19}F{^{1}H} NMR (377 MHz, $CDCl_3$, 25 °C): δ = -162.28 (t, 2F, *J* = 19.4 Hz), -153.04 (t, 1F, *J* = 20.9 Hz), -145.08 (q, 2F, *J* = 28.6 Hz), -137.09 (d, 2F, *J* = 21.2 Hz) ppm; ^{11}B NMR (128 MHz, $CDCl_3$, 25 °C): δ = 0.25 (t, *J* = 28.8 Hz) ppm; UV-Vis (DCM) λ_{max} [log(ε/M^{-1} cm^{-1})] = 290 [4.69], 303 [4.68], 443 [5.63], 506 [4.72], 567 [4.24], 614 [4.47] nm; HRMS (MALDI): *m/z* calcd. for $C_{74}H_{42}BN_6F_7Zn$ $[M]^+$: 1222.2744; found 1222.2703.

1-(4-((15-Pentafluorophenyl-10,20-diphenylporphyrinato)zinc(II)-5-yl)ethynylphenyl)-3-(4-(1-pyrenylethynyl)phenyl)bicyclo[1.1.1]pentane (**5.33**)

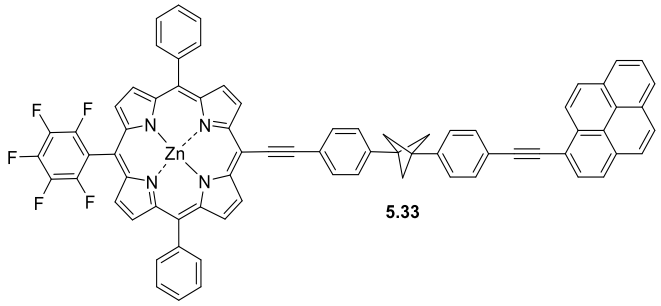

5.33

In a Schlenk tube, 1-(4-((15-pentafluorophenyl-10,20-diphenylporphyrinato)zinc(II)-5-yl)ethynylphenyl)-3-(4-iodophenyl)bicyclo[1.1.1]pentane (**5.29**) (20 mg, 18.9 µmol) was dissolved in a mixture of THF (1.2 mL) and triethylamine (0.6 mL) and argon was bubbled through the mixture for 10 min. $Pd(PPh_3)_2Cl_2$ (2.6 mg, 3.77 µmol) and CuI (1.1 mg, 5.66 µmol) were added and argon was bubbled for another 3 min. At the end, 1-ethynylpyrene (**4.27**) (6.0 mg, 26.4 µmol) was added and argon was bubbled for 3 min. The reaction mixture was stirred under argon at 40 °C. The progression of the reaction was monitored by TLC analysis. Batches of 1-ethynylpyrene (**4.27**) (3.0 mg, 13.2 µmol and 1.5 mg, 6.6 µmol) were added after 4.5 h and 5.5 h of the total reaction time. After 6 h the reaction was determined to be complete. The solvent was removed *in vacuo* and the crude solids were purified by column chromatography (SiO_2, *n*-hexane/EtOAc 20:1, 10:1, v/v). Removal of the solvents *in vacuo* afforded compound **5.33** as a green solid (12.8 mg, 11.5 µmol, 58%); M.p. = 266–268 °C dec.; R_f = 0.29 (SiO_2, *n*-hexane/DCM 1:1, v/v); ^{1}H NMR (600 MHz, $CDCl_3$, 25 °C): δ = 2.48 (s, 6H, CH_2), 7.40 (d, *J* = 7.7 Hz, 2H, Ar-H), 7.50 (d, *J* = 7.7 Hz, 2H, Ar-H), 7.71 (d, *J* = 7.7 Hz, 2H, Ar-H), 7.74–7.79 (m, 6H, Ar-H), 7.99–8.07 (m, 5H, Ar-H, pyrenyl-H), 8.11 (d, *J* = 7.8 Hz, 1H, pyrenyl-H), 8.15–8.19 (m, 2H, pyrenyl-H), 8.20 (d, *J* = 7.4 Hz, 6H, Ar-H, pyrenyl-H), 8.67 (d, *J* = 9.1 Hz, 1H, pyrenyl-H), 8.72 (d, *J* = 4.5 Hz, 2H, β-H), 8.89 (d, *J* = 4.6 Hz, 2H, β-H), 8.95 (d, *J* = 4.4 Hz, 2H, β-H), 9.81 (d, *J* = 4.4 Hz, 2H, β-H) ppm; ^{13}C{^{1}H} NMR (151 MHz, $CDCl_3$ + MeOD, 25 °C): δ = 41.2, 41.2, 54.4, 88.8, 93.0, 95.4, 96.7, 101.5, 102.1, 118.0, 121.8, 122.3, 122.5, 124.4, 124.6, 124.7, 125.7, 125.7, 126.3, 126.5, 126.7, 126.7, 127.4, 127.7, 128.2, 128.4, 129.7, 129.7, 131.2, 131.2, 131.3, 131.4, 131.6, 131.7, 132.0, 132.9, 133.3, 134.7, 137.5 (d, 2C, J_{CF} = 251.5 Hz), 141.3, 141.4, 141.7 (d, 2C, J_{CF} = 257.0 Hz), 146.6 (d, 2C, J_{CF} = 240.0 Hz), 142.7, 149.3, 150.4, 150.7, 152.2 ppm; ^{19}F{^{1}H} NMR (377 MHz, $CDCl_3$ + MeOD, 25 °C) δ = -162.74 (td, 2F, *J* = 24.1, 8.2 Hz), -153.67 (t, 1F, *J* = 20.7 Hz), -137.49 (dd, 2F, *J* = 24.5, 8.2 Hz) ppm; UV-Vis (DCM) λ_{max} [log(ε/M^{-1} cm^{-1})] = 288 [4.54], 300 [4.65], 368 [4.59], 394 [4.57], 442 [5.44], 567 [4.06], 614 [4.28] nm; HRMS (MALDI): *m/z* calcd. for $C_{75}H_{41}N_4F_5Zn$ $[M]^+$: 1156.2543; found 1156.2501.

1-(4-((15-Pentafluorophenyl-10,20-diphenylporphyrinato)zinc(II)-5-yl)ethynylphenyl)-3-(4-((10,15,20-triphenylporphyrinato)zinc(II)-5-yl)phenyl)bicyclo[1.1.1]pentane (**5.35**)

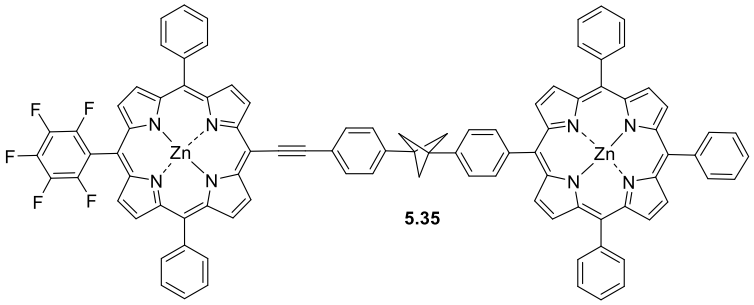

In a Schlenk tube, 1-(4-((15-pentafluorophenyl-10,20-diphenylporphyrinato)zinc(II)-5-yl)ethynylphenyl)-3-(4-iodophenyl)bicyclo[1.1.1]pentane (**5.29**) (25 mg, 23.6 µmol), (5-(4',4',5′,5′-tetramethyl-[1′,3′,2]-dioxaborolan-2′-yl)-10,15,20-triphenylporphyrinato)zinc(II) (**5.34**) (17.2 mg, 23.6 µmol) and K_2CO_3 (39 mg, 0.283 mmol) were dissolved in anhydrous DMF (1.5 mL). Argon was bubbled through the mixture for 10 min. $Pd(PPh_3)_4$ (5.5 mg, 4.72 µmol) was added and argon was bubbled for another 3 min. The reaction mixture was stirred under argon at 90 °C for 15 h. The solvent was removed *in vacuo* and the crude solids were purified by column chromatography (SiO_2, *n*-hexane/DCM 1:1, 2:3, v/v). After removal of the solvents *in vacuo*, compound **5.35** was obtained as a purple solid (18.5 mg, 12.1 µmol, 51%); M.p. > 300 °C; R_f = 0.45 (SiO_2, *n*-hexane/DCM 1:3, v/v); ^{1}H NMR (600 MHz, $CDCl_3$, 25 °C): δ = 2.73 (s, 6H, CH_2), 7.64 (d, 2H, *J* = 7.7 Hz, Ar-H), 7.74 (d, 2H, *J* = 7.6 Hz, Ar-H), 7.77–7.85 (m, 15H, Ar-H), 8.08 (s, 2H, Ar-H), 8.23–8.29 (m, 12H, Ar-H), 8.84 (d, 2H, *J* = 4.4 Hz, β-H), 8.98–9.01 (m, 8H, β-H), 9.04–9.07 (m, 4H, β-H), 9.92 (d, *J* = 4.4 Hz, 2H, β-H) ppm; ^{13}C{^{1}H} NMR (151 MHz, $CDCl_3$, 25 °C): δ = 41.4, 54.7, 92.4, 97.4, 102.5, 102.8, 121.3, 122.3, 122.8, 124.6, 126.7, 126.9, 126.9, 127.7, 128.0, 130.0, 131.6, 131.8, 132.1, 132.2, 132.3, 133.2, 133.7, 134.6, 134.6, 140.1, 141.3, 142.0, 142.3, 143.0, 143.0, 149.5, 150.4, 150.5, 150.6, 150.8, 152.3 ppm; ^{19}F{^{1}H} NMR (377 MHz, $CDCl_3$, 25 °C): δ = -162.43 – -162.20 (m, 2F), -153.08 (t, 1F, *J* = 20.8 Hz), -137.18 – -137.01 (m, 2F) ppm; UV-Vis (DCM) λ_{max} [log(ε/M^{-1} cm^{-1})] = 422 [5.85], 442 [5.74], 553 [4.54], 614 [4.57] nm; HRMS (MALDI): *m/z* calcd. for $C_{95}H_{55}N_8F_5Zn_2$ $[M]^+$: 1530.3053; found 1530.3059.

(5-Bromo-10,20-diphenyl-15-pentafluorophenylporphyrinato)copper(II) (**5.36**)

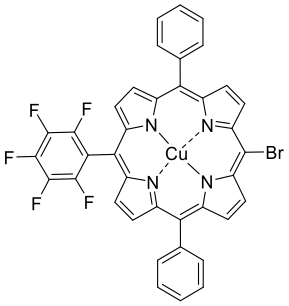

5.36

In a round-bottomed flask, 5-bromo-10,20-diphenyl-15-pentafluorophenylporphyrin (**5.23**) (100 mg, 0.153 mmol) was dissolved in DCM (15 mL) and $Cu(OAc)_2$ (83.5 mg, 0.460 mmol), dissolved in methanol (5 mL), were added. The mixture was stirred at 40 °C for 1.5 h. The solvent was removed *in vacuo*, the crude solids were dissolved in DCM and purified on a SiO_2 pad, eluting with *n*-hexane/DCM 10:1 (v/v). After removal of the solvents *in vacuo*, compound **5.36** was isolated as red crystals (101 mg, 0.131 mmol, 93%); M.p. > 300 °C. R_f = 0.43 (SiO_2, *n*-hexane/DCM 3:1, v/v); UV-Vis (DCM) λ_{max} [log(ε/M^{-1} cm^{-1})] = 418 [5.69], 544 [4.33], 578 (sh) [3.77] nm; HRMS (MALDI): *m/z* calcd. for $[C_{38}H_{18}BrCuF_5N_4]$ $[M]^+$: 766.9931; found 766.9956.

(5-Bromo-10,20-diphenyl-15-pentafluorophenylporphyrinato)nickel(II) (**5.37**)

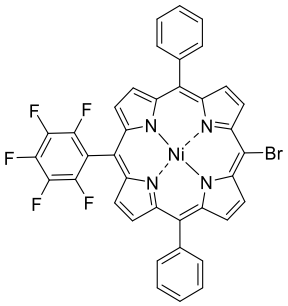

5.37

In a round-bottomed flask, 5-bromo-10,20-diphenyl-15-pentafluorophenylporphyrin (**5.23**) (80 mg, 0.113 mmol) was dissolved in toluene (20 mL) and $Ni(acac)_2$ (116 mg, 0.452 mmol) was added. The mixture was stirred at 100 °C for 18 h. The solvent was removed *in vacuo*, the crude solids were dissolved in DCM and purified on a SiO_2 pad, eluting with *n*-hexane/DCM 1:1 (v/v). After removal of the solvents *in vacuo*, compound **5.37** was isolated as brown crystals (91 mg, 0.121 mmol, quant.); M.p. > 300 °C; R_f = 0.38 (SiO_2, *n*-hexane/DCM 3:1, v/v); ^{1}H NMR (400 MHz, $CDCl_3$, 25 °C): δ = 7.65–7.75 (m, 6H, Ar-H), 7.94–7.98 (m, 4H, Ar-H), 8.60 (d, *J* = 5.0 Hz, 2H, β-H), 8.76 (t, *J* = 4.6 Hz, 4H, β-H), 9.49 (d, *J* = 5.0 Hz, 2H, β-H) ppm; ^{13}C{^{1}H} NMR (101 MHz, $CDCl_3$, 25 °C): δ = 101.0, 104.1, 120.2, 127.2, 128.2, 130.6, 133.7, 133.8, 133.9, 134.3, 140.2, 142.6, 142.6, 143.2, 143.9 ppm; ^{19}F{^{1}H} NMR (377 MHz, $CDCl_3$, 25 °C): δ = -161.82 (dt, 2F, *J* = 23.6, 8.1 Hz), -152.45 (t, 1F, *J* = 20.9 Hz), -136.93 (dd, 2F, *J* = 23.8, 8.0 Hz) ppm; UV-Vis (DCM) λ_{max} [log(ε/M^{-1} cm^{-1})] = 416 [5.60], 533 [4.44], 563 (sh) [4.01] nm; HRMS (MALDI): *m/z* calcd. for $[C_{38}H_{18}N_4F_5NiBr]$ $[M]^+$: 761.9988; found 761.9976.

(5-Trimethylsilylethynyl-10,20-diphenyl-15-pentafluorophenylporphyrinato)nickel(II) (**5.39**)

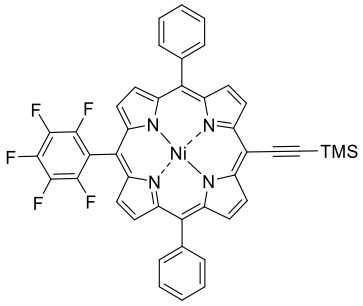

5.39

In a Schlenk tube, (5-bromo-10,20-diphenyl-15-pentafluorophenylporphyrinato)nickel(II) (**5.37**) (60 mg, 78.5 µmol) was dissolved in a mixture of anhydrous THF (1 mL) and anhydrous triethylamine (1 mL) and the mixture was purged with argon for 10 min. $Pd(PPh_3)_2Cl_2$ (5.5 mg, 7.85 µmol) and CuI (3.0 mg, 15.7 µmol) were added and the mixture was purged with argon for 3 min. At the end, trimethylsilylacetylene (0.040 mL, 0.314 mmol) was added and the mixture was purged with argon for another 3 min. The mixture was stirred under argon at r.t. for 3 h. The solvent was removed *in vacuo* and the crude solids were purified by silica gel column chromatography (SiO_2, *n*-hexane/DCM 10:1, 5:1, v/v) to afford compound **5.39** as red crystals (51.8 mg, 66.3 µmol, 84%); M.p. = 193–196 °C; R_f = 0.33 (SiO_2, *n*-hexane/DCM 3:1, v/v); ^{1}H NMR (400 MHz, $CDCl_3$, 25 °C): δ = 0.55 (s, 9H, TMS-CH_3), 7.67–7.75 (m, 6H, Ar-H), 7.98–8.01 (m, 4H, Ar-H), 8.58 (d, *J* = 4.9 Hz, 2H, β-H), 8.75 (d, *J* = 5.0 Hz, 2H, β-H), 8.80 (d, *J* = 4.9 Hz, 2H, β-H), 9.54 (d, *J* = 4.9 Hz, 2H, β-H) ppm; ^{13}C{^{1}H} NMR (151 MHz, $CDCl_3$, 25 °C): δ = 0.3, 100.5, 101.8, 103.3, 105.1, 120.5, 127.1, 128.2, 130.3, 132.4, 133.4, 133.7, 133.8, 140.4, 142.1, 143.3, 143.6, 145.3 ppm; ^{19}F{^{1}H} NMR (377 MHz, $CDCl_3$, 25 °C): δ = -161.93 (dt, 2F, *J* = 22.9, 8.0 Hz), -152.60 (t, 1F, *J* = 20.9 Hz), -136.98 (dd, 2F, *J* = 23.7, 8.2 Hz) ppm; UV-Vis (DCM) λ_{max} [log(ε/M^{-1} cm^{-1})] = 425 [5.41], 542 [4.21], 577 [4.10] nm; HRMS (APCI): *m/z* calcd. for [$C_{43}H_{28}N_4F_5NiSi$] $[M+H]^+$: 781.1351; found 781.1336.

(5-Ethynyl-10,20-diphenyl-15-pentafluorophenylporphyrinato)copper(II) (**5.40**)

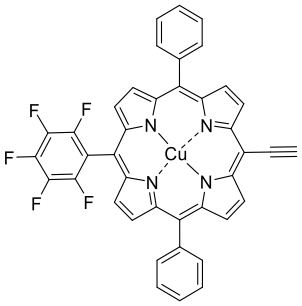

5.40

In a Schlenk tube, (5-bromo-10,20-diphenyl-15-pentafluorophenylporphyrinato)copper(II) (**5.36**) (66 mg, 85.8 µmol) was dissolved in a mixture of anhydrous THF (1.2 mL) and anhydrous triethylamine (1.2 mL) and the mixture was purged with argon for 15 min. $Pd(PPh_3)_2Cl_2$ (6.0 mg, 8.58 µmol) and CuI (3.3 mg, 17.2 µmol) were added and argon was bubbled for 3 min. At the end, trimethylsilylacetylene (0.050 mL, 0.343 mmol) was added and the mixture was purged with argon another 3 min. The mixture was stirred under argon at r.t. for 3 h. The solvent was removed *in vacuo* and the crude solids were purified by column chromatography (SiO_2, *n*-hexane/DCM 4:1, v/v). After removal of the solvents *in vacuo*, (5-trimethylsilylethynyl-10,20-diphenyl-15-pentafluorophenylporphyrinato)copper(II) (**5.38**) was obtained as red crystals (62 mg, 78.8 µmol, 81%). In a Schlenk flask, (5-trimethylsilylethynyl-10,20-diphenyl-15-pentafluorophenylporphyrinato)copper(II) (62 mg, 78.8 µmol) was dissolved anhydrous DCM (6 mL). A 1 M solution of TBAF in THF (0.087 mL, 87 µmol) was added and the mixture was stirred under argon at r.t. for 1 h. DCM was added to the reaction mixture and the mixture was washed with water (2 ×) and brine (1 ×). The organic layer was dried over $MgSO_4$, filtered and the solvent was removed *in vacuo*. Column chromatography (SiO_2, *n*-hexane/DCM 1:1, v/v) followed by removal of the solvents *in vacuo* afforded compound **5.40** as red crystals (58 mg, 81 µmol, quant.); M.p. > 300 °C; R_f = 0.32 (SiO_2, *n*-hexane/DCM 3:1, v/v); UV-Vis (DCM) λ_{max} [log(ε/M^{-1} cm^{-1})] = 422 [5.79], 550 [4.40], 589 [4.24] nm; HRMS (MALDI): *m/z* calcd. for $[C_{40}H_{19}CuF_5N_4]$ $[M]^+$: 713.0826; found 713.0834.

(5-Ethynyl-10,20-diphenyl-15-pentafluorophenylporphyrinato)nickel(II) (**5.41**)

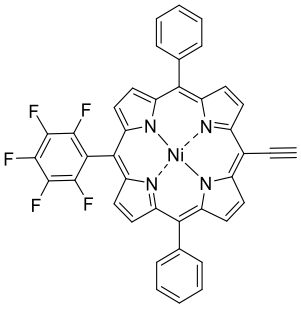

5.41

In a Schlenk flask, (5-trimethylsilylethynyl-10,20-diphenyl-15-pentafluorophenylporphyrinato)nickel(II) (**5.39**) (44.6 mg, 57.1 µmol) was dissolved anhydrous DCM (4 mL). A 1 M solution of TBAF in THF (0.070 mL, 70 µmol) was added and the mixture was stirred under argon at r.t. for 40 min. When TLC analysis showed incomplete conversion of the starting material, more of the 1 M TBAF solution was added (0.010 mL, 10 µmol) and the mixture was stirred for another 10 min. DCM (15 mL) was added and the mixture was washed with water (2 ×). The organic layer was dried over $MgSO_4$, filtered and the solvent was removed *in vacuo*. The crude product was passed through a SiO_2 pad, eluting with *n*-hexane/DCM 1:1 (v/v) and the solvents were removed *in vacuo* to afford compound **5.41** as red crystals (37 mg, 52 µmol, 91%). M.p. > 300 °C; R_f = 0.27 (SiO_2, *n*-hexane/DCM 3:1, v/v); ^{1}H NMR (600 MHz, $CDCl_3$, 25 °C): δ = 4.07 (s, 1H, acetylene-H), 7.68–7.71 (m, 4H, Ar-H), 7.72–7.75 (m, 2H, Ar-H), 7.98–8.00 (m, 4H, Ar-H), 8.61 (d, *J* = 4.9 Hz, 2H, β-H), 8.77 (d, *J* = 4.9 Hz, 2H, β-H), 8.81 (d, *J* = 4.9 Hz, 2H, β-H), 9.54 (d, *J* = 4.8 Hz, 2H, β-H) ppm; ^{13}C{^{1}H} NMR (151 MHz, $CDCl_3$, 25 °C) δ = 83.8, 85.1, 99.0, 102.0, 120.5, 127.2, 128.2, 130.5, 132.2, 133.6, 133.8, 133.8, 137.6 (d, J_{CF} = 252.0 Hz, 2C), 140.4, 142.0, 142.0 (d, J_{CF} = 256.9 Hz, 1C), 143.3, 143.6, 145.4, 146.3 (d, J_{CF} = 246.5 Hz, 2C) ppm; ^{19}F{^{1}H} NMR (377 MHz, $CDCl_3$, 25 °C) δ = -161.88 (dt, 2F, *J* = 23.3, 8.2 Hz), -152.51 (t, 1F, *J* = 20.9 Hz), -136.97 (dd, 2F, *J* = 23.8, 8.0 Hz) ppm; UV-Vis (DCM) λ_{max} [log(ε/M^{-1} cm^{-1})] = 420 [5.21], 538 [4.05], 576 [3.89] nm; HRMS (APCI): *m/z* calcd. for [$C_{40}H_{20}N_4F_5Ni$] $[M+H]^+$: 709.0956; found 709.0943.

1-(4-((15-Pentafluorophenyl-10,20-diphenylporphyrinato)copper(II)-5-yl)ethynylphenyl)-3-(4-((10,15,20-triphenylporphyrinato)zinc(II)-5-yl)phenyl)bicyclo[1.1.1]pentane (**5.42**)

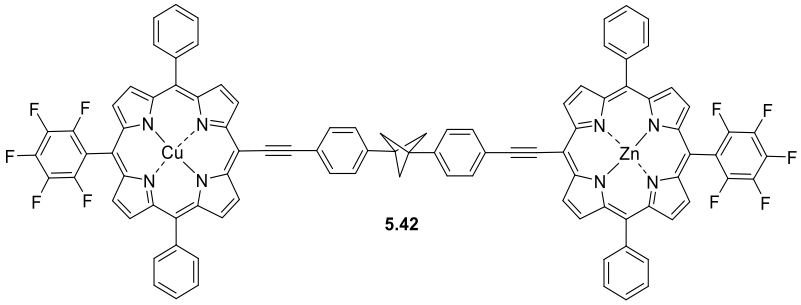

In a Schlenk tube, 1-(4-((15-pentafluorophenyl-10,20-diphenylporphyrinato)zinc(II)-5-yl)ethynylphenyl)-3-(4-iodophenyl)bicyclo[1.1.1]pentane (**5.29**) (23 mg, 21.7 µmol) was dissolved in a mixture of anhydrous THF (1.4 mL) and anhydrous triethylamine (0.7 mL) and the mixture was purged with argon for 10 min. $Pd(PPh_3)_2Cl_2$ (3.0 mg, 4.34 µmol) and CuI (1.2 mg, 6.51 µmol) were added and the mixture was purged with argon for 3 min. At the end, (5-ethynyl-10,20-diphenyl-15-pentafluorophenylporphyrinato)copper(II) (**5.40**) (18.6 mg, 26.0 µmol) was added and the mixture was purged with argon for another 3 min. The mixture was stirred under argon at r.t. for 1.5 h. More (5-ethynyl-10,20-diphenyl-15-pentafluorophenylporphyrinato)copper(II) (**5.40**) (9.3 mg, 13.0 µmol) was added and the mixture was stirred for another 18.5 h. The solvent was removed *in vacuo* and the crude solids were purified by column chromatography (SiO_2, *n*-hexane/DCM 2:1, 1:1, v/v). Removal of the solvents *in vacuo* afforded compound **4.42** as dark green crystals (17.3 mg, 10.5 µmol, 48%); M.p. > 300 °C; R_f = 0.61 (SiO_2, *n*-hexane/DCM 1:2, v/v); UV-Vis (DCM) λ_{max} [log(ε/M^{-1} cm^{-1})] = 442 [5.93], 562 [4.60], 608 [4.73] nm; HRMS (MALDI): *m/z* calcd. for $[C_{97}H_{50}CuF_{10}N_8Zn]$ $[M]^+$: 1643.2586; found 1643.2562.

1-(4-((15-pentafluorophenyl-10,20-diphenylporphyrinato)nickel(II)-5-yl)ethynylphenyl)-3-(4-((10,15,20-triphenylporphyrinato)zinc(II)-5-yl)phenyl)bicyclo[1.1.1]pentane (**5.43**)

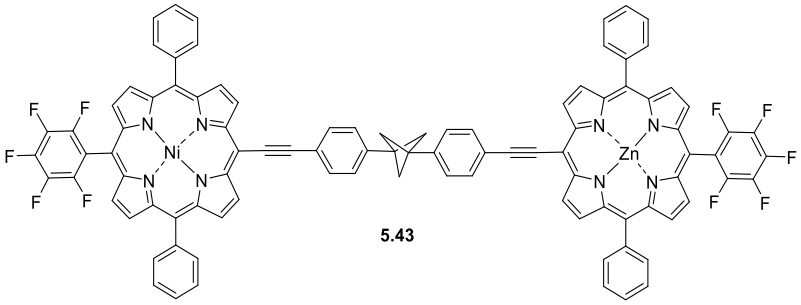

5.43

In a Schlenk tube, 1-(4-((15-pentafluorophenyl-10,20-diphenylporphyrinato)zinc(II)-5-yl)ethynylphenyl)-3-(4-iodophenyl)bicyclo[1.1.1]pentane (**5.29**) (30 mg, 28.2 µmol) was dissolved in a mixture of anhydrous THF (2 mL) and anhydrous triethylamine (1 mL) and the mixture was purged with argon for 10 min. $Pd(PPh_3)_2Cl_2$ (4.0 mg, 5.64 µmol) and CuI (1.6 mg, 3.96 µmol) were added and the mixture was purged with argon for 3 min. At the end, (5-ethynyl-10,20-diphenyl-15-pentafluorophenylporphyrinato)nickel(II) (**5.41**) (22 mg, 31.0 µmol) was added and argon was bubbled for another 3 min. The mixture was stirred under argon at r.t. for 4.5 h. More (5-ethynyl-10,20-diphenyl-15-pentafluorophenylporphyrinato)nickel(II) (**5.41**) (2 mg, 2.82 µmol) was added and the mixture was stirred for another 1.5 h. The solvent was removed *in vacuo* and the crude solids were purified by column chromatography (SiO_2, *n*-hexane/EtOAC 20:1, 25:2, 10:1, v/v). After removal of the solvents *in vacuo*, compound **5.43** was obtained as dark green crystals (10.3 mg, 10.5 µmol, 22%); M.p. > 300 °C; R_f = 0.50 (SiO_2, *n*-hexane/DCM 1:2, v/v); ^{1}H NMR (600 MHz, $CDCl_3$, 25 °C): δ = 2.53 (s, 6H, CH_2), 7.50 (d, *J* = 7.9 Hz, 2H, Ar-H), 7.54 (d, *J* = 7.9 Hz, 2H, Ar-H), 7.70–7.76 (m, 6H, Ar-H), 7.77–7.83 (m, 6H, Ar-H), 7.93 (d, *J* = 7.9 Hz, 2H, Ar-H), 8.01–8.04 (m, 6H, Ar-H), 8.20–8.23 (m, 4H, Ar-H), 8.59 (d, *J* = 4.8 Hz, 2H, β-H), 8.76 (d, *J* = 4.9 Hz, 2H, β-H), 8.81 (d, *J* = 4.5 Hz, 2H, β-H), 8.84 (d, *J* = 4.8 Hz, 2H, β-H), 8.97 (d, *J* = 4.6 Hz, 2H, β-H), 9.03 (d, *J* = 4.5 Hz, 2H, β-H), 9.64 (d, *J* = 4.8 Hz, 2H, β-H), 9.88 (d, *J* = 4.5 Hz, 2H, β-H) ppm; ^{13}C{^{1}H} NMR (151 MHz, $CDCl_3$, 25 °C): δ = 14.3, 29.9, 41.3, 41.3, 54.5, 90.1, 92.4, 97.3, 97.9, 101.1, 101.7, 102.5, 102.8, 120.5, 121.9, 122.3, 122.8, 126.8, 126.8, 126.9, 127.2, 128.0, 128.2, 129.3, 130.0, 130.3, 131.6, 131.8, 131.8, 132.2, 133.2, 133.4, 133.7, 133.8, 133.8, 134.6, 140.4, 141.6, 141.8, 142.2, 142.2, 143.2, 143.5, 145.0, 149.5, 150.6, 150.9, 152.4 ppm; ^{19}F{^{1}H} NMR (377 MHz, $CDCl_3$, 25 °C): δ = -162.43 – -162.26 (m, 2F), -161.78 (td, 2F, *J* = 23.2, 7.8 Hz), -153.13 (t, 1F, *J* = 20.4 Hz), -152.38 (t, 1F, *J* = 20.8 Hz), -137.14 (dd, 2F, *J* = 24.1, 8.2 Hz), -136.96 (dd, 2F, *J*

= 23.8, 8.1 Hz) ppm; UV-Vis (DCM) λ_{max} [log(ε/M^{-1} cm^{-1})] = 442 [5.90], 579 [4.58], 613 [4.64] nm; HRMS (MALDI): *m/z* calcd. for [$C_{97}H_{50}F_{10}N_8ZnNi$] $[M]^+$: 1638.2644; found 1638.2664.

4,4''-Bis((15-pentafluorophenyl-10,20-diphenylporphyrinato)zinc(II)-5-yl)terphenyl (**5.45**)

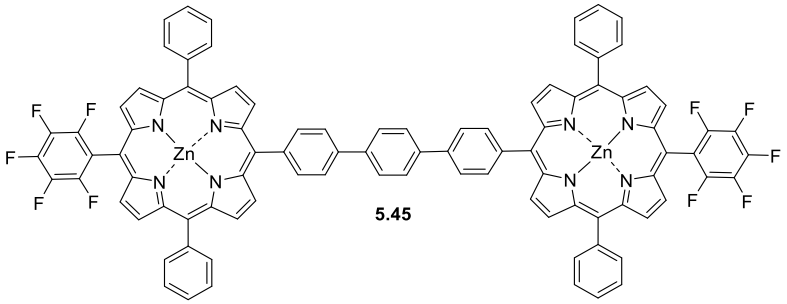

In a Schlenk tube, (5-(4,4,5,5-tetramethyl-1,3,2-dioxaborolan-2-yl)-10,20-diphenyl-15-pentafluorophenylporphyrinato)zinc(II) (**5.24**) (53 mg, 64.8 µmol) and 4,4″-dibromo-*p*-terphenyl (**5.44**) (12.6 mg, 32.4 µmol) were dissolved in anhydrous DMF (3 mL) and the mixture was purged with argon for 15 min. $Pd(PPh_3)_4$ (7.5 mg, 6.48 µmol) and anhydrous K_2CO_3 (53.7 mg, 0.389 mmol) were added and the mixture was purged with argon for another 5 min. The reaction mixture was stirred under argon at 100 °C for 15 h. The solvent was removed *in vacuo* and crude solids were purified by gel column chromatography (SiO_2, *n*-hexane/DCM gradient 2:1, 1:1, 1:2, v/v). After removal of the solvents *in vacuo* compound **5.45** was obatined as a red-brown solid (17.3 mg, 10.7 µmol, 33%); M.p. > 300 °C. R_f = 0.50 (SiO_2, *n*-hexane/DCM 1:3, v/v); ^{1}H NMR (400 MHz, $CDCl_3$ + MeOD, 25 °C): δ = 7.76–7.83 (m, 12H, Ar-H), 8.16 (d, *J* = 8.1 Hz, 4H, Ar-H), 8.19 (s, 4H, Ar-H), 8.27–8.23 (m, 8H, Ar-H), 8.38 (d, *J* = 8.0 Hz, 4H, Ar-H), 8.89 (d, *J* = 4.6 Hz, 4H, β-H), 9.01 (d, *J* = 4.7 Hz, 4H, β-H), 9.06 (d, *J* = 4.7 Hz, 4H, β-H), 9.12 (d, *J* = 4.7 Hz, 4H, β-H) ppm; $^{13}C\{^1H\}$ NMR (151 MHz, $CDCl_3$ + pyridine-d_5, 25 °C): δ = 100.2, 121.4, 122.2, 123.6, 125.1, 126.4, 127.4, 128.0, 129.4, 132.0, 132.2, 133.3, 134.6, 135.3, 135.9, 139.6, 140.1, 142.6, 143.2, 149.8, 150.1, 150.2, 150.7 ppm ($^{13}C\{^1H\}$ NMR spectrum was recorded in $CDCl_3$ + pyridine-d_5 due to low intensity of the signals in neat $CDCl_3$ and a mixture of $CDCl_3$ + MeOD.); $^{19}F\{^1H\}$ NMR (377 MHz, $CDCl_3$, 25 °C): δ = -162.44 (td, 2F, *J* = 24.1, 8.4 Hz), -153.26 (t, 1F, *J* = 20.7 Hz), -137.07 (dd, 2F, *J* = 24.4, 8.3 Hz) ppm; UV-Vis (DCM) λ_{max} [log(ε/M^{-1} cm^{-1})] = 423 [6.14], 549 [4.52], 588 [3.86] nm; HRMS (MALDI): *m/z* calcd. for [$C_{94}H_{48}F_{10}N_8Zn_2$] $[M]^+$: 1606.2426; found 1606.2425.

Methyl 3-phenylbicyclo[1.1.1]pentane-1-carboxylate (**5.66**)[371]

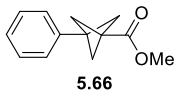

5.66

BCP **5.66** was synthesised according to a modified literature procedure.[200c] In a microwave vial, Magnesium turnings (0.131 g, 5.37 mmol) were dried under vacuum and heated with a heat gun. The vial was evacuated and refilled with argon (3 ×) followed by the addition of anhydrous diethyl ether (2 mL) under argon. Bromobenzene (0.28 mL, 2.69 mmol) was added dropwise to the reaction mixture. A turbidity appeared and the mixture started to reflux gently. After the reflux had stopped the mixture was stirred for another 10 min before a 0.54 M solution of [1.1.1]propellane in diethyl ether (2.5 mL) was added dropwise. The vial was sealed with a pressure cap and the mixture was stirred at 100 ˚C for 3 h. After this time, the reaction was left to cool to room temperature and then transferred to an ethanol/$N_{2(l)}$ cold bath. Methyl chloroformate (0.42 mL, 5.37 mmol) was added at -60 ˚C and the mixture was left to stir at r.t. for 30 min. A saturated aqueous NH_4Cl solution was added followed by diethyl ether. The aqueous layer was extracted with diethyl ether (3 ×), the combined organic layers were dried over $MgSO_4$, filtered and the solvent was removed *in vacuo*. The crude product was purified by column chromatography (SiO_2, *n*-hexane/diethyl ether 30:1, v/v) followed by removal of the solvents *in vacuo* to yield **5.66** as a light-yellow oil (93.4 mg, 0.462 mmol, 34%); ^{1}H NMR (400 MHz, $CDCl_3$, 25 °C): δ = 2.33 (s, 6H, CH_2), 3.72 (s, 3H, OCH_3), 7.20–7.25 (m, 3H, Ar-H), 7.29–7.34 (m, 2H, Ar-H) ppm; ^{13}C{^{1}H} NMR (101 MHz, $CDCl_3$, 25 °C): 51.8, 53.5, 126.2, 127.1, 128.4, 139.8, 163.9, 170.9 ppm. Characterisation data in accordance with the literature.[370]

(5-Pentafluorophenyldipyrromethan-1-yl)-(3-phenylbicyclo[1.1.1]pentan-1-yl)methanone (**5.70**)

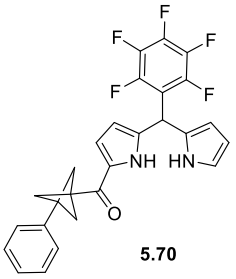

5.70

In a Schlenk tube, 5-pentafluorophenyldipyrromethane (202 mg, 0.646 mmol) was dissolved in anhydrous toluene (10 mL) and the solution was purged with argon for 10 min. A 1M solution of ethylmagnesium bromide in THF (3.22 mL, 3.22 mmol) was added and the mixture was stirred for 1 h at r.t. 3-Phenylbicyclo[1.1.1]pentane-1-carbonyl chloride **5.68** was prepared *in situ* from phenylbicyclo[1.1.1]pentane-1-carboxylic acid **5.67** as follows: Phenylbicyclo[1.1.1]pentane-1-carboxylic acid (304 mg, 1.62 mmol) was dissolved in a mixture of anhydrous DCM (10 mL) and anhydrous DMF (0.3 mL) and oxalyl chloride (166 µL, 1.94 mmol) was added dropwise at 0 °C. The reaction mixture was stirred at 40 °C for 2 h. This solution was then added dropwise to the Schlenk tube containing the DPM mixture and the reaction mixture was stirred for 3 h at r.t. A saturated aqueous NH_4Cl

solution was added until no effervescence was observed anymore, the mixture was extracted with DCM (4 ×), the organic layers were combined and washed with water (2 ×) and brine (1 ×). The organic layer was dried over $MgSO_4$ and the solvent was removed *in vacuo*. Two column chromatographies (1. SiO_2, *n*-hexane/EtOAc 5:1, v/v, 2. SiO_2, *n*-hexane/EtOAc 10:1, v/v) followed by removal of the solvents *in vacuo* afforded compound **5.70** as a brown solid (78 mg, 0.161 mmol, 25%); M.p. = 115 °C dec.; R_f = 0.36 (SiO_2, *n*-hexane/EtOAc 5:1, v/v). ^{1}H NMR (400 MHz, $CDCl_3$, 25 °C): δ = 2.46 (s, 6H, C*H*$_2$), 5.92 (s, 1H, meso-C*H*), 6.06–6.09 (m, 1H, pyrrolic-H), 6.12 (s, 1H, pyrrolic-H), 6.18 (q, *J* = 2.7 Hz, 1H, pyrrolic-H), 6.75–6.78 (m, 1H, pyrrolic-H), 6.98–7.01 (m, 1H, pyrrolic-H), 7.27 (d, *J* = 6.5 Hz, 3H, Ar-H), 7.31–7.36 (m, 2H, Ar-H), 8.33 (s, 1H, N*H*), 9.47 (s, 1H, N*H*) ppm; ^{13}C{^{1}H} NMR (151 MHz, $CDCl_3$, 25 °C): δ = 33.3, 41.9, 41.9, 54.7, 108.8, 109.1, 110.2, 118.2, 119.0, 126.2, 126.5, 127.1, 128.4, 130.9, 136.4, 134.0, 139.0–137.0 (m, 2C), 141.8–139.9 (m, 1C), 146.1–144.0 (m, 2C), 187.5 ppm; ^{19}F{^{1}H} NMR (377 MHz, $CDCl_3$, 25 °C) δ = -160.55 (td, 2F, *J* = 22.3, 7.7 Hz), -154.59 (t, 1F, *J* = 21.1 Hz), -141.18 (dd, 2F, *J* = 21.2, 5.7 Hz) ppm; HRMS (APCI): *m/z* calcd. for [$C_{27}H_{20}F_5N_2O$] [M+H]$^+$: 483.1490, found 483.1496.

5,15-Bis(pentafluorophenyl)-10,20-bis(3-phenylbicyclo[1.1.1]pentan-1-yl)porphyrin (**5.72**)

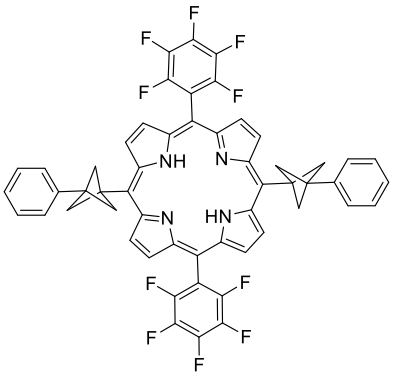

5.72

In a Schlenk tube, compound **5.70** (77.7 mg, 161 mmol) was dried under vacuum. The vessel was evacuated and refilled with argon (3 ×) and anhydrous THF (2.25 mL) and MeOH (0.75 mL) were added under argon. $NaBH_4$ (150 mg, 3.96 mmol) was added in batches under an argon stream. The reaction was left to stir at r.t. for 30 min. Saturated aqueous NH_4Cl solution (6.3 mL) was added, followed by DCM. The mixture was extracted with DCM (4 ×) and the combined organic layers were washed with water (3 ×). The organic layer was dried over $MgSO_4$, filtered and the solvent was removed *in vacuo*. The crude product was used without further purification for the next step. The solids were dissolved in acetonitrile (32 mL) and the solution was purged with argon for 20 min. The condensation was initiated by addition of TFA (70 µL, 0.914 mmol) and the reaction was left to stir at r.t. for 16 h. DDQ (72 mg, 0.317 mmol) was added and the mixture was stirred further for 1 h. The reaction was neutralised by addition of TEA and the solvent was removed *in vacuo*. The solids were dissolved in DCM and passed through a pad of aluminium oxide, eluting with DCM. Purification by column chromatography (SiO_2, *n*-hexane/EtOAc 25:1, v/v) followed by removal of the solvents *in*

vacuo yielded compound **5.72** as purple crystals (3.8 mg, 4.10 µmol, 5%); M.p. = 145 °C dec.; R_f = 0.44 (SiO_2, *n*-hexane/EtOAc 20:1, v/v); ^{1}H NMR (600 MHz, $CDCl_3$, 25 °C): δ = -2.16 (s, 2H, N*H*), 3.56 (s, 12H, CH_2), 7.37–7.41 (m, 2H, Ar-H), 7.50 (t, *J* = 7.6 Hz, 4H, Ar-H), 7.58–7.62 (m, 4H, Ar-H), 8.81 (d, *J* = 4.8 Hz, 4H, β-H), 9.87 (d, *J* = 4.9 Hz, 4H, β-H) ppm; ^{13}C{^{1}H} NMR (151 MHz, $CDCl_3$, 25 °C): δ = 43.9, 44.9, 61.7, 101.8, 119.4, 126.4, 127.2, 128.7, 130.2, 130.6, 140.2, 143.4, 148.7 ppm; ^{19}F{^{1}H} NMR (377 MHz, $CDCl_3$, 25 °C): δ = -162.19 (td, 2F, *J* = 23.8, 8.2 Hz), -152.61 (t, 1F, *J* = 20.9 Hz), -136.82 (dd, 2F, *J* = 23.8, 8.1 Hz) ppm; UV-Vis (DCM) λ_{max} [log(ε/M^{-1} cm^{-1})] = 421 [4.98], 521 [3.71], 554 [3.29], 596 [3.23], 653 [3.01] nm; HRMS (MALDI): *m/z* calcd. for [$C_{54}H_{32}$ N_4F_{10}] $[M]^+$: 926.2467; found 926.2484.

Methyl 3-(4-((trimethylsilyl)ethynyl)phenyl)bicyclo[1.1.1]pentane-1-carboxylate (**5.80**)

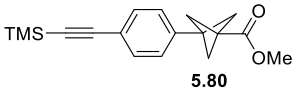

5.80

BCP **5.80** was synthesised according to a modified literature procedure.[200c] In a microwave vial, Magnesium turnings (0.181 g, 7.43 mmol) were dried under vacuum and heated with a heat gun. The vial was evacuated and refilled with argon (3 ×) followed by the addition of anhydrous diethyl ether (4.3 mL) under argon. ((4-Bromophenyl)ethynyl)trimethylsilane (939 mg, 3.72 mmol) was added dropwise to the reaction mixture followed by the addition of 1,2-dibromoethane (0.2 mL) as an initiator. A turbidity appeared and the mixture started to reflux gently. After the reflux had stopped the mixture was stirred for another 10 min before a 1.5 M solution of [1.1.1]propellane in diethyl ether (2.5 mL) was added dropwise. The vial was sealed with a pressure cap and the mixture was stirred at 100 ˚C for 3 h. After this time, the reaction was left to cool to room temperature and then transferred to an ethanol/$N_{2(l)}$ cold bath. Methyl chloroformate (0.58 mL, 7.43 mmol) was added at -60 ˚C and the mixture was left to stir at r.t. for 30 min. A saturated aqueous NH_4Cl solution was added followed by diethyl ether. The aqueous layer was extracted with diethyl ether (3 ×), the combined organic layers were dried over $MgSO_4$, filtered and the solvent was removed *in vacuo*. The crude product was purified by column chromatography (SiO_2, *n*-hexane/EtOAc 20:1 v/v) followed by removal of the solvents *in vacuo* to yield **5.80** as a white solid (63.9 mg, 0.214 mmol, 12%); M.p. = 106 °C; R_f = 0.36 (SiO_2, *n*-hexane/EtOAc 20:1, v/v); ^{1}H NMR (400 MHz, $CDCl_3$, 25 °C): δ = 0.24 (s, 9H, TMS-CH_3), 2.31 (s, 6H, CH_2), 3.71 (s, 3H, OCH_3), 7.13 (d, J = 8.4 Hz, 2H, Ar-H), 7.40 (d, J = 8.3 Hz, 2H, Ar-H) ppm; ^{13}C{^{1}H} NMR (101 MHz, $CDCl_3$, 25 °C): δ = 0.1, 37.1, 41.8, 51.9, 53.5, 94.4, 105.1, 121.9, 126.1, 132.0, 140.2, 170.7 ppm. No HRMS spectrum of **5.83** could be obtained due to instability of the material under all tried conditions (ESI, APCI).

6.6 Details of XRD Data Collection and Refinement

X-ray diffraction data collection and refinement of the compounds listed herein was performed by Dr. Brendan Twamley and Dr. Christopher Kingsbury.

Crystals were grown following the protocol developed by Hope, by dissolving the compounds in $CDCl_3$ and allowing for slow evaporation over time.[372] Data for samples **4.24**, **4.47**, **4.45**, **4.46**, **4.52** were collected on a Bruker D8 Quest ECO using Mo Kα (λ = 0.71073 Å) radiation. Data for samples **3.42**, **3.38**, **4.36**, **4.41**, **4.14**, **4.53**, **4.56**, **5.21**, **5.23**, **5.27**, **5.29**, **5.32**, **5.36**, **5.45**, **5.81** were collected on a Bruker Kappa Apex Duo using Mo Kα (λ = 0.71073 Å; **3.42**, **4.14**, **4.53**) and Cu Kα (λ = 1.54178 Å; **3.38**, **4.36**, **4.41**, **4.56**, **5.21**, **5.23**, **5.27**, **5.29**, **5.32**, **5.36**, **5.45**, **5.81**). Samples were mounted on a MiTeGen microloop and data collected at 100(2) K (**3.38**, **3.42**, **4.36**, **4.40**, **4.41**, **4.14**, **4.45**, **4.52**, **4.53**, **4.56**, **5.21**, **5.23**, **5.27**, **5.29**, **5.32**, **5.36**, **5.45**, **5.81**), 120(2) K (**4.46**) and room temperature (**4.24**) using an Oxford Instruments Cryostream (Bruker ECO) and Cobra (Bruker Kappa Apex Duo) low temperature device. Bruker APEX[373] software was used to collect and reduce data and determine the space group. Structures were solved with the SHELXT[374] structure solution program using Intrinsic Phasing and refined with the SHELXL[375] refinement package using Least Squares minimisation with Olex2.[376] Absorption corrections were applied using SADABS.[377] Crystal data, details of data collection and refinement are given in Tables S1-S4. In **4.40**, the partially occupied solvent in the void, $CHCl_3$ was modelled disordered over two locations with occupancies of 43:20% using restraints (SIMU). Two hexane molecules were also modelled with restraints (DFIX, SIMU, ISOR) and with occupancies of 23:15%. The solvent molecule occupancies were refined using SUMP. The structure of **4.41** consists of two independent molecules in the asymmetric unit. There are also solvent molecules – one fully occupied $CHCl_3$, a half occupied DCM, modelled using a rigid group and restraints (SIMU), and a quarter occupied MeOH, modelled using restraints (DFIX, ISOR). In **4.52** and **5.29**, the bicyclopentyl moiety was disordered and modelled over two locations with occupancies 57:43% with restraints (SADI, SIMU) (**4.52**) and 61:39% with restraints (SIMU, ISOR) (**5.29**). In **5.29** a SQUEEZE model was for one molecule of chloroform solvent. The *ipso* and *para* atoms on the phenyliodide ring were evidently suffering from crystallographic Fourier issues, as well as an unmodelled minor disorder. Aryl ring and BCP atoms were held to SIMU restraints. **4.56** was modelled as a rotational twin around (0 0 1) [1 0 4], angle = 0.07 °, matrix of (-1.000, 0.000, 0.000, 0.000, -1.000, 0.000, 0.492, 0.000, 1.000), with a refined BASF of 0.0757(14). In **5.27**, chloroform solvates were held to a loose SIMU restraint to account for rotational thermal motion. In **5.32**, disordered solvent molecules were held with SIMU, ISOR and SADI restraints. The crystal of **5.36** demonstrated twinning by

pseudomerohedry (rotation around *a**, with *a*- as the stacking direction) which was compensated using a standard SADABS and hklf4 TWIN card. The largest Q-peak (≈1e$^-$) is at the approximate position of a Br-atom at the porphyrin-3 position – possibly not due to over-bromination of 1% of the structure but more likely residual Fourier issues. Twin law is [[-1 0 0] [0 -1 0] [1.171 0.631 1]]. The terphenyl bridge of **5.45** shows minor disorder in the central ring, across two equivalent orientations, and was held to SIMU restraints. A water molecule at the axial position of the Zn was refined for occupancy, refining to 0.57 per formula (0.29/Zn) – H atoms were constrained to likely orientations. Two chloroform molecules were ordered, with a third disordered over 3 sites, this was held to SUMP, SAME and SIMU restraints. Significant crystallographic ripples were found adjacent to the Zn atom. In **5.81**, the pentafluorophenyl and dichloromethane components were held to SIMU restraints, and DCM to SADI restraint. Total solvate occupancy was held to 0.25 per F.U. to give an integer formula. The pentafluorophenyl ring in the crystal of **5.21** was disordered and modelled in two positions with 56:44% occupancy. The distance from the porphyrin to each ring was restrained (SADI) and the displacement parameters for each atom in the pentafluorophenyl ring were also restrainted (SIMU, ISOR for fluorine only). The rings were also modelled with a coordinate constraint (AFIX). Pyrrole hydrogen atoms located on the difference map and refined with restraints (DFIX). Partial deuterosolvent $CDCl_3$ is also present and was modelled with a rigid group with an occupancy of 15% (disordered over the inversion centre).

Table 6.1. Crystal Details and Structure refinement for **3.38**, **3.42**, **4.24** and **4.36**.

Parameter	**3.38**	**3.42**	**4.24**	**4.36**
Empirical Formula	$C_{35}H_{27}BF_2N_2$	$C_{25}H_{30}B_2F_2N_2O_2$	$C_{21}H_{19}BF_2N_2$	$C_{26}H_{25}BF_2IN_5$
Temperature (K)	100(2)	100(2)	299(2)	100(2)
Crystal System	triclinic	triclinic	Triclinic	monoclinic
Space group	$P\bar{1}$	$P\bar{1}$	$P\bar{1}$	$P2_1/c$
a (Å)	9.8550(3)	6.7972(11)	9.8219(11)	6.5571(3)
b (Å)	11.4791(4)	12.2622(19)	9.8350(12)	15.7993(8)
c (Å)	13.4833(4)	15.062(2)	10.5448(12)	23.7215(12)
α **(º)**	70.9641(18)	106.925(2)	116.635(4)	90
β **(º)**	72.5879(18)	95.757(2)	90.175(5)	94.1280(10)
γ (º)	79.1869(19)	102.712(2)	92.636(5)	90
Volume (Å^3)	1368.97(8)	1153.2(3)	909.23(19)	2451.1(2)
Z	2	2	2	4
ρ_{calc} (g/cm^3)	1.272	1.296	1.272	1.580
μ (mm^{-1})	0.664	0.091	0.088	1.347
F(000)	548	476	364	1168
Crystal size (mm^3)	0.15 × 0.12 × 0.07	0.36 × 0.09 × 0.03	0.4 × 0.38 × 0.17	0.19 × 0.09 × 0.09
Radiation	Cu Kα	Mo Kα	Mo Kα	Cu Kα
2θ (º)	3.59 to 68.49	1.80 to 25.33	5.916 to 53.84	3.1 to 55.172
Reflections collected	16546	31162	12695	35440
Independent reflections	4977	4205	3931	5681
R_{int}	0.0492	0.0994	0.0639	0.0523
R_{sigma}	0.0489	0.0638	0.0694	0.0367
Restraints	363	306	0	0
Parameters	0	0	240	320
GooF (*S*)	1.059	1.022	0.996	1.008
R_1 [I> 2σ (I)]	0.0513	0.0533	0.0538	0.0278
wR_2 [I> 2σ (I)]	0.1441	0.1213	0.1160	0.0570
R_1 [all data]	0.0647	0.1061	0.1364	0.0437
wR_2 [all data]	0.1547	0.1445	0.1511	0.0612
Largest peak (e Å^{-3})	0.273	0.494	0.18	0.53
Deepest hole (e Å^{-3})	-0.242	0.280	-0.16	-0.87
Flack parameter	–	–	–	–
CCDC no.	–	–	2030937	2030938

Table 6.2. Crystal Details and Structure refinement for **4.14, 4.40**, **4.41** and **4.45**.

Parameter	**4.14**	**4.40**	**4.41**	**4.45**
Empirical Formula	$C_{13}H_{12}IN_3$	$C_{24.45}H_{17.97}Cl_{0.93}I_2N_3$	$C_{109.75}H_{85}Cl_4I_4N_{14}O_{2.25}Zn_2$	$C_{13}H_{11}I_2N_3$
Temperature (K)	100(2)	100(2)	100(2)	100(2)
Crystal System	monoclinic	triclinic	triclinic	monoclinic
Space group	$P2_1$	$P\bar{1}$	$P\bar{1}$	$P2_1/c$
a (Å)	5.5693(6)	11.4298(5)	14.8736(5)	13.1815(8)
b (Å)	21.395(2)	13.6227(7)	15.7052(5)	15.1379(9)
c (Å)	5.5706(5)	16.7424(8)	22.1531(6)	7.1660(4)
α (º)	90	69.3293(14)	99.4667(18)	90
β (º)	107.4585(12)	75.6176(16)	96.1130(19)	93.5530(14)
γ (º)	90	82.5218(16)	91.6518(19)	90
Volume (Å^3)	633.20(11)	2360.0(2)	5069.6(3)	1427.16(15)
Z	2	4	2	4
ρ_{calc} (g/cm^3)	1.768	1.803	1.583	2.155
μ (mm^{-1})	2.510	2.787	11.574	4.393
F(000)	328	1230	2399	864
Crystal size (mm^3)	0.28 × 0.12 × 0.05	0.37 × 0.286 ×	0.12 × 0.1 × 0.03	0.40 × 0.15 × 0.02
Radiation	Mo K_α	Mo Kα	Cu Kα	Mo Kα
2θ (º)	3.808 to 61.026	4.798 to 55.32	4.07 to 139.938	5.382 to 57.618
Reflections collected	35051	43574	71856	23435
Independent reflections	3855	10961	18862	3730
R_{int}	0.0240	0.0351	0.1110	0.0426
R_{sigma}	0.0139	0.0304	0.1181	0.0275
Restraints	1	271	31	0
Parameters	154	685	1262	163
GooF (*S*)	1.026	1.073	1.036	1.115
R_1 [I> 2σ (I)]	0.0198	0.0341	0.0759	0.0295
wR_2 [I> 2σ (I)]	0.0436	0.0757	0.2005	0.0549
R_1 [all data]	0.0200	0.0489	0.1121	0.0484
wR_2 [all data]	0.0436	0.0835	0.2291	0.0607
Largest peak (e Å^{-3})	0.98	2.14	1.92	1.52
Deepest hole (e Å^{-3})	-1.57	-1.45	-1.64	-1.29
Flack parameter		-	-	-
CCDC no.		2030939	2036122	2030941

Table 6.3. Crystal Details and Structure refinement for **4.46**, **4.52**, **4.53** and **4.56**.

Parameter	**4.46**	**4.52**	**4.53**	**4.56**
Empirical Formula	$C_{12}H_{10}I_2N_4$	$C_{21}H_{16}IN_3$	$C_{19}H_{14}IN_5$	$C_{12}H_{11}IN_4$
Temperature (K)	120(2)	100(2)	100(2)	100(2)
Crystal System	monoclinic	monoclinic	monoclinic	monoclinic
Space group	$P2_1/m$	$P2_1/c$	C2/c	$P2_1/c$
a (Å)	8.7892(4)	11.3814(6)	36.210(4)	7.8158(5)
b (Å)	7.4625(4)	13.3117(7)	5.5976(6)	5.5129(3)
c (Å)	10.5505(5)	11.9166(6)	20.841(2)	28.5940(16)
α (º)	90	90	90	90
β (º)	101.0921(12)	91.9135(14)	123.6746(11)	93.852(3)
γ (º)	90	90	90	90
Volume (Å^3)	679.07(6)	1804.43(16)	3515.5(7)	1229.27(12)
Z	2	4	8	4
ρ_{calc} (g/cm^3)	2.269	1.610	1.660	1.827
μ (mm^{-1})	4.619	1.782	1.833	20.330
F(000)	432	864	1728	656
Crystal size (mm^3)	0.28 × 0.11 × 0.068	0.5 × 0.36 × 0.17	0.38 × 0.07 × 0.07	0.17 × 0.06 × 0.03
Radiation	Mo Kα	Mo Kα	Mo Kα	Cu Kα
2θ (º)	6.706 to 61.484	5.752 to 61.4	3.91 to 59.174	3.098 to 69.867
Reflections collected	19589	42159	47574	2313
Independent reflections	2263	5590	4930	2313
R_{int}	0.0395	0.0493	0.0255	0.0589
R_{sigma}	0.0210	0.0257	0.0120	0.0511
Restraints	0	180	0	0
Parameters	116	254	226	155
GooF (*S*)	1.132	1.047	1.132	1.115
R_1 [I> 2σ (I)]	0.0193	0.0317	0.0209	0.0464
wR_2 [I> 2σ (I)]	0.0412	0.0613	0.0474	0.1105
R_1 [all data]	0.0242	0.0517	0.0242	0.0500
wR_2 [all data]	0.0431	0.0695	0.0489	0.1126
Largest peak (e Å^{-3})	0.94	0.96	0.52	1.896
Deepest hole (e Å^{-3})	-0.93	-1.00	-0.89	-0.851
Flack parameter	-	-	-	-
CCDC no.	2030942	2030943	2030944	2036123

Table 6.4. Crystal Details and Structure refinement for **5.23**, **5.23**, **5.27** and **5.29**.

Parameter	**5.21**	**5.23**	**5.27**	**5.29**
Empirical Formula	$C_{38}H_{21}F_5N_4$	$C_{40}H_{20}BrCl_6F_5N_4Zn$	$C_{101}H_{64}Cl_{18}F_{10}N_8O_2Zn_2$	$C_{59}H_{34}Cl_6F_5IN_4Zn$
Temperature (K)	100(2)	100(2)	100(2)	100(2)
Crystal System	monoclinic	triclinic	triclinic	monoclinic
Space group	$P2_1/c$	$P\bar{1}$	$P\bar{1}$	C2/c
a (Å)	16.8175(5)	7.8374(4)	11.4657(4)	49.8304(18)
b (Å)	12.9633(4)	13.8052(7)	11.7262(4)	8.9418(4)
c (Å)	14.5193(5)	18.3297(10)	19.7668(7)	25.0931(11)
α (º)	90	83.244(4)	96.761(2)	90
β (º)	107.9453(11)	78.929(4)	97.881(2)	104.802(3)
γ (º)	90	74.405(4)	109.3960(10)	90
Volume ($Å^3$)	3011.37(17)	1870.08(17)	2444.92(15)	10809.8(8)
Z	4	2	1	8
ρ_{calc} (g/cm^3)	1.426	1.793	1.617	1.596
μ (mm^{-1})	1.253	6.665	5.767	8.358
F(000)	1323	1000	1198	5168
Crystal size (mm^3)	0.10 × 0.25 × 0.30	0.029 × 0.07 × 0.21	0.15 × 0.15 × 0.03	0.384 × 0.066 × 0.017
Radiation	Cu Kα	Cu Kα	Cu Kα	Cu Kα
2θ (º)	2.762 to 70.011	2.46 to 67.96	2.29 to 70.05°	1.83 to 69.06
Reflections collected	40080	29035	38541	37777
Independent reflections	5676	6682	9156	9839
R_{int}	0.0415	0.0690	0.0545	0.0625
R_{sigma}	0.0240	0.0584	0.0408	0.0675
Restraints	183	545	652	678
Parameters	538	189	48	126
GooF (*S*)	1.078	1.078	1.006	0.809
R_1 [I> 2σ (I)]	0.0470	0.0692	0.0805	0.1086
wR_2 [I> 2σ (I)]	0.1240	0.1814	0.2199	0.2911
R_1 [all data]	0.0483	0.0899	0.0862	0.1348
wR_2 [all data]	0.1251	0.1976	0.2255	0.3183
Largest peak (e $Å^{-3}$)	0.467	0.955	2.227	1.352
Deepest hole (e $Å^{-3}$)	-0.322	-0.766	-2.142	-3.116
Flack parameter	-	-	-	-
CCDC no.	-	-	-	-

Table 6.5. Crystal Details and Structure refinement for **5.32**, **5.36**, **5.45** and **5.81**.

Parameter	**5.32**	**5.36**	**5.45**	**5.81**
Empirical Formula	$C_{79.24}H_{53.73}BCl_{1.13}F_7N_6Zn$	$C_{38.50}H_{19}BrClCuF_5N_4$	$C_{100}H_{55.15}Cl_{18}F_{10}N_8O_{0.57}Zn_2$	$C_{38.25}H_{19.50}Cl_{0.50}F_5N_4Zn$
Temperature (K)	100(2)	100(2)	100(2)	100(2)
Crystal System	monoclinic	triclinic	triclinic	monoclinic
Space group	Cc	$P\bar{1}$	$P\bar{1}$	$P2_1/c$
a (Å)	20.5835(9)	7.4047(3)	11.1950(4)	16.6005(7)
b (Å)	20.5119(9)	13.9903(6)	12.2069(4)	13.3563(7)
c (Å)	15.2423(6)	16.3999(7)	19.3024(7)	13.9214(6)
α (º)	90	101.968(2)	98.769(2)	90
β (º)	104.858(3)	101.623(2)	98.363(2)	105.489(2)
γ (º)	90	103.502(2)	110.333(2)	90
Volume (Å^3)	6220.2(5)	1559.31(12)	2387.83(15)	2974.6(2)
Z	4	2	1	4
ρ_{calc} (g/cm^3)	1.430	1.728	1.625	1.593
μ (mm^{-1})	1.615	3.869	5.883	2.157
F(000)	2754	808	1172	1442
Crystal size (mm^3)	0.41 × 0.03 × 0.02	0.26 × 0.14 × 0.01	0.31 × 0.18 × 0.02	0.24 × 0.23 × 0.02
Radiation	Cu Kα	Cu Kα	Cu Kα	Cu Kα
2θ (º)	3.09 to 68.70	2.85 to 68.29	2.371 to 68.742	2.76 to 68.38
Reflections	34852	17557	44636	24257
Independent	10430	5626	8773	5448
R_{int}	0.0783	0.0576	0.0877	0.0692
R_{sigma}	0.0937	0.0601	0.0696	0.0656
Restraints	931	470	725	507
Parameters	314	0	415	878
GooF (*S*)	1.077	1.143	1.067	1.067
R_1 [I> 2σ (I)]	0.0625	0.0804	0.0862	0.0526
wR_2 [I> 2σ (I)]	0.1573	0.2380	0.2378	0.1343
R_1 [all data]	0.0805	0.0910	0.1072	0.0746
wR_2 [all data]	0.1702	0.2553	0.2612	0.1514
Largest peak (e Å^{-3}	0.565	1.066	1.848	0.627
Deepest hole (e Å^{-3}	-0.373	-0.965	-0.795	-0.564
Flack parameter	-	-	-	-
CCDC no.	-	-	-	-

Chapter 7. References

[1] a) S. K. Chapman, S. Daff, A. W. Munro in *Metal Sites in Proteins and Models: Iron Centres* (Eds.: H. A. O. Hill, P. J. Sadler, A. J. Thomson), Springer Berlin Heidelberg, Berlin-Heidelberg, **1997**, pp. 39–70; b) T. L. Poulos, *Chem. Rev.* **2014**, *114*, 3919–3962.

[2] a) A. R. Battersby, *Nat. Prod. Rep.* **2000**, *17*, 507–526; b) M. O. Senge, A. A. Ryan, K. A. Letchford, S. A. MacGowan, T. Mielke, *Symmetry* **2014**, *6*, 781–843; c) A. A. Ryan, M. O. Senge, *Photochem. Photobiol. Sci.* **2015**, *14*, 638–660.

[3] B. Kräutler, *Biochem. Soc. Trans.* **2005**, *33*, 806–810.

[4] a) T. J. Dougherty, C. J. Gomer, B. W. Henderson, G. Jori, D. Kessel, M. Korbelik, J. Moan, Q. Peng, *J. Natl. Cancer Inst.* **1998**, *90*, 889–905; b) J. Moan, *Photochem. Photobiol.* **1986**, *43*, 681–690; c) A. P. Castano, T. N. Demidova, M. R. Hamblin, *Photodiagnosis Photodyn. Ther.* **2004**, *1*, 279–293; d) S. Callaghan, M. A. Filatov, E. Sitte, H. Savoie, R. W. Boyle, K. J. Flanagan, M. O. Senge, *Photochem. Photobiol. Sci.* **2017**, *16*, 1371–1374.

[5] a) B. Meunier, *Chem. Rev.* **1992**, *92*, 1411–1456; b) K. Rybicka-Jasińska, W. Shan, K. Zawada, K. M. Kadish, D. Gryko, *J. Am. Chem. Soc.* **2016**, *138*, 15451–15458; c) L. Feng, K.-Y. Wang, E. Joseph, H.C. Zhou, *Trends Chem.* **2020**, *2*, 555–568; d) J. C. Barona-Castaño, C. C. Carmona-Vargas, T. J. Brocksom, K. T. de Oliveira, *Molecules* **2016**, *21*, 310–336; e) M. Roucan, M. Kielmann, S. J. Connon, S. S. R. Bernhard, M. O. Senge, *Chem. Commun.* **2018**, *54*, 26–29.

[6] a) R. Paolesse, D. Monti, S. Nardis, C. di Natale, in *Handbook of Porphyrin Science* (Eds.: K. M. Kadish, K. M. Smith, R. Guilard), World Scientific Publishing, Singapore, **2011**, Vol. 12, pp. 121–225; b) K. Norvaiša, K. J. Flanagan, D. Gibbons, M. O. Senge, *Angew. Chem. Int. Ed. Engl.* **2019**, *58*, 16553–16557; c) M. Kielmann, C. Prior, M. Senge, *New J. Chem.* **2018**, *42*, 7529–7550; d) K. Norvaiša, M. Kielmann, M. O. Senge, *ChemBioChem* **2020**, *21*, 1–16.

[7] a) D. M. Guldi, *Chem. Soc. Rev.* **2002**, *31*, 22–36; b) L.-L. Li, E. W.-G. Diau, *Chem. Soc. Rev.* **2013**, *42*, 291–304; c) G. Pellegrino, G. G. Condorelli, V. Privitera, B. Cafra, S. Di Marco, A. Alberti, *J. Phys. Chem. C* **2011**, *115*, 7760–7767.

[8] a) E. Hückel, *Z. Phys.* **1931**, *70*, 204–286; b) E. Hückel, *Z. Phys.* **1931**, *72*, 310–337; c) E. Hückel, *Z. Phys.* **1932**, *76*, 628–648.

[9] a) L. E. Webb, E. B. Fleischer, *J. Chem. Phys.* **1965**, *43*, 3100–3111; b) B. M. L. Chen, A. Tulinsky, *J. Am. Chem. Soc.* **1972**, *94*, 4144–4151.

[10] a) E. Vogel, W. Haas, B. Knipp, J. Lex, H. Schmickler, Angew. Chem. Int. Ed. Engl. **1988**, *27*, 406–409; b) E. Steiner, P. W. Fowler, *ChemPhysChem* **2002**, *3*, 114–116.

[11] a) H. Fliegl, D. Sundholm, *J. Org. Chem.* **2012,** *77*, 3408–3414; b) J. Jusélius, D. Sundholm, *Phys. Chem. Chem. Phys.* **2000**, *2*, 2145–2151.

[12] a) A. Ghosh, J. Almloef, *J. Phys. Chem.* **1995**, *99*, 1073–1075; b) V. A. Kuzmitsky, K. N. Solovyov, *J. Mol. Struct.* **1980**, *65*, 219–230; c) T. J. Butenhoff, C. B. Moore, *J. Am. Chem. Soc.* **1988**, *110*, 8336–8341; d) K. E. Thomas, L. J. McCormick, H. Vazquez-Lima, A. Ghosh, *Angew. Chem. Int. Ed. Engl.* **2017**, *56*, 10088–10092.

[13] a) M. Gouterman, *J. Mol. Spectrosc.* **1961**, *6*, 138–163; b) R. Giovannetti, in *Macro To Nano Spectroscopy* (Ed.: J. Uddin), InTech, Rijeka, **2012**, pp. 87–108; c) T. Hashimoto, Y.-K. Choe, H. Nakano, K. Hirao, *J. Phys. Chem. A* **1999**, *103*, 1894–1904.

[14] a) A. Rosa, G. Ricciardi, E. J. Baerends, *J. Phys. Chem. A* **2006**, *110*, 5180–5190; b) T. Wolfle, A. Gorling, W. Hieringer, *Phys. Chem. Chem. Phys.* **2008**, *10*, 5739–5742; c) S. S. Eaton, G. R. Eaton, *J. Am. Chem. Soc.* **1975**, *97*, 3660–3666; d) C. J. Medforth, R. E. Haddad, C. M. Muzzi, N. R. Dooley, L. Jaquinod, D. C. Shyr, D. J. Nurco, M. M. Olmstead, K. M. Smith, J.-G. Ma, J. A. Shelnutt, *Inorg. Chem.* **2003**, *42*, 2227–2241; e) J. W. Dirks, G. Underwood, J. C. Matheson, D. Gust, *J. Org. Chem.* **1979**, *44*, 2551–2555.

[15] a) R. S. Ajioka, J. D. Phillips, J. P. Kushner, *Biochim. Biophys. Acta* **2006**, *1763*, 723–736; b) H. A. Dailey, T. A. Dailey, S. Gerdes, D. Jahn, M. Jahn, M. R. O'Brian, M. J. Warren, *Microbiol. Mol. Biol. Rev.* **2017**, *81*, e00048–16.

[16] G. G. Stokes, *J. Chem. Soc.* **1864**, *17*, 304–318.

[17] R. Robinson, *Obituary Notices of Fellows of the Royal Society* **1953**, *8*, 609–634.

[18] H. Fischer, K. Zeile, *Liebigs Ann. Chem.* **1929**, *468*, 98–116.

[19] H. Fischer, H. Wenderoth, *Liebigs Ann. Chem.* **1940**, *545*, 140–147.

[20] R. B. Woodward, W. A. Ayer, J. M. Beaton, F. Bickelhaupt, R. Bonnett, P. Buchschacher, G. L. Closs, H. Dutler, J. Hannah, F. P. Hauck, S. Itô, A. Langemann, E. Le Goff, W. Leimgruber, W. Lwowski, J. Sauer, Z. Valenta, H. Volz, *J. Am. Chem. Soc.* **1960**, *82*, 3800–3802.

[21] a) R. B. Woodward, *Pure Appl. Chem.* **1968**, *17*, 519–547; b) R. B. Woodward, *Pure Appl. Chem.* **1971**, *25*, 283–304; c) R. B. Woodward, *Pure Appl. Chem.* **1973**, *33*, 145–177; d) A. Eschenmoser, *Q. Rev. Chem. Soc.* **1970**, *24*, 366–415; e) A. Eschenmoser, C. E. Wintner, *Science* **1977**, *196*, 1410–1420.

[22] a) K. M. Smith, *New J. Chem.* **2016**, *40*, 5644–5649; b) M. O. Senge, N. N. Sergeeva, K. J. Hale, *Chem. Soc. Rev.* **2021**, *50*, 4730–4789.

[23] a) P. Rothemund, *J. Am. Chem. Soc.* **1935**, *57*, 2010–2011; b) P. Rothemund, *J. Am. Chem. Soc.* **1936**, *58*, 625–627.

[24] A. D. Adler, F. R. Longo, J. D. Finarelli, J. Goldmacher, J. Assour, L. Korsakoff, *J. Org. Chem.* **1967**, *32*, 476–476.

[25] a) J. S. Lindsey, I. C. Schreiman, H. C. Hsu, P. C. Kearney, A. M. Marguerettaz, *J. Org. Chem.* **1987**, *52*, 827–836; b) J. S. Lindsey, H. C. Hsu, I. C. Schreiman, *Tetrahedron Lett.* **1986**, *27*, 4969–4970.

[26] I. P. Beletskaya, V. S. Tyurin, A. Uglov, C. Stern, R. Guilard, in *Handbook of Porphyrin Science* (Eds.: K. M. Kadish, K. M. Smith, R. Guilard), World Scientific Publishing, Singapore, **2012**, vol. 23, pp. 81–279.

[27] a) M. O. Senge, S. Plunkett, *ECS Trans.* **2011**, *35*, 147–157; b) M. O. Senge, *Chem. Commun.* **2011**, *47*, 1943–1960.

[28] G. P. Arsenault, E. Bullock, S. F. MacDonald, *J. Am. Chem. Soc.* **1960**, *82*, 4384–4389.

[29] a) J. S. Lindsey, *Acc. Chem. Res.* **2010**, *43*, 300–311; b) P. D. Rao, S. Dhanalekshmi, B. J. Littler, J. S. Lindsey, *J. Org. Chem.* **2000**, *65*, 7323–7344.

[30] A. Wiehe, C. Ryppa, M. O. Senge, *Org. Lett.* **2002**, *4*, 3807–3809.

[31] a) A. Boudif, M. Momenteau, *J. Chem. Soc., Perkin Trans. 1* **1996**, 1235–1242; b) S. Hatscher, M. O. Senge, *Tetrahedron Lett.* **2003**, *44*, 157–160; c) A. Meindl, S. Plunkett, A. A. Ryan, K. J. Flanagan, S. Callaghan, M. O. Senge, *Eur. J. Org. Chem.* **2017**, 3565–3583.

[32] D. K. Dogutan, S. H. H. Zaidi, P. Thamyongkit, J. S. Lindsey, *J. Org. Chem.* **2007**, *72*, 7791–7714.

[33] a) M. O. Senge, M. Davis, *J. Porphyrins Phthalocyanines* **2010**, *14*, 557–567; b) S. Neya, N. Funasaki, *Tetrahedron Lett.* **2002**, *43*, 1057–1058; c) S. Neya, J. Quan, T. Hoshino, M. Hata, N. Funasaki, *Tetrahedron Lett.* **2004**, *45*, 8629–8630.

[34] M. G. H. Vicente, K. M. Smith, *Curr. Org. Synth.* **2014**, *11*, 3–28.

[35] a) L. R. Nudy, H. G. Hutchinson, C. Schieber, F. R. Longo, *Tetrahedron* **1984**, *40*, 2359–2363; b) S. G. DiMagno, V. S.-Y. Lin, M. J. Therien, *J. Am. Chem. Soc.* **1993**, *115*, 2513–2515; c) S. G. DiMagno, V. S.-Y. Lin, M. J. Therien, *J. Org. Chem.* **1993**, *58*, 5983–5993.

[36] R. W. Boyle, C. K. Johnson, D. Dolphin, *J. Chem. Soc., Chem. Commun.* **1995**, 527–528.

[37] a) S. Hiroto, Y. Miyake, H. Shinokubo, *Chem. Rev.* **2017**, *117*, 2910–3043; b) A. Ryan, A. Gehrold, R. Perusitti, M. Pintea, M. Fazekas, O. B. Locos, F. Blaikie, M. O. Senge, *Eur. J. Org. Chem.* **2011**, 5817–5844.

[38] a) N. Miyaura, K. Yamada, A. Suzuki, *Tetrahedron Lett.* **1979**, *20*, 3437–3440; b) A. G. Hyslop, M. A. Kellett, P. M. Iovine, M. J. Therien, *J. Am. Chem. Soc.* **1998**, *120*, 12676–12677.

[39] K. Sonogashira, Y. Tohda, N. Hagihara, *Tetrahedron Lett.* **1975**, *50*, 4467–4470.

[40] a) K. Sonogashira, Y. Tohda, N. Hagihara, *Tetrahedron Lett.* **1975**, *50*, 4467–4470; b) V. Lin, S. G. DiMagno, M. J. Therien, *Science* **1994**, *264*, 1105–1111.

[41] J. K. Stille, *Angew. Chem. Int. Ed. Engl.* **1986**, *25*, 508–524.

[42] a) R. F. Heck, *J. Am. Chem. Soc.* **1968**, *90*, 5518–526; b) I. K. Morris, K. M. Snow, N. W. Smith, K. M. Smith, *J. Org. Chem.* **1990**, *55*, 1231–1236.

[43] a) F. Paul, J. Patt, J. F. Hartwig, *J. Am. Chem. Soc.* **1994**, *116*, 5969–5970; b) A. S. Guram, S. L. Buchwald, *J. Am. Chem. Soc.* **1994**, *116*, 7901–7902; c) T. Takanami, M. Hayashi, F. Hino, K. Suda, *Tetrahedron Lett.* **2003**, *44*, 7353–7357.

[44] a) M. O. Senge, *Acc. Chem. Res.* **2005**, *38*, 733–743; b) W. W. Kalish, M. O. Senge, *Angew. Chem. Int. Ed. Engl.* **1998**, *37*, 1107–1109; c) M. O. Senge, W. W. Kalish, I. Bischoff, *Chem. Eur. J.* **2000**, *6*, 2721–2738.

[45] M. O. Senge, I. Bischoff, *Eur. J. Org. Chem.* **2001**, 1735–1751.

[46] a) M. O. Senge, X. Feng, *Tetrahedron Lett.* **1999**, *40*, 4165–4168; b) M. O. Senge, X. Feng, *J. Chem. Soc., Perkin Trans. 1* **2000**, 3615–3621.

[47] a) Z.-X. Xia, F. S. Mathews, *J. Mol. Biol.* **1990**, *212*, 837–863; b) A. W. Munro, K. Malarkey, J. McKnight, A. J. Thomson, S. M. Kelly, N. C. Price, J. G. Lindsay, J. R. Coggins, J. S. Miles, *Biochem. J.* **1994**, *303*, 423–428; c) M. J. J. M. Zvelebil, C. R. Wolf, M. J. E. Sternberg, *Protein Eng. Des. Sel.* **1991**, *4*, 271–282; d) S. Schneider, J. Marles-Wright, K. H. Sharp, M. Paoli, *Nat. Prod. Rep.* **2007**, *24*, 621–630.

[48] T. Shimizu, A. Lengalova, V. Martinek, M. Martinkova, *Chem. Sov. Rev.* **2019**, *48*, 5624–5657.

[49] a) X. Wen, Y. Li, M. R. Hamblin, *Photodiagnosis Photodyn. Ther.* **2017**, *19*, 140–152; b) Y. Hisamatsu, N. Umezawa, H. Yagi, K. Kato, T. Higuchi, *Chem. Sci.* **2018**, *9*, 7455–7467; c) M. Sun, L. Xu, J. H. Bahng, H. Kuang, S. Alben, N. A. Kotov, C. Xu, *Nat. Commun.* **2017**, *8*, 1847; d) Y. Xu, L. Wang, X. Zhu, C.-Q. Wang, *RSC Adv.* **2016**, *6*, 31053–31058; e) C. Fowley, N. Nomikou, A. P. McHale, B. McCaughan, J. F. Callan, *Chem. Commun.* **2013**, *49*, 8934–8936; f) H. Koo, H. Lee, S. Lee, K. H. Min, M. S. Kim, D. S. Lee, Y. Choi, I. C. Kwon, K. Kim, S. Y. Jeong, *Chem. Commun.* **2010**, *46*, 5668–5670.

[50] a) F. Harris, L. Pierpoint, *Med. Res. Rev.* **2012**, *32*, 1292–1327; b) A. Wiehe, J. M. O'Brien, M. O. Senge, *Photochem. Photobiol. Sci.* **2019**, *18*, 2565–2612.

[51] a) B. R. Vummidi, J. Alzeer, N. W. Luedtke, *ChemBioChem* **2013**, *14*, 540–558; b) R. Hou, X. Niu, F. Cui, *RSC Adv.* **2016**, *6*, 7765–7771; c) Q. Xue, Y. Lv, H. Cui, X. Gu, S. Zhang, J. Liu, *Anal. Chim. Acta* **2015**, *856*, 103–109.

[52] a) H. Han, Q. Jin, H. Wang, W. Teng, J. Wu, H. Tong, T. Chen, J. Ji, *Small* **2016**, *12*, 3870–3878; b) F. B. Barlas, B. Demir, E. Guler, A. M. Senisik, H. A. Arican, P. Unak, S. Timur, *RSC Adv.* **2016**, *6*, 30217–30225; c) M. Yao, M. Ma, H. Zhang, Y. Zhang, G. Wan, J. Shen, H. Chen, R. Wu, *Adv. Funct. Mater.* **2018**, *28*, 1804497.

[53] a) O. F. Brandenberg, R. Fasan, F. H. Arnold, *Curr. Opin. Biotech.* **2017**, *47*, 102–111; b) R. K. Zhang, X. Huang, F. H. Arnold, *Curr. Opin. Chem. Biol.* **2019**, *49*, 67–75; c) R. Kato, Y. Kobayashi, M. Akiyama, T. Komatsu, *Dalton Trans.* **2013**, *42*, 15889–15892.

[54] a) H. J. Vreman, D. A. Cipkala, D. K. Stevenson, *Can. J. Physiol. Pharmacol.* **1996**, *74*, 278–285; b) S.-I. Ozaki, A. Nakahara, T. Sato, *Chem. Lett.* **2011**, *40*, 362–363; c) Y. Lu, A. Sousa, R. Franco, A. Mangravita, G. C. Ferreira, I. Moura, J. A. Shelnutt, *Biochemistry* **2002**, *41*, 8253–8262.

[55] a) M. O. Senge, S. A. MacGowan, J. M. O'Brien, *Chem. Commun.* **2015**, *51*, 17031–17063; b) S. A. MacGowan, M. O. Senge, *Inorg. Chem.* **2013**, *52*, 1228–1237.

[56] V. Y. Pavlov, *Russ. J. Org. Chem.* **2007**, *43*, 1–34.

[57] Z. S. Seddigi, S. A. Ahmed, S. Sardar, N. H. Yarkandi, M. Abdulaziz, S. K. Pal, *RSC Adv.* **2017**, *7*, 12277–12282.

[58] a) N. Alderman, L. Danos, L. Fang, M. C. Grossel, T. Markvart, *Chem. Commun.* **2017**, *53*, 12120–12123; b) K. Oohora, T. Mashima, K. Ohkubo, S. Fukuzumi, T. Hayashi, *Chem. Commun.* **2015**, *51*, 11138–11140; c) S. V. Lepeshkevich, M. V. Parkhats, A. S. Stasheuski, V. V. Britikov, E. S. Jarnikova, S. A. Usanov, B. M. Dzhagarov, *J. Phys. Chem. A* **2014**, *118*, 1864–1878.

[59] a) T. S. Metzger, R. Tel-Vered, I. Willner, *Small* **2016**, *12*, 1605–1614; b) N. Lalaoui, A. Le Goff, M. Holzinger, S. Cosnier, *Chem. Eur. J.* **2015**, *21*, 16868–16873.

[60] a) H. C. Fry, J. M. Garcia, M. J. Medina, U. M. Ricoy, D. J. Gosztola, M. P. Nikiforov, L. C. Palmer, S. I. Stupp, *J. Am. Chem. Soc.* **2012**, *134*, 14646–14649; b) S. V. Bhosale, S. V. Bhosale, G. V. Shitre, S. R. Bobe, A. Gupta, *Eur. J. Org. Chem.* **2013**, 3939–3954.

[61] H. Fischer, A. Kirstahler, *Liebigs Ann. Chem.* **1928**, *466*, 178–188.

[62] a) J. A. S. Cavaleiro, A. M. d. A. R. Gonsalves, G. W. Kenner, K. M. Smith, *J. Chem. Soc., Perkin Trans. 1* **1974**, 1771–1781; b) Y. K. Shim, R. K. Pandey, K. M. Smith, *J. Porphyrins Phthalocyanines* **2000**, *4*, 185–191; c) K. M. Smith, *Acc. Chem. Res.* **1979**, *12*, 374–381; d) K. M. Smith, F. Eivazi, Z. Martynenko, *J. Org. Chem.* **1981**,

46, 2189–2193; e) K. M. Smith, R. K. Pandey, *J. Heterocycl. Chem.* **1983**, *20*, 1383–1388; f) K. M. Smith, R. K. Pandey, *J. Heterocycl. Chem.* **1985**, *22*, 1041–1044; g) K. M. Smith, D. W. Parish, W. S. Inouye, *J. Org. Chem.* **1986**, *51*, 666–671; h) K. M. Smith, M. Miura, I. K. Morris, *J. Org. Chem.* **1986**, *51*, 4660–4667; i) K. M. Smith, E. M. Fujinari, R. K. Pandey, H. D. Tabba, *J. Org. Chem.* **1986**, *51*, 4667–4676; j) K. M. Snow, K. M. Smith, *J. Org. Chem.* **1989**, *54*, 3270–3281; K. M. Smith, F. Eivazi, K. C. Langry, J. A. P. B. de Almeida, G. W. Kenner, *Bioorg. Chem.* **1979**, *8*, 485–495; l) K. M. Smith, J. A. P. B. De Almeida, W. M. Lewis, *J. Heterocycl. Chem.* **1980**, *17*, 481–487; m) K. M. Smith, G. W. Craig, *J. Org. Chem.* **1983**, *48*, 4302–4306.

[63] a) R. T. Holmes, J. Lu, C. Mwakwari, K. M. Smith, *Arkivoc* **2009**, *2010*, 5–16; b) I. Bronshtein, S. Aulova, A. Juzeniene, V. Lani, L.-W. Ma, K. M. Smith, Z. Malik, J. Moan, B. Ehrenberg, *Photochem. Photobiol.* **2006**, *82*, 1319–1325.

[64] P. Martin, M. Müller, D. Flubacher, A. Boudier, H.-U. Blaser, D. Spielvogel, *Org. Process Res. Dev.* **2010**, *14*, 799–804.

[65] a) E. D. Sternberg, D. Dolphin, C. Brückner, *Tetrahedron* **1998**, *54*, 4151–4202; b) K. M. Smith, J. A. S. Cavaleiro, *Heterocycles* **1987**, *26*, 1947–1963; c) H. Fischer, H. Orth, *Die Chemie des Pyrrols*, Akademische Verlagsgesellschaft, Leipzig, **1934**; d) H. Brunner, K. M. Schellerer, B. Treittinger, *Inorg. Chim. Acta* **1997**, *264*, 67–79; e) G. Karagianis, J. Reiss, *Austr. J. Chem* **1995**, *48*, 1693–1705; f) Z.-L. Chen, W.-Q. Wan, J.-R. Chen, F. Zhao, D.-Y. Xu, *Heterocycles* **1998**, *48*, 1739–1745.

[66] a) S. B. Kahl, J. J. Schaeck, M.-S. Koo, *J. Org. Chem.* **1997**, *62*, 1875–1880; b) J.-H. Fuhrhop, K. M. Smith in *Porphyrins and Metalloporphyrins* (Ed.: K. M. Smith), Elsevier, Amsterdam, **1975**, pp. 757–661.

[67] a) M. F. Isaac, S. B. Kahl, *J. Organomet. Chem.* **2003**, *680*, 232–243; b) R. K. Pandey, M. Isaac, C. J. Medforth, M. O. Senge, T. J. Dougherty, K. M. Smith, *J. Org. Chem.* **1997**, *62*, 1463–1472.

[68] X. Jiang, K. M. Smith, *J. Chem. Soc., Perkin Trans. 1* **1996**, 1601–1606.

[69] F.-P. Montforts, B. Gerlach, F. Hoeper, *Chem. Rev.* **1994**, *94*, 327–347.

[70] A. Peixoto, M. M. Pereira, M. G. P. M. S. Neves, A. M. S. Silva, J. A. S. Cavaleiro, *Tetrahedron Lett.* **2003**, *44*, 5593–5595.

[71] a) X. Liu, E. Sternberg, D. Dolphin, *Chem. Commun.* **2004**, 852–853; b) X. Liu, E. Sternberg, D. Dolphin, *J. Org. Chem.* **2008**, *73*, 6542–6550.

[72] a) X. Jiang, R. K. Pandey, K. M. Smith, *J. Chem. Soc., Perkin Trans. 1* **1996**, 1607–1615; b) M. Castella, F. Calahorra, D. Sainz, D. Velasco, *Org. Lett.* **2001**, *3*, 541–544; c) I. K. Morris, K. M. Snow, N. W. Smith, K. M. Smith, *J. Org. Chem.* **1990**, *55*, 1231–1236.

[73] a) R. P. Evstigneeva, V. N. Luzgina, P. S. Timashev, V. A. Ol'shevskaya, L. I. Zakharkin, *Russ. J. Gen. Chem.* **2003**, *73*, 1648–1652; b) V. A. Ol'shevskaya, R. G. Nikitina, A. V. Zaitsev, M. A. Gyul'malieva, V. N. Luzgina, E. G. Kononova, T. G. Morozova, V. V. Drozhzhina, M. A. Kaplan, V. N. Kalinin, A. A. Shtil, *Dokl. Chem.* **2004**, *399*, 245–249; c) H. Murakami, R. Matsumoto, Y. Okusa, T. Sagara, M. Fujitsuka, O. Ito, N. Nakashima, *J. Mater. Chem.* **2002**, *12*, 2026–2033; d) E. Tsuchida, T. Komatsu, N. Toyano, S.-I. Kumamoto, H. Nishide, *J. Chem. Soc., Chem.Commun.* **1993**, 1731–1733.

[74] M. E. El-Zaria, H. S. Ban, H. Nakamura, *Chem. Eur. J.* **2010**, *16*, 1543–1552.

[75] a) V. Sol, F. Lamarche, M. Enache, G. Garcia, R. Granet, M. Guilloton, J. C. Blais, P. Krausz, *Bioorg. Med. Chem.* **2006**, *14*, 1364–1377; b) S. K. Sahoo, T. Sawa, J. Fang, S. Tanaka, Y. Miyamoto, T. Akaike, H. Maeda, *Bioconjugate Chem.* **2002**, *13*, 1031–1038; c) J. H. Fuhrhop, C. Demoulin, C. Boettcher, J. Koening, U. Siggel, *J. Am. Chem. Soc.* **1992**, *114*, 4159–4165; d) I. Hamachi, S. Tanaka, S. Tsukiji, S. Shinkai, S. Oishi, *Inorg. Chem.* **1998**, *37*, 4380–4388; e) R. P. Evstigneeva, G. A. Zheltukhina, V. Khalil, E. I. Efimova, *Bioorg. Khim.* **1999**, *25*, 572–580; f) T. Hayashi, T. Ando, T. Matsuda, H. Yonemura, S. Yamada, Y. Hisaeda, *J. Inorg. Biochem.* **2000**, *82*, 133–139; g) H. Sato, M. Watanabe, Y. Hisaeda, T. Hayashi, *J. Am. Chem. Soc.* **2005**, *127*, 56–57; h) S. M. Sondhi, S. Rajvanshi, M. Johar, S. G. Dastidar, *Ind. J. Chem.* **2002**, *41B*, 388–393; i) S. M. Sondhi, N. Singhal, R. P. Verma, S. K. Arora, S. G. Dastidar, *Ind. J. Chem.* **2001**, *40B*, 113–119; j) S. M. Sondhi, M. Johar, N. Singh, S. G. Dastidar, *Ind. J. Chem.* **2004**, *43B*, 162–167.

[76] S. E. Brantley, B. Gerlach, M. M. Olmstead, K. M. Smith, *Tetrahedron Lett.* **1997**, *38*, 937–940.

[77] K. Miyata, S. Yasuda, T. Masuya, S. Ito, Y. Kinoshita, H. Tamiaki, T. Oba, *Tetrahedron* **2018**, *74*, 3707–3711.

[78] G. Kenner, S. McCombie, K. M. Smith, *J. Chem. Soc., Perkin Trans. 1* **1973**, 2517–2523.

[79] R. Loska, A. Janiga, D. Gryko, *J. Porphyrins Phthalocyanines* **2013**, *17*, 104–117.

[80] A. F. Uchoa, C. S. Oliveira, M. S. Baptista, *J. Porphyrins. Phthalocyanines* **2010**, *14*, 832–845.

[81] S. Tachikawa, M. E. El-Zaria, R. Inomata, S. Sato, H. Nakamura, *Bioorg. Med. Chem.* **2014**, *22*, 4745–4751.

[82] a) S. B. Kahl, M.-S. Koo, *J. Chem. Soc., Chem. Commun.* **1990**, 1769–1771; b) S. Mathai, T. A. Smith, K. P. Ghiggino, *Photochem. Photobiol. Sci.* **2007**, *6*, 995–1002; c) P. Dozzo, M.-S. Koo, S. Berger, T. M. Forte, S. B. Kahl, *J. Med. Chem.* **2005**, *48*,

357–359; d) J. Lee, Y. S. Park, Y. I. Kim, H. C. Kang, *Bull. Korean Chem. Soc.* **1999**, *20*, 1371–1372; e) V. I. Bregadze, I. B. Sivaev, D. Gabel, D. Wöhrle, *J. Porphyrins Phthalocyanines* **2001**, *5*, 767–781; f) S. Mathai, D. K. Bird, S. S. Stylli, T. A. Smith, K. P. Ghiggino, *Photochem. Photobiol. Sci.* **2007**, *6*, 1019–1026.

[83] A. R. Morgan, D. H. Kohli, *Tetrahedron Lett.* **1995**, *36*, 7603–7606.

[84] a) J. S. Hill, S. B. Kahl, S. S. Stylli, Y. Nakamura, M.-S. Koo, A. H. Kaye, *Proc. Natl. Acad. Sci. USA* **1995**, *92*, 12126–12130.; b) M. A. Rosenthal, B. Kavar, J. S. Hill, D. J. Morgan, R. L. Nation, M. Daniel, G. Varigos, M. Searle, S. S. Stylli, R. L. Basser, S. Uren, H. Gerald, M. D. Green, S. B. Kahl, A. H. Kaye, *J. Clin. Oncol.* **2001**, *19*, 519–524.

[85] K. T. de Oliveira, A. M. S. Silva, A. C. Tomé, M. G. P. M. S. Neves, C. R. Neri, V. S. Garcia, O. A. Serra, Y. Iamamoto, J. A. S. Cavaleiro, *Tetrahedron* **2008**, *64*, 8709–8715.

[86] A. F. Uchoa, K. T. de Oliveira, M. S. Baptista, A. J. Bortoluzzi, Y. Iamamoto, O. A. Serra, *J. Org. Chem.* **2011**, *76*, 8824–8832.

[87] J. C. J. M. D. S. Menezes, M. A. F. Faustino, K. T. de Oliveira, M. P. Uliana, V. F. Ferreira, S. Hackbarth, B. Röder, T. Teixeira Tasso, T. Furuyama, N. Kobayashi, A. M. S. Silva, M. G. P. M. S. Neves, J. A. S. Cavaleiro, *Chem. Eur. J.* **2014**, *20*, 13644–13655.

[88] F. de C. da Silva, V. F. Ferreira, M. C. B. V. de Souza, A. C. Tomé, M. G. P. M. S. Neves, A. M. S. Silva, J. A. S. Cavaleiro, *Synlett* **2008**, 1205–1207.

[89] a) S. V. Bhosale, M. B. Kalyankar, S. V. Nalage, S. V. Bhosale, C. H. Lalander, S. J. Langford, *Supramol. Chem.* **2011**, *23*, 563–569; b) S. V. Bhosale, M. B. Kalyankar, S. V. Bhosale, S. G. Patil, C. H. Lalander, S. J. Langford, S. V. Nalage, *Supramol. Chem.* **2011**, *23*, 263–268.

[90] a) T. Asano, K. Yabusaki, P.-C. Wang, A. Iwasaki, *Spectrochim. Acta A* **2010**, *75*, 819–824; b) T. Asano, P.-C. Wang, A. Iwasaki, *Spectrochim. Acta A* **2010**, *75*, 305–309; c) T. Umemura, H. Hotta, T. Abe, Y. Takahashi, H. Takiguchi, M. Uehara, T. Odake, K.-i. Tsunoda, *Anal. Chem.* **2006**, *78*, 7511–7516; d) S. Belali, H. Savoie, J. M. O'Brien, A. A. Cafolla, B. O'Connell, A. R. Karimi, R. W. Boyle, M. O. Senge, *Biomacromolecules* **2018**, *19*, 1592–1601; e) B. Khurana, P. Gierlich, A. Meindl, L. C. Gomes-da-Silva, M. O. Senge, *Photochem. Photobiol. Sci.* **2019**, *18*, 2613–2656; f) W. J. R. Santos, P. R. Lima, C. R. T. Tarley, L. T. Kubota, *J. Braz. Chem. Soc.* **2009**, *20*, 820–825; g) C. Raja, K. Ananthanarayanan, P. Natarajan, *Eur. Polym. J.* **2006**, *42*, 495–506.

[91] L. E. O'Leary, M. J. Rose, T. X. Ding, E. Johansson, B. S. Brunschwig, N. S. Lewis, *J. Am. Chem. Soc.* **2013**, *135*, 10081–10090.

[92] a) K. Han, J.-Y. Zhu, S.-B. Wang, Z.-H. Li, S.-X. Cheng, X.-Z. Zhang, *J. Mater. Chem. B* **2015**, *3*, 8065–8069; b) M. Ashjari, S. Dehfuly, D. Fatehi, R. Shabani, M. Koruji, *RSC Adv.* **2015**, *5*, 104621–104628; c) J. L. Vivero-Escoto, D. L. Vega, *RSC Adv.* **2014**, *4*, 14400–14407; d) T. D. Schladt, K. Schneider, M. I. Shukoor, F. Natalio, H. Bauer, M. N. Tahir, S. Weber, L. M. Schreiber, H. C. Schröder, W. E. G. Müller, W. Tremel, *J. Mater. Chem.* **2010**, *20*, 8297–8304; e) L. M. Rossi, P. R. Silva, L. L. R. Vono, A. U. Fernandes, D. B. Tada, M. S. Baptista, *Langmuir* **2008**, *24*, 12534–12538; f) N. Gharibi, K. Kailass, A. A. Beharry, *ChemBioChem* **2019**, *20*, 345–349; g) F. Taba, A. Onoda, U. Hasegawa, T. Enoki, Y. Ooyama, J. Ohshita, T. Hayashi, *ChemMedChem* **2018**, *13*, 15–19; h) S.-Y. Li, W.-X. Qiu, H. Cheng, F. Gao, F.-Y. Cao, X.-Z. Zhang, *Adv. Funct. Mater.* **2017**, *27*, 1604916; i) K. Han, Q. Lei, S.-B. Wang, J.-J. Hu, W.-X. Qiu, J.-Y. Zhu, W.-N. Yin, X. Luo, X.-Z. Zhang, *Adv. Funct. Mater.* **2015**, *25*, 2961–2971; j) S. Singh, A. Chakraborty, V. Singh, A. Molla, S. Hussain, M. K. Singh, P. Das, *Phys. Chem. Chem. Phys.* **2015**, *17*, 5973–5981; k) C. Aggelidou, T. A. Theodossiou, K. Yannakopoulou, *Photochem. Photobiol.* **2013**, *89*, 1011–1019; l) T. Sagir, S. Gencer, N. Kemikli, M. F. Abasiyanik, S. Isik, R. Ozturk, *Med. Chem. Res.* **2012**, *21*, 4499–4505; m) M. Sibrian-Vazquez, X. Hu, T. J. Jensen, M. G. H. Vicente, *J. Porphyrins Phthalocyanines* **2012**, *16*, 603–615; n) C. L. Conway, I. Walker, A. Bell, D. J. H. Roberts, S. B. Brown, D. I. Vernon, *Photochem. Photobiol. Sci.* **2008**, *7*, 290–298; o) M. Kwitniewski, D. Kunikowska, B. Dera-Tomaszewska, E. Tokarska-Pietrzak, H. Dziadziuszko, A. Graczyk, R. Glosnicka, *J. Photochem. Photobiol. B: Biol.* **2005**, *81*, 129–135; p) A.-N. Zhang, W. Wu, C. Zhang, Q.-Y. Wang, Z.-N. Zhuang, H. Cheng, X.-Z. Zhang, *J. Mater. Chem. B* **2019**, *7*, 1087–1095; q) J. Dong, R. A. Ghiladi, Q. Wang, Y. Cai, Q. Wei, *Nanotechnology* **2018**, *29*, 265601; r) C. Ringot, N. Saad, F. Brégier, P. Bressollier, E. Poli, V. Chaleix, T. S. Ouk, V. Sol, *Photochem. Photobiol. Sci.* **2018**, *17*, 1780–1786; s) G. Zampini, O. Planas, F. Marmottini, O. Gulías, M. Agut, S. Nonell, L. Latterini, *RSC Adv.* **2017**, *7*, 14422–14429; t) F. Liu, A. Soh Yan Ni, Y. Lim, H. Mohanram, S. Bhattacharjya, B. Xing, *Bioconjugate Chem.* **2012**, *23*, 1639–1647; u) I. Banerjee, M. P. Douaisi, D. Mondal, R. S. Kane, *Nanotechnology* **2012**, *23*, 105101; v) I. Banerjee, D. Mondal, J. Martin, R. S. Kane, *Langmuir* **2010**, *26*, 17369–17374; w) M. E. Bakleh, V. Sol, R. Granet, G. Déléris, K. Estieu-Gionnet, P. Krausz, *Chem. Commun.* **2010**, *46*, 2115–2117.

[93] N. Kemikli, H. Kavas, S. Kazan, A. Baykal, R. Ozturk, *J. Alloys Compd.* **2010**, *502*, 439–444.

[94] S. Banerjee, A. Dhir, T. Banerjee, A. K. Singh, A. Datta, *J. Chem. Sci.* **2011**, *123*, 901–907.

[95] a) B. Yan, Y.-Y. Li, X.-F. Qiao, *Micropor. Mesopor. Mat.* **2012**, *158*, 129–136; b) M. Shirakawa, N. Fujita, A. Takada, S. Shinkai, *Chem. Lett.* **2014**, *43*, 1330–1332; c) S. Boufi, M. Rei Vilar, V. Parra, A. M. Ferraria, A. M. Botelho do Rego, *Langmuir* **2008**, *24*, 7309–7315.

[96] a) J. Zhu, G. Sun, *J. Mater. Chem.* **2012**, *22*, 10581–10588; b) M. Trytek, A. Lipke, M. Majdan, S. Pisarek, D. Gryko, *Eur. J. Org. Chem.* **2013**, 1653–1658.

[97] a) T. S. Metzger, R. Tel-Vered, H. B. Albada, I. Willner, *Adv. Funct. Mater.* **2015**, *25*, 6470–6477; b) A. Onoda, Y. Kakikura, T. Uematsu, S. Kuwabata, T. Hayashi, *Angew. Chem. Int. Ed.* **2012**, *51*, 2628–2631.

[98] a) V. Pirota, F. Gennarini, D. Dondi, E. Monzani, L. Casella, S. Dell'Acqua, *New J. Chem.* **2014**, *38*, 518–528; b) C. Dallacosta, W. A. Alves, A. M. da Costa Ferreira, E. Monzani, L. Casella, *Dalton Trans.* **2007**, 2197–2206.

[99] a) R.-H. Pan, T.-L. Zhang, D.-X. Han, C.-L. Liu, *Chin. J. Chem.* **2006**, *24*, 1037–1044; b) G. Delaittre, I. C. Reynhout, J. J. L. M. Cornelissen, R. J. M. Nolte, *Chem. Eur. J.* **2009**, *15*, 12600–12603.

[100] a) V. Singh, M. Monisha, R. Anindya, P. Das, *RSC Adv.* **2015**, *5*, 89025–89029; b) S. V. Bhosale, S. V. Nalage, J. M. Booth, A. Gupta, S. K. Bhargava, S. V. Bhosale, *Supramol. Chem.* **2012**, *24*, 779–786; c) M. Mirzaei Salehabady, F. Mehrnejad, A. Heidari, M. N. Sarbolouki, H. Naderi-Manesh, *Iran. J. Chem. Chem. Eng.* **2011**, *30*, 109–112; d) S. V. Bhosale, S. V. Bhosale, M. B. Kalyankar, S. J. Langford, C. H. Lalander, *Austr. J. Chem.* **2010**, *63*, 1326–1329; e) H. Kitagishi, K. Oohora, H. Yamaguchi, H. Sato, T. Matsuo, A. Harada, T. Hayashi, *J. Am. Chem. Soc.* **2007**, *129*, 10326–10327.

[101] C. C. Fernández, C. Spedalieri, D. H. Murgida, F. J. Williams, *J. Phys. Chem. C* **2017**, *121*, 21324–21332.

[102] K. Maximova, S. Pisarek, D. Gryko, *Synthesis* **2013**, *45*, 1099–1105.

[103] E. Sitte, M. O. Senge, *Eur. J. Org. Chem.* **2020**, 3171–3191.

[104] a) R. Rodriguez, K. M. Miller, J. V. Forment, C. R. Bradshaw, M. Nikan, S. Britton, T. Oelschlaegel, B. Xhemalce, S. Balasubramanian, S. P. Jackson, *Nat. Chem. Biol.* **2012**, *8*, 301–310; b) N. Maizels, *Curr. Biol.* **2008**, *18*, R613–R614; c) H. J. Lipps, D. Rhodes, *Trends Cell Biol.* **2009**, *19*, 414–422; d) J. Eddy, N. Maizels, *Nucleic Acids Res.* **2006**, *34*, 3887–3896.

[105] a) J. Ida, S. K. Chan, J. Glökler, Y. Y. Lim, Y. S. Choong, T. S. Lim, *Molecules* **2019**, *24*, 1079–1108; b) B. Ruttkay-Nedecky, J. Kudr, L. Nejdl, D. Maskova, R. Kizek, V. Adam, *Molecules* **2013**, *18*, 14760–14779.

[106] a) J. L. Neo, K. Kamaladasan, M. Uttamchandani, *Curr. Pharm. Des.* **2012**, *18*, 2048–2057; b) I. Willner, B. Shlyahovsky, M. Zayats, B. Willner, *Chem. Soc. Rev.* **2008**, *37*, 1153–1165; c) J. Kosman, B. Juskowiak, *Anal. Chim. Acta* **2011**, *707*, 7–17; d) D. Sen, L. C. H. Poon, *Crit. Rev. Biochem. Mol. Biol.* **2011**, *46*, 478–492.

[107] a) H. Yaku, T. Murashima, D. Miyoshi, N. Sugimoto, *Molecules* **2012**, *17*, 10586–10613; b) I. Rozas, M. O. Senge, *Future Med. Chem.* **2016**, *8*, 609–612.

[108] a) A.-M. Chiorcea-Paquim, R. Eritja, A. M. Oliveira-Brett, *J. Nucleic Acids* **2018**, *2018*, 1–20; b) H. Funabashi, *Electrochemistry* **2016**, *84*, 290–295.

[109] T. B. Melø, G. Reisæter, *Biophys. Chem.* **1986**, *25*, 99–104.

[110] T. Li, E. Wang, S. Dong, *Anal. Chem.* **2010**, *82*, 7576–7580.

[111] T. Li, E. Wang, S. Dong, *J. Am. Chem. Soc.* **2009**, *131*, 15082–15083.

[112] a) Z.-Z. Yang, Z.-B. Wen, X. Peng, Y.-Q. Chai, W.-B. Liang, R. Yuan, *Chem. Commun.* **2019**, *55*, 6453–6456; b) Q. Xue, C. Liu, X. Li, L. Dai, H. Wang, *Bioconjugate Chem.* **2018**, *29*, 1399–1405; c) Z. Zhang, E. Sharon, R. Freeman, X. Liu, I. Willner, *Anal. Chem.* **2012**, *84*, 4789–4797; d) Q. Xue, Y. Lv, Y. Zhang, S. Xu, R. Li, Q. Yue, H. Li, L. Wang, X. Gu, S. Zhang, J. Liu, *Biosens. Bioelectron.* **2014**, *61*, 351–356; e) J. Zhu, L. Zhang, Z. Zhou, S. Dong, E. Wang, *Anal. Chem.* **2014**, *86*, 312–316.

[113] J. Zhu, L. Zhang, E. Wang, *Chem. Commun.* **2012**, *48*, 11990–11992.

[114] C. Wang, H. Yang, S. Wu, Y. Liu, W. Wei, Y. Zhang, M. Wei, S. Liu, *Trends Anal. Chem.* **2018**, *105*, 404–412.

[115] N. W. Kim, M. A. Piatyszek, K. R. Prowse, C. B. Harley, M. D. West, P. L. Ho, G. M. Coviello, W. E. Wright, S. L. Weinrich, J. W. Shay, *Science* **1994**, *266*, 2011–2015.

[116] a) Q. Xue, Y. Zhang, S. Xu, H. Li, L. Wang, R. Li, Y. Zhang, Q. Yue, X. Gu, S. Zhang, J. Liu, H. Wang, *Analyst* **2015**, *140*, 7637–7644; b) Q. Xue, Y. Lv, S. Xu, Y. Zhang, L. Wang, R. Li, Q. Yue, H. Li, X. Gu, S. Zhang, J. Liu, *Biosens. Bioelectron.* **2015**, *66*, 547–553; c) Z. Zhou, J. Zhu, L. Zhang, Y. Du, S. Dong, E. Wang, *Anal. Chem.* **2013**, *85*, 2431–2435; d) F. Yang, X. Li, J. Li, Y. Xiang, R. Yuan, *Talanta* **2019**, *204*, 812–816.

[117] P. W. Laird, R. Jaenisch, *Annu. Rev. Genet.* **1996**, *30*, 441–464.

[118] G. Ma, Z. Yu, W. Zhou, Y. Li, L. Fan, X. Li, *J. Phys. Chem. B* **2019**, *123*, 5405–5411.

[119] a) Z. Yu, W. Zhou, J. Han, Y. Li, L. Fan, X. Li, *Anal. Chem.* **2016**, *88*, 9375–9380; b) Y. Bai, F. Feng, L. Zhao, Z. Chen, H. Wang, Y. Duan, *Anal. Methods* **2014**, *6*, 662–665; c) T. Li, S. Dong, E. Wang, *J. Am. Chem. Soc.* **2010**, *132*, 13156–13157.

[120] a) C. R. Geyer, D. Sen, *J. Mol. Biol.* **2000**, *299*, 1387–1398; b) Y. Li, D. Sen, *Biochemistry* **1997**, *36*, 5589–5599; c) Y. Li, D. Sen, *Nat. Struct. Biol.* **1996**, *3*, 743–747.

[121] L. Zhang, J. Zhu, J. Ai, Z. Zhou, X. Jia, E. Wang, *Biosens. Bioelectron.* **2013**, *39*, 268–273.

[122] a) F. Liu, A. Ding, J. Zheng, J. Chen, B. Wang, *Sensors* **2018**, *18*, 1769–1778; b) J.-H. Park, J.-Y. Byun, H. Jang, D. Hong, M.-G. Kim, *Biosens. Bioelectron.* **2017**, *97*, 292–298; c) B. H. Kang, N. Li, S. G. Liu, N. B. Li, H. Q. Luo, *Anal. Sci.* **2016**, *32*, 887–892.

[123] Y. Lv, Q. Xue, X. Gu, S. Zhang, J. Liu, *Analyst* **2014**, *139*, 2583–2588.

[124] a) J. Ai, T. Li, B. Li, Y. Xu, D. Li, Z. Liu, E. Wang, *Anal. Chim. Acta* **2012**, *741*, 93–99; b) Z. Zhou, D. Li, L. Zhang, E. Wang, S. Dong, *Talanta* **2015**, *134*, 298–304.

[125] T. Hayashi, D. Hilvert, A. P. Green, *Chem. Eur. J.* **2018**, *24*, 11821–11830.

[126] a) E. M. Boon, M. A. Marletta, *J. Am Chem. Soc.* **2006**, *128*, 10022–10023; b) E. E. Weinert, L. Plate, C. A. Whited, C. Olea Jr., M. A. Marletta, *Angew. Chem. Int. Ed.* **2010**, *49*, 720–723; c) M. B. Winter, E. J. McLaurin, S. Y. Reece, C. Olea Jr., D. G. Nocera, M. A. Marletta, *J. Am. Chem. Soc.* **2010**, *132*, 5582–5583.

[127] M. B. Winter, P. J. Klemm, C. M. Phillips-Piro, K. N. Raymond, M. A. Marletta, *Inorg. Chem.* **2013**, *52*, 2277–2279.

[128] A. Nierth, M. A. Marletta, *Angew. Chem. Int. Ed.* **2014**, *53*, 2611–2614.

[129] a) T. M. Makris, K. v. Koenig, I. Schlichting, S. G. Sligar, *J. Inorg. Biochem.* **2006**, *100*, 507–518; b) M. S. Mondal, S. Mitra, *Biochim. Biophys. Acta, Protein Struct. Mol. Enzymol.* **1996**, *1296*, 174–180; c) T. Yonetani, T. Asakura, *J. Biol. Chem.* **1968**, *243*, 3996–3998; d) K. K. Khan, M. S. Mondal, S. Mitra, *J. Chem. Soc., Dalton Trans.* **1996**, 1059–1062; e) L. M. Landino, L. J. Marnett, *Biochemistry* **1996**, *35*, 2637–2643; f) R. J. Nick, G. B. Ray, K. M. Fish, T. G. Spiro, J. T. Groves, *J. Am. Chem. Soc.* **1991**, *113*, 1838–1840; g) K. Kumar Khan, M. Sudan Mondal, S. Mitra, *J. Chem. Soc., Dalton Trans.* **1998**, 533–536; h) A. Gengenbach, S. Syn, X. Wang, Y. Lu, *Biochemistry* **1999**, *38*, 11425–11432; i) C. Veeger, *J. Inorg. Biochem.* **2002**, *91*, 35–45; j) J.-L. Primus, S. Grunenwald, P.-L. Hagedoorn, A.-M. Albrecht-Gary, D. Mandon, C. Veeger, *J. Am. Chem. Soc.* **2002**, *124*, 1214–1221; k) M. S. Mondal, S. Mazumdar, S. Mitra, *Inorg. Chem.* **1993**, *32*, 5362–5367; l) D. W. Low, S. Abedin, G. Yang, J. R. Winkler, H. B. Gray, *Inorg. Chem.* **1998**, *37*, 1841–1843.

[130] Y.-B. Cai, X.-H. Li, J. Jing, J.-L. Zhang, *Metallomics* **2013**, *5*, 828–835.

[131] a) L. K. Stone, J. Hua, H. Choudhry, *Inorganics* **2015**, *3*, 219–229; b) Y.-B. Cai, S.-Y. Yao, M. Hu, X. Liu, J.-L. Zhang, *Inorg. Chem. Front.* **2016**, *3*, 1236–1244.

[132] Y. Daijima, T. Komatsu, *Chem. Commun.* **2014**, *50*, 14716–14719.

[133] a) K. Oohora, Y. Kihira, E. Mizohata, T. Inoue, T. Hayashi, *J. Am. Chem. Soc.* **2013**, *135*, 17282–17285; b) M. Bordeaux, R. Singh, R. Fasan, *Bioorg. Med. Chem.* **2014**, *22*, 5697–5704.

[134] a) H. M. Key, P. Dydio, D. S. Clark, J. F. Hartwig, *Nature* **2016**, *534*, 534–537; b) S. N. Natoli, J. F. Hartwig, *Acc. Chem. Res.* **2019**, *52*, 326–335.

[135] P. Dydio, H. M. Key, A. Nazarenko, J. Y. E. Rha, V. Seyedkazemi, D. S. Clark, J. F. Hartwig, *Science* **2016**, *354*, 102.

[136] H. M. Key, P. Dydio, Z. Liu, J. Y. E. Rha, A. Nazarenko, V. Seyedkazemi, D. S. Clark, J. F. Hartwig, *ACS Cent. Sci.* **2017**, *3*, 302–308.

[137] a) P. Dydio, H. M. Key, H. Hayashi, D. S. Clark, J. F. Hartwig, *J. Am. Chem. Soc.* **2017**, *139*, 1750–1753; b) Y. Gu, S. N. Natoli, Z. Liu, D. S. Clark, J. F. Hartwig, *Angew. Chem. Int. Ed.* **2019**, *58*, 13954–13960.

[138] G. Sreenilayam, E. J. Moore, V. Steck, R. Fasan, *Adv. Synth. Catal.* **2017**, *359*, 2076–2089.

[139] T. Komatsu, R.-M. Wang, P. A. Zunszain, S. Curry, E. Tsuchida, *J. Am. Chem. Soc.* **2006**, *128*, 16297–16301.

[140] a) T. Hayashi, Y. Hisaeda, *Acc. Chem. Res.* **2002**, *35*, 35–43; b) T. Hayashi, T. Takimura, H. Ogoshi, *J. Am. Chem. Soc.* **1995**, *117*, 11606–11607; c) Y. Hitomi, T. Hayashi, K. Wada, T. Mizutani, Y. Hisaeda, H. Ogoshi, *Angew. Chem. Int. Ed.* **2001**, *40*, 1098–1101.

[141] T. Matsuo, A. Asano, T. Ando, Y. Hisaeda, T. Hayashi, *Chem. Commun.* **2008**, *31*, 3684–3686.

[142] A. Onoda, Y. Kakikura, T. Hayashi, *Dalton Trans.* **2013**, *42*, 16102–16107.

[143] D. J. Sommer, M. D. Vaughn, G. Ghirlanda, *Chem. Commun.* **2014**, *50*, 15852–15855.

[144] a) G. M. Locke, S. S. R. Bernhard, M. O. Senge, *Chem. Eur. J.* **2019**, *25*, 4590–4647; b) N. Grover, M. O. Senge, *Synthesis* **2020**, *52*, 3295–3325.

[145] a) M. P. Johnson, *Essays Biochem.* **2016**, 60, 255–273; b) N. Nelson, A. Ben-Shem, *Nat. Rev. Mol. Cell Bio.* ***2004***, *5*, 971–982.

[146] a) H. Kurreck, M. Huber, *Angew. Chem. Int. Ed.* **1995**, *34*, 849–866; b) M. R. Wasielewski, *Chem. Rev.* **1992**, *92*, 435–461.

[147] R. A. Marcus, N. Sutin, *Biochim. Biophys. Acta* **1985**, *811*, 265–322.

[148] a) H. B. Gray, J. R. Winkler, *Proc. Natl. Acad. Sci. U.S.A.* **2005**, *102*, 3534–3539; b) H. Oevering, M. N. Paddon-Row, M. Heppener, A. M. Oliver, E. Cotsaris, J. W. Verhoeven, N. S. Hush, *J. Am. Chem. Soc.* **1987**, *109*, 3258–3269; c) M. D. Johnson, J. R. Miller, N. S. Green, G. L. Cross, *J. Phys. Chem.* **1989**, *93*, 1173–1176.

[149] W. B. Davis, W. A. Svec, M. A. Ratner, M.R. Wasielewski, *Nature* **1998**, *396*, 60–63.

[150] D. Holten, D. F. Bocian, J. S. Lindsey, *Acc. Chem. Res.* **2002**, *35*, 57–69.

[151] K. B. Wiberg, D. S. Connor, G. M. Lampman, *Tetrahedron Lett.* **1964**, *5*, 531–534.

[152] K. B. Wiberg, D. S. Connor, *J. Am. Chem. Soc.* **1966**, *88*, 4437–4441.

[153] K. B. Wiberg, F. H. Walker, *J. Am. Chem. Soc.* **1982**, *104*, 5239–5240.

[154] J. Altman, E. Babad, J. Itzchaki, D. Ginsburg, *Tetrahedron* **1966**, *22*, 279–304.

[155] a) J. Belzner, U. Bunz, K. Semmler, G. Szeimies, K. Opitz, A.-D. Schlüter, *Chem. Ber.* **1989**, *122*, 397–398; b) M. Werner, D. S. Stephenson, G. Szeimies, *Liebigs Ann.***1996**, *1996*, 1705–1715; c) K. R. Mondanaro, W. P. Dailey, *Org. Synth.* **1998**, *75*, 98.

[156] T. Matsunaga, J. Kanazawa, T. Ichikawa, M. Harada, Y. Nishiyama, N. T. Duong, T. Matsumoto, K. Miyamoto, M. Uchiyama, *Angew. Chem. Int. Ed.* **2021**, *60*, 2578–2582.

[157] a) M. D. Levin, P. Kaszynski, J. Michl, *Chem. Rev.* **2000**, *100*, 169–234; b) P. Kaszynski, J. Michl, in *The Chemistry of the Cyclopropyl Group* (Ed.: Z. Rappoport), John Wiley, New York, **1995**, Vol. 2, pp. 773–812; c) V. Galasso, *Chem. Phys. Lett.* **1994**, *230*, 387–390; d) E. Honegger, H. Huber, E. Heilbronner, W. P. Dailey, K. B. Wiberg, *J. Am. Chem. Soc.* **1985**, *107*, 7172–7174; e) O. Schafer, M. Allan, G. Szeimies, M. Sanktjohanser, *J. Am. Chem. Soc.* **1992**, *114*, 8180–8186.

[158] a) W. Wu, J. Gu, J. Song, S. Shaik, P. C. Hiberty, *Angew. Chem. Int. Ed.* **2009**, *48*, 1407–1410; b) M. Messerschmidt, S. Scheins, L. Grubert, M. Pätzel, G. Szeimies, C. Paulmann, P. Luger, *Angew. Chem. Int. Ed.* **2005**, *44*, 3925–3928.

[159] a) D. Feller, E. R. Davidson, *J. Am. Chem. Soc.* **1987**, *109*, 4133–4139; b) K. B. Wiberg, C. M. Hadad, S. Sieber, P. v. R. Schleyer, *J. Am. Chem. Soc.* **1992**, *114*, 5820–5828.

[160] K. B. Wiberg, *Angew. Chem. Int. Ed.* **1986**, *25*, 312–322.

[161] A. Baeyer, *Ber. Dtsch. Chem. Ges.* **1885**, *18*, 2269–2281.

[162] a) K. S. Pitzer, *J. Chem. Phys.* **1937**, *5*, 473–479; b) J. D. Kemp, K. S. Pitzer, *J. Chem. Phys.* **1936**, *4*, 749–750.

[163] J. D. Dunitz, V. Prelog, *Angew. Chem.* **1960**, *72*, 896–902.

[164] J. F. Chiang, S. H. Bauer, *J. Am. Chem. Soc.* **1970**, *92*, 1614–1617.

[165] A. Almenningen, B. Andersen, B. A. Nyhus, P. Beronius, J. E. Engebretsen, L. Ehrenberg, *Acta Chem. Scand.* **1971**, *25*, 1217–1223.

[166] a) E. W. Della, E. Cotsaris, P. T. Hine, P. E. Pigou, *Aust. J. Chem.* **1981**, *34*, 913–916; b) C. J. Rhodes, J. C. Walton, E. W. Della, *J. Chem. Soc., Perkin Trans. 2* **1993**, 2125–2128.

[167] K. B. Wiberg, *Tetrahedron Lett.* **1985**, *26*, 599–602.

[168] R. Srinivasan, *J. Am. Chem. Soc.* **1968**, *90*, 2752–2754.

[169] J. L. Adcock, A. A. Gakh, J. L. Pollitte, C. Woods, *J. Am. Chem. Soc.* **1992**, *114*, 3980–3981.

[170] a) G. S. Murthy, K. Hassenruck, V. M. Lynch, J. Michl, *J. Am. Chem. Soc.* **1989**, *111*, 7262–7263; b) J. D. Daniel Rehm, B. Ziemer, G. Szeimies, *Eur. J. Org. Chem.* **1999**, 2079–2085.

[171] P. Kaszynski, J. Michl, in *Advances in Strain in Organic Chemistry* (Ed. B. Halton), JAI Press, Greenwich, **1995**, Vol. 4, pp. 283–331.

[172] a) K. B. Wiberg, B. S. Ross, J. J. Isbell, N. McMurdie, *J. Org. Chem.* **1993**, *58*, 1372–1376; b) K. B. Wiberg, V. Z. Williams, *J. Org. Chem.* **1970**, *35*, 369–373.

[173] A. d. Meijere, L. Zhao, V. N. Belov, M. Bossi, M. Noltemeyer, S. W. Hell, *Chem. Eur. J.* **2007**, *13*, 2503–2516.

[174] A. Sella, H. Basch, S. Hoz, *Tetrahedron Lett.* **1996**, *37*, 5573–5576.

[175] A. J. Sterling, A. B. Dürr, R. C. Smith, E. A. Anderson, F. Duarte, *Chem. Sci.* **2020**, 11, 4895–4903.

[176] E. W. Della, P. E. Pigou, C. H. Schiesser, D. K. Taylor, *J. Org. Chem.* **1991**, *56*, 4659–4664.

[177] P. Kaszynski, J. Michl, *J. Am. Chem. Soc.* **1988**, *110*, 5225–5226.

[178] a) K. B. Wiberg, S. T. Waddell, K. Laidig, *Tetrahedron Lett.* **1986**, *27*, 1553–1556; b) K. B. Wiberg, S. T. Waddell, *J. Am. Chem. Soc.* **1990**, *112*, 2194–2216.

[179] P. Kaszynski, J. Michl, *J. Org. Chem.* **1988**, *53*, 4594–4596.

[180] K. Donnelly, M. Baumann, *Chem. Commun.* **2021**, *57*, 2871-2874.

[181] N. Grover, G. M. Locke, K. J. Flanagan, M. H. Beh, A. Thompson, M. O. Senge, *Chem. Eur. J.* **2020**, *26*, 2405−2416.

[182] a) A. M. Dilmaç, E. Spuling, A. de Meijere, S. Bräse, *Angew. Chem. Int. Ed.* **2017**, *56*, 5684–5718; b) R. Pellicciari, M. Raimondo, M. Marinozzi, B. Natalini, G. Costantino, C. Thomsen, *J. Med. Chem.* **1996**, *39*, 2874–2876; c) M. Pätzel, M. Sanktjohanser, A. Doss, P. Henklein, G. Szeimies, *Eur. J. Org. Chem.* **2004**, 493–498; d) A. F. Stepan, C. Subramanyam, I. V. Efremov, J. K. Dutra, T. J. O'Sullivan,

K. J. DiRico, W. S. McDonald, A. Won, P. H. Dorff, C. E. Nolan, S. L. Becker, L. R. Pustilnik, D. R. Riddell, G. W. Kauffman, B. L. Kormos, L. Zhang, Y. Lu, S. H. Capetta, M. E. Green, K. Karki, E. Sibley, K. P. Atchison, A. J. Hallgren, C. E. Oborski, A. E. Robshaw, B. Sneed, C. J. O'Donnell, *J. Med. Chem.* **2012**, *55*, 3414–3424; e) K. C. Nicolaou, J. Yin, D. Mandal, R. D. Erande, P. Klahn, M. Jin, M. Aujay, J. Sandoval, J. Gavrilyuk, D. Vourloumis, *J. Am. Chem. Soc.* **2016**, *138*, 1698–1708.

[183] F. Toriyama, J. Cornella, L. Wimmer, Tie-Gen Chen, D. D. Dixon, G. Creech, P. S. Baran, *J. Am. Chem. Soc.* **2016**, *138*, 11132–11135.

[184] K. Semmler, G. Szeimies, J. Belzner, *J. Am. Chem. Soc.* **1985**, *107*, 6410–6411.

[185] a) R. M. Bär, S. Kirschner, M. Nieger, S. Bräse, *Chem. Eur. J.* **2018**, *24*, 1373–1382; b) R. M. Bär, P. J. Gross, M. Nieger, S. Bräse, *Chem. Eur. J.* **2020**, *26*, 4242–4245; c) R. M. Bär, L. Langer, M. Nieger, S. Bräse, *Adv. Synth. Catal.* **2020**, *362*, 1356–1361.

[186] S. O. Kokhan, Y. B. Valter, A. V. Tymtsunik, I. V. Komarov, O. O. Grygorenko, *Eur. J. Org. Chem.* **2020**, 2210–2216.

[187] R. M. Bär, G. Heinrich, M. Nieger, O. Fuhr, S. Bräse, *Beilstein J. Org. Chem.* **2019**, *15*, 1172–1180.

[188] a) Z. Wu, Y. Xu, J. Liu, X. Wu, C. Zhu, *Sci. China Chem.* **2020**, *63*, 1025–1029; b) Z. Wu, Y. Xu, X. Wu, C. Zhu, *Tetrahedron* **2020**, *76*, 131692–131698.

[189] a) K. B. Wiberg, V. Z. Williams, *J. Org. Chem.* **1970**, *35*, 369–373; b) Md. T. Hossain, J. W. Timberlake, *J. Org. Chem.* **2001**, *66*, 6282–6285; c) M. R. Barbachyn, D. K. Hutchinson, D. S. Toops, R. J. Reid, G. E. Zurenko, B. H. Yagi, R. D. Schaadt, J. W. Allison, *Bioorg. Med. Chem. Lett.* **1993**, *3*, 671–676.

[190] a) Y. L. Goh, V. A. Adsool, *Org. Biomol. Chem.* **2015**, *13*, 11597–11601; b) C. Zarate, M. Ardolino, G. J. Morriello, K. M. Logan, W. P. Kaplan, L. Torres, D. Li, M. Chen, H. Li, J. Su, P. Fuller, M. L. Maddess, Z. J. Song, *Org. Process Res. Dev.* **2021**, *25*, 642–647.

[191] D. S. Toops, M. R. Babachyn, *J. Org. Chem.* **1993**, *58*, 6505–6508.

[192] K. D. Bunker, N. W. Sach, Q. Huang, P. F. Richardson, *Org. Lett.* **2011**, *13*, 4746–4748.

[193] J. Kanazawa, K. Maeda, M. Uchiyama, *J. Am. Chem. Soc.* **2017**, *139*, 17791–17794.

[194] Y. L. Goh, E. K. W. Tam, P. H. Bernardo, C. B. Cheong, C. W. Johannes, A. D. Williams, V. A. Adsool, *Org. Lett.* **2014**, *16*, 1884–1887.

[195] N. T. Thirumoorthi, C. J. Shen, V. A. Adsool, *Chem. Commun.* **2015**, *51*, 3139–3142.

[196] a) R. Gianatassio, J. M. Lopchuk, J. Wang, C.-M. Pan, l. R. Malins, L. Prieto, T. A. Brandt, M. R. Collins, G. M. Gallego, N. W. Sach, J. E. Spangler, H. Zhu, J. Zhu, P.

S. Baran, *Science* **2016**, *351*, 241–246; b) J. M. Lopchuk, K. Fjelbye, Y. Kawamata, L. R. Malins, C.-M. Pan, R. Gianatassio, J. Wang, L. Prieto, J. Bradow, T. A. Brandt, M. R. Collins, J. Elleraas, J. Ewanicki, W. Farrell, O. O. Fadeyi, G. M. Gallego, J. J. Mousseau, R. Oliver, N. W. Sach, J. K. Smith, J. E. Spangler, H. Zhu, J. Zhu, P. S. Baran, *J. Am. Chem. Soc.* **2017**, *139*, 3209–3226.

[197] S. O. Kokhan, Y. B. Valter, A. V. Tymtsunik, I. V. Komarov, O. O. Grygorenko, *Eur. J. Org. Chem.* **2017**, 6450–6456.

[198] J. M. E. Hughes, D. A. Scarletta, A. C.-Y. Chen, J. D. Burch, J. L. Gleason, *Org. Lett.* **2019**, *21*, 6800–6804.

[199] S. Shin, S. Lee, W. Choi, N. Kim, S. Hong, *Angew. Chem. Int. Ed.* **2021**, *60*, 7873–7879.

[200] a) J. D. Daniel Rehm, B. Ziemer, G. Szeimies, *Eur. J. Org. Chem.* **1999**, 2079–2085; b) M. Messner, S. I. Kozhushkov, A. de Meijere, *Eur. J. Org. Chem.* **2000**, 1137–1155; c) I. S. Makarov, C. E. Brocklehurst, K. Karaghiosoff, G. Koch, P. Knochel, *Angew. Chem. Int. Ed.* **2017**, *56*, 12774–12777.

[201] S. Yu, C. Jing, A. Noble, V. K. Aggarwal, *Angew. Chem. Int. Ed.* **2020**, *59*, 3917–3921.

[202] S. Yu, C. Jing, A. Noble, V. K. Aggarwal, *Org. Lett.* **2020**, *22*, 5650–5655.

[203] V. K. Vyas, G. J. Clarkson, M. Wills, *Org. Lett.* **2021**, *23*, 3179–3183.

[204] K. B. Wiberg, S. T. Waddell, *Tetrahedron Lett.* **1988**, *29*, 289–292.

[205] P. Kaszynski, N. D. McMurdie, J. Michl, *J. Org. Chem.* **1991**, *56*, 307–316.

[206] D. F. J. Caputo, C. Arroniz, A. B. Dürr, J. J. Mousseau, A. F. Stepan, S. J. Mansfield, E. A. Anderson, *Chem. Sci.* **2018**, *9*, 5295–5300.

[207] J. Nugent, B. R. Shire, D. F. Caputo, H. D. Pickford, F. Nightingale, I. T. T. Houlsby, J. J. Mousseau, E. A. Anderson, *Angew. Chem. Int. Ed.* **2020**, *59*, 11866–11870.

[208] M. L. J. Wong, J. J. Mousseau, S. J. Mansfield, E. A. Anderson, *Org. Lett.* **2019**, *21*, 2408–2411.

[209] Z. J. Garlets, J. N. Sanders, H. Malik, C. Gampe, K. N. Houk, H. M. L. Davies, *Nat. Catal.* **2020**, *3*, 351–357.

[210] M. Konodo, J. Kanazawa, T. Ichikawa, T. Shimokawa, Y. Nagashima, K. Miyamoto, M. Uchiyama, *Angew. Chem. Int. Ed.* **2020**, *59*, 1970–1974.

[211] S. K. Rout, G. Marghem, J. Lan, T. Leyssens, O. Riant, *Chem. Commun.* **2019**, *55*, 14976–14979.

[212] a) J. Nugent, C. Arroniz, B. R. Shire, A. J. Sterling, H. D. Pickford, M. L. J. Wong, S. J. Mansfield, D. F. Caputo, B. Owen, J. J. Mousseau, F. Duarte, E. A. Anderson,

ACS Catal. **2019**, *9*, 9568–9574; b) H. Zhang, M. Wang, X. Wu, C. Zhu, *Chin. J. Org. Chem.* **2020**, *40*, 3431–3438.

[213] M .L. J. Wong, A. J. Sterling, J. J. Mousseau, F. Duarte, E. A. Anderson, *Nat. Commun.* **2021**, *12*, 1644–1652.

[214] X. Zhang, R. T. Smith, C. Le, S. J. McCarver, B. T. Shireman, N. I. Carruthers, D. W. C. MacMillan, *Nature* **2020**, *580*, 220–226.

[215] M. D. VanHeyst, J. Qi, A. J. Roecker, J. M. E. Hughes, L. Cheng, Z. Zhao, J. Yin, *Org. Lett.* **2020**, *22,* 1648–1654.

[216] R. A. Shelp, P. J. Walsh, *Angew. Chem. Int. Ed.* **2018**, *57*, 15867–15861.

[217] N. Trongsiriwat, Y. Pu, Y. Nieves-Quinones, R. A. Shelp, M. C. Kozlowski, P. J. Walsh, *Angew. Chem. Int. Ed.* **2019**, *58*, 13416–13420.

[218] a) F. Lovering, J. Bikker, C. Humblet, *J. Med. Chem.* **2009**, *52*, 6752–6756; b) F. Lovering, *Med. Chem. Commun.* **2013**, *4*, 515–519; c) T. P. Stockdale, C. M. Williams, *Chem. Soc. Rev.* **2015**, *44*, 7737–7763.

[219] a) P. K. Mykhailiuk, *Org. Biomol. Chem.* **2019**, *17*, 2839–2849; b) Y. L. Goh, Y. T. Cui, V. Pendharkar, V. A. Adsool, *ACS Med. Chem. Lett.* **2017**, *8*, 516–520; c) Y. P. Auberson, C. Brocklehurst, M. Furegati, T. C. Fessard, G. Koch, A. Decker, L. La Vecchia, E. Briard, *ChemMedChem* **2017**, *12*, 590–598; d) K. C. Nicolaou, D. Vourloumis, S. Totokotsopoulos, A. Papakyriakou, H. Karsunky, H. Fernando, J. Gavrilyuk, D. Webb, A. F. Stepan, *ChemMedChem* **2016**, *11*, 31–37; e) N. D. Measom, K. D. Down, D. J. Hirst, C. Jamieson, E. S. Manas, V. K. Patel, D. O. Somers, *ACS Med. Chem. Lett.* **2017**, *8*, 43–48; f) N. T. Thirumoorthi, V. Adsool, *Org. Biomol. Chem.* **2016**, *14*, 9485–9489; g) G. Costantino, K. Maltoni, M. Marinozzi, E. Camaioni, L. Prezeau, J.-P. Pin, R. Pellicciari, *Bioorg. Med. Chem.* **2001**, *9*, 221–227; h) R. Pellicciari, G. Costantino, E. Giovagnoni, L. Mattoli, I. Brabet, J.-P. Pin, *Bioorg. Med. Chem. Lett.* **1998**, *8*, 1569–1574; i) G. Mannaioni, S. Attucci, A. Missanelli, R. Pellicciari, R. Corradetti, F. Moroni, *Neuropharmacology*, **1999**, *38*, 917–926; j) D. E. Pellegrini-Giampietro, F. Peruginelli, E. Meli, A. Cozzi, S. Albani-Torregrossa, R. Pellicciari, F. Moroni, *Neuropharmacology* **1999**, *38*, 1607–1619; k) R. Pellicciari, R. Filosa, M. Carmela Fulco, M. Marinozzi, A. Macchiarulo, C. Novak, B. Natalini, M. B. Hermit, S. Nielsen, T. N. Sager, T. B. Stensbøl, C. Thomsen, *ChemMedChem* **2006**, *1*, 358–365; l) R. Filosa, M. Carmela Fulco, M. Marinozzi, N. Giacchè, A. Macchiarulo, A. Peduto, A. Massa, P. de Caprariis, C. Thomsen, C. T. Christoffersen, R. Pellicciari, *Bioorg. Med. Chem.* **2009**, *17*, 242–250.

[220] M. H. Keylor, B. S. Matsuura, C. R. J. Stephenson, *Chem. Rev.* **2015**, *115*, 8976–9027.

[221] R. Filosa, M. Marinozzi, G. Costantino, M. B. Hermit, C. Thomsen, R. Pellicciari, *Bioorg. Med. Chem.* **2006**, *14*, 3811–3817.

[222] a) K. J. Eastman, K. Parcella, K.-S. Yeung, K. A. Grant-Young, J. Zhu, T. Wang, Z. Zhang, Z. Yin, B. R. Beno, S. Sheriff, K. Kish, J. Tredup, A. G. Jardel, V. Halan, K. Ghosh, D. Parker, K. Mosure, H. Fang, Y.-K. Wang, J. Lemm, X. Zhuo, U. Hanumegowda, K. Rigat, M. Donoso, M. Tuttle, T. Zvyaga, Z. Haarhoff, N. A. Meanwell, M. G. Soars, S. B. Roberts, J. F. Kadow, *Med. Chem. Commun.* **2017**, *8*, 796–806; b) M. V. Westphal, B. T. Wolfstädter, J.-M. Plancher, J. Gatfield, E. M. Carreira, *ChemMedChem* **2015**, *10*, 461–469.

[223] D. Bouzard, P. Di Cesare, M. Essiz, J. P. Jacquet, J. R. Kiechel, P. Remuzon, A. Weber, T. Oki, M. Masuyoshi, R. E. Kessler, *J. Med. Chem.* **1990**, *33*, 1344–1352.

[224] D. Bouzard, P. Di Cesare, M. Essiz, J. P. Jacquet, P. Remuzon, A. Weber, T. Oki, M. Masuyoshi, *J. Med. Chem.* **1989**, *32*, 537–542.

[225] a) C. R. Butler, K. Ogilvie, L. Martinez-Alsina, G. Barreiro, E. M. Beck, C. E. Nolan, K. Atchison, E. Benvenuti, L. Buzon, S. Doran, C. Gonzales, C. J. Helal, X. Hou, M.-H. Hsu, E. F. Johnson, K. Lapham, L. Lanyon, K. Parris, B. T. O'Neill, D. Riddell, A. Robshaw, F. Vajdos, M. A. Brodney, *J. Med. Chem.* **2017**, *60*, 386–402; b) D. Marcoux, J. J.-W. Duan, Q. Shi, R. J. Cherney, A. S. Srivastava, L. Cornelius, D. G. Batt, Q. Liu, M. Beaudoin-Bertrand, C. A. Weigelt, P. Khandelwal, S. Vishwakrishnan, K. Selvakumar, A. Karmakar, A. K. Gupta, M. Basha, S. Ramlingam, N. Manjunath, S. Vanteru, S. Karmakar, N. Maddala, M. Vetrichelvan, A. Gupta, R. A. Rampulla, A. Mathur, S. Yip, P. Li, D.-R. Wu, J. Khan, M. Ruzanov, J. S. Sack, J. Wang, M. Yarde, M. E. Cvijic, S. Li, D. J. Shuster, V. Borowski, J. H. Xie, K. W. McIntyre, M. T. Obermeier, A. Fura, K. Stefanski, G. Cornelius, J. Hynes Jr., J. A. Tino, J. E. Macor, L. Salter-Cid, R. Denton, Q. Zhao, P. H. Carter, T. G. Murali Dhar, *J. Med. Chem.* **2019**, *62*, 9931–9946; c) X. Gao, J. Wang, J. Liu, D. Guiadeen, A. Krikorian, S. B. Boga, A.-B. Alhassan, O. Selyutin, W. Yu, Y. Yu, R. Anand, S. Liu, C. Yang, H. Wu, J. Cai, A. Cooper, H. Zhu, K. Maloney, Y.-D. Gao, T. O. Fischmann, J. Presland, M. Mansueto, Z. Xu, E. Leccese, J. Zhang-Hoover, I. Knemeyer, C. G. Garlisi, N. Bays, P. Stivers, P. E. Brandish, A. Hicks, R. Kim, J. A. Kozlowski, *Bioorg. Med. Chem. Lett.* **2017**, *27*, 1471–1477; d) S. Pritz, M. Pätzel, G. Szeimies, M. Dathe, M. Bienert, *Org. Biomol. Chem.* **2007**, *5*, 1789–1794; e) M. Meier, J. Seelig, *J. Am. Chem. Soc.* **2008**, *130*, 1017–1024; f) P. K. Mikhailiuk, S. Afonin, A. N. Chernega, E. B. Rusanov, M. O. Platonov, G. G. Dubinina, M.

Berditsch, A. S. Ulrich, I. V. Komarov, *Angew. Chem. Int. Ed.* **2006**, *45*, 5659–5661; g) S. Afonin, P. K. Mikhailiuk, I. V. Komarov, A. S. Ulrich, *J. Pept. Sci.* **2007**, *13*, 614–623; h) P. K. Mykhailiuk, N. M. Voievoda, S. Afonin, A. S. Ulrich, I. V. Komarov, *J. Fluor. Chem.* **2010**, *131*, 217–220; i) P. Wadhwani, E. Strandberg, N. Heidenreich, J. Bürck, S. Fanghänel, A. S. Ulrich, *J. Am. Chem. Soc.* **2012**, *134*, 6512–6515; j) M. Salwiczek, P. K. Mikhailiuk, S. Afonin, I. V. Komarov, A. S. Ulrich, B. Koksch, *Amino Acids* **2010**, *39*, 1589–1593; k) S. Fanghänel, P. Wadhwani, E. Strandberg, W. P. R. Verdurmen, J. Bürck, S. Ehni, P. K. Mykhailiuk, S. Afonin, D. Gerthsen, I. V. Komarov, R. Brock, A. S. Ulrich, *PLOS One* **2014**, *9*, e99653–e99666; l) P. Wadhwani, J. Reichert, E. Strandberg, J. Bürck, J. Misiewicz, S. Afonin, N. Heidenreich, S. Fanghänel, P. K. Mykhailiuk, I. V. Komarov, A. S. Ulrich, *Phys. Chem. Chem. Phys.* **2013**, *15*, 8962–8971.

[226] a) M. D. Andrews, S. K. Bagal, K. R. Gibson, K. Omoto, T. Ryckmans, S. E. Skerratt, P. A. Stupple, U.S. Patent Appl. US2014364415A1, **2014**; b) R. B. Gammill, S. N. Bisaha, J. M. Timko, T. M. Judge, M. R. Barbachyn, K. S. Kim, U.S. Patent Appl. US5262417A, **1993**; c) H. J. Breslin, B. D. Dorsey, B. J. Dugan, K. M. Fowler, R. L. Hudkins, E. F. Mesaros, N. J. T. Monck, Int. Patent Appl. WO2013US62085A1, **2013**; d) K. Hayashi, T. Watanabe, K. Toyama, J. Kamon, M. Minami, M. Uni, Int. Patent WO2012JP70876A1, **2012**; e) M. J. Bennett, L. R. Zehnder, S. Ninkovic, P. Kung, J. J. Meng, B. Huang, U.S. Patent Appl. US2010093696A1, **2010**; f) T. W. Johnson, P. F. Richardson, M. R. Collins, D. T. Richter, B. J. Burke, K. Gajiwala, S. Ninkovic, M. A. Linton, P. T. Q. Le, J. E. Hoffman, Can. Patent Appl. CA2915356A1, **2016**.

[227] A. R. Campanelli, A. Domenicano, G. Piacente, F. Ramondo, *J. Phys. Chem. A*, **2010**, *114*, 5162–5170.

[228] Y. S. Obeng, M. E. Laing, A. C. Friedli, H. C. Yang, D. Wang, E. W. Thulstrup, A. J. Bard, J. Michl, *J. Am. Chem. Soc.* **1992**, *114*, 9943–9952.

[229] a) J.-Y. Cho, M. K. Tse, D. Holmes, R. E. Maleczka Jr., M. R. Smith III, *Science* **2002**, *295*, 305–308; b) H. Hata, H. Shinokubo, A. Osuka, *J. Am. Chem. Soc.* **2005**, *127*, 8264–8265.

[230] D. E. Chumakov, A. V. Khoroshutin, A. V. Anisimov, K. I. Kobrakov, *Chem. Heterocycl. Compd.* **2009**, *45*, 259–283.

[231] a) W. S. Caughey, J. O. Alben, W. Y. Fujimoto, J. L. York, *J. Org. Chem.* **1966**, *31*, 2631–2640; b) M. Castella, F.R. Trull, F. López, Calahorra, D. Velasco, M. M. González, *Tetrahedron* **2000**, *56*, 4017–4025.

[232] J. Clayden, N. Greeves, S. Warren, *Organic Chemistry*, Oxford University Press, New York, **2012**.

[233] K. M. Smith, K. C. Langry, *J. Chem. Soc., Chem. Commun.* **1980**, 217–218.

[234] O. M. Minnetian, I. K. Morris, K. M. Snow, K. M. Smith, *J. Org. Chem.* **1989**, *54*, 5567–5574.

[235] a) R. Gauler, N. Risch, *Eur. J. Org. Chem.* **1998**, 1193–1200; b) N. Risch, R. Gauler, R. Keuper, *Tetrahedron Lett.* **1999**, *40*, 2925–2926.

[236] H. Ali, J. E. van Lier, *Tetrahedron* **1994**, *50*, 11933–11944.

[237] I. Stojiljkovic, V. Kumar, N. Srinivasan, *Mol. Microbiol.* **1999**, *31*, 429–442.

[238] a) I. Stojiljkovic, B. D. Evavold, V. Kumar, *Expert Opin. Investig. Drugs* **2001**, *10*, 309–320; b) K. J. McLean, A. W. Munro, *Drug Discov. Today* **2017**, *22*, 566–575; c) Y. Kaneko, M. Thoendel, O. Olakanmi, B. E. Britigan, P. K. Singh, *J. Clin. Invest.* **2007**, *117*, 877–888.

[239] C. P. Owens, N. Chim, C. W. Goulding, *Future Med. Chem.* **2013**, *5*, 1391–1403.

[240] D. E. Hultquist, M. Morrison, *J. Biol. Chem.* **1963**, *238*, 2843–2846.

[241] J. A. Cowan, J. K. M. Sanders, *J. Chem. Soc., Perkin Trans. 1* **1987**, 2395–2402.

[242] C.-Z. Li, I. Taniguchi, A. Mulchandani, *Bioelectrochemistry* **2009**, *75*, 182–188.

[243] a) A. Khadira, Y. de Coene, P. Gawal, C. Roche, K. Clays, H. L. Anderson, *Org. Biomol. Chem.* **2017**, *15*, 947– 965; b) L. Cao, X. Guo, L. Wang, S. Wang, Y. Li, W. Zhao, *New J. Chem.* **2017**, *41*, 14279–14287.

[244] a) T. Araki, T. Ozawa, H. Yokoe, M. Kanematsu, M. Yoshida, K. Shishido, *Org. Lett.* **2013**, *15*, 200–203; b) T. Ohgiya, N. Kutsumura, S. Nishiyama, *Synlett* **2008**, *20*, 3091–3105.

[245] M. P. Moon, R. D. Crouch, C.R. Jones. Pyridinium Hydrobromide Perbromide. In *Encyclopedia of Reagents for Organic Synthesis*, **2020**, doi: 10.1002/047084289X.rp292.pub3

[246] X. Feng, H. Zhang, W. Lu, Y. Yamamoto, A. I. Almansour, N. Arumugam, R. S. Kumar, M. Bao, *Synthesis* **2017**, *49*, 2727–2732.

[247] I. Maluenda, O. Navarro, *Molecules* **2015**, *20*, 7528–7557.

[248] A. Suzuki, *J. Organomet. Chem.* **2002**, *653*, 83–90.

[249] C. Moylan, L. Rogers, Y. M. Shaker, M. Davis, H.-G. Eckhardt, R. Eckert, Aoife A. Ryan, M. O. Senge, *Eur. J. Org. Chem.* **2016**, 185–195.

[250] C. Glaser, *Ber. Dtsch. Chem. Ges.* **1869**, *2*, 422−424.

[251] K. L. Billingsley, S. L. Buchwald, *Angew. Chem.* **2008**, *120*, 4773–4776

[252] I.-W. Hwang, T. Kamada, T. K. Ahn, D. M. Ko, T. Nakamura, A. Tsuda, A. Osuka, D. Kim, *J. Am. Chem. Soc.* **2004**, *126*, 16187–16198.

[253] a) T. Ishiyama, M. Murata, N. Miyaura, *J. Org. Chem.* **1995**, *60*, 7508-7510; b) K. C. Lam, T. B. Marder, Z. Lin, *Organometallics* **2010**, *29*, 1849–1857.

[254] M. Murata, S. Watanabe, Y. Masuda, *J. Org. Chem.* **1997**, *62*, 6458–6459.

[255] M. A. Bakar, N. N. Sergeeva, T. Juillard, M. O. Senge, *Organometallics* **2011**, *30*, 3225–3228.

[256] R. Chinchilla, C. Nájera, *Chem. Rev.* **2007**, *107*, 874–922.

[257] T. Asma, N. Serge, J. Anny, *Chem. Eur. J.* **2007**, *13*, 666–676.

[258] T. Liungdahl, T. Bennur, A. Dallas, H. Emtenäs, J. Mårtensson, *Organometallics* **2008**, *27*, 2490–2498.

[259] a) C. W. Tornøe, C. Christensen, M. Meldal, *J. Org. Chem.* **2002**, *67*, 3057–3064; b) V. V. Rostovtsev, L. G. Green, V. V. Fokin, K. B. Sharpless, *Angew. Chem. Int. Ed.* **2002**, *41*, 2596–2599.

[260] R. Huisgen, *Proc. Chem. Soc.* **1961**, 357−396.

[261] H. C. Kolb, M. G. Finn, K. B. Sharpless, *Angew. Chem. Int. Ed.* **2001**, *40*, 2004−2021.

[262] J. P. Collman, Y.-L. Yan, J. Lei, P. H. Dinolfo, *Inorg. Chem.* **2006**, *45*, 7581-7583.

[263] K. Ladomenou, V. Nikolaou, G. Charalambidis, A. G. Coutsolelos, *Coord. Chem. Rev.* **2016**, *306*, 1−42.

[264] M. Matoba, T. Kajimoto, K. Nishide, M. Node, *Chem. Pharm. Bull.* **2006**, *54*, 141–146.

[265] a) M. F. Romine, D. A. Rodionov, Y. Maezato, L. N. Anderson, P. Nandhikonda, I. A. Rodionova, A. Carre, X. Li, C. Xu, T. R. W. Clauss, Y.-M. Kim, T. O. Metz, A. T. Wright, *Proc. Natl. Acad. Sci. U. S. A.* **2017**, *114*, E1205–E1214; b) A. Amirshaghaghi, B. Altun, K. New, L. Yan, J. M. Stein, Z. Cheng, A. Tsourkas, *J. Am. Chem. Soc.* **2018**, *140*, 13550–13553.

[266] a) M. C. DeRosa, R. J. Crutchley. *Coord. Chem. Rev.* **2002**, *233*, 351–371; b) M. O. Senge, M. W. Radomski. *Photodiagnosis Photodyn. Ther.* **2013,** *10*, 1–16.

[267] a) L. Rogers, N. N. Sergeeva, E. Paszko, G. M. F. Vaz, M. O. Senge, *PLOS ONE* **2015**, *10*, e0125372; b) D. E. J. G. J. Dolmans, D. Fukumura, R. K. Jain, *Nat. Rev. Cancer* **2003**, *3*, 380–387; c) F. Cieplik, D. Deng, W. Crielaard, W. Buchalla, E. Hellwig, A. Al-Ahmad, T. Maisch, *Crit. Rev. Microbiol.* **2018**, *44*, 571–589.

[268] a) H. Ding, H. Yu, Y. Dong, R. Tian, G. Huang, D. A. Boothman, B. D. Sumer, J. Gao, *J. Control. Release* **2011**, *156*, 276–280; b) H. I. Pass, *J. Natl. Cancer Inst.* **1993**, *85*, 443–456; c) A. P. Castano, P. Mroz, M. R. Hamblin, *Nat. Rev. Cancer* **2006**, *6*, 535–545; d) Á. Juarranz, P. Jaén, F. Sanz-Rodríguez, J. Cuevas, S. González, *Clin. Transl. Oncol.* **2008**, *10*, 148–154.

[269] A. M. Joussen, *Retinale Gefäßerkrankungen*, Springer-Verlag, Berlin Heidelberg, **2012**.

[270] R. R. Allison, G. H. Downie, R. Cuenca, X.-H. Hu, C. J. H. Childs, C. H. Sibata, *Photodiagnosis Photodyn. Ther*. **2004**, *1*, 27–42.

[271] a) E. S. Nyman, P. H. Hynninen, *J. Photochem. Photobiol. B* **2004**, *73*, 1–28; b) A. De Rosa, D. Naviglio, A. Di Luccia, *Curr. Canc. Ther. Rev.* **2011**, *7*, 234–247.

[272] H. Abrahamse, M. R. Hamblin, *Biochem. J.* **2016**, *473*, 347–364.

[273] I. Yoon, J. Z. Li, Y. K. Shim, *Clin. Endosc.* **2013**, *46*, 7–23.

[274] W. Zhu, Y.-H. Gao, P.-Y. Liao, D.-Y. Chen, N.-N. Sun, P. A. Nguyen Thi, Y.-J. Yan, X.-F. Wu, Z.-L. Chen, *Eur. J. Org. Chem.* **2018**, *160*, 146–156.

[275] Y. Zhang, J. F. Lovell, *Theranostics* **2012**, *2*, 905–915.

[276] J. Sandland, N. Malatesi, R. Boyle, *Photodiagnosis Photodyn. Ther.* **2018**, *23*, 281–294.

[277] T. Förster, *Ann. Phys. (Leipzig)* **1948**, *437*, 55–75.

[278] D. L. Dexter, *J. Chem. Phys.* **1953**, *21*, 836–850.

[279] a) G. A. Jones, D. S. Bradshaw, *Front. Phys.* **2019**, *7*, 100–118; b) A. West in *Self-Assembly Processes at Interfaces. Multiscale Phenomena.* (Ed.: V. Ball), Academic Press, London, **2017**, Vol. 21, pp. 131–241.

[280] F. Scandola, V. Balzani, *J. Chem. Educ.* **1983**, *60*, 814–823.

[281] Y. Chen, A. Gryshuk, S. Achilefu, T. Ohulchansky, W. Potter, T. Zhong, J. Morgan, B. Chance, P. N. Prasad, B. W. Henderson, A. Oseroff, R. K. Pandey, *Bioconjugate Chem.* **2005**, *16*, 1264–1274.

[282] M. A. Grin, P. V. Toukach, V. B. Tsvetkov, R. I. Reshetnikov, O. V. Kharitonova, A. S. Kozlov, A. A. Krasnovsky, A. F. Mironov, *Dyes Pigment.* **2015**, *121*, 21–29.

[283] P. A. Panchenko, M. A. Grin, O. A. Fedorova, M. A. Zakharko, D. A. Pritmov, A. F. Mironov, A. N. Arkhipova, Y. V. Fedorov, G. Jonusauskas, R. I. Yakubovskaya, N. B. Morozova, A. A. Ignatova, A. V. Feofanov, *Phys. Chem. Chem. Phys.* **2017**, *19*, 30195–30206.

[284] S. Osati, H. Ali, J. E. van Lier, *Tetrahedron Lett.* **2015**, *56*, 2049–2053.

[285] A. Loudet, K. Burgess, *Chem. Rev.* **2007**, *107*, 4891–4932.

[286] T. K. Khan, M. Bröring, S. Mathur, M. Ravikanth, *Coord. Chem. Rev.* **2013**, *257*, 2348–2387.

[287] M. Sachar, K. E. Anderson, X. Ma, *J. Pharmacol. Exp. Ther.* **2016**, *356*, 267–275.

[288] K. R. Rollakanti, S. C. Kanick, S. C. Davis, B. W. Pogue, E. V. Maytin, *Photonics Lasers Med.* **2013**, *2*, 287–303.

[289] M. Bai, J. Huang, X. Zheng, Z. Song, M. Tang, W. Mao, L. Yuan, J. Wu, X. Weng, X. Zhou, *J. Am. Chem. Soc.* **2010**, *132*, 15321–15327.

[290] E. G. Azenha, A. C. Serra, M. Pineiro, M. M. Pereira, J. Seixas de Melo, L. G. Arnaut, S. J. Formosinho, A. M. d'A. Rocha Gonsalves, *Chem. Phys.* **2002**, *280*, 177–190.

[291] A. A. Kumar, L. Giribabu, B. G. Maiya, *J. Chem. Sci.* **2002**, *114*, 565–578.

[292] V. S. Shetti, Y. Pareek, M. Ravikanth, *Coord. Chem. Rev.* **2021**, *256*, 2816–2842.

[293] T. Lazarides, S. Kuhri, G. Charalambidis, M. K. Panda, D. M. Guldi, A. G. Coutsolelos, *Inorg. Chem.* **2012**, *51*, 4193-4204.

[294] D. P. Arnold, J. Block, *Coord. Chem. Rev.* **2004**, *248*, 299–319.

[295] V. S. Shetti, M. Ravikanth, *Inorg. Chem.* **2010**, *49*, 2692–2700.

[296] D. Badgurjar, K. Sudhakar, K. Jain, V. Kalantri, Y. Venkatesh, N. Duvva, S. Prasanthkumar, A. K. Sharma, P. R. Bangal, R. Chitta, L. Giribabu, *J. Phys. Chem. C* **2016**, *120*, 16305–16321.

[297] T. Shiragami, J. Matsumoto, H. Inoue, M. Yasuda, *J. Photochem. Photobiol. C: Photochem. Rev.* **2005***, 6,* 227–248.

[298] G. Ulrich, R. Ziessel, A. Harriman, *Angew. Chem. Int. Ed.* **2008**, *47*, 1184–1201.

[299] A. Gorman, J. Killoran, C. O'Shea, T. Kenna, W. M. Gallagher, D. F. O'Shea, *J. Am. Chem. Soc.* **2004**, *126*, 10619–10631.

[300] a) S. Pascal, L. Bucher, N. Desbois, C. Bucher, C. Andraud, C. P. Gros, *Chem. Eur. J.* **2016**, *22*, 4971–4979; b) J. Zhou, L. Gai, Z. Zhou, J. Mack, K. Xu, J. Zhao, H. Qiu, K. S. Chan, Z. Shen, *RCS Adv.* **2016**, *6*, 72115–72120; c) A. Koch, M. Ravikanth, *J. Org. Chem.* **2019**, *84*, 10775–10784.

[301] Q. Bellier, S. Pégaz, C. Aronica, B. L. Guennic, C. Andraud, O. Maury, *Org. Lett.* **2011**, *13*, 22–25.

[302] K. Rurack, M. Kollmannsberger, J. Daub, *New J. Chem.* **2001**, *25*, 289–292.

[303] a) Z. Dost, S. Atilgan, E. U. Akkaya, *Tetrahedron* **2006**, *62*, 8484–8488; b) S. Atilgan, Z. Ekmekci, A. L. Dogan, D. Guc, E. U. Akkaya, *Chem. Commun.* **2006**, 4398–4400.

[304] A. Meares, A. Satraitis, N. Santhanam, Z. Yu, M. Ptaszek, *J. Org. Chem.* **2015**, *80*, 3858−3869.

[305] L. Huang, X. Cui, B. Therrien, J. Zhao, *Chem. Eur. J.* **2013**, *19,* 17472−17482.

[306] A. Quaranta, G. Charalambidis, C. Herrero, S. Margiola, W. Leibl, A. Coutsolelos, A. Aukauloo, *Phys. Chem. Chem. Phys*. **2015**, *17*, 24166−24172.

[307] H. Sugimoto, M. Muto, T. Tanaka, A. Osuka, *Eur. J. Org. Chem*. **2011**, 71−77.

[308] O. Galangau, C. Dumas-Verdes, R. Méallet-Renault, G. Clavier, *Org. Biomol. Chem.* **2010**, *8*, 4546−4553.

[309] L. Liang, D. Astruc, *Coord. Chem. Rev.* **2011**, *255*, 2933−2945.

[310] M. Breugst, H.U. Reissig, *Angew. Chem. Int. Ed*. **2020**, *59*, 12293−12307.

[311] J. E. Moses, A. D. Moorhouse, *Chem. Soc. Rev*. **2007**, *36*, 1249−1262.

[312] a) K. J. Flanagan, B. Twamley, M. O. Senge, *Inorg. Chem.* **2019**, *58*, 15769−15787; b) O. B. Locos, C. C. Heindl, A. Corral, M. O. Senge, E. M. Scanlan, *Eur. J. Org. Chem.* **2010**, 1026−1028; c) C. Moylan, A. M. K. Sweed, Y. M. Shaker, E. M. Scanlan, M. O. Senge, *Tetrahedron* **2015**, *71*, 4145−4153.

[313] B. T. Worrell, J. A. Malik, V. V. Fokin, *Science* **2013**, *340*, 457−460.

[314] N. J. Agard, J. A. Prescher, C. R. Bertozzi, *J. Am. Chem. Soc*. **2004**, *126*, 15046−15047.

[315] J. C. Morris, J. Chiche, C. Grellier, M. Lopez, L. F. Bornaghi, A. Maresca, C. T. Supuran, J. Pouysségur, S.A. Poulsen*, J. Med. Chem*. **2011**, *54*, 6905−6918.

[316] a) B. R. Mullaney, A. L. Thompson, P. D. Beer, *Angew. Chem. Int. Ed.* **2014**, *53*, 11458−11462; b) N. L. Kilah, M. D. Wise, C. J. Serpell, A. L. Thompson, N. G. White, K. E. Christensen, P. D. Beer, *J. Am. Chem. Soc*. **2010**, *132*, 11893−11895; c) B. R. Mullaney,B. E. Partridge, P. D. Beer, *Chem. Eur. J*. **2015**, *21*, 1660−1665.

[317] R. Yan, E. El-Emir, V. Rajkumar, M. Robson, A. P. Jathoul, R. B. Pedley, E. Årstad, *Angew. Chem. Int. Ed.* **2011**, *50*, 6793−6795.

[318] D. N. Barsoum, N. Okashah, X. Zhang, L. Zhu, *J. Org. Chem.* **2015**, *80*, 9542−9551.

[319] a) Y.-M. Wu, J. Deng, Y. Li, Q.-Y. Chen, *Synthesis* **2005**, *8*, 1314−1318; b) D. N. Barsoum, C. J. Brassard, J. H. A. Deeb, N. Okashah, K. Sreenath, J. Tyler Simmons, L. Zhu, *Synthesis* **2013**, *45*, 2372−2386; c) L. Li, G. Hao, A. Zhu, S. Liu, G. Zhang, *Tetrahedron Lett*. **2013**, *54*, 6057−6060; d) L. Li, G. Zhang, A. Zhu, L. Zhang, *J. Org. Chem.* **2008**, *73*, 3630−3633; e) W. S. Brotherton, R. J. Clark, L. Zhu, *J. Org. Chem.* **2012**, *77*, 6443−6455; f) B. Wang, J. Zhang, X. Wang, N. Liu, W. Chen, Y. Hu*, J. Org. Chem*. **2013**, *78*, 10519−10523; g) R. Yan, K. Sander, E. Galante, V. Rajkumar, A. Badar, M. Robson, E. El-Emir, M. F. Lythgoe, R. B. Pedley, E. Årstad, *J. Am. Chem. So*c. **2013**, *135*, 703−709; h) L. Li, X. Xing, C. Zhang, A. Zhu, X. Fan, C. Chen, G. Zhang, *Tetrahedron Lett. **2018**, 59,* 3563−3566.

[320] Z. Chen, Z. Liu, G. Cao, H. Li, H. Ren, *Adv. Synth. Catal.* **2017**, *359*, 202−224.

[321] a) J. E. Hein, J. C. Tripp, L. B. Krasnova, K. B. Sharpless, V. V. Fokin, *Angew. Chem. Int. Ed.* **2009**, *48*, 8018−8021; b) J. García-Álvarez, J. Díez, J. Gimeno, *Green Chem.* **2010**, *12*, 2127−2130.

[322] L. Ackermann, H. K. Potukuchi, *Org. Biomol. Chem.* **2010**, *8*, 4503−4513.

[323] F. Alonso, Y. Moglie, G. Radivoy, M. Yus, *Synlett* **2012**, *23*, 2179−2182.

[324] D. Yang, N. Fu, Z. Liu, Y. Li, B. Chen, *Synlett* **2007**, *2*, 278−282.

[325] B. Gerard, J. Ryan, A. B. Beeler, J. A. Porco, *Tetrahedron* **2006**, *62*, 6405−6411.

[326] L.-J. Li, Y.-Q. Zhang, Y. Zhang, A.-L. Zhu, G.-S. Zhang, *Chin. Chem. Lett.* **2014**, *25*, 1161−1164.

[327] K. Yamamoto, T. Bruun, J. Yun Kim, L. Zhang, M. Lautens, *Org. Lett.* **2016**, *18*, 2644−2647.

[328] W. Wang, F. Wei, Y. Ma, C.-H. Tung, Z. Xu, *Org. Lett.* **2016**, *18*, 4158−4161.

[329] X. Jiang, X. Hao, L. Jing, G. Wu, D. Kang, X. Liu, P. Zhan, *Expert Opin. Drug Discov.* **2019**, *14*, 779–789.

[330] M. Kanai, T. Hirano, I. Azumaya, I. Okamoto, H. Kagechika, A.Tanatani, *Tetrahedron* **2012**, *68*, 2778−2783.

[331] X. Zhang, P. Liu, L. Zhu, *Molecules* **2016**, *21*, 1697−1714.

[332] a) K. Tanaka, C. Kageyama, K. Fukase, *Tetrahedron Lett*. **2007**, *48*, 6475−6479; b) I. Pérez-Castro, O. Caamaño, F. Fernández, M. D. García, C. López, E. De Clercq, *Org. Biomol. Chem.* **2007**, *5*, 3805−3813; c) N. W. Smith, B. P. Polenz, S. B. Johnson, S. V. Dzyuba, *Tetrahedron Lett.* **2010**, *51*, 550−553; d) R. Berg, B. F. Straub, *Beilstein J. Org. Chem.* **2013**, *9*, 2715−2750.

[333] L. Li, J. Wang, G. Zhang, Q. Liu, *Tetrahedron Lett*. **2009**, *50*, 4033−4036.

[334] a) R. Schmidt, R. Thorwirth, T. Szuppa, A. Stolle, B. Ondruschka, H. Hopf, *Chem. Eur. J*. **2011**, *17*, 8129−8138; b) X. Jia, K. Yin, C. Li, J. Li, H. Bian, *Green Chem.* **2011**, *13*, 2175−2178.

[335] a) S. G. Agalave, S. R. Mauja, V. S. Pore, *Chem. Asian J*. **2011**, *6*, 2696−2718; b) T. Ostrowski, P. Januszczyk, M. Cieslak, J. Kazmierczak-Baranska, B. Nawrot, E. Bartoszak-Adamska, J. Zeidler, *Bioorg. Med. Chem*. **2011**, *19*, 4386−4398.

[336] D. Goyard, A. S. Chajistamatiou, A. I. Sotiropoulou, E. D. Chrysina, J.-P. Praly, S. Vidal, *Chem. Eur. J.* **2014**, *20*, 1−11.

[337] M. Rakshit, G. K. Kar, M. Chakrabarty, *Monatsh. Chem.* **2015**, *146*, 1681−1688.

[338] P. Siemsen, R. C. Livingston, F. Diederich, *Angew. Chem. Int. Ed*. **2000**, *39*, 2632−2657.

[339] M. Gazvoda, M. Virant, B. Pinter, J. Košmrlj, *Nat. Commun.* **2018**, *9*, 4814−4822.

[340] a) J. Černý, P. Hobza, *Phys. Chem. Chem. Phys.* **2007**, *9*, 5291−5303; b) P. Zhou, J. Huang, F. Tian, *Curr. Med. Chem*. **2012**, *19*, 226−238.

[341] A. K. Nangia, G. R. Desiraju, *Angew. Chem. Int. Ed.* **2018**, *58*, 4100−4107.

[342] G. R. Desiraju, P. S. Ho, L. Kloo, A. C. Legon, R. Marquardt, P. Metrangolo, P. Politzer, G. Resnati, K. Rissanen, *Pure Appl. Chem.* **2013**, *85*, 1711−1713.

[343] a) J. P. M. Lommerse, A. J. Stone, R. Taylor, F. H. Allen, *J. Am. Chem. Soc*. **1996**, *118*, 3108−3116; b) P. Politzer, J. S. Murray, T. Clark, *Phys. Chem. Chem. Phys.*

2020, *12*, 7748−7757; c) G. Cavallo, P. Metrangolo, R. Milani, T. Pilati, A. Priimagi, G. Resnati, G. Terraneo*, Chem. Rev*. **2016**, *116*, 2478−2601.

[344] a) G. R. Desiraju, R. Parthasarathy, *J. Am. Chem. Soc.* **1989**, *111*, 8725−8726; b) A. Mukherjee, S. Tothadi, G. R. Desiraju, *Acc. Chem. Res.* **2014**, *47*, 2514−2524.

[345] L. Brammer, E. A. Bruton, P. Sherwood, *Cryst. Growth Des.* **2001**, *1*, 277−290.

[346] E. Arunan, G. R. Desiraju, R. A. Klein, J. Sadlej, S. Scheiner, I. Alkorta, D. C. Clary, R. H. Crabtree, J. J. Dannenberg, P. Hobza, H. G. Kjaergaard, A.C. Legon, B. Mennucci, D. J. Nesbitt, *Pure Appl. Chem.* **2011**, *83*, 1619−1636.

[347] a) M. Amati, F. Lelj, R. Liantonio, P. Metrangolo, S. Luzzati, T. Pilati, G. Resnati, *J. Fluor. Chem.* **2004**, *125*, 629−640; b) S. Rosokha, J. Kochi in *Halogen Bonding. Fundamentals and Applications* (Eds.: P. Metrangolo, G. Resnati), Springer-Verlag: Berlin, Heidelberg, **2008**, Vol. 126, pp. 137−160.

[348] a) M. Erdélyi, *Chem. Soc. Rev.* **2012**, *41*, 3547−3557; b) B. Hawthorne, H. Fan-Hagenstein, E. Wood, J. Smith, T. Hanks, *Int. J. Spectrosc.* **2013**, *2013*, 216518.

[349] a) A. K. Burrell, D. L. Officer, P. G. Plieger, D. C. W. Reid, *Chem. Rev.* **2001**, *101*, 2751–2796; b) D. Gust, T. A. Moore, A. L. Moore, *Acc. Chem. Res.* **2001**, *34*, 40–48; c) T. Tanaka, A. Osuka, *Chem. Soc. Rev.* **2015**, *44*, 943–969.

[350] J.-P. Strachan, S. Gentemann, J. Seth, W. A. Kalsbeck, J. S. Lindsey, D. Holten, D. F. Bocian, *J. Am. Chem. Soc.* **1997**, *119*, 11191–11201.

[351] F. Ginia, F. Foliab, A. M. Maruccoc, J. Facchetti, I. Fenoglioc, L. Serpeb, **2020**, OSF preprint DOI: 10.31219/osf.io/qky6s.

[352] A. Osuka, N. Tanabe, S. Kawabata, I. Yamazaki, Y. Nishimura, *J. Org. Chem.* **1995**, *60*, 7177–7185.

[353] a) B. Ventura, F. Barigelletti, F. Lodato, D. L. Officer, L. Flamigni, *Phys. Chem. Chem. Phys.* **2009**, *11*, 2166–2176; b) A. Helms, D. Heiler, G. McLendon, *J. Am. Chem. Soc.* **1992**, *114*, 6227–6238; c) A. Helms, D. Heiler, G. McLendon, *J. Am. Chem. Soc.* **1991**, *113*, 4325–4327.

[354] selected examples: a) J. R. Bolton, T.-F. Ho, S. Liauw, A. Siemiarczuk, C. S. K. Wan, A. C. Weedon, *J. Chem. Soc., Chem. Commun.* **1985,** 559–560; b) A. D. Joran, B. A. Laland, G. G. Geller, J. J. Hopfield, P. B. Dervan, *J. Am. Chem. Soc.* **1984**, *106*, 6090–6092; c) L. M. Urner, M. Sekita, N. Trapp, W. B. Schweizer, M. Wörle, J.-P. Gisselbrecht, C. Boudon, D. M. Guldi, F. Diederich, *Eur. J. Org. Chem.* **2015**, 91–108; d) T. A. Reekie, M. Sekita, L. M. Urner, S. Bauroth, L. Ruhlmann, J.-P. Gisselbrecht, C. Boudon, N. Trapp, T. Clark, D. M. Guldi, F. Diederich, *Chem. Eur. J.* **2017**, *23*, 6357–6369; e) O. Atsuhiro, Z. Run-Ping, M. Kazuhiro, O. Takeshi, N. Koichi, *Bull. Chem. Soc. Jpn.* **1993**, *66*, 3773–3782.

[355] selected examples: a) M. R. Wasielewski, M. P. Niemczyk, *J. Am. Chem. Soc.* **1984**, *106*, 5043–5045; b) M. R. Wasielewski, M. P. Niemczyk, D. G. Johnson, W. A. Svec, D. W. Minsek, *Tetrahedron* **1989**, *45*, 4785–4806; c) K. Dahms, M. O. Senge, *Tetrahedron Lett.* **2008**, *49*, 5397–5399; d) E. M. Finnigan, R. Rein, N. Solladié, K. Dahms, D. C. G. Götz, G. Bringmann, M. O. Senge, *Tetrahedron* **2011**, *67*, 1126–1134; e) G. Emandi, Y. M. Shaker, K. J. Flanagan, J. M. O'Brien, M. O. Senge, *Eur. J. Org. Chem.* **2017**, 6680–6692; f) G. M. Locke, K. J. Flanagan, M. O. Senge, *Beilstein J. Org. Chem.* **2020**, *16*, 763–777.

[356] S. S. R. Bernhard, G. M. Locke, S. Plunkett, A. Meindl, K. J. Flanagan, M. O. Senge, *Chem. Eur. J.* **2018**, *24*, 1026–1030.

[357] a) A. Shimojima, H. Takahashi, *J. Phys. Chem.* **1993**, *97*, 9103–9112; b) S. Toyota, *Chem. Rev.* **2010**, *110*, 5398–5424.

[358] a) M. Braga, *Chem. Phys.* **1996**, *213*, 159–164; b) R. Gleitner, K.-H. Pfeifer, G. Szeimies, U. Bunz, *Angew. Chem. Int. Ed.* **1990**, *29*, 413–415; c) O. Schafer, M. Allan, G. Szeimies, M. Sanktjohanser, *Chem. Phys. Lett.* **1992**, *195*, 293–297.

[359] M. Rickhaus, A. Vargas Jentzsch, L. Tejerina, I. Grübner, M. Jirasek, T. D. W. Claridge, H. L. Anderson, *J. Am. Chem. Soc.* **2017**, *139*, 16502–16505.

[360] C.-H. Lee, F. Li, K. Iwamoto, J. Dadok, A. A. Bothner-By, J. S. Lindsey, *Tetrahedron* **1995**, *51*, 11645–11672.

[361] S. Hayashi, M. Yotsukura, M. Noji, T. Takanami, *Chem. Commun.* **2015**, *51*, 11068–11071.

[362] a) K. Ladomenou, V. Nikolaou, G. Charalambidis, A. Charisiadis, A. G. Coutsolelos, *C. R. Chimie* **2017**, *20*, 314–322; b) S. M. Rojas-Montoya, M. Vonlanthen, P. Porcu, G. Flores-Rojas, A. Ruiu, D. Morales-Morales, E. Rivera, *Dalton Trans.* **2019**, *48*, 10435–10447; c) G. Zaragoza-Galán, M. Fowler, R. Rein, N. Solladié, J. Duhamel, E. Rivera, *J. Phys. Chem. C* **2014**, *118*, 8280–8294.

[363] M. R. Rao, S. M. Mobin, M. Ravikanth, *Tetrahedron* **2010**, *66*, 1728–1734.

[364] P. Bhyrappa, M. Sankar, B. Varghese, *Inorg. Chem.* **2006**, *45*, 4136–4149.

[365] R. J. Cave, S. J. Klippenstein, R. A. Marcus, *J. Chem. Phys.* **1986**, *84*, 3089–3098.

[366] P. D. Rao, B. L. Littler, G. R. Geier III, J. S. Lindsey, *J. Org. Chem.* **2000**, *65*, 1084–1092.

[367] C. J. Kingsbury, M. O. Senge, *Coord. Chem. Rev.* **2021**, *431*, 213760–213782.

[368] M. Z. Atassi, *Biochem. J.* **1967**, *103*, 29–35.

[369] V. Eck, M. Marcus, G. Stange, J. Westerhausen, J. F. Holzwarth, *Ber. Bunsenges. Phys. Chem.* **1981**, *85*, 869–876.

[370] N. Sugita, I. Tsuchiy, T. Takanami, *Heterocycles* **2016**, *93*, 483−511.

[371] D. E. Applequist, T. L. Renken, J. W. Wheeler, *J. Org. Chem.* **1982**, *47*, 4985−4995.

[372] H. Hope, *Prog. Inorg. Chem.* **2007**, *41*, 1−19.

[373] Bruker, *APEX3*, Bruker AXS Inc., Madison, WI, USA, **2017.**

[374] G. M. Sheldrick, *Acta Cryst. Sect. A* **2015**, *71*, 3−8.

[375] G. M. Sheldrick, *Acta Cryst. Sect. C*, **2015**, *71*, 3−8.

[376] O. V. Dolomanov, L.J. Bourhis, R.J. Gildea, J.A.K. Howard, H. Puschmann, *J. Appl. Cryst.* **2009**, *42*, 339−341.

[377] Bruker, *SADABS*, Bruker AXS Inc., Madison, Wisconsin, USA, **2016**.